LUANA LUCAS DUTRA

Pharmacological potential of withanolides from the subtribe Withaninae for Alzheimer's disease treatment and investigation of *Atheanea* species as a source of antitumor compounds.

Tese apresentada à Universidade Federal de Viçosa, como parte das exigências do Programa de Pós-Graduação em Bioquímica Aplicada, para obtenção do título de *Doctor Scientiae*.

Orientador: João Paulo Viana Leite

Coorientadores: Gustavo Costa Bressan
Tiago Antônio de Oliveira Mendes

VIÇOSA - MINAS GERAIS
2024

Ficha catalográfica elaborada pela Biblioteca Central da Universidade Federal de Viçosa - Campus Viçosa

T
D978p
2024

Dutra, Luana Lucas, 1994-
Pharmacological potential of with anolides from the subtribe withaninae for Alzheimer's diseasetreatment and investigation of *Atheanea* species as a source of antitumor compounds / Luana Lucas Dutra. – Viçosa, MG, 2024.
1 tese eletrônica (191 f.): il. (algumas color.).

Texto em inglês.
Inclui apêndices.
Orientador: João Paulo Viana Leite.
Tese (doutorado) - Universidade Federal de Viçosa, Departamento de Bioquímica e Biologia Molecular, 2024.
Inclui bibliografia.
DOI: https://doi.org/10.47328/ufvbbt.2024.277
Modo de acesso: World Wide Web.

1. Matéria médica vegetal. 2. *Athenaea*. 3. Produtos naturais. 4. Câncer - Tratamento. 5. Alzheimer, Doença de - Tratamento. 6. Agentes antineoplásicos. I. Leite, João Paulo Viana, 1972-. II. Universidade Federal de Viçosa. Departamento de Bioquímica e Biologia Molecular. Programa de Pós-Graduação em Bioquímica Aplicada. III. Título.

CDD 22. ed. 615.321

Bibliotecário(a) responsável: Alice Regina Pinto Pires CRB-6/2523

LUANA LUCAS DUTRA

Pharmacological potential of withanolides from the subtribe Withaninae for Alzheimer's disease treatment and investigation of *Atheanea* species as a source of antitumor compounds.

Tese apresentada à Universidade Federal de Viçosa, como parte das exigências do Programa de Pós-Graduação em Bioquímica Aplicada, para obtenção do título de *Doctor Scientiae*.

APROVADA: 29 de fevereiro de 2024.

Assentimento:

Documento assinado digitalmente
gov.br
LUANA LUCAS DUTRA
Data: 11/07/2024 15:12:58-0300
Verifique em https://validar.iti.gov.br

Luana Lucas Dutra

Autora

Documento assinado digitalmente
gov.br
JOAO PAULO VIANA LEITE
Data: 11/07/2024 15:57:04-0300
Verifique em https://validar.iti.gov.br

João Paulo Viana Leite

Orientador

AGRADECIMENTOS

À minha filha, Fernanda, e ao meu marido, Cleyton, por todo o amor e companheirismo. Esta tese não existiria sem o apoio de vocês.

Às minhas irmãs, meus pais e meus sogros, pelo apoio não só nos últimos quatro anos, mas durante toda a minha jornada acadêmica.

À Universidade Federal de Viçosa e ao Programa de Bioquímica Aplicada, pela oportunidade de realizar a pós-graduação. Ao professor Dr. João Paulo Leite, pela incrível orientação e paciência, e por me manter motivada mesmo durante períodos tão difíceis que atravessamos.

Ao Dr. Alisson Andrade Almeida, pelo auxílio na obtenção dos vitanolídeos, por todas as reuniões e sugestões, e aos demais colegas do Grupo de Pesquisa de Bioprospecção Molecular para o Uso Sustentável da Biodiversidade (BIOPROS). Agradeço especialmente à Dra. Lais Azevedo Rodrigues por ter sido minha mãe de bancada e melhor companheira de café. Aos colegas Vitor, Milena, Thaís, Guilherme, Juliana e Luciana, agradeço por todos os dias e algumas noites de companhia e conversas.

Ao professor Dr. Gustavo Bressan e a todos os membros do Laboratório de Bioquímica Celular e Bioprodutos pela orientação, disponibilização de toda a infraestrutura e treinamento necessários para os estudos envolvendo cultivo celular. Ao professor Dr. Tiago Mendes e aos membros do Laboratório de Bioquímica Molecular pelo suporte e orientações.

À Dra. Ana Zanatta pela disponibilidade em compartilhar seu conhecimento e por ter contribuído muito para a minha formação. Ao professor Dr. Vinícius G. Maltarollo, da Faculdade de Farmácia da UFMG, e ao Dr. Rafael J. Borges pela colaboração no primeiro capítulo deste trabalho e durante toda a árdua jornada em busca da publicação, espero trabalhar novamente com vocês. À Dra. Betânia Barros Cota e ao Dr. Markus Kohlhoff, do Laboratório de Produtos Bioativos do Centro de Pesquisa René Rachou, Fundação Oswaldo Cruz, pela colaboração com as análises de LC-MSMS, e ao prof. Dr. Geraldo Célio Brandão, da Faculdade de Farmácia da Universidade Federal de Ouro Preto, pelos experimentos de RMN. Ao viveiro do Departamento de Engenharia Florestal pelo cultivo de Athenaea velutina e pelo fornecimento de material vegetal. O presente trabalho foi realizado com apoio da Coordenação de Aperfeiçoamento de Pessoa de Nível Superior - Brasil (CAPES) - Código de Financiamento 001. Agradecemos também ao Conselho Nacional de Desenvolvimento Científico e Tecnológico (CNPq) e à Fundação de Amparo à Pesquisa do Estado de Minas Gerais (FAPEMIG), pelo financiamento da pesquisa.

RESUMO

DUTRA, L.L., Universidade Federal de Viçosa, março de 2024. **Potencial farmacológico de vitanolídeos da subtribo Withaninae para o tratamento de doença de Alzheimer e investigação de espécies de *Atheanea* como fonte de compostos antitumorais**. Orientador: João Paulo Viana Leite. Coorientadores: Gustavo Costa Bressan e Tiago Antônio de Oliveira Mendes.

Produtos naturais, compostos derivados do metabolismo secundário de plantas, desempenham um papel significativo como medicamentos ou precursores de medicamentos sintéticos. Vitanolídeos são um grupo de lactonas esteroidais polioxigenadas, que apresentam grande diversidade estrutural e são encontrados predominantemente em espécies da família Solanaceae. *Withania somnifera*, também conhecida como ginseng indiano, é uma fonte notável de vitanolídeos e amplamente utilizada na Medicina Tradicional Indiana. Estes produtos naturais estão associados a diversas atividades biológicas, incluindo efeitos antitumorais, inseticidas, antimicrobianos, anti-inflamatórios e imunorreguladores. Withaferin A, um vitanolideo proeminente de *W. somnifera*, demonstra atividade inibitória contra marcadores moleculares-chave na doença de Alzheimer (DA), sugerindo potencial terapêutico. Além disso, vitanolideos são promissores agentes anticancerígenos, com estudos indicando atividade citotóxica contra várias linhagens celulares cancerígenas. Neste trabalho investigamos se a diversidade estrutural dos vitanolídeos da subtribo Withaninae influencia suas propriedades farmacocinéticas e interação com alvos moleculares implicados na DA. Em nosso estudo *in silico* destacamos insaturações nos carbonos C5-C6 como favoráveis para farmacocinética e interação com enzimas colinesterases, alvos potenciais da DA. Este estudo destacou as potenciais características estruturais na melhoria da eficácia de medicamentos contra a DA. A partir de pesquisas anteriores demonstrando a atividade citotóxica dos vitanolideos, foram realizadas investigações sobre sua citotoxicidade em modelos de células cancerígenas humanas. A vitalutina, vitacnistina e acetato de vitacnistina, vitanolídeos isolados de *Athenaea velutina*, apresentaram alta citotoxicidade em linhagens de melanoma e câncer de mama, além de significativa atividade antiproliferativa no modelo de melanoma. Simulações de docking molecular sugerem um possível mecanismo envolvendo a interação com o fator de transcrição STAT3. A exploração subsequente dos vitanolideos em outras espécies de *Athenaea* revelou atividade citotóxica promissora, especialmente no extrato etanólico de *A. fasciculata*. O fracionamento deste extrato resultou no aumento da citotoxicidade nas frações orgânicas e a análise de composição por LC-HRMS sugere a presença de vitanolídeos como compostos bioativos potenciais. Em conclusão, os vitanolideos representam uma classe diversificada de produtos naturais com significativo potencial farmacológico. A diversidade estrutural influencia sua atividade contra doenças multifatoriais como a AD e o câncer. Pesquisas adicionais sobre vitanolideos, incluindo a elucidação de seus mecanismos moleculares e a exploração de fontes naturais adicionais, oferecem promessa para o desenvolvimento de novos tratamentos visando doenças complexas.

Palavras-chave: Vitanolideos; *Athenaea;* Produtos Naturais; Câncer; Doença de Alzheimer

ABSTRACT

DUTRA, L. L., Federal University of Viçosa, March 2024. **Pharmacological potential of withanolides from the Withaninae subtribe for Alzheimer's disease treatment and investigation of Athenaea species as a source of antitumor compounds.** Supervisor: João Paulo Viana Leite. Co-supervisors: Gustavo Costa Bressan and Tiago Antônio de Oliveira Mendes.

Natural products, compounds derived from the secondary metabolism of plants, play a significant role as drugs or precursors for synthetic drugs. Withanolides are a group of polyoxygenated steroidal lactones, presenting structural diversity and predominantly found in species of the Solanaceae family. *Withania somnifera*, also known as Indian ginseng, is a notable source of withanolides, widely used in Traditional Indian Medicine. These natural products are associated with various biological activities, including antitumor, insecticidal, antimicrobial, anti-inflammatory, and immunoregulatory effects. Withaferin A, a prominent withanolide from *W. somnifera*, demonstrates inhibitory activity against key molecular markers in Alzheimer's disease (AD), suggesting therapeutic potential. Moreover, withanolides show promise as anticancer agents, with studies indicating cytotoxic activity against various cancer cell lines. In this study, we investigated whether the structural diversity of withanolides from the Withaninae subtribe influences their pharmacokinetic properties and interaction with molecular targets implicated in AD. In our *in silico* study, we highlighted unsaturations at carbons C5-C6 as favorable for pharmacokinetics and interaction with cholinesterase enzymes, potential targets of AD. This study emphasized the structural features in enhancing the effectiveness of drugs against AD. Building upon previous research demonstrating the cytotoxic activity of withanolides, investigations were conducted on their cytotoxicity in human cancer cell models. Withalutin, withacnistin, and withacnistin acetate, withanolides isolated from *Athenaea velutina*, showed high cytotoxicity in melanoma and breast cancer cell lines, along with significant antiproliferative activity in the melanoma model. Molecular docking simulations suggest a possible mechanism involving interaction with the STAT3 transcription factor. Subsequent exploration of withanolides in other *Athenaea* species revealed promising cytotoxic activity, especially in the ethanolic extract of *A. fasciculata*. Fractionation of this extract resulted in increased cytotoxicity in organic fractions, and LC-HRMS composition analysis suggests the presence of withanolides as potential bioactive compounds. In conclusion, withanolides represent a diverse class of natural products with significant pharmacological potential. Structural diversity influences their activity against multifactorial diseases such as AD and cancer. Further research on withanolides, including elucidation of their molecular mechanisms and exploration of additional natural sources, holds promise for the development of new treatments targeting complex diseases.

Keywords: Withanolides; *Athenaea*; Natural Products; Cancer; Alzheimer's disease

Para Fernanda. Com todo o meu amor, mamãe.

SUMÁRIO

Introduction

Withanolides: natural products with pharmacological applications

Multifactorial diseases result from a combination of elements, including genetic predisposition, environmental factors, and lifestyle, leading to the development of complex pathologies such as cancer, Alzheimer's disease, hypertension, and schizophrenia (STOLK et al., 2008). Due to the complexity of these diseases, there is a significant interest in drugs that can modulate different molecular pathways (RAMSAY et al., 2018). Compounds from the secondary metabolism of plants, known as natural products, play a significant role as drugs (phytopharmaceuticals and herbal medicines) or as precursors for new synthetic drugs (NEWMAN and CRAGG, 2020), and many of these compounds operate synergistically and on multiple targets, given their wide diversity of chemical structures (EFFERT and KOCH, 2011). Withanolides steroids are part of a group of polyoxygenated steroidal lactones that vary mainly in terms of the number and position of oxygenated substituents, as well as the degree of unsaturation (CHEN et al., 2011). The fundamental structure of withanolides (Figure 1) comprises a C-28 skeleton, in which C-26 and C-22 or C-26 and C-23 are oxidized, forming δ- or γ-lactones, respectively (CHEN et al., 2011).

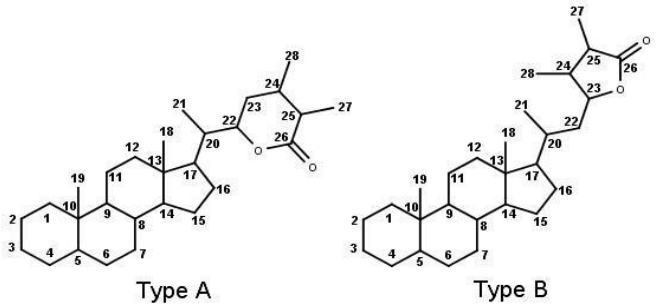

Figure 1: Structures of A-type withanolide (delta lactone) and B-type withanolide (gamma lactone).

This complex array of molecules exhibits significant structural diversity (CHEN et al., 2011; DUTRA et al., 2023) and is predominantly found in species of the Solanaceae family, including genera such as *Acnistus, Datura, Deprea, Dunalis, Discopodium, Exodeconus, Hyoscyamus, Iochroma, Jaborosa, Larnax, Lycium, Nicandra, Physalis, Salpichroa, Trechonaetes, Tubocapsicum, Vassobia, Withania* e *Witheringia*, and less frequently in the families Fabaceae (*Cassia siamea*), Labiatae (*Ajuga parviflora* and *Ajuga bracteosa*), Myrtaceae (*Eucalyptus globulus*) and Taccaceae (*Tacca plantaginea* and *Tacca chantrieri*) (CHEN et al., 2011; XIA et al., 2022).

Withania somnifera, also known as Indian ginseng, stands out as a notable source of withanolides, with extensive application in Traditional Indian Medicine or *Ayurveda* (DHAR et al., 2015). Phytotherapeutic formulations derived from *W. somnifera* primarily use roots and leaves and are intended to treat various disorders associated with the inflammatory process (CHEN et al., 2011; DAR et al., 2015). Isolated withanolides are linked to a variety of biological activities such as antitumor, insecticidal, trypanocidal, leishmanicidal, antimicrobial, anti-inflammatory, immunoregulatory, neuronal interaction reconstruction, cholinesterase inhibition, and phytotoxic activity (CHEN et al., 2011; XIA et al., 2022). Around 40 withanolides have been identified in *W. somnifera*, with withaferin A being one of the main compounds, known for its antitumor, anti-inflammatory, and cholinesterase inhibitory properties (CHEN et al., 2011; DAR et al., 2015).

Within the Solanaceae family, the genus *Withania* is phylogenetically associated with seven other genera: *Mellissia*, *Athenaea, Tubocapsicum, Nothocestrum, Discopodium, Deprea,* and *Cuatresia*, composing the Withaninae subtribe (OLMSTEAD et al., 2008; DEANNA et al., 2019). The *Aureliana* genus was recently incorporated into the *Athenaea* genus (RODRIGUES et al., 2019).

It is possible that the biosynthesis of withanolides occurs through the mevalonate (MVA) and non-mevalonate (MEP or DOXP) pathways, with a relative ratio of 1:3 (XIA et al., 2022). Although 24-methylenecholesterol is known to be a vital precursor for the synthesis of various withanolides, the molecular mechanisms of these conversions are not yet completely elucidated (Figure 1) (XIA et al., 2022).

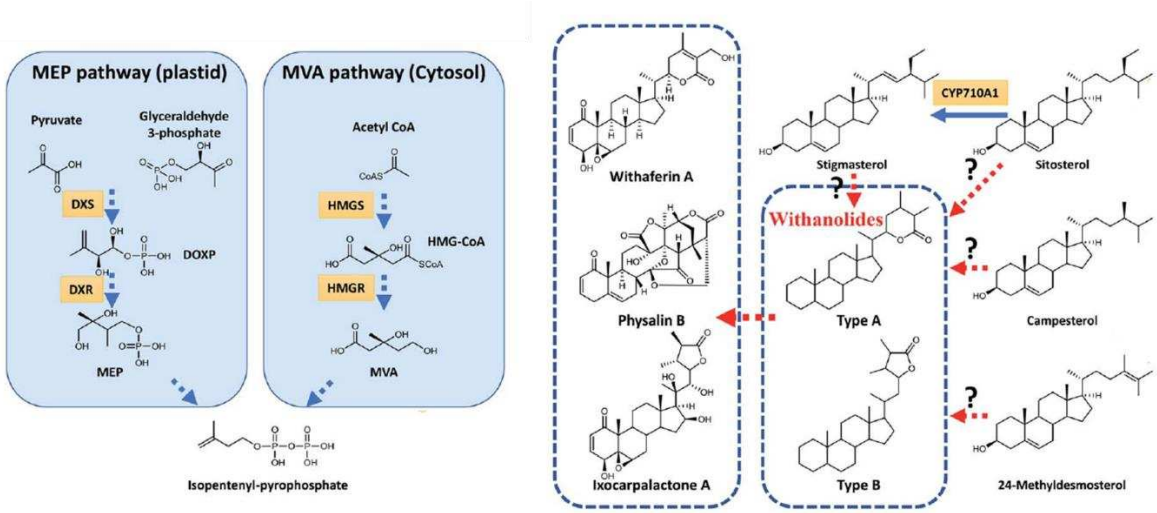

Figure 1: Summarized mechanism of withanolide biosynthesis proposed by Xia and colleagues (2022).

Anti-Alzheimer's disease activities of withanolides

The multi-target action of withanolides makes these molecules promising precursors for new drugs to treat Alzheimer's disease (AD). AD's exact cause is still unclear, but it is characterized by insoluble β-amyloid aggregates, hyperphosphorylation of the Tau protein in the cytoskeleton, hyperactivation of cholinesterases, and interference with inflammatory and oxidative pathways (DU et al., 2018).

The cholinergic hypothesis, the oldest and most widely used approach, suggests that reduced acetylcholine biosynthesis is linked to AD development. Inhibiting acetylcholinesterase (AChE) and butyrylcholinesterase (BChE) can increase acetylcholine levels and slow the disease's progression (HAMPEL et al., 2019; AMBURE et al., 2019). The amyloid hypothesis posits that inhibiting β-secretase (BACE-1) prevents the formation of insoluble β-amyloid (βA) aggregates. The Tau hypothesis suggests that hyperphosphorylation of Tau leads to cytoskeleton breakdown and fibrillar tangles, with cyclin-dependent kinase 5 (CDK5) and glycogen synthase kinase 3β (GSK-3β) being key targets (AMBURE et al., 2019). Additionally, the oxidative stress hypothesis implicates increased oxidative stress in neuronal death and the formation of AD markers, with monoamine oxidase (MAO-B) producing ROS that cause cellular damage (AMBURE et al., 2019).

Withaferin A, a well-studied withanolide in *W. somnifera*, shows inhibitory activity against crucial molecular markers in AD. It reduces β-amyloid aggregates and fibrillar tangles, regulates heat shock proteins, and inhibits oxidative and inflammatory pathways (DAS et al., 2015). Additionally, both the leaf extract of *W. somnifera* and the withanolide S compound found in the extract have demonstrated AChE inhibition, providing protection against hemolysis, anti-inflammatory action, and antioxidant activity (MAHROUS et al., 2017).

In light of the pharmacological potential of this class of natural products, we aimed to elucidate how the structural diversity of withanolides occurring in the Withaninae subtribe interferes with their pharmacokinetic properties and their interaction with potential molecular targets involved in the development of AD. The *in silico* investigation highlighted the presence of unsaturations at carbons C5 and C16 or C17 as promoters of a better pharmacokinetic profile and participated interaction with the catalytic site of cholinesterase enzymes. These enzymes are potential targets, and their inhibition characterizes one of the main mechanism of action of commercial drugs against AD. This study, published by Dutra and colleagues (2023), is detailed in Chapter 1.

Anticancer activities of withanolides

Another promising pharmacological application for withanolides is as anticancer agents. The antitumor activity of these compounds has been extensively evaluated in more than 80 cell lines, demonstrating excellent cytotoxicity of this class of natural products (XIA et al., 2022). The mechanism of action of withanolides in tumour cells has not been extensively explored, but evidence indicates that these molecules promote the induction of reactive oxygen species (ROS), inhibit the inflammatory response via NF-κB, and modulate the activity of different kinases (XIA et al., 2022).

Specific studies have described the impact of the withanolide withacnistin on breast cancer cells, observing alterations in the functioning of the STAT3 transcription factor (ZANG et al., 2014). This withanolide was also isolated from the dichloromethane extract of *A. velutina* leaves (ALMEIDA et al., 2022), along with the acetate analogue of withacnistin and the previously unreported molecule, withalutin (Figure 2). The enriched withanolide fraction from *A. velutina* exhibited promising cytotoxic activity against murine melanoma B16F10 cells, significantly reducing proliferation, migration, and invasion processes, as well as inducing cell cycle arrest in the G0/G1 phase and apoptosis (ALMEIDA et al., 2021). The isolated withanolides from this fraction not only demonstrated excellent cytotoxicity (IC_{50} = 1.50 µM, 3.12 µM, and 5.39 µM, respectively) but also showed promising properties related to ADMET (ALMEIDA et al., 2022).

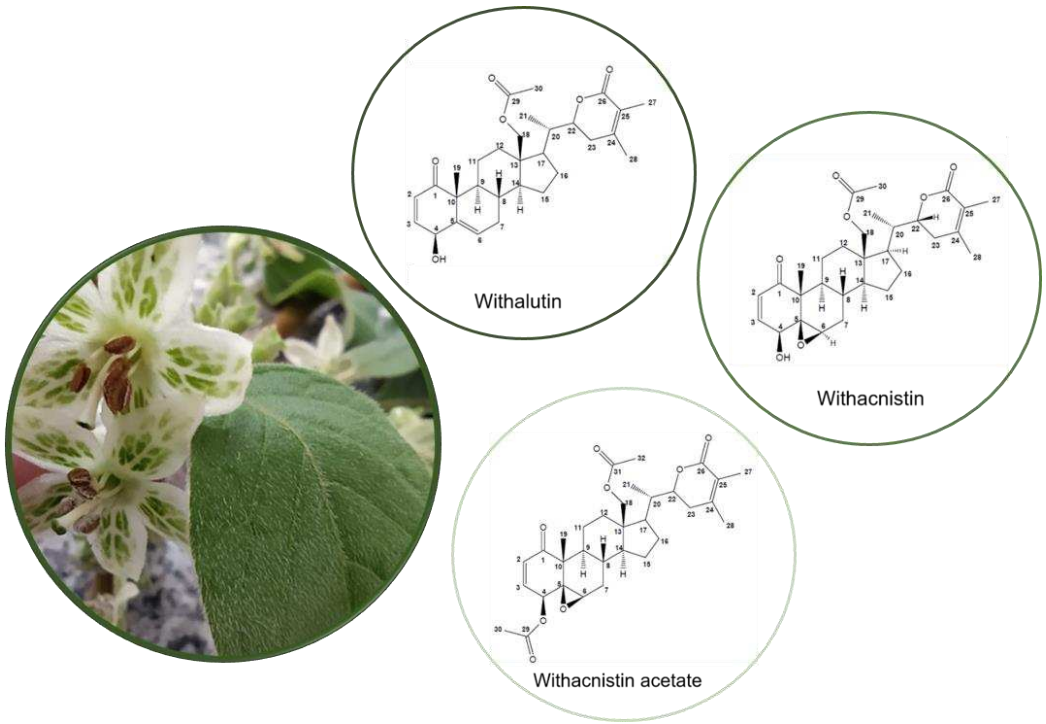

Figure 2: Structure of withanolides isolated from *A. velutina* (ALMEIDA et al., 2022).

Building upon the work of Almeida and colleagues (2022), which demonstrated the cytotoxic activity of three withanolides isolated from *A. velutina* in a murine B16F10 melanoma cell model, we decided to investigate how the structural differences in these molecules reflect on cytotoxicity and antiproliferative activity in other cancer cell models (human melanoma and breast cancer, MV3, and MCF-7). Additionally, we computationally assessed the possible mechanism of action responsible for these activities through interaction with the STAT3 transcription factor in a blind molecular docking simulation. This study is reported in Chapter 2. Further analyses are needed to confirm the interaction with STAT3 and explore other molecular targets that justify the promising anticancer activity of these molecules.

The results obtained after prospecting bioactive molecules in *A. velutina* (ALMEIDA et al., 2020; 2021, and 2022) were surprising enough to prompt the search for withanolides in other species of the *Athenaea* genus. Using melanoma and breast cancer cell models, we evaluated the cytotoxic activity of dichloromethane and ethanol extracts generated by percolation from dried leaves of other species of this genus: *A. fasciculata, A. martiana, and A. tomentosa*. We selected the extract with the highest cytotoxicity and fractionated it by liquid-liquid partition to assess the activity of the fractions as well as their composition by LC-MS/MS. This study is detailed in Chapter 3.

Rational drug design

The application of *in silico* studies in medicinal chemistry has become increasingly common due to the advancement of biomolecule characterization techniques and computational methods for analyzing these data. Determining the molecular target is a crucial step in screening potential drugs, as a good target must have a confirmed role in the pathology under study, an unequal distribution of target expression across tissues, an experimentally elucidated three-dimensional structure, and measurable *in vitro* validation assays (GASHAW et al., 2011).

For selecting the molecular target, the deconvolution method can be followed. In this method, phenotypic alterations caused by the molecules under study (ligands) are observed, and the ligand-target interactions responsible for these alterations are determined. This method requires cellular or animal models, meaning it starts with *in vitro* or *in vivo* studies to guide which targets will be analyzed in the computational step. This ensures greater reliability for *in silico* analyses but comes at a high cost (MOFFAT et al., 2017).

Another widely used method is based on the structure of the ligand under study and information described in the literature about molecular targets that interact with them. In this method, although the cellular context is excluded, the target selection is faster and less

expensive, allowing screening of a large number of ligands and the establishment of structure-activity relationships (CROSTON, 2017).

Molecular docking is widely used in the screening of potential drugs based on the target structure (structure-based virtual screening - SBVS). This technique provide a computational prediction of the binding mode of a molecule to a receptor of interest (pose) and the affinity of the ligand-target interaction. It is an interdisciplinary area of study that involves knowledge of bioinformatics, molecular biology, biotechnology, mathematics, and computer science (GUPTA, SHARMA, and KUMAR, 2018; LI et al., 2016).

The selection of the best candidates (hits) can be based on interaction affinity parameters, molecular dynamics, determination of pharmacophore groups, or ligand-based methods (ligand-based drug design - LBDD) (FERREIRA et al., 2015; VIEIRA, SANTOS, and FERREIRA et al., 2018).

Computational chemistry has advanced in predicting pharmacokinetic properties like absorption, distribution, metabolism, excretion, and toxicity (ADMET). These properties often cause drug candidates that perform well *in vitro* to fail in clinical trials (MAKHOBA et al., 2020). Due to the structural diversity of withanolides, understanding their pharmacokinetic properties is crucial for discovering new drug leads (LIU, 2022). *In silico* studies that predict physicochemical, pharmacokinetic, and toxicity properties can effectively screen small molecules, guiding experimental testing and improving drug development.

References

ALMEIDA, A.A., COTA, B.B., RODRIGUES, L. M., DUTRA, L. L., KOHLHOFF, M., BRESSAN, G. C., BRANDÃO. G. C., LEITE, J. P. V. Withalutin, a new cytotoxic withanolide from *Athenaea velutina* (Sendtn.) D'Arcy. *Natural Product Research*, v. 13, p. 1-8, 2022. DOI: 10.1080/14786419.2022.2039135

ALMEIDA, A.A., LIMA, G.D.A., EITERER, M., RODRIGUES, L.A., DO VALE, J.A., ZANATTA, A.C., BRESSAN, G.C., DE OLIVEIRA, L.L., LEITE, J.P.V. A withanolide-rich fraction of *Athenaea velutina* induces apoptosis and cell cycle arrest in melanoma B16F10 cells. *Planta Medica*, 2021. DOI: 10.1055/a-1395-9046

ALMEIDA, A.A., LIMA, G.D.A., SIMÃO, M.V.R.C., MOREIRA, G.A., SIQUEIRA, R.P., ZANATTA, A.C., VILEGAS, W., MACHADO-NEVES, M., BRESSAN, G.C., LEITE, J.P.V. Screening of plants from the Brazilian Atlantic Forest led to the identification of *Athenaea velutina* (Solanaceae) as a novel source of antimetastatic agentes. *International Journal of Experimental Pathology*, v.10, n.3-4, p. 106-121, 2020.

ALMEIDA-LAFETÁ, R. C., FERREIRA, M. J. P., EMERENCIANO, V. P., KAPLAN, M. A. C. Withanolides from *Aureliana fasciculata var. fasciculata. Helvetica Chimica Acta*, v. 93, 2010.

AMBURE, P., BHAT, J., PUZYN, T. e ROY, K. Identifying natural compounds as multi-target directed ligands against Alzheimer's disease: an in silico approach. *Journal of Biomolecular Structure and Dynamics*, v. 35, p. 1282-1306, 2019. DOI: 10.1080/07391102.2018.1456975

CHEN, L., HE, H. e QIU, F. Natural withanolides: an overview. *Natural Product Reports*, v. 28, p. 705-740, 2011. DOI: 10.1039/c0np00045k

CROSTON, G. E. The utility of target-based discovery. *Expert Opinion on Drug Discovery*, v. 12, p. 427-429, 2017. DOI: 10.1080/17460441.2017.1308351

DEANNA, R., LARTER, M. D., BARBOZA, G. E., SMITH, S. D. Repeated evolution of a morphological novelty: a phylogenetic analysis of the inflated fruiting calyx in the *Physalideae* tribe (Solanaceae). *American Journal of Botany*, v. 106, n. 2, p. 270-279, 2019. DOI: 10.1002/ajb2.1242

DHAR, N., RAZDAN, S., RANA, S., BHAT, W. W., VISHWAKARMA, R. e LATTOO, S. K. A decade of molecular understanding of withanolide biosynthesis and in vitro studies in *Withania somnifera* (L.) Dunal: prospects and perspectives for pathway engineering. *Frontiers in Plant Science*, v. 6, 2015. DOI: 0.3389/fpls.2015.01031

DU,X, WANG, X. e GENG, M. Alzheimer's disease hypothesis and related therapies. *Translational Neurodegeneration*. 2018. DOI: 10.1186/s40035-018-0107-y

DUTRA, L.L., BORGES, R.J., MALTAROLLO, V.G., MENDES, T.A., BRESSAN, G.C. AND LEITE, J.P.V. *In silico* evaluation of pharmacokinetics properties of withanolides and simulation of their biological activities against Alzheimer's disease. *Journal of Biomolecular Structure and Dynamics*, p.1-16, 2023. DOI: 10.1080/07391102.2023.2206909

EFFERTH, T. e KOCH, E. Complex interactions between phytochemicals. The mult-target therapeutic concept of phytotherapy. *Current drug Targets*, v. 12, p. 122-132, 2011.

FERREIRA, L. G., dos SANTOS, R. N., OLIVIA, G. e ANDRICOPULO, A. D. Molecular docking and structure-based drug design strategies. *Molecules*, v. 20, p. 13384-13421, 2015.

GASHAW, I., ELLINGHAUS, P., SOMMER, A. e ASADULLAH, K. What makes a good drug target? *Drug Discovery Today*, v. 16, p. 1037-1043, 2011. DOI: https://doi.org/10.1016/j.drudis.2011.09.007

GUPTA, M., SHARMA, R. e KUMAR, A. Docking techniques in pharmacology: how much promising? *Computational Biology and Chemistry,* v. 76, p. 210-217, 2018.

LIEBESCHUETZ, J.W., COLE, J.C., KORB, O. Pose prediction and virtual screening performance of GOLD scoring functions in a standardized test. *Journal of computer-aided molecular design*, v. 26, p.737-748, 2012. DOI: 10.1007/s10822-012-9551-4

LIMA, S.C.D.M., PACHECO, J.D.S., MARQUES, A.M., VELTRI, E.R.P., ALMEIDA-LAFETÁ, R.D.C., FIGUEIREDO, M.R., KAPLAN, M.A.C., TORRES-SANTOS, E.C. Leishmanicidal activity of Withanolides from *Aureliana fasciculata var. fasciculata. Molecules*, v. 23, n.12, p.3160, 2018. DOI: 10.3390/molecules23123160

LIU, Y. *In silico* evaluation of pharmacokinetics and acute toxicity of withanolides in ashawagandha. *Phytochemistry Letters*, v. 47, p.130–135, 2022.

MAHROUS, R. S. R., GHAREEB, D. A., FATHY, H. M., EL-KHAIR, R. M. A. e OMAR, A. A. The Protective Effect of Egyptian Withania somnifera Against Alzeheimer's. *Medicinal and Aromatic Plants*, v. 6, p. 1-6, 2017. 10.4172/2167-0412.1000285

MAKHOBA, X.H., VIEGAS JR, C., MOSA, R.A., VIEGAS, F.P., POOE, O.J. Potential impact of the multi-target drug approach in the treatment of some complex diseases. *Drug Design, Development and Therapy,* v.14, p.3235, 2020.

MOFFAT, J. G., VINCENT, F., LEE, J. A., EDER, J. e PRUNOTTO, M. Opportunities and challenges in phenotypic drug discovery: an industry perspective. *Nature Reviews Drug Discovery*, v. 16, p. 531-543, 2017.

NEWMAN, D. J., CRAGG, G. M. Natural Products as Sources of New Drugs over the Nearly Four Decades from 01/1981 to 09/2019. *Journal of Natural Products*, v. 83, n. 3, p. 770-803, 2020. DOI: 10.1021/acs.jnatprod.9b01285

OLMSTEAD, R. G., BOHS, L., MIGID, H. A., SANTIAGO-VALENTIN, E., GARCIA, V. F. E COLLIERET S. M. A molecular phylogeny of the Solanaceae. *Taxon*, v. 57, p. 1159-1181, 2008.

PERES, R.B., FIUZA, L.F.D.A., DA SILVA, P.B., BATISTA, M.M., CAMILLO, F.D.C., MARQUES, A.M., DE C. BRITO, L., FIGUEIREDO, M.R., SOEIRO, M.D.N. *In vitro* phenotypic activity and in silico analysis of natural products from Brazilian biodiversity on *Trypanosoma cruzi*. *Molecules*, v. 26, n. 18, p.5676, 2021. DOI: 10.3390/molecules26185676

RAMSAY, R. R., POPOVIC-NIKOLIC, M. R., NIKOLIC, K., ULIASSI, E., BOLOGNESI, M. L. A perspective on multi-target drug discovery and design for complex diseases. *Clinical and Translational Medice*, v. 7, p. 1-14, 2018.

RODRIGUES, I. M. C., KNAPP, S., STEHMANN, J. R. The nomenclatural re-establishment of *Athenaea Sendtn.* (Solenaceae) with a nomenclatural synopsis of the genus. *Taxon*, 2019. DOI: 10.1002/tax.12089

STOLK, R. P., ROSMALEN, J. G. M., POSTMA, D. S., BOER, R. A., NAVIS, G., SLAETS, J. P. J., ORMEL, J., WOLFFENBUTTEL, B. H. R. Universal risk factors for multifactorial diseases. *Eur J Epidemiol*, v. 23, p. 67-74, 2008.

TUNYASUVUNAKOOL, K., ADLER, J., WU, Z., et al. Highly accurate protein structure prediction for the human proteome. *Nature*, v. 596, 2021. DOI: 10.1038/s41586-021-03828-1

VIEIRA, R. P., SANTOS, V. C. e FERREIRA, R. S. Structure-based approaches targeting parasite cysteine proteases. *Current Medicinal Chemistry*, v. 25, p. 1-18, 2018.

WANG, M., CARVER, J. J., PHELAN, V. V., SANCHEZ, L. M., GARG, N., PENG, Y., NGUYEN, D. D., et al. Sharing and community curation of mass spectrometry data with Global Natural Products Social Molecular Networking. *Nature biotechnology*, v. 34, n. 8, 2016. DOI: 10.1038/nbt.3597

XIA, G.Y., CAO, S.J., CHEN, L.X., QIU, F. Natural withanolides, an update. *Natural Product Reports*, v. 39, n.4, p.784-813, 2022. DOI: 10.1039/D1NP00055A

ZHANG, X., BLASKOVICH, M.A., FORINASH, K.D., SEBTI, S.M. Withacnistin inhibits recruitment of STAT3 and STAT5 to growth factor and cytokine receptors and induces regression of breast tumours. *British journal of cancer*, v. 111, n.5, p. 894-902, 2014.

Chapter 1: *In silico* evaluation of pharmacokinetics properties of withanolides and simulation of their biological activities against Alzheimer's disease

[1]Luana L. Dutra, [1]Rafael J. Borges, [2]Vinícius G. Maltarollo, [1]Tiago A. O. Mendes, [1]Gustavo C. Bressan and [1]João Paulo V. Leite

[1]Department of Biochemistry and Molecular Biology, Universidade Federal de Viçosa, Minas Gerais Brazil.

[2]Pharmaceutical Products Department- Faculty of Pharmacy, Universidade Federal de Minas Gerais, Minas Gerais Brazil.

Contributing authors: luanalucasdutra@gmail.com; rafael.j.borges@ufv.br; maltarollo@ufmg.br; tiagomendes@gmail.com; gustavo.bressan@ufv.br; pvleite@ufv.br.

To link to this article: https://doi.org/10.1080/07391102.2023.2206909

Article history: received 26 August 2022, accepted 19 April 2023.

1.1 Abstract

The withanolides are naturally occurring steroidal lactones found mainly in plants of the Solanaceae family. The subtribe Withaninae includes species like *Withania sominifera*, which are a source of many bioactive withanolides. In this work, we selected and evaluated the ADMET-related properties of 91 withanolides found in species of the subtribe Withaninae computationally, to predict the relationship between their structures and their pharmacokinetic profiles. We also evaluated the interaction of these withanolides with known targets of Alzheimer's disease (AD) through molecular docking and molecular dynamics. Withanolides presented favorable pharmacokinetic properties, like high gastrointestinal absorption, lipophilicity (logP $\leq$ 5), good distribution and excretion parameters, and a favorable toxicity profile. The specie *Withania aristata* stood out as an interesting source of the promising withanolides classified as 5-ene with 16-ene or 17-ene. These withanolides presented a favourable pharmacokinetic profile and were also highlighted as the best candidates for inhibition of AD-related targets. Our results also suggest that withanolides are likely to act as cholinesterase inhibitors by interacting with the catalytic pocket in an energy favorable and stable way.

Keywords: Withanolide, Withaninae, ADMET, Molecular docking, Alzheimer's Disease

1.2 Introduction

The many traditional medicines are a rich source of knowledge that lead to important discoveries about the biological potential of several species of plants [1]. The natural steroids called withanolides are an important class of natural products found mainly in species of the Solanaceae family, such as the Indian ginseng *Withania somnifera*, a plant widely used in Traditional Indian Medicine Ayurveda [2].

The Solanaceae family is represented by approximately 100 genera and 2,500 species, occurring on all temperate and tropical continents. Within this family, the Physalideae tribe contains the greatest diversity at the generic level, with 29 genera and about 300 species arranged in three subtribes (Iochrominae, Physalidinae and Withaninae) [3, 4]

Withania is a genus belonging to Withaninae subtribe and is characterized by the presence of a large number of withanolides [5]. Others Withaninae species phylogenetically related and also sources of withanolides are grouped in the genera *Discopodium, Tubocapsicum, Depra,* and *Athenaea* [6–8]. *Cuatresia, Mellissia* and *Nothocestrum* also belong to the Withaninae subtribe but, so far, there is no report on the presence of withanolides [3, 4].

Those natural products are defined as polyoxygenated steroidal lactones with a C-28 skeleton [9]. Their triterpenoide backbone are biosynthesized by the mevalonic acid and the methylerythritol phosphate pathways, but the complete synthetic mechanism is unknown [2]. Based on the side-chain substituents on C17 they can be divided into two classes: type A, where C-26 and C-22 are oxidized to form δ- lactone, and type B, where the oxidation of C-26 and C-23 form a γ- lactone [9] (Figure 1).

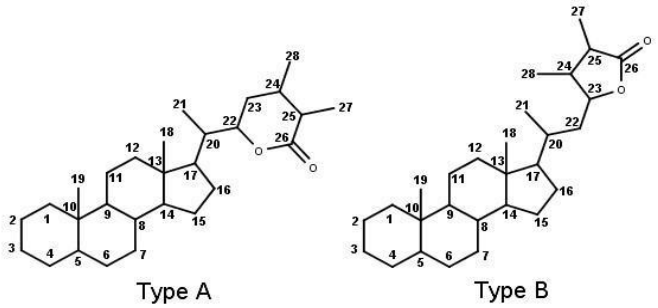

Fig. 1 Structure of withanolides type A and B.

The type A withanolides are the largest class and can be divided into two groups: group I, withanolides with an unmodified skeleton, is subdivided into four subgroups and represent approximately 75% of all type A withanolides. The withanolides with a modified skeleton belongs to group II that contains thirteen subgroups. Type B withanolides are more diverse class and are divided into four groups. Some withanolides do not conserve the type A or B

skeleton and are grouped as other types [8]. The withanolides found in plants of the subtribe Withaninae belong mainly to the Type A-class, but there are a few other types of withanolides recently isolated from *Withania aristata* and *Tubocapsicum anomalum* [8].

The withanolides have numerous promising biological activities, such as antitumor, insecticide, trypanocidal and leishmanicidal, antimicrobial, antiinflammatory, immunoregulatory, reconstruction of neuronal interactions, cholinesterase inhibition, and phytotoxic activity [2, 8, 9]. That large number of biological activities can be due to the high structure diversity among withanolides.

The interest in molecules able to act over more than one molecular target (multi-target drugs) has been growing in recent years. That is because these drugs hold the possibility of reduced dosage or length of treatment and also their mode of action is consistent with multifactorial pathologies like cancer, metabolic, cardiovascular, and neurological diseases [10, 11].

For the development of multi-target drugs the use of computational tools has been shown to be crucial. The construction of protein-protein interaction networks, molecular docking and modeling of potential targets are important methods that gives pieces of evidence about the mode of action, efficacy, and safety of new molecules with therapeutic potential [12].

Computational chemistry also has been able to predict pharmacokinetic properties related to absorption, distribution, metabolism, excretion and toxicity (ADMET). These properties are related to the failure of many drugs that seem promise in *in vitro* tests when are evaluated in clinical trials [11]. Due to the structural diversity among the withanolides, the understanding of how specific characteristics of the different subgroups affect their pharmacokinetic properties is important for the search for a new drug leads [13]. Thus, the conduction of *in silico* studies to assess the structure–activity relationship of small molecules by predicting physicochemical, pharmacokinetic and toxicity properties can be used as a virtual screening strategy to select desired structural features that will be tested experimentally. That kind of study is essential to guide future analyses and improve the process of drug development.

The diverse biological activities attributed to withanolides also makes these molecules promising precursors of new drugs for the treatment of multifactorial diseases like Alzheimer's disease (AD).

AD is a pathology associated with the accumulation of insoluble *β*amyloid clusters, hyperphosphorylation of the Tau protein present in the cytoskeleton, hyperactivation of cholinesterases and interference of inflammatory and oxidative pathways [14]. Plant extracts containing withanolides, as well as these purified compounds have the ability to inhibit the

enzymes acetylcholinesterase (AChE) and butyrylcholinesterase (BChE), modulate the β-amyloid metabolism, and also neuroprotective, anti-inflammatory and antioxidant activities [15–21], but there is still no application of withanoliderich extracts or even isolated compounds in clinical trials against AD.

Newman and Cragg define natural products as the best option for the discovery of new agents/active templates against different human diseases [22]. There are three major barriers to drug development against AD: the drug must enter the central nervous system by passing through the blood-brain barrier without being eliminated by efflux transporters like P-glycoproteins; there are many overlapping phenomena related to AD and the understanding of its basic pathology is still limited; the lack of tools for early identification of molecular changes when the degenerative damage are not at an irreversible stage [23]. Currently, there are only six chemical entities approved by the FDA against AD: one natural product (galanthamine), two synthetic molecules that mimic a natural product (donepezil and rivastigmine), one synthetic molecule (memantine), and one recently accelerated approved antibody (aducanumab) [22, 24].

Evidence suggests that withanolides are promising molecules against AD [15]. Molecular docking showed that withanolide S had favorable binding affinity with BACE-1 and interacted with key residues at the entrance of the catalytic gorge of AChE and formed hydrogen bonds and Van der Walls interactions with residues around its catalytic triad [15]. Withanolide A is also known as a neuritogenic agent, and its mechanism has an indirect effect on glucocorticoid receptor (GR) putative mediated through closely related pathways such ERK, Akt, NF-κB, TRα, or Hsp90 [25]. Withaferin A possesses inhibitory activities against AD biochemical markers by reducing Aβ and tau accumulation, regulating heat shock proteins, and inhibiting oxidative and inflammatory constituents [21].

In the present study we selected 91 withanolides reported from species of the Withaninae subtribe and evaluated their ADMET-related properties according to each subgroup, to correlate the different structures to their pharmacokinetic potential. Furthermore, we investigated the inhibitory potential of these molecules against multiple targets involved in AD through molecular docking.

1.3 Methodology

Identification of withanolides

We organized the revised structures of the withanolides according to the species of origin [8, 26], and selected 91 withanolide structures identified in plant species from the subtribe Withaninae. A total of 87 compounds were classified into 12 subgroups of type-A withanolides

and 4 as other type. Their names, groups, molecular formula, and specie of origin are listed in Table 1. Since the withanolide 87 is the only one classified as 5*β*,6*β*-epoxides with a 17(20)-ene (Table 1) we included it in the group L, along with the non-type A withanolides classified as other types, for the further analysis.

Table 1: Withanolides selected for ADMET and molecular docking studies.

ID	Name	Molecular Formula	Origin Species
	5*β*,6*β*-Epoxides with a 17*β*-side chain (group A)		
1	Withacnistine	C30H40O7	*Athenaea velutina*
2	Withanolide D	C28H38O6	*Withania somnifera*
3	Withacnistin-acetate	C32H42O8	*Athenaea velutina*
4	Aurelianolide A	C30H40O8	*Athenaea fasciculata*
5	28- Hydroxytubocapsanolide A	C28H36O7	*Tubocapsicum anomalum*
6	27-O-acetyl-withaferin A	C30H40O7	*Withania aristata*
7	5*β*,6*β*-Epoxy4*β*-hydroxy-27(1-formyloxy-1methylethoxy)-1-oxowitha-2,24-dienolide	C32H44O8	*Withania aristata*
8	27-O-acetylviscosalactone B	C30H42O8	*Withania aristata*
9	Tubocaapsanolide MAP	C29H40O7	*Tubocapsicum anomalum*
10	2,3-Dihydrotubocapsanolide A	C28H38O6	*Tubocapsicum anomalum*
11	3*β*-Ethoxy-2,3- Dihydrotubocapsanolide A	C30H42O7	*Tubocapsicum anomalum*
12	3*α*-(Uracil-1-yl)-2,3dihydrowithaferin A	C32H42N2O8	*Withania somnifera*
13	3*β*-(Uracil-1-yl)-2,3dihydrowithaferin A	C32H42N2O8	*Withania somnifera*
14	3*β*-(Adenin-9-yl)-2,3dihydrowithaferin A	C33H43N5O6	*Withania somnifera*
15	14*α*,15*α*Epoxywithaferin A	C28H36O7	*Withania somnifera*
16	Withaoxylactone	C28H38O8	*Withania somnifera*
	5-Enes with a 17*β*-side chain (group B)		

17	Withalutin	C30H40O6	*Athenaea velutina*
18	5,6-deoxywithaferin A	C28H38O5	*Withania somnifera*
19	Aurelianolide B	C30H40O7	*Athenaea fasciculata*
20	Obtusifonolide	C30H40O6	*Withania obtusifolia*
21	Withacoagulin D	C28H38O7	*Withania coagulans*
22	Withacoagulin G	C28H38O6	*Withania coagulans*
23	Withacoagulin H	C28H36O6	*Withania coagulans*
24	(22R)-4α,17α,27Trihydroxy-1-oxowitha-2,5,24-trienolide	C28H38O6	*Withania aristata*
25	Withacoagulide C	C28H38O6	*Withania coagulans*
26	Withasilolide A	C28H38O5	*Withania somnifera*
27	Withasilolide B	C28H40O5	*Withania somnifera*
28	5,6-De-epoxy-5-en7-one-17-hydroxy withaferin A	C28H36O7	*Withania somnifera*
29	Withacoagulin I	C28H38O7	*Withania coagulans*
30	Withacoagulide D	C28H38O6	*Withania coagulans*
31	27-Hydroxywithanolide K	C28H38O7	*Withania coagulans*
32	27-Hydroxywithanolide I	C28H38O5	*Withania coagulans*
33	Withacoagulin F	C28H38O4	*Withania coagulans*
34	Withanolide H	C28H38O6	*Withania coagulans*
35	Withacoagulin E	C28H38O5	*Withania coagulans*
36	2,3-Dihydro-3β,27dihydroxywithanolide I	C28H40O7	*Withania coagulans*
37	2,3-Dihydro3β-O-β-D-Glucopyranosylwithanolide I	C34H50O11	*Withania coagulans*
38	14-Epicoagulin O	C34H50O11	*Withania coagulans*
39	14-Epicoagulansin B	C28H42O6	*Withania coagulans*
40	Withacoagulin A	C28H36O5	*Withania coagulans*

41	Withanolide P	C28H38O5	*Withania somnifera*
42	Wadpressine	C40H60O16	*Withania adpressa*
43	(20R,22R)14*α*,17,20*β*,27Trihydroxy-1oxowitha-5,24dienolide-27-(O-*β*-Dglucopyranoside)	C34H50O13	*Withania coagulans*
44	Withanolide F	C28H38O6	*Withania coagulans*
45	27- Hydroxywithanolide F	C28H38O7	*Withania coagulans*
46	2,3-Dihydro-3*β*hydroxywithanolide F	C28H40O7	*Withania coagulans*
47	15*α*-Hydroxycoagulin L	C34H50O13	*Withania coagulans*
48	14*α*,15*α*,17*β*,20Tetrahydroxy-1oxowitha-2,5,24trienolide	C28H38O7	*Withania coagulans*
49	Withacoagulin C	C28H38O7	*Withania coagulans*
50	14*α*,15*α*-Epoxy17*β*,20-dihydroxy1-oxowitha-3,5,24trienolide	C28H36O6	*Withania coagulans*
	5-Enes with 16-ene or 17-ene groups (group C)		
51	(4S,20S,22R)-4,27Dihydroxy-1-oxowitha-2,5,16,24tetraenolide	C28H36O5	*Withania aristata*
52	(4S,20S,22R)-4Hydroxy-1-oxo-witha-2,5,16,24-tetraenolide	C28H36O4	*Withania aristata*
53	(20S,22R)-27Hydroxy-1,4-dioxowitha-2,5,16,24tetraenolide	C28H34O5	*Withania aristata*
54	(4S,22R)-4,16*β*,27Trihydroxy-1-oxowitha-2,5,17(20),24tetraenolide	C28H36O6	*Withania aristata*
55	(22R)-16*β*,27Dihydroxy-1-oxowitha-2,5,17(20),24tetraenolide	C28H36O5	*Withania aristata*
56	(22R)-16β,27-Dihydroxy-1,4-dioxowitha-2,5,17(20),24tetraenolide	C28H3406	*Withania aristata*
	6*α*,7*α*-Epoxides (group D)		
57	Withasilolide D	C28H38O7	*Withania somnifera*
58	Withasilolide C	C28H40O6	*Withania somnifera*
59	Withasilolide E	C28H36O7	*Withania somnifera*
60	Withasilolide F	C30H38O8	*Withania somnifera*
	Intermediate withanolides with a 17*β*-side chain (group E)		
61	Withacoagulinyl tetraglucoside	C30H41ClO7	*Withania coagulans*

62	27-Acetoxy-4β,6αdihydroxy-5β-chloro1-oxowitha-2,24dienolide	C30H41ClO7	*Withania somnifera*
63	6α-Chloro-5β,17αdihydroxywithaferin A	C28H39ClO7	*Withania somnifera*
64	3β,4β,5α,6β,27Pentahydroxy-1-oxowitha-24-enolide	C28H42O8	*Withania aristata*
65	Withasomniferolide A	C28H36O4	*Withania somnifera*
66	Withasomniferolide B	C28H36O4	*Withania somnifera*
	Intermediate withanolides with a 17α-side chain (group F)		
67	Physaperuvin G, withanolide S	$C_{28}H_{40}O_8$	*Withania coagulans*
68	Tubocapsanolide D	$C_{28}H_{40}O_7$	*Withania coagulans*
	Withaphysalins (group G)		
69	Withaphysalin V	C28H36O6	*Deprea bitteriana*
70	Withaphysalin W	C28H36O6	*Deprea bitteriana*
71	Withaphysalin X	C28H36O8	*Deprea cuyacensis*
	Epiacnistins (group H)		
72	4β-Hydroxyacnistin I	C28H38O7	*Tubocapsicum anomalum*
73	25-Epi-anomanolide A	C28H38O7	*Tubocapsicum anomalum*
74	4β-Hydroxyanomanolide E	C28H40O9	*Tubocapsicum anomalum*
75	2,3-Dihydroanomanolide A	C28H40O7	*Tubocapsicum anomalum*
76	3β-Methoxy-2,3dihydroanomanolide C	C29H42O9	*Tubocapsicum anomalum*
	Withajardins (group I)		
77	Withajardin J	C28H38O7	*Tubocapsicum anomalum*
78	Withajardin K	C28H36O6	*Tubocapsicum anomalum*
79	17-Epi-withajardin J	C28H38O7	*Tubocapsicum anomalum*
	14α,20α-Epoxides (group J)		
80	Withacoagulin J	$C_{28}H_{36}O_5$	*Withania coagulans*

81	Withacogulanoside-B	$C_{34}H_{48}O_{11}$	*Withania coagulans*
	13,17-seco Withanolides (group K)		
82	Physangulidine D	C28H36O7	*Deprea zamorae*
83	Physangulidine E	C28H36O7	*Deprea zamorae*
84	Physangulidine F	C28H36O8	*Deprea zamorae*
85	Physangulidine G	C28H36O10	*Deprea zamorae*
86	Physangulidine H	C28H36O9	*Deprea zamorae*
	5*β*,6*β*-epoxides with a 17(20)-ene and other types (group L)		
87	5*β*,6*β*-epoxy-4*β*,16*β*,27-trihydroxy-1-oxo-witha-2,17(20),24-trienolide	$C_{28}H_{36}O_7$	*Withania aristata*
88	4*β*-Formyl-6*β*,27dihydroxy-1-oxowitha-2,24-dienolide	C28H38O6	*Withania aristata*
89	4*β*-Formyl-6*β*,27dihydroxy-1-oxowitha-24-enolide	C28H40O6	*Withania aristata*
90	28-Hydroxytubocapsenolide A	C28H36O7	*Tubocapsicum anomalum*
91	3*β*-Ethoxy-2,3-dihydrotubocapsenolide A	C30H42O7	*Tubocapsicum anomalum*

Similarity with reported databases

We performed a principal component analysis (PCA) to characterize the dataset and compare it with other databases reported in the literature [27] using the space of physicochemical properties related to drug-likeness (logP, HBA, HBD, MW, PSA, Fsp3, rtB) and structural space (calculated using Morgan fingerprints). Calculations were performed using the KNIME analytical platform [28]. The withanolides selected in this work were compared with the following databases: NuBBE [29] from Brazil, BIOFACQUIM [30] from Mexico, ANPDB [31] from Africa, TCM [32] from China, and FDA-approved drugs [33]. PCA was performed with all compounds together and, for ease of visualization and comparison, withanolides were plotted separately with each database.

Prediction of ADMET-related properties

We submitted the structures in SMILES format to the web servers SwissADME [34], pkCSM [35], and ADMET Lab 2 [36] to analyze the properties related to ADMET and druglikeness. In this paper we discuss consensus properties predicted by at least two servers aiming to increase the confidence of predictions [37]. The raw data generated by the servers are in Supplementary Material (Tables S1-S14).

Molecular docking

To assess the activity against Alzheimer's Diseases we selected the central targets of the four main hypotheses that describe the underlying cause of AD progression [38]: amyloid hypothesis target BACE-1 (PDB 2qp8, [39]), cholinergic hypothesis targets AChE (PDB 1eve, [40]) and BChE (PDB 6esj, [41]), tau hypothesis targets CDK5 (PDB 4au8, [42]) and GSK-3B (PDB 6hk7, [43]), and oxidative stress hypothesis target MAO-B (PDB 2v5z, [44]). All the protein structures described are experimentally determined with a resolution range between 1.5 and 3.2 Å, in complex with inhibitor with no mutations.

We performed the molecular docking of each one of the five proteins described in previous paragraph with the 91 withanolide compounds of section 2.1. We used the software Gold 2021.3 using the defaul score function ChemPLP, that treats neutral and repulsive contacts with a piecewise linear potential (PLP) [45]. We selected the top-ranked poses of each complex and used their score values to evaluate the effect of withanolide structural diversity over the interaction with the targets. We used the docking score average of each group to assess discrimination, which can be employed to rationalize the choice of small molecules for experimental trials.

The 3D structure of each withanolide was generated by National Cancer Institute web service (cactus.nci.nih.gov/index) and the protonation states of the targets was defined at pH 7.4 [46]. The grid box was chosen based on the redocking of the experimental ligand of each PDB ID (RMSD $\leq$ 1.5Å) and was defined as the region 6 Å around the redocking ligand site, except for the targets 2qp8 (4Å) and 2v5z (7Å).

The docking results figures were generated with PyMOL (The PyMOL Molecular Graphics System, Version 1.8.4.0, Schr¨odinger, LLC., http://www.pymol.org/).

Molecular dynamics and binding affinity

The stability of the protein-withanolide complexes generated in the docking step was evaluated through molecular dynamics (MD). MD simulations were calculated with the software GROMACS (Groningen Machine for Chemical Simulation) 2020.4 [47] with

CHARMM36 force fields [48]. The input files were generated by CHARMM-GUI (http://www.charmm-gui.org) v3.7 [49]. Protein charged groups used were the correspondent of pH 7.0 calculated with PROPKA webserver [50]. The complexes were placed in a periodic rectangular box of 12.0 Å of edge distance with explicit water molecules neutralized by addition of counter ions (approximately 100 mM sodium and chloride ions) under constant temperature (310 K) and pressure (1.0 bar) held by coupling to an isotropic pressure and external heat bath [51, 52]. This was succeeded by minimization, equilibration, and production steps of 500 ns.

The generated trajectory was analyzed using root-mean-square deviations (RMSD) using the protein C-alpha (RMSD-protein) and all ligand atoms (RMSD-ligand) after protein C-alphas were superimposed. The conformational changes caused by the ligands were also evaluated through the root-mean-square fluctuation (RMSF) of the complex (protein-ligand) and unbound protein (native protein) and the differences in motion of the analysed complexes were determined using Principal component analysis (PCA). We also calculated the number of hydrogen bonds formed between the protein and the ligand throughout the simulation (H-bond), the solvent accessible surface areas of the protein (SASA) and Radius of Gyration (RG) of each complex and native protein.

The binding affinity was estimated using the Molecular Mechanics/Poisson–Boltzmann surface area (MM-PBSA) [53]. A total of 100 snapshots were chosen from the end of molecular dynamics trajectory and the ΔG_{bind} value can be described as:

$$(1)\ \Delta G_{Total} = \Delta G_{Binding\ (complex)} - (\Delta G_{Binding\ (protein)} + \Delta G_{Binding\ (ligand)})$$

The energy values (ΔG_{Biding}) prediction are based in two componentes: the enthalpy changes upon the complex formation (summation of the van der Waals and the electrostatic interaction energies) and the solvation free energy contribution (summation of the polar and nonpolar componentes).

All the analyses mentioned above were performed with GROMACS utilities (gmx rms; gmx rmsf; gmx covar and anaeig; gmx hbond; gmx sasa; gmx gyrate; gmx mmpbsa) and visualizations were plot with Gnuplot (http://www.gnuplot.info/).

Statistics and visualization

The distribution of predicted ADMET-related properties and molecular docking results were analysed by One-way ANOVA followed by Tukey's multiple comparisons tests (p-value ≤ 0.05). The molecular docking scores are listed in the Table S20 and the interaction with the targets surfaces were visualized with software PyMol.

1.4 Results and discussion

Withanolides from subtribe Withaninae

The selected withanolides were identified from eleven species of the Withaninae subtribe: *Athenaea fasciculata, Athenaea velutina, Deprea bitteriana, Deprea cuyacensis, Deprea zamorae, Tubocapsicum anomalum, Withania adpressa, Withania aristata, Withania coagulans, Withania obtusifolia,* and *Withania somnifera*. Withanolides from the groups 5*β*,6*β*-epoxides with a 17*β*-side chain (group A) and 5-enes with a 17*β*-side chain (group B) showed more significant diversity concerning the species of origin, while the other groups of withanolides were isolated from one to three species (Figure 2). Among the subtribe Withaninae, the genus *Withania* has the largest number of species with identified withanolides (species 8-11), having found molecules of all groups, except withaphysalins. Withaphysains were isolated from *Deprea* spp. Withanolides from the epiacnistins and withajardins groups were initially isolated from *Tubocapsicum anomalum*. That latter species has become an important source of structurally diverse withanolides with promising anti-cancer activity [55, 56].

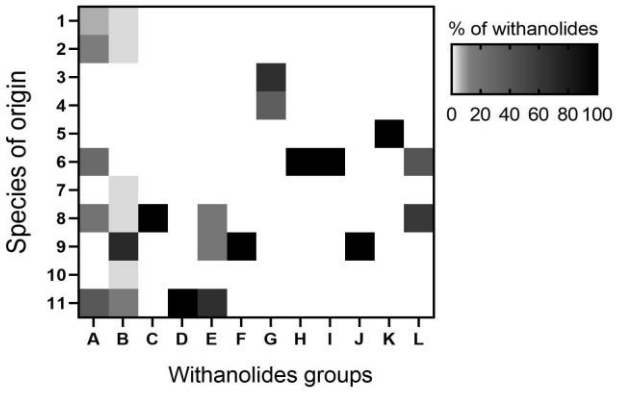

Fig. 2 Heatmap of Withaninae species and groups of withanolides evaluated. There were eleven species of plants: **1:** *Athenaea fasciculata*, **2:** *Athenaea velutina*, **3:** *Deprea bitteriana*, **4:** *Deprea cuyacensis*, **5:** *Deprea zamorae*, **6:** *Tubocapsicum anomalum*, **7:** *Withania adpressa*, **8:** *Withania aristata*, **9:** *Withania coagulans*, **10:** *Withania obtusifolia* and **11:** *Withania somnifera*. Twelve structural groups of withanolides were evaluated: **A:** 5*β*,6*β*epoxides with a 17*β*-side chain, **B:** 5-enes with a 17*β*-side chain, **C:** 5-enes with 16-ene or 17-ene groups, **D:** 6*α*,7*α*-epoxides, **E:** Intermediate withanolides with a 17*β*-side chain, **F:** Intermediate withanolides with a 17*α*-side chain, **G:** Withaphysalins, **H:** Epiacnistins, **I:** Withajardins, **J:** 14*α*,20*α*-epoxides, **K:** 13,17-seco Withanolides, and **L:** 5*β*,6*β*-epoxides with a 17(20)-ene group and Other types.

Similarity with reported databases

The comparison of the canonical SMILES indicated that the withanolides are structurally unique in all the databases studied. This indicates that its general structure is unique as a class of compounds, they can be considered little explored and with potential for innovation (patent

filing, for example). Furthermore, it is possible to notice that the withanolides are located in spatial regions similar to all the databases compared (NuBBE, BIOFAQUIM, ANPDB, TCM, and FDA-approved drugs) both in the structural space and in the physicalchemical space. Therefore, it is possible to affirm that, although withanolides are substances with unique structures, they are very similar to natural products from different sources and locations, both concerning their structure and physicochemical properties, presenting an enormous potential to be used as pharmaceuticals (Figure 3).

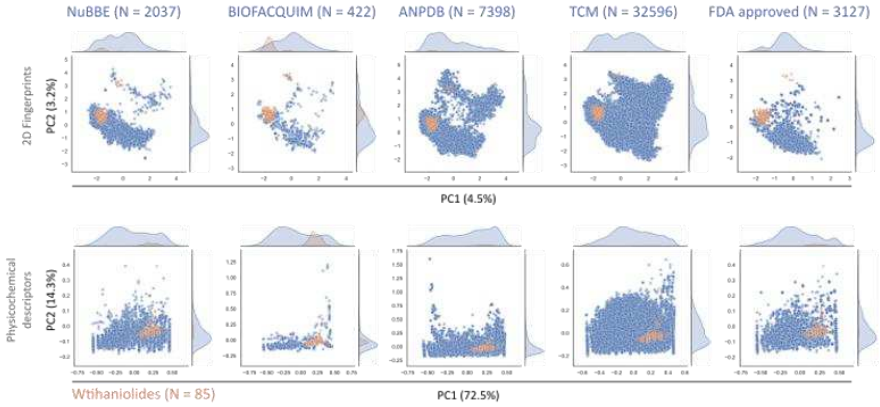

Fig. 3 Comparison between the set of withanolides and different databases reported in the literature.

ADME-related properties

To assess how the structural diversity of withanolides may affect their pharmacokinetic potential, we predicted the ADMET-related properties of 89 withanolides. The withanolides wadpressine (42) and withacoagulinyl tetraglucoside (61) were excluded from this analysis because of their large SMILES structure (over 200 characters).

The ”Lipinski’s rules” is one of the most used parameters to assess whether a given molecule has favorable pharmacological properties and good oral bioavailability. An efficient and safe drug does not necessarily need to satisfy all the five rules, but this parameter is valuable regarding the bioavailability profile of small molecules, especially in the early stages of screening for new drugs. [34, 57].

In general, the withanolides have favorable pharmacological properties according to Lipinski’s rule, since 60.8% have no violation and 30.3% have 1. Group B (5-enes with a 17β-side chain) is the largest one (34 structures) and was the only group to present 3 violations of Lipinski’s rule. Among these, the withanolides 37, 38, 43, and 47 have molecular weight higher than 500 g/mol, total Nitrogen or Oxigen higher than 10, and the number of -NH or OH groups higher than 5, which results in molecules with a high polarity that are difficult to absorb. Only 7.9% of the withanolides have 2 or 3 violations.

Violations of Lipinski's rule are not an impediment to the use of a natural product as a drug precursor or even as the final drug [58]. The rule that proved to be fundamental regarding natural products was lipophilicity (log P). There are FDA-approved natural products, such as Taxol (Paclitaxel), Avermectin B1a (Ivermectin), and Daptomycin, that violate up to 4 rules but maintain logP value ≤ 5. This indicates that Lipinski's rule is still a valid selection filter if one is working with large library of molecules, but it should be applied with precaution and jointly with other ADMET parameters when it comes to natural products [57, 58].

The SwissADME server provides four druglikeness filters besides Lipinski (Ghose, Veber, Egan, Muegge). Each filter evaluate a set of parameters that are likely to be correlated with good oral drug-candidates. The consensus of those parameters among the five SwissADME druglikeness filter are presented in Table 2, along with the distribution of withanolides that violated them. Group C seems to be the most promising regarding drug-likeness properties since presented only one member that violated the consensus lipophilicity threshold (withanolide 52) along with just 8.8% of the total withanolides. Approximately 80% of the withanolides exceeded the number of atoms considered favorable to oral bioavailability but there was no violation of the minimum carbon and heteroatoms content and maximum number of rotatable bonds, suggesting that withanolides posses a large backbone but with limited flexibility.

Table 2 Distribution of withanolides that violate the consensus drug-like parameters of the SwissADME drug-likeness filters.

Consensus Drug-like parameters	% withanolides (all)	% withanolides (by group)
Molecular weight (200 ≤ MW ≤480)	34.1	A (87.5), B (50.0)
LOG P (-0.4 ≤ LOGP ≤ 4.15)	8.8	A (18.8), B (5.9), C (16.7), E(16.7), F(50.0),
TPSA (TPSA ≤ 131.6)	15.4	A (18.8), B (11.8), E (16.7), F (50.0), H (20.0), I (33.3), K (40.0), L (20.0)
Num. of rings (R ≤ 7)	3.3	A (6.3), K (20.0), L (20.0)
Num. H-bond acceptors (H-ACC ≤ 10)	5.5	B (11.8), K (20.0)
Num. H-bond donors (H-DON ≤ 5)	5.5	B (11.8), H (20.0)
Num. of atoms (20 ≤ A ≤ 70)	80.2	A (100), B (88.2), D (100), E (50.0), F (50.0), G (33.3), H (100), I (66.7), J (50.0), K (100), L (100)
Molar Refractivity (40 ≤ MR ≤ 130)	40.7	A (75.0), B (44.1), E (66.7), F (50.0), G (33.3), H (20,0), I (33.3), K (20.0), L (20.0)
Num. of heteroatoms (HA >1)	0	-

Num. of carbons (C ≥ 4)	0	-
Num. of rotatable bonds (RB ≤ 10)	0	-

A: 5*β*,6*β*-epoxides with a 17*β*-side chain, **B:** 5-enes with a 17*β*-side chain, **C:** 5-enes with 16-ene or 17-ene groups, **D:** 6*α*,7*α*-epoxides, **E:** Intermediate withanolides with a 17*β*-side chain, **F:** Intermediate withanolides with a 17*α*-side chain, **G:** Withaphysalins, **H:** Epiacnistins, **I:** Withajardins, **J:** 14*α*,20*α*-epoxides, **K:** 13,17-seco Withanolides, and **L:** 5*β*,6*β*-epoxides with a 17(20)-ene group and Other types.

Oral bioavailability is primarily driven by gastrointestinal absorption (GI), a ADMET parameter that rely on two physicochemical properties: lipophilicity (log P) and polar surface area (TPSA) [59]. Most of the withanolides were predicted to have high GI absorption (Figure 4) and there were no statistically significant difference between the groups. The Caco-2 cell permeability prediction model also did not show statistically significant difference between the groups, and among the total withanolides 25,5% presented high permeability and 56.6% moderated permeability (Table S3). These results are consistent with other *in silico* and *in vitro* published data about withanolides GI absorption [60–62].

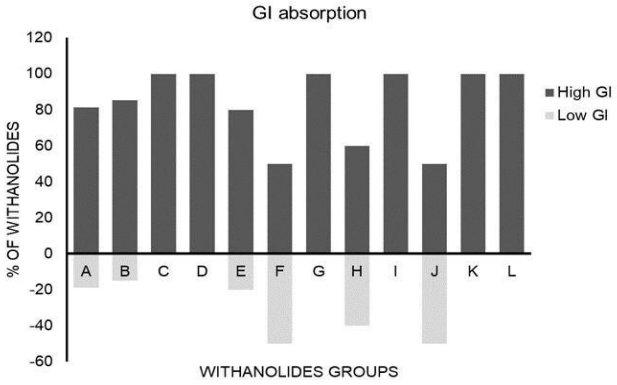

Fig. 4 Gastrointestinal absorption (GI) of withanolides from each group. The pkCSM GI absorption values were converted to high GI (if higher than 30%) and low GI (if lower than 30%). The bars indicate the percentage of withanolides in the groups that have High GI predicted by both servers (above the x axis) and Low GI (below the x axis). **A:** 5*β*,6*β*epoxides with a 17*β*-side chain, **B:** 5-enes with a 17*β*-side chain, **C:** 5-enes with 16-ene or 17-ene groups, **D:** 6*α*,7*α*-epoxides, **E:** Intermediate withanolides with a 17*β*-side chain, **F:** Intermediate withanolides with a 17*α*-side chain, **G:** Withaphysalins, **H:** Epiacnistins, **I:** Withajardins, **J:** 14*α*,20*α*-epoxides, **K:** 13,17-seco Withanolides, and **L:** 5*β*,6*β*-epoxides with a 17(20)-ene group and Other types.

The water solubility differs among the withanolides groups, being the groups F, G, H, I, and K totally above the global mean -4.32 (Figure 5-I). The water solubility of group K was significantly higher than groups A and E (p value ≤ 0.05, Table 3) suggesting that the unusual carbon scaffold of the group K (13,17-seco withanolides), characterized by the typical arrangement of withajardins (group I) with the ketal functionality at the C-17 position [8], may be improving the water solubility of those withanolides. Overall the withanolides present moderated-low water solubility (Table S1) and the group B had the most heterogeneous values

of logS ranging between -5.57 to -2.15. The water solubility has also influence on the rout of administration to be chosen, where a water-soluble drug is better absorbed by enteral administration. In case of withanolides, it seems that the transdermal drug delivery system is an alternative to the moderate-low water solubility, since all the groups presented high skin permeability (log KP ≤ -2.5) (Figure 5-II) [35]. The withanolides from group K were isolated from *Deprea zamorae* and the studies regarding their biological activities are scarce [63]. Our results suggest that this group of withanolides, also found in *Physalis angulata*, has an interesting pharmacological potential.

Beside the GI absorption, it is also crucial to know if a given molecule is capable of crossing the blood-brain barrier (BBB permeability). Only a few withanolides were predicted to have that capacity (withanolide 8, 9, 18, 28, 33, 52, 60, and 89) according to at leats two predictors. Those withanolides belong to groups A (8, 9), B (18, 28, 33), C (52), D (60), and L (89) and were isolated from *T. anomalum* and *withania* species. Another way to measured the blood-brain permeability is through the CNS permeability parameter, that is a more direct measurement because it lacks the systemic distribution effects. That parameter states that a given molecule is able to penetrate the CNS if log PS ≥ -2, and the molecule is unable to penetrate the CNS if log PS ≤ -3 [35]. All the groups of withanolides presented similar CNS permeability prediction evaluated by only one predictor (Table S4) and the compounds 18, 26, 27, 40 (group B), 51, 52, 53, 55 (group C), 61, 65, and 66 (group E) were predicted as capable of penetrating the CSN (log PS ≥ -2). That suggests that this withanolides may be promising against nervous system-related diseases. In fact the withanolides 65 and 66 (withasomniferolide A and B) shown the ability to modulate the $GABA_A$ receptor function [64], and also the withanolide CR-777, a withaferin A conjugated at C-6 with glutathione derivative, has protective effect against a large panel of neuronal stressors [8].

The volume of distribution at steady state (VDss) is an essential pharmacokinetic parameter that measures the relative affinity of a drug for tissues and plasma. A high VDss value (above 2.81 L/kg) means that the drug is extensively taken up by tissues, whereas a low VDss value (below 0.71 L/kg) indicates that the drug binds extensively to plasma proteins. The VDss parameter is important for developing dose measurement plans, calculating the mean residence time (MRT) and half-life (t½) of a drug. VDss is affected by the pKa of the drug, whereas acidic drugs have low, neutrals and zwitterions have moderate, and basic drugs have high VDss values [35, 65]. Most of the withanolides presented a low-moderate VDss value (Figure 5-III), except the group E, that had high variability and its mean was significantly lower than groups B, G, and K (Table 3).

The fraction of unbound drug concentration (Fu) represents the concentration of drugs capable of interacting with pharmacological targets since the degree to which a given drug binds to serum proteins affects how efficiently it can transverse cellular membranes or diffuse. The value of Fu affects the volume of distribution (VDss) and the total clearance (CLtot) of a drug. The total clearance is the volume of blood from which all drug is removed per minute, considering both renal and hepatic clearance. Those parameters foreshadow how a given drug is distributed and removed from the body, which can reflect both its efficacy and toxicity. The Fu values of withanolide from all groups were slightly different from each other (Table 3) and ranged between 0.015-0.362 (Figure 5-IV). That difference were increased with the clearance values (Figure 5-V), where group C was higher than B, E, and H (Table 3).

Most of the withanolides were identified as substrates and inhibitors of the efflux transporter P-gp by at least two predictors. According to the predictors ADMET LAb 2 and pkCSM only the compounds 6, 7 (group B), 66, and 86 (group E) are not likely to be eliminated by this efflux transporter, and the withanolides 14 (group A), 16, 42, 43, 46 (group B), 67 (group F), 74, 76 (group H), and 81 (group J) were predicted as non-inhibitors of them.

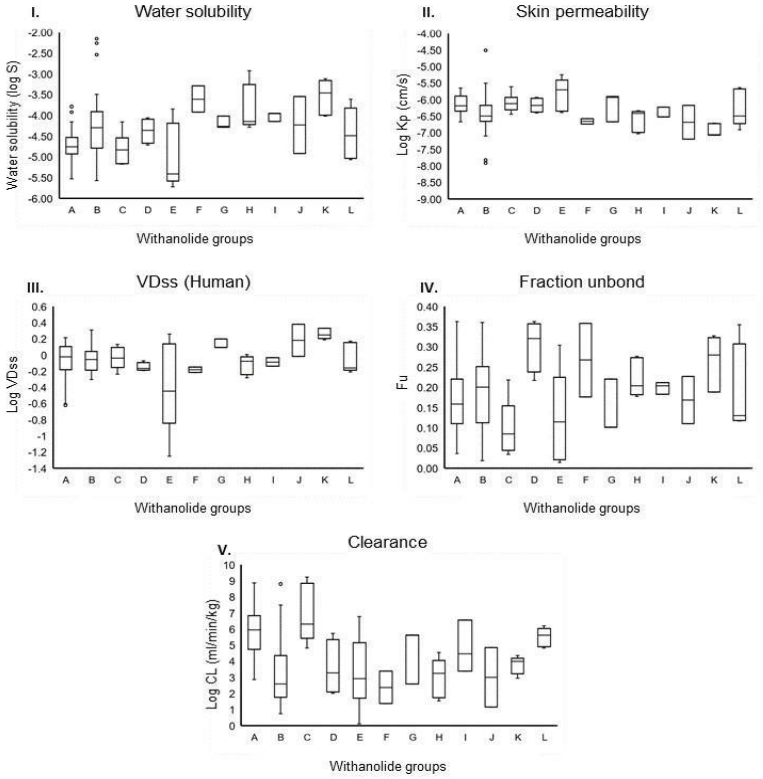

Fig. 5 Box and whisker plots of ADME-related properties of each group of withanolides. I: Water solubility, given as the mean between SwissADME and pkCSM logarithm of molar concentration (log mol/L). II: Skin permeability, given as the mean between SwissADME and pkCSM logarithm of Kp (cm/s), is considered to be low if the log Kp ≥ -2.5. III: Steady state volume of distribution (VDss) is given as the mean between ADMET Lab 2 and pkCSM logarithm of the volume of a drug per kg (log VDss) and is considered low if below 0.71 L/kg

(log VDss ≤ -0.15) and high if above 2.18 L/kg (log VDss ≥ 0.45). IV: Fraction unbond (Fu) is given as the mean between ADMET Lab 2 and pkCSM of the fraction unbound in plasms. Drugs less bonded to serum proteins are more likely to transverse cellular membranes and be more efficient. V: Clearance (CL) is given as the mean between ADMET Lab 2 and pkCSM of the logarithm of the CL penetration (log ml/min/kg). **A:** 5*β*,6*β*-epoxides with a 17*β*-side chain, **B:** 5-enes with a 17*β*-side chain, **C:** 5-enes with 16-ene or 17-ene groups, **D:** 6*α*,7*α*epoxides, **E:** Intermediate withanolides with a 17*β*-side chain, **F:** Intermediate withanolides with a 17*α*-side chain, **G:** Withaphysalins, **H:** Epiacnistins, **I:** Withajardins, **J:** 14*α*,20*α*epoxides, **K:** 13,17-seco Withanolides, and **L:** 5*β*,6*β*-epoxides with a 17(20)-ene group and Other types.

Table 3 Results of one-way ANOVA followed by Tukey's multiple comparisons test among the withanolides groups means of each ADME-related properties.

ADME-related proertie ANOVA summary					
	Water solubility	Skin permeability	VDss	Fraction unbond	Clearance
F	2.55	1.89	3.07	2.11	4.69
P value	0.01	0.053	0.0021	0.029	<0.0001
P value summary	*	-	**	*	****
Significant diff. among means (P <0.05)?	Yes	No	Yes	Yes	Yes
Tukey's multiple comparisons test summary	*(AK, EK)	-	*(BE, EG), **(EK)	*(CD)	*(CE, CH), **(AB, BC)

A: 5*β*,6*β*-epoxides with a 17*β*-side chain, **B:** 5-enes with a 17*β*-side chain, **C:** 5-enes with 16-ene or 17-ene groups, **D:** 6*α*,7*α*-epoxides, **E:** Intermediate withanolides with a 17*β*-side chain, **F:** Intermediate withanolides with a 17*α*-side chain, **G:** Withaphysalins, **H:** Epiacnistins, **I:** Withajardins, **J:** 14*α*,20*α*-epoxides, **K:** 13,17-seco Withanolides, and **L:** 5*β*,6*β*-epoxides with a 17(20)-ene group and Other types.

The cytochrome P450 is an important detoxification enzyme found in the liver. Most of the withanolides were predicted as substrate and non-inhibitors of the isoform CYP3A4, except the withanolide 32, the only cytochrome P450 inhibitor identified by SwissADME and pkCSM (Table S5 and S11).

Regarding toxicity, the consensus properties between ADMET Lab 2 and pkCSM were promising (Tables S7, S18, and S19). AMES toxicity, also know as Ames test, is based on the *Salmonella*/mammalian-microsome mutagenicity. That procedure was developed by Bruce Ames and consist in evaluate genetic damage produced by a given molecule [66]. No withanolide was classified as potentially mutagenic. Another essential toxicity parameter to be evaluated is the inhibition of hERG channels. That feature has resulted in the removal of many substances from the pharmaceutical market because it is the principal cause of the development of acquired long QT syndrome (increase of the indirect measurement of ventricular refractory period) that leads to fatal ventricular arrhythmia. No withanolide was predicted as hERG inhibitor and 68% of the evaluated molecules were described as unlikely inhibitors by both predictors. Skin sensitization was another positive toxicity parameter since no withanolides was classified as sensitizer and 53% of the evaluated molecules was classified as unlikely to be skin

sensitizer. Only three withanolides were predicted to be hepatotoxic (withanolides 12, 13, and 14).

These results suggest that withanolides have favorable pharmacokinetics properties and promising toxicity profile that can guide further works based on their structural relationship with ADMET properties.

Molecular docking with AD-related targets

The multi-targeted action of withanolides also makes these molecules promising precursors of new drugs for the treatment of AD. From the first description of the disease made by the psychiatrist and neuropathologist Alois Alzheimer in 1906 to the present day, different hypotheses have emerged that aim to explain the causes of AD.

The cholinergic hypothesis, the most applied one nowadays to the development of treatments, proposes that AD is caused by reduced acetylcholine biosynthesis. Thus, both acetylcholinesterase (AChE) and butyrylcholinesterase (BChE) are the main targets for the selection of inhibitors, aiming to decrease the degradation of this neurotransmitter [38, 67]. AChE (PDB ID: 1eve) and BChE (PDB ID: 6esj) are serine hydrolases responsible for the termination of impulse signaling at cholinergic synapses [19].

The cholinesterases had the best score values with withanolides (Figure 6). No differences among the groups were observed with AChE and with BChE the groups F, G, I, and K had significant lower scores than groups A, B, C, and E (Table 4). A few withanolides had scores above the original ligand of the cholinesterases. The withanolide 81 (group J) was the first and third best ligand to AChE and BChE, respectively. The steroidal backbone was responsible for the hydrophobic interaction with the deep active site of the cholinesterases and the hydrogen bonds formed between the glucose group and the residues at the bottom of the catalytic gorge (Figure 7), including the BChE catalytic residue His 438, suggest that glucose-withanolides may be promising inhibitors candidates through the use of polar drug delivery systems, like lipossomal particles.

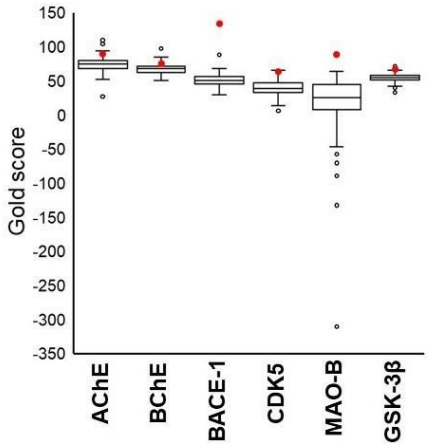

Fig. 6 Box and whisker plot of Gold score of the withanolides with AD-related targets.The whiskers represent the minimum and maximum values of score and the red dots are the redocking score value of the ligands extracted from the original PDB.

Table 4 Results of one-way ANOVA followed by Tukey's multiple comparisons test among the docking score means of each withanolides groups for the AD-related target

ANOVA summary of docking score among AD-related targets						
	AChE	BChE	BACE-1	CDK5	MAO-B	GSK-3β
F	2.28	5.90	2.36	2.34	2.15	6.66
P value	0.0176	<0.0001	0.014	0.015	0.025	<0.0001
Significant diff. among means (P <0.05)?	Yes	Yes	Yes	Yes	Yes	Yes
Tukey's multiple compaission test summary	-	*(AH, AI, BF, BH, CI, CK, EF, EH), **(AK, BI, BK, EI, EK)	-	*(CH, CI)	*(BK), **(CK)	**(AK, BK, CK, DK, EH, EK, GK, IK, JK, KL)

A: 5β,6β-epoxides with a 17β-side chain, **B:** 5-enes with a 17β-side chain, **C:** 5-enes with 16-ene or 17-ene groups, **D:** 6α,7α-epoxides, **E:** Intermediate withanolides with a 17β-side chain, **F:** Intermediate withanolides with a 17α-side chain, **G:** Withaphysalins, **H:** Epiacnistins, **I:** Withajardins, **J:** 14α,20α-epoxides, **K:** 13,17-seco Withanolides, and **L:** 5β,6β-epoxides with a 17(20)-ene group and Other types.

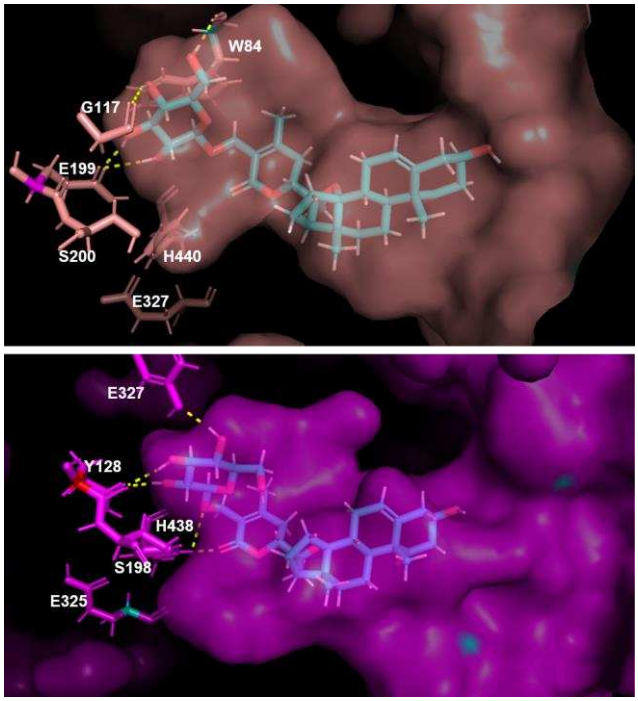

Fig. 7 Molecular docking of the cholinesterases AChE (1eve) and BChE (6esj) with the hit withanolides 81 (cyan). The proteins are represented as surface and colored by the secondary structure (AChE: cyan-helix, magenta-sheet, pink-loop; BChE: cyan-helix, pinksheet, magenta-loop). The catalytic residues and the ones that formed polar interactions with the ligand are represented as sticks and labeled. The ligand is represented as sticks (cyan-carbon, red-oxygen, white-hydrogen) and the hydrogen bonds are represented as dashed lines.

Two other very influential hypotheses are based on the main markers of AD, amyloid plaques and fibrillar tangles of Tau protein. The amyloid hypothesis presents as a critical target the β-secretase (BACE-1, PDB ID: 2qp8), responsible for the cleavage of the amyloid precursor protein (APP) and formation of insoluble β-amyloid (βA) aggregates [38]. There was no difference among the groups with the BACE-1 target (Table 4) and the score values of the withanolides were lower than the original ligand but above zero, suggesting that the interaction with that target is also favorable.

The tau hypothesis suggests that hyperphosphorylation of the protein Tau leads to the disintegration of the cytoskeleton and formation of fibrillary tangles, with glycogen synthase 3β (GSK-3β, PDB ID: 6hk7) and cyclindependent 5 (CDK5, PDB ID: 4au8) kinases being important targets that act in that process [38]. With the kinase CDK5 the groups H and I had the lowest score values but the original ligand was similar to the withanolides. The GSK-3β had less variation among the withanolides score values than the other targets and the withanolides 61 and 65 were better than its original ligand.

Among the AD-related target evaluated, only the monoamine oxidase B (MAO-B, PDB ID: 2v5z) presented negative score values (Figure 6). The groups J and K were significantly worst than most of the other groups (Table 4) and the original ligand had a score far above the

withanolides score values. There is a hypothesis that suggests that increased oxidative stress would be responsible for leading to neuronal death and the formation of AD molecular markers, with monoamine oxidase (MAO-B) being the enzyme responsible for the production of ROS that causes cell damage [38]. In relation to the other enzymes, our results suggest that MAO-B is not a potential target for withanolides.

The structural differences among the withanolide groups had no effect on the docking results of AChE and BACE-1 (Table 4). For the other targets, the significant differences among the mean docking scores of the groups can be visualized in Figure 8. The group C had one of the highest score value average among all AD-related targets, followed by groups E and J (Figure 8). These withanolides all share an insaturation on ring A, but their steroidal backbone is overall different. Group C also stood out as promising regarding its ADMET-related properties, which make these withanolides strong candidates for multi-target drugs against Alzheimer‘s disease. The withanolide 53 (group C) were chosen as ligand for the molecular dynamics simulations with the most promissing targets AChE, BChE, and GSK-3*β*.

Fig. 8 Heatmap representing the mean of the docking score values of each withanolide group and the corresponding AD-related target.

Molecular dynamics and binding affinity

The aim of the study was to filter the library of ligands to identify the most promising chemical structures for the biological activity in question. We therefore followed molecular dynamics with only the three most promising targets indicated by the docking result. The cholinesterases AChE and BChE and the kinase GSK-3B were the targets that had the mean docking score values closer to the score value of the experimental ligand (Figure 6). To confirm complex stability, we performed MD simulations with the three enzymes complexed with the withanolide 53 (group C). The proteins remained stable during the simulations as shown by a RMSD below 3.5 Å (Figure 9). The RMSD of complex and native structures from MD calculations had similar RMSD (Figure 9).

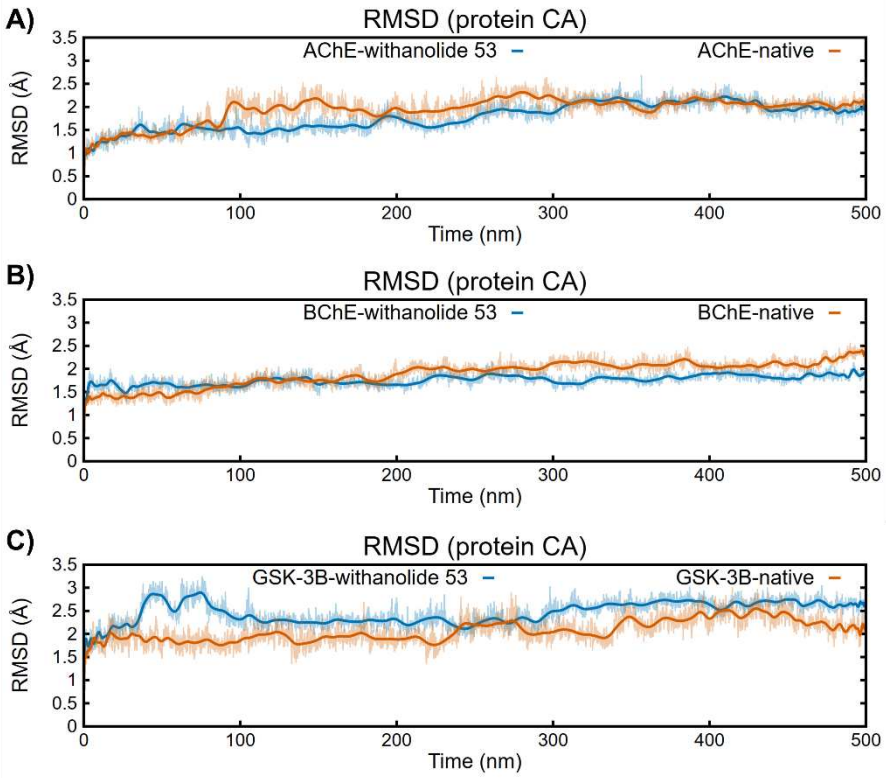

Fig. 9 RMSD of the protein C-alpha during a Molecular dynamics (MD) simulations of 500 ns.

Comparing the local variation between C-alpha of AChE-withanolide 53 complex and the native protein, the groups of TRP58-ASN98 (atoms 900-1500) and LYS325-LEU391 (atoms 5000-6000) showed highest variation in RMSF (Figure 10-A and B). These regions contain TPR84, component of the anionic site responsible for guiding the substrate, and GLU327, which together with SER200 and HIS440 makes up the catalytic triad [15]. This indicates that the interaction with the withanolide 53 resulted in changes in the conformation of the catalytic gorge compared to the native structure without changing the overall structure of the target. This global stability can also be observed with the low variation of RG and SASA (Figure S3, S4). BChE cholinesterase showed the smallest RMS fluctuation between the complex and the native protein, but for both cholinesterases the largest conformational fluctuation occurred in the N- and C-terminal regions (Figure 10-A and B). The cholinesterases BChE show maximum eigenvalues along PC1 and PC3 in the range of −4.0 to 3.0 nm and −1.5 to 3.5 nm, which means that their binding to withanolide 53 is more stable as compared to AChE-withanolide 53 complex (Figure 11).

The GSK-3B kinase complexed with the vitanolide 53 showed a higher RMSD compared to the native structure (Figure 9-C). This structural modification was concentrated around atoms 250-600, 2500-3100 and 3600-4300 (Figure 10-C), corresponding to residues GLN52-CYS76,

ASN186-ARG223, and PHE257-TRP301. Despite the stability of the protein being maintained throughout the simulation, the interaction with the withanolide 53 was not maintained and the ligand left the active site after 200 ns (Figure 12). However, withanolide 53 remained within the catalytic gorge of cholinesterases, indicating that these correspond to more promising targets among those studied in this work.

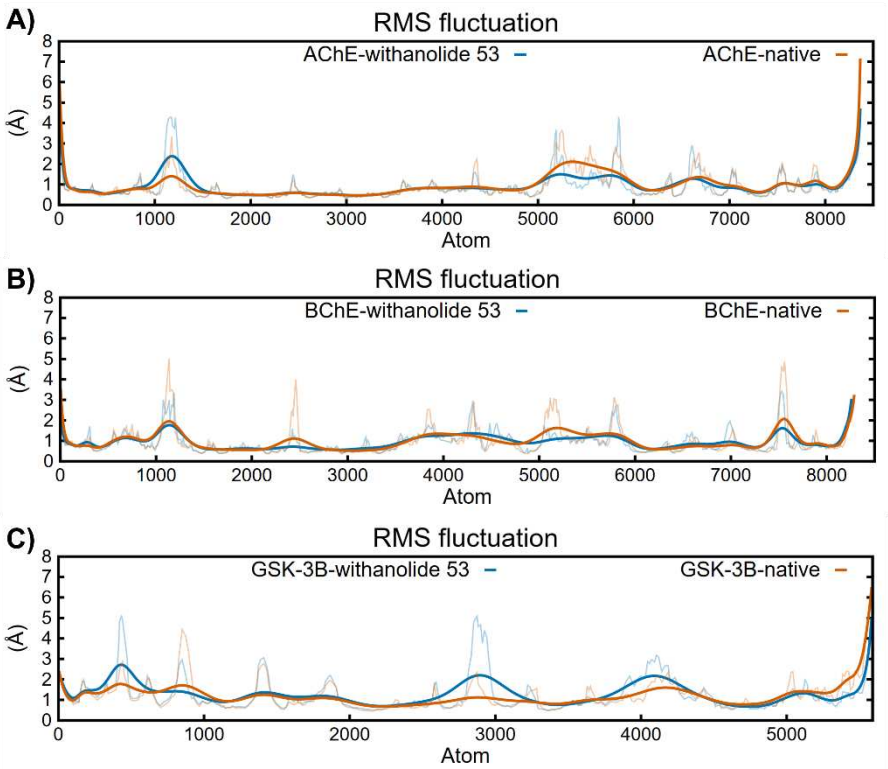

Fig. 10 1 RMSF of the protein backbone during a Molecular dynamics (MD) simulations of 500 ns.

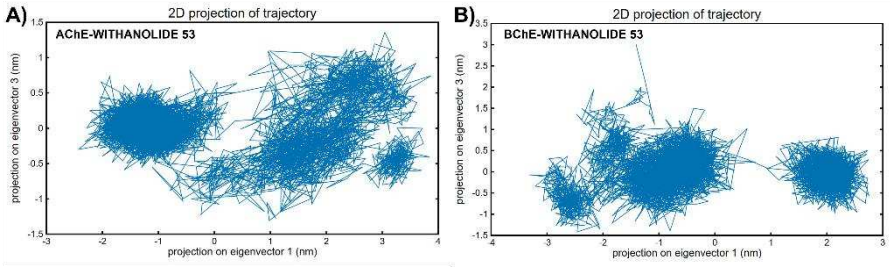

Fig. 11 2D projection of trajectory of A) AChE-withanolide 53 and B) BChE-withanolide 53.

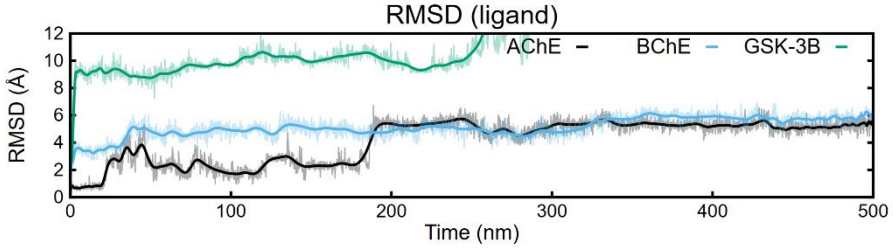

Fig. 12 RMSD of the ligands after the protein C-alpha are superimposed during a Molecular dynamics (MD) simulations of 500 ns.

Post MD-simulation analysis with AChE and BChE were also performed to understand the binding affinity of withanolide 53 against the cholinesterases during MD trajectory. Withanolide 53 showed 2 hydrogen bonds with both cholinesterases with residues TYR121 and HSE440 from AChE, and ASP70 and THR20 from BChE that maintained in most of MD simulations. Although, higher number of van der Walls and hydrophobic interaction were seen for the complex (Figure 13). The binding affinity between withanolide 53 and the targets, measured by MM-PBSA, was favorable and similar for both cholinesterases (Table 5). The energetic component that exerted the greatest influence on the total energy was the van der Waals interaction, especially with the residues that make up the catalytic triad and the anionic sub-site (Figure 13). The variation in electrostatic energy had a significant effect on binding but was not the primary component due to the absence of charged groups in the ligand structure. This mode of interaction and binding energy value are consistent with the acetylcholinesterase inhibition prediction model proposed by Borioni et al [69], which establishes the relationship between the predicted $\Delta G_{binding}$ value by MM-PBSA (E) and the IC_{50} value of the compound (Equation 2).

$$(2)\ E = 7.19\ (\pm 0.87)\ log\ log\ (IC50) - 52.23\ (\pm 1.04)$$

Withanolide 53 presented a predicted IC_{50} value of 1.99 μM (±3.47), suggesting its great potential as an inhibitor of this enzyme.

Table 5 Binding energy decomposition per target with withanolide 53, obtained with MM-PBSA method.

Delta Energy Componentes (Complex - Receptor - Ligand) (kcal/mol)	AChE	BChE
Van der Walls	-41.85 ± 3.14	-50.9 ± 2.39
Eletrostatic	-15.81 ± 8.03	-19.27 ± 5.28
ΔG polar	35.49 ± 8.27	56.8 ± 5.82
ΔG non-polar	-30.36 ± 2.42	-37.34 ± 1.15
ΔG binding	-52.53 ± 5.03	-50.72 ± 4.83

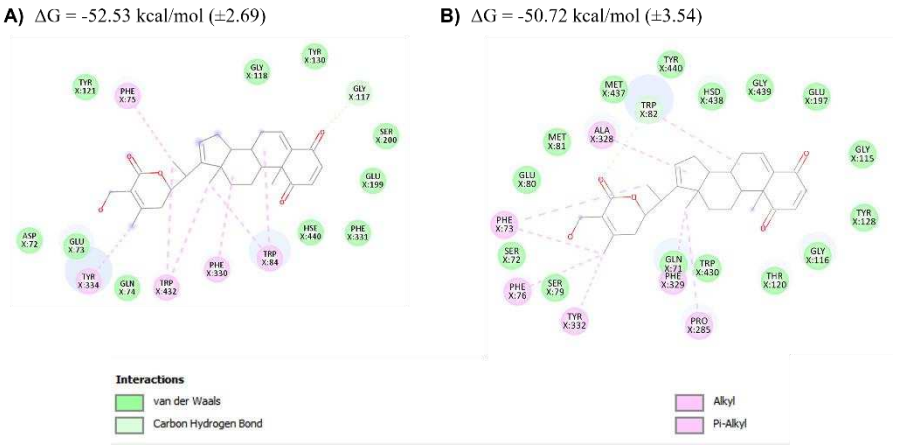

Fig. 13 Protein-ligand interactions between the withanolide 53 and the targets AChE (A) and BChE (B) The affinity energy was predicted by MM-PBSA.

1.5 Conclusions

Withanolides are a large class of natural products with amazing structure diversity. We evaluated 91 withanolides, from 12 structurally different groups, found in plants from the Withaninae subtribe.

Overall, these molecules have very promising pharmacokinetic properties, and even the ones with Lipinski's rule-of-five violations regarding size or number of heteroatoms are likely to be well-absorbed and metabolized by the organism. The structural differences among the groups had a moderate impact on their ADMET-related properties, whereas groups C (5-enes with a 17βside chain) and E (intermediate withanolides with a 17β-side chain) stood out as a promising drug candidates and were more likely to be able to reach the nervous system.

Among the AD-related targets, the cholinesterases were the most promising ones and the structural differences had no significant impact on the docking score values with AChE, suggesting that the core of the withanolides are responsible for most of the interactions. The presence of glicoside groups at carbon C3 can improve its potential to interact with the target, despite the high polarity.

The enzymes BACE-1, GSK-3β, and CDK5 also seem like promising targets, specially the kinases, since the docking values were similar to the original ligand present on these targets. The enzyme MAO-B was the only one with unfavorable docking score and unlikely to be a proper target for withanolides.

The group C, represented by withanolide 53, had intresting results after Molecular dynamics simulations. The interaction with GSK-3β kinase was not strong enough to keep the

withanolide inside the active site, unlike cholinesterases that had a favorable interaction with the ligand, maintained mostly by hydrophobic interactions.

Our results described crucial pharmacokinetics properties and their relationship with the withanolide structures. We also provide a guide to further experimental studies regarding the mechanism of action of those natural products, improving the understanding of their biological activities, and supporting the development of new drugs against AD based on withanolides.

The raw results of the ADMET-related properties and docking biding affinity values can be found in the Supplementary Material.

1.6 Acknowledgements

This study was financed by the Fundação de Amparo à Pesquisa do Estado de Minas Gerais (FAPEMIG) and the Coordenação de Aperfeiçoamento de Pessoal de Nível Superior - Brasil (CAPES) - Finance Code 001.

1.7 Conflict of Interest

Authors have no conflict of interest to declare.

1.8 References

[1] Saslis-Lagoudakis, C.H., Savolainen, V., Williamson, E.M., Forest, F., Wagstaff, S.J., Baral, S.R., Watson, M.F., Pendry, C.A., Hawkins, J.A.: Phylogenies reveal predictive power of traditional medicine in bioprospecting. Proceedings of the National Academy of Sciences **109**(39), 15835–15840 (2012)

[2] Dhar, N., Razdan, S., Rana, S., Bhat, W.W., Vishwakarma, R., Lattoo, S.K.: A decade of molecular understanding of withanolide biosynthesis and in vitro studies in withania somnifera (l.) dunal: prospects and perspectives for pathway engineering. Frontiers in plant science **6**, 1031 (2015)

[3] Olmstead, R.G., Bohs, L., Migid, H.A., Santiago-Valentin, E., Garcia, V.F., Collier, S.M.: A molecular phylogeny of the solanaceae. Taxon **57**(4), 1159–1181 (2008)

[4] Deanna, R., Larter, M.D., Barboza, G.E., Smith, S.D.: Repeated evolution of a morphological novelty: a phylogenetic analysis of the inflated fruiting calyx in the physalideae tribe (solanaceae). American Journal of Botany **106**(2), 270–279 (2019)

[5] Schirmer Pigatto, A.G., Mentz, L.A., Gon¸calves Soares, G.L.: Chemotaxonomic characterization and chemical similarity of tribes/genera of the solanoideae subfamily (solanaceae) based on occurrence of withanolides. Biochemical Systematics and Ecology **54**, 40–47 (2014). https: //doi.org/10.1016/j.bse.2013.12.026

[6] Almeida-Lafet´a, R.C., Ferreira, M.J., Emerenciano, V.P., Kaplan, M.A.: Withanolides from aureliana fasciculata var. fasciculata. Helvetica Chimica Acta **93**(12), 2478–2487 (2010)

[7] Misico, R.I., Nicotra, V.E., Oberti, J.C., Barboza, G., Gil, R.R., Burton, G.: Withanolides and related steroids. Progress in the Chemistry of Organic Natural Products Vol. 94, 127–229 (2011)

[8] Xia, G.-y., Cao, S.-j., Chen, L.-x., Qiu, F.: Natural withanolides, an update. Natural Product Reports (2022)

[9] Chen, L.-X., He, H., Qiu, F.: Natural withanolides: an overview. Natural product reports **28**(4), 705–740 (2011)

[10] Ramsay, R.R., Popovic-Nikolic, M.R., Nikolic, K., Uliassi, E., Bolognesi, M.L.: A perspective on multi-target drug discovery and design for complex diseases. Clinical and translational medicine **7**(1), 1–14 (2018)

[11] Makhoba, X.H., Viegas Jr, C., Mosa, R.A., Viegas, F.P., Pooe, O.J.: Potential impact of the multi-target drug approach in the treatment of some complex diseases. Drug Design, Development and Therapy **14**, 3235 (2020)

[12] Torres, P.H., Sodero, A.C., Jofily, P., Silva-Jr, F.P.: Key topics in molecular docking for drug design. International journal of molecular sciences **20**(18), 4574 (2019)

[13] Liu, Y.: In silico evaluation of pharmacokinetics and acute toxicity of withanolides in ashawagandha. Phytochemistry Letters **47**, 130–135 (2022)

[14] Du, X., Wang, X., Geng, M.: Alzheimer's disease hypothesis and related therapies. Translational neurodegeneration **7**(1), 1–7 (2018)

[15] Mahrous, R., Ghareeb, D.A., Fathy, H.M., EL-Khair, R.M.A., Omar, A.A.: The protective effect of egyptian withania somnifera against alzheimer's. Med. Aromat Plants **6**(285), 2167–0412 (2017)

[16] Patil, S.P., Maki, S., Khedkar, S.A., Rigby, A.C., Chan, C.: Withanolide a and asiatic acid modulate multiple targets associated with amyloid-β precursor protein processing and amyloid-β protein clearance. Journal of natural products **73**(7), 1196–1202 (2010)

[17] Sehgal, N., Gupta, A., Valli, R.K., Joshi, S.D., Mills, J.T., Hamel, E., Khanna, P., Jain, S.C., Thakur, S.S., Ravindranath, V.: Withania somnifera reverses alzheimer's disease pathology by enhancing low-density lipoprotein receptor-related protein in liver. Proceedings of the National Academy of Sciences **109**(9), 3510–3515 (2012)

[18] Kumar, S., Seal, C.J., Howes, M., Kite, G.C., Okello, E.J.: In vitro protective effects of withania somnifera (l.) dunal root extract against hydrogen peroxide and β-amyloid (1–42)-induced cytotoxicity in differentiated pc12 cells. Phytotherapy Research **24**(10), 1567–1574 (2010)

[19] Choudhary, M.I., Yousuf, S., Nawaz, S.A., Ahmed, S., *et al.*: Cholinesterase inhibiting withanolides from withania somnifera. Chemical and pharmaceutical bulletin **52**(11), 1358–1361 (2004)

[20] A Khan, S., B Khan, S., Shah, Z., M Asiri, A.: Withanolides: biologically active constituents in the treatment of alzheimer's disease. Medicinal Chemistry **12**(3), 238–256 (2016)

[21] Das, R., Rauf, A., Akhter, S., Islam, M.N., Emran, T.B., Mitra, S., Khan, I.N., Mubarak, M.S.: Role of withaferin a and its derivatives in the management of alzheimer's disease: Recent trends and future perspectives. Molecules **26**(12), 3696 (2021)

[22] Newman, D.J., Cragg, G.M.: Natural products as sources of new drugs over the nearly four decades from 01/1981 to 09/2019. Journal of natural products **83**(3), 770–803 (2020)

[23] Ovais, M., Zia, N., Ahmad, I., Khalil, A.T., Raza, A., Ayaz, M., Sadiq, A., Ullah, F., Shinwari, Z.K.: Phyto-therapeutic and nanomedicinal approaches to cure alzheimer's disease: present status and future opportunities. Frontiers in aging neuroscience, 284 (2018)

[24] Cummings, J.L., Goldman, D.P., Simmons-Stern, N.R., Ponton, E.: The costs of developing treatments for alzheimer's disease: A retrospective exploration. Alzheimer's & Dementia **18**(3), 469–477 (2022)

[25] Crane, E.A., Heydenreuter, W., Beck, K.R., Strajhar, P., Vomacka, J., Smiesko, M., Mons, E., Barth, L., Neuburger, M., Vedani, A., *et al.*: Profiling withanolide a for therapeutic targets in neurodegenerative diseases. Bioorganic & medicinal chemistry **27**(12), 2508–2520 (2019)

[26] Almeida, A.A., Cota, B.B., Rodrigues, L.M., Dutra, L.L., Kohlhoff, M., Bressan, G.C., Brand˜ao, G.C., Leite, J.P.: Withalutin, a new cytotoxic withanolide from athenaea velutina (sendtn.) d'arcy. Natural Product Research, 1–8 (2022)

[27] Ver´ıssimo, G.C., dos Santos Ju´nior, V.S., de Almeida, I.A.d.R., Ruas, M.S.M., Coutinho, L.G., de Oliveira, R.B., Alves, R.J., Maltarollo, V.G.: The brazilian compound library (bracoli) database: a repository of chemical and biological information for drug design. Molecular Diversity, 1–11 (2022)

[28] Berthold, M.R., Cebron, N., Dill, F., Gabriel, T.R., K¨otter, T., Meinl, T., Ohl, P., Thiel, K., Wiswedel, B.: Knime-the konstanz information miner: version 2.0 and beyond. AcM SIGKDD explorations Newsletter **11**(1), 26–31 (2009)

[29] Pilon, A.C., Valli, M., Dametto, A.C., Pinto, M.E.F., Freire, R.T., CastroGamboa, I., Andricopulo, A.D., Bolzani, V.S.: Nubbedb: an updated database to uncover chemical and biological information from brazilian biodiversity. Scientific Reports **7**(1), 1–12 (2017)

[30] Pil´on-Jim´enez, B.A., Sald´ıvar-Gonz´alez, F.I., D´ıaz-Eufracio, B.I., MedinaFranco, J.L.: Biofacquim: a mexican compound database of natural products. Biomolecules **9**(1), 31 (2019)

[31] Simoben, C.V., Qaseem, A., Moumbock, A.F., Telukunta, K.K., Gu¨nther, S., Sippl, W., Ntie-Kang, F.: Pharmacoinformatic investigation of medicinal plants from east africa. Molecular informatics **39**(11), 2000163 (2020)

[32] Chen, C.Y.-C.: Tcm database@ taiwan: the world's largest traditional chinese medicine database for drug screening in silico. PloS one **6**(1), 15939 (2011)

[33] Wishart, D.S., Feunang, Y.D., Guo, A.C., Lo, E.J., Marcu, A., Grant, J.R., Sajed, T., Johnson, D., Li, C., Sayeeda, Z., *et al.*: Drugbank 5.0: a major update to the drugbank database for 2018. Nucleic acids research **46**(D1), 1074–1082 (2018)

[34] Daina, A., Michielin, O., Zoete, V.: Swissadme: a free web tool to evaluate pharmacokinetics, drug-likeness and medicinal chemistry friendliness of small molecules. Scientific reports **7**(1), 1–13 (2017)

[35] Pires, D.E., Blundell, T.L., Ascher, D.B.: pkcsm: predicting smallmolecule pharmacokinetic and toxicity properties using graph-based signatures. Journal of medicinal chemistry **58**(9), 4066–4072 (2015)

[36] Xiong, G., Wu, Z., Yi, J., Fu, L., Yang, Z., Hsieh, C., Yin, M., Zeng, X., Wu, C., Lu, A., *et al.*: Admetlab 2.0: an integrated online platform for accurate and comprehensive predictions of admet properties. Nucleic Acids Research **49**(W1), 5–14 (2021)

[37] Pantale˜ao, S.Q., Fernandes, P.O., Gonc¸alves, J.E., Maltarollo, V.G., Honorio, K.M.: Recent advances in the prediction of pharmacokinetics properties in drug design studies: a review. ChemMedChem **17**(1), 202100542 (2022)

[38] Ambure, P., Bhat, J., Puzyn, T., Roy, K.: Identifying natural compounds as multi-target-directed ligands against alzheimer's disease: an in silico approach. Journal of Biomolecular Structure and Dynamics **37**(5), 1282– 1306 (2019)

[39] Iserloh, U., Wu, Y., Cumming, J., Pan, J., Wang, L., Stamford, A., Kennedy, M., Kuvelkar, R., Chen, X., Parker, E., *et al.*: Potent pyrrolidine-and piperidine-based bace-1 inhibitors. Bioorganic & medicinal chemistry letters **18**(1), 414–417 (2008)

[40] Kryger, G., Silman, I., Sussman, J.L.: Structure of acetylcholinesterase complexed with e2020 (aricept®): implications for the design of new antialzheimer drugs. Structure **7**(3), 297–307 (1999)

[41] Rosenberry, T.L., Brazzolotto, X., Macdonald, I.R., Wandhammer, M., Trovaslet-Leroy, M., Darvesh, S., Nachon, F.: Comparison of the binding of reversible inhibitors to human butyrylcholinesterase and acetylcholinesterase: A crystallographic, kinetic and calorimetric study. Molecules **22**(12), 2098 (2017)

[42] Malmstr¨om, J., Viklund, J., Slivo, C., Costa, A., Maudet, M., Sandelin, C., Hiller, G., Olsson, L.-L., Aagaard, A., Geschwindner, S., *et al.*: Synthesis and structure-activity relationship of 4-(1, 3-benzothiazol-2yl)-thiophene-2-sulfonamides as cyclin-dependent kinase 5 (cdk5)/p25 inhibitors. Bioorganic & medicinal chemistry letters **22**(18), 5919–5923 (2012)

[43] Gobbo, D., Piretti, V., Di Martino, R.M.C., Tripathi, S.K., Giabbai,B., Storici, P., Demitri, N., Girotto, S., Decherchi, S., Cavalli, A.:Investigating drug–target residence time in kinases through enhanced sampling simulations. Journal of Chemical Theory and Computation **15**(8), 4646–4659 (2019)

[44] Binda, C., Wang, J., Pisani, L., Caccia, C., Carotti, A., Salvati, P., Edmondson, D.E., Mattevi, A.: Structures of human monoamine oxidase b complexes with selective noncovalent inhibitors: safinamide and coumarin analogs. Journal of medicinal chemistry **50**(23), 5848–5852 (2007)

[45] Liebeschuetz, J.W., Cole, J.C. & Korb, O. Pose prediction and virtual screening performance of GOLD scoring functions in a standardized test. J Comput Aided Mol Des 26, 737–748 (2012). https://doi.org/10.1007/s10822-012-9551-4

[46] Dolinsky, T.J., Nielsen, J.E., McCammon, J.A., Baker, N.A.: Pdb2pqr: an automated pipeline for the setup of poisson–boltzmann electrostatics calculations. Nucleic acids research **32**(suppl 2), 665–667 (2004)

[47] Abraham, M.J., Murtola, T., Schulz, R., P´all, S., Smith, J.C., Hess, B., Lindahl, E.: Gromacs: High performance molecular simulations through multi-level parallelism from laptops to supercomputers. SoftwareX **1**, 19– 25 (2015)

[48] Huang, J., Rauscher, S., Nawrocki, G., Ran, T., Feig, M., De Groot, B.L., Grubmu¨ller, H., MacKerell, A.D.: Charmm36m: an improved force field for folded and intrinsically disordered proteins. Nature methods **14**(1), 71–73 (2017)

[49] Jo, S.: T.; iyer, vg; im, w. CHARMM-GUI: a web-based graphical user interface for CHARMM, 1859–1865 (2008)

[50] Olsson, M.H., Søndergaard, C.R., Rostkowski, M., Jensen, J.H.: Propka3: consistent treatment of internal and surface residues in empirical p k a predictions. Journal of chemical theory and computation **7**(2), 525–537 (2011)

[51] Berendsen, H.J., Postma, J.P., van Gunsteren, W.F., Hermans, J.: Interaction models for water in relation to protein hydration. In: Intermolecular Forces, pp. 331–342. Springer, ??? (1981)

[52] Parrinello, M., Rahman, A.: Strain fluctuations and elastic constants. The Journal of Chemical Physics **76**(5), 2662–2666 (1982)

[53] Valdés-Tresanco, M.S., Valdés-Tresanco, M.E., Valiente, P.A. and Moreno E. gmx_MMPBSA: A New Tool to Perform End-State Free Energy Calculations with GROMACS. Journal of Chemical Theory and Computation, 2021 17 (10), 6281-6291. https://pubs.acs.org/doi/10.1021/acs.jctc.1c00645.

[54] Adasme, M.F., Linnemann, K.L., Bolz, S.N., Kaiser, F., Salentin, S., Haupt, V.J., Schroeder, M.: Plip 2021: expanding the scope of the protein– ligand interaction profiler to dna and rna. Nucleic acids research **49**(W1), 530–534 (2021)

[55] Hsieh, P.-W., Huang, Z.-Y., Chen, J.-H., Chang, F.-R., Wu, C.-C., Yang, Y.-L., Chiang, M.Y., Yen, M.-H., Chen, S.-L., Yen, H.-F., *et al.*: Cytotoxic withanolides from tubocapsicum anomalum. Journal of natural products **70**(5), 747–753 (2007)

[56] Xiang, K., Li, C., Li, M.-X., Song, Z.-R., Ma, X.-X., Sun, D.-J., Li, H., Chen, L.-X.: Withanolides isolated from tubocapsicum anomalum and their antiproliferative activity. Bioorganic Chemistry **110**, 104809 (2021)

[57] Zhang, M.-Q., Wilkinson, B.: Drug discovery beyond the 'rule-of-five'. Current Opinion in Biotechnology **18**(6), 478–488 (2007). https://doi.org/ 10.1016/j.copbio.2007.10.005. Chemical biotechnology / Pharmaceutical biotechnology

[58] Ganesan, A.: The impact of natural products upon modern drug discovery. Current opinion in chemical biology **12**(3), 306–317 (2008)

[59] Daina, A., Zoete, V.: A boiled-egg to predict gastrointestinal absorption and brain penetration of small molecules. ChemMedChem **11**(11), 1117 (2016)

[60] Devkar, S.T., Kandhare, A.D., Sloley, B.D., Jagtap, S.D., Lin, J., Tam, Y.K., Katyare, S.S., Bodhankar, S.L., Hegde, M.V.: Evaluation of the bioavailability of major withanolides of withania somnifera using an in vitro absorption model system. Journal of advanced pharmaceutical technology & research **6**(4), 159 (2015)

[61] Baig, M.W., Nasir, B., Waseem, D., Majid, M., Khan, M.Z.I., Haq, I.-u.: Withametelin: A biologically active withanolide in cancer, inflammation, pain and depression. Saudi Pharmaceutical Journal **28**(12), 1526–1537 (2020)

[62] Khanal, P., Chikhale, R., Dey, Y.N., Pasha, I., Chand, S., Gurav, N., Ayyanar, M., Patil, B., Gurav, S.: Withanolides from withania somnifera as an immunity booster and their therapeutic options against covid-19. Journal of Biomolecular Structure and Dynamics, 1–14 (2020)

[63] Castro, S.J., Casero, C.N., Padr´on, J.M., Nicotra, V.E.: Selective antiproliferative withanolides from species in the genera eriolarynx and deprea. Journal of natural products **82**(5), 1338–1344 (2019)

[64] Sonar, V.P., Fois, B., Distinto, S., Maccioni, E., Meleddu, R., Cottiglia,

F., Acquas, E., Kasture, S., Floris, C., Colombo, D., *et al.*: Ferulic acid esters and withanolides: in search of withania somnifera gabaa receptor modulators. Journal of natural products **82**(5), 1250–1257 (2019)

[65] Kumar, V., Faheem, M., Lee, K.W., et al.: A decade of machine learningbased predictive models for human pharmacokinetics: Advances and challenges. Drug discovery today (2021)

[66] Zeiger, E.: The test that changed the world: The ames test and the regulation of chemicals. Mutation Research/Genetic Toxicology and Environmental Mutagenesis **841**, 43–48 (2019)

[67] Hampel, H., Mesulam, M.-M., Cuello, A.C., Khachaturian, A.S., Vergallo, A., Farlow, M., Snyder, P., Giacobini, E., Khachaturian, Z.: Revisiting the cholinergic hypothesis in alzheimer's disease: emerging evidence from translational and clinical research. The journal of prevention of Alzheimer's disease **6**(1), 2–15 (2019)

[68] Thomas Kramer, Boris Schmidt, Fabio Lo Monte, "Small-Molecule Inhibitors of GSK-3: Structural Insights and Their Application to Alzheimer's Disease Models", International Journal of Alzheimer's Disease, vol. 2012, Article ID 381029, 32 pages, 2012. https://doi.org/10.1155/2012/381029

Chapter 2: Antitumor potential of withanolides isolated from *Atheanaea velutina* on melanoma and breast câncer cell lines

[1]Luana L. Dutra, [1]Ananda Aguilar, [1]Tiago A. O. Mendes, [1]Gustavo C. Bressan, [2]Betania B. Cota, [2]Markus Kohlhoff and [1]João Paulo V. Leite

[1]Department of Biochemistry and Molecular Biology, Universidade Federal de Viçosa, Minas Gerais Brazil.

[2]Instituto Rene-Rachou, Fundação Oswaldo Cruz (Fiocruz), Belo Horizonte, Brazil.

Contributing authors: luanalucasdutra@gmail.com; ananda.aguilar@ufv.br; tiagomendes@gmail.com; gustavo.bressan@ufv.br; pvleite@ufv.br.

Manuscript under preparation.

2.1 Abstract

Withanolides, naturally occurring steroidal lactones found in Solanaceae family plants, exhibit diverse biological activities, including antitumoral and, in general, display favorable pharmacokinetic properties and structural similarity to known bioactive compounds. We evaluated the anticancer activity of three withanolides isolated from *Athenaea velutina* (Solanaceae) in human melanoma (MV3) and breast cancer (MCF-7) cell lines. Withalutin, withacnistin, and withacnistin acetate exhibited remarkable cytotoxicity in breast cancer and melanoma models, marking the first report of withalutin's biological activity in human cell lines. Structural differences among the molecules, as the absence of the epoxide ring on withalutin, affected the cytotoxicity but had no effect over the antiproliferative activity. This study evaluated the cytotoxic and antiproliferative activities of these natural products and computationaly explored their interaction with the transcription factor STAT3. Notably, withalutin displayed a preferential binding site distinct from the other two withanolides, potentially linked to its lower cytotoxic activity. Further investigations are required to validate the hypothesis that STAT3 inhibition contributes, at least partially, to the anticancer activity of these withanolides.

2.2 Introduction

Withanolides are naturally occurring steroidal lactones found in plants of the Solanaceae family and are associated with various biological activities such as antitumor, anti-inflammatory, hypoglycemic, hypolipidemic, immunomodulatory, anti-cognitive dysfunction, antioxidant, leishmanicidal, antibacterial, antifungal, and anticholinesterase (CHOUDHARY et al., 2005; XIA, 2022). In recent years, researchers have increasingly investigated the antitumor potential of this chemical class. (ZHANG, 2023).

Withaferin A, one of the most studied molecules in this class, exhibits antitumor activity against different cell types evaluated in *in vitro* and *in vivo* models (XIA et al, 2020). A recent clinical study on the safety and pharmacokinetics of this molecule in patients with advanced osteosarcoma observed good tolerability but low oral bioavailability (PIRES et al., 2020). In an *in silico* study, withanolides demonstrated favorable pharmacokinetic properties and structural similarity to databases of natural bioactive molecules and even FDA-approved drugs (DUTRA et al., 2023). Most of the known withanolides have been isolated or are the active compound of formulations from the leaves and roots of *Withania somnifera* (L.) Dun. (Solanaceae), a plant of great importance in traditional Indian medicine called Ayurveda. The genus *Athenaea* is phylogenetically related to *Withania somnifera* (OLMSTEAD et al., 2008), belonging to subtribo Withaninae, but there are still few studies on the composition of secondary metabolites and biological activities associated with species of this genus.

Two withanolides, aurelianolide A and B, were isolated from the leaves of *A. fasciculata*, but only their leishmanicidal and trypanocidal effects have been described (ALMEIDA-LAFETÁ et al., 2010; LIMA et al., 2018; PERES et al., 2021). Almeida and colleagues reported the promising antitumor activity of *A. velutina* due to the presence of different withanolides (ALMEIDA et al., 2020 and 2021). Indeed, three withanolides were isolated from this plant (Fig. 1) and showed excellent cytotoxicity in a murine melanoma *in vitro* model (ALMEIDA et al., 2022).

Withacnistin was isolated through bio-guided fractionations for antitumoral activity from the leaves of *Acnistus arborescens* and *W. somnifera* , along with Withaferin A (KUPCHAN et al, 1968). The acetylated derivative of withacnistin was reported as a semi-synthetic product and first found as a natural product from the leaves of *A. velutina* (ALMEIDA et al, 2022).

Structurally, withacnistin and its acetylated derivative belong to the group 5β, 6β-epoxides with a 17β-side chain, while withalutin belongs to the group 5-enes with a 17β-side chain (DUTRA et al, 2023). Various pharmacokinetic properties of these three withanolides were computationally evaluated, highlighting high gastrointestinal absorption, a favorable

toxicity profile, and good drug-likeness properties such as logP < 5 (ALMEIDA et al, 2022; DUTRA et al, 2023).

In this study, we aim to expand our understanding of the antitumor activity of these molecules by evaluating their cytotoxicity in two human tumor cell lines (MV3 and MCF-7), their selectivity against normal cells (BGM), and evaluate for the first time their antiproliferative activity through Ki-67 immunostaining. Additionally, we investigate the hypothesis based on Zhang and colleagues (2014) work that the withacnistin and the other withanolides possess cytotoxic activity partially due to interaction with the transcriptiona factor STAT3.

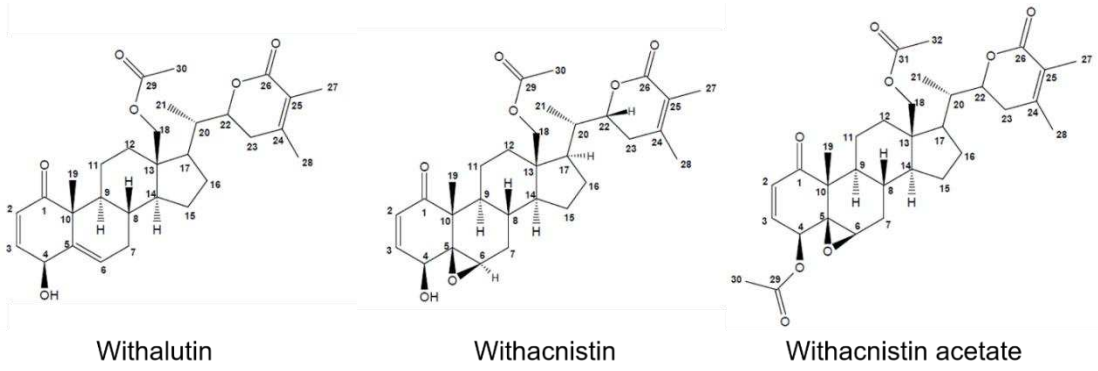

Fig. 1: Structure of the withanolides isolated from *A. velutina* (ALMEIDA et al., 2022).

2.3 Methodology

Obtaining the analyzed withanolide compounds

Our own phytochemical investigation of the species *Athenaea velutina* led to the obtaining of withalutin, withacnistin and withacnistin acetate. Their structures were determined by ESI-HRMS and 2D NMR experiments (ALMEIDA et al., 2022).

Cell culture, culture conditions, and compound dilution

The anticancer activity of the withanolides were assessed with human melanoma (MV3), human breast cancer (MCF-7), and non-tumoral African green monkey kidney cells (BGM). They were kindly provided by Dr. Anésia Aparecida dos Santos (Department of General Biology, Universidade Federal de Viçosa, Viçosa, Minas Gerais, Brazil). The MV3 and BGM cells were cultured in high-glucose DMEM medium, supplemented with 1% sodium pyruvate and 10% fetal bovine serum, while MCF-7 were cultured in RPMI medium, supplemented with 0.1% insulin and 20% fetal bovine serum. The cells were maintained in 25 cm^2 culture flasks at 37ºC, 5% CO_2 until reaching approximately 90% confluence. The withanolides withalutin

(1), withacnistin (2) and withacnistin acetate (3) were solubilyzed in dimethilsulphoxide (DMSO) at 50 mM and kept under -20ºC until the application on the cells.

Cell viability assay

The MV3 and MCF-7 cells were seeded onto 96-well plates so that each well contained 1 x 10^4 and 2 x 10^4 cells/well, respectively. After 24h under culture conditions, the cells were treated with withanolides at different concentrations (50, 25, 12.5, 6.25, 3.12, 1.56, 0.78, 0.39 µM) or the vehicle solvent (DMSO). After 48h of incubation, 10 µL of MTT (3-(4,5-dimethylthiazol-2-yl)-2,5-diphenyltetrazolium bromide; Sigma Aldrich, 5 mg/ml) were added to each well and incubated for 3 hours at 37ºC. The culture medium was removed, and the formazan salts formed by the metabolism of the MTT reagent were solubilized in 100 µL of DMSO and quantified at 540 nm using a plate reader (Synergy HT, Biotek, Winooski, Vermont, USA). The results were normalized considering the control culture, and the IC_{50} value was defined by nonlinear regression after normalization with the software GraphPad Prism v.5. To determine the selectivity index (SI) for tumor cell lines, we performed the same assay with the non-tumor cell line BGM, under the same culture conditions as MV3.

Ki-67 immunofluorescence assay

Ki-67 immunofluorescence was evaluated in MV3 and MCF-7 cells (1 x 10^4 and 2 x 10^4 cells/well, respectively, on coverslips) treated with withanolides at the IC_{50} concentration or DMSO (0.1% v/v; control) for 48 hours. The cells were fixed with 4% paraformaldehyde for 20 minutes and rinsed with PBS. Subsequently, they were permeabilized and blocked with 0.5% v/v Triton X-100/PBS and 2% m/v bovine serum albumin (BSA) for 60 minutes. After three washes with PBS, the cells were incubated with the primary antibody anti-Ki-67 (1:100, Abcam, #ab16667) for 60 minutes. Following PBS washing, the cells underwent a 60-minute incubation with a secondary antibody anti-rabbit IgG Alexa Fluor 488 (1:100, ThermoFisher Scientific, #A11008). Slides were mounted using Prolong Diamond® with 4′,6-diamidino-2-phenylindole (DAPI, Thermo Fisher Scientific) as a nuclear counterstain. Fluorescence signals were captured using an inverted fluorescence microscope EVOS® (Life Technologies) equipped with DAPI LED CUBE and GFP LED CUBE filters.

Molecular docking simulation

A blind molecular docking simulation was conducted using the AlphaFold-derived structure of the transcription factor STAT3 (AF-P40763-F1-model_v4) (JUMPER et al, 2021)

and the three previously mentioned withanolides as ligands. The AutoDock Vina software was employed for the docking simulations, and preparation of structure files. This approach aimed to explore the potential binding interactions between the STAT3 protein and the withanolides, providing insights into the withanolides site and conformational preferences around STAT3 and afinity predictions.

2.4 Results and discussion

Cell viability assays

The cytotoxic effects of the three withanolides were investigated on two tumoral cell lines (MV3 and MCF-7) and one non-tumoral cell line (BGM). Although, their performance on both tumoral cells was similar, withalutin showed slightly lower cytotoxicity compared to withacnistin and its acetylated analog (Figure 2). Indeed, the IC_{50} value determined for withalutin with the MV3 cell line was approximately 4-fold higher than the other two withanolides, and 3-fold higher with the MCF-7 cell line (Table 1). There was a significant difference among withalutin and the other two withanolides on both tumoral cell lines.

The three withanolides demonstrated significantly higher cytotoxicity compared to Dacarbazine when evaluated in an *in vitro* model similar to the one used in this study (IC_{50}= 175 µM). Dacarbazine is a standard treatment for melanoma with limited efficacy across various melanoma types (GUO et al, 2023). In the breast cancer model, both withacnistin and its acetylated analogue exhibited a lower IC_{50} than that observed for doxorubicin, a first-line treatment for breast cancer, under similar experimental conditions (IC_{50}= 4.13 µM) (ABUHAMMAD and ZIHlIF, 2013).

Regarding the mechanism of action behind the significant cytotoxic activity on both cell lines, we can speculate that the structural variation among the withanolides affects their efficiency. Indeed, Dutra and colleagues described the influence of different classes of withanolides on their pharmacokinetic properties and observed a promising profile through the prediction of drug-likeness and ADMET properties of various withanolides, including the three discussed in this study (ALMEIDA et al, 2022; DUTRA et al, 2023).

According to Dutra and colleagues (2023) the three withanolides isolated from *A. velutina* and evaluated in this study have a logP below 5, a highly relevant structural characteristic for a natural product that can become a drug candidate. Additionally, these three withanolides also demonstrate high intestinal and cutaneous absorption but are unlikely to surpass the blood-brain

barrier. Regarding metabolism and excretion parameters, these withanolides are possible substrates of P-glycoprotein, are not predicted as inhibitors of cytochrome P450, and exhibit a low to moderate Steady state volume of distribution (VDss). As for toxicity, the three withanolides were predicted to be non-carcinogenic, non-hepatotoxic, and non-inhibitors of hERG channels.

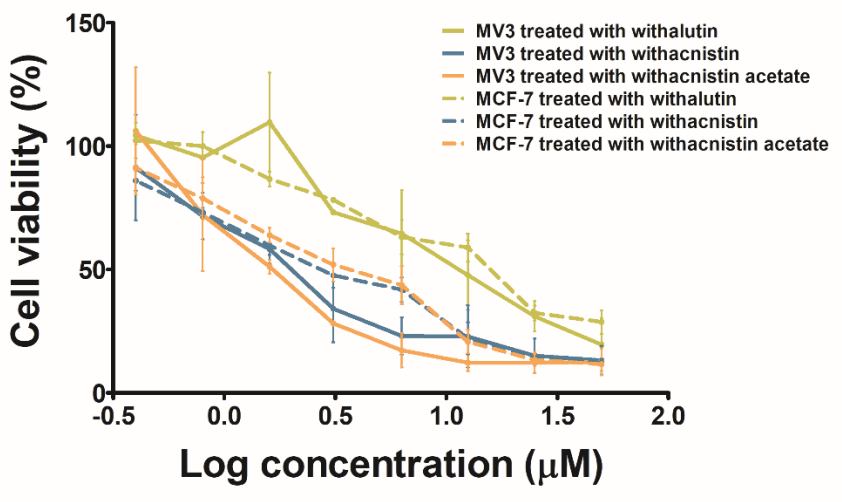

Fig. 2: MTT/formazan assay results depict the cytotoxic effects of withanolides: withalutin (in yellow), withacnistin (in blue), and withacnistin acetate (in orange) on MCF-7 (dashed line) and MV3 (continuous line) cells. Cell viability was calculated relative to the control group (DMSO), and the graph represents the mean of two independent experiments, each conducted in triplicate.

Table 1: *In vitro* cytotoxic activity of the withanolides using the MTT/formazan assay.

	IC_{50} of each treatment, in µM (SD)			**SI (MV3, MCF-7)**
	MV3	MCF-7	BGM	
Withalutin	6.18 (1.84)[a]	6.78 (0.13)[a]	6.96 (5.63)	1.13, 1.03
Withacnistin	1.33 (0.02)[b]	2.10 (0.09)[b]	3.09 (2.29)	2.33, 1.47
Withacnistin acetate	1.25 (0.14)[b]	2.66 (0.73)[b]	1.33 (0.02)	1.07, 0.50

SI (selectivity index) = $IC_{50}^{BGM}/IC_{50}^{\text{cancer cell line}}$, Nonlinear regression analysis were performed to calculate de IC_{50} values, based on two independent experiment with three replicates each. Different superscript letters indicate statical significance differences between means after 1-way ANOVA and Bonferroni posttests (p-value < 0.01).

Ki-67 immunofluorescence assays

We evaluated the expression of the proliferative marker Ki-67 in MCF-7 and MV3 tumor cells after treatment with withanolides, comparing the results to the control group treated with the vehicle solvent (DMSO). We observed a difference in the staining pattern between the treatments and the control groups. As reported by Miller and colleagues (2018),

immunofluorescence labeling of the Ki-67 protein should not be interpreted as a binary marker of cell proliferation. In fact, the Ki-67 protein is gradually degraded during the G0/G1 phases and accumulates gradually during the other phases of the cell cycle. Thus, the amount of protein observed in a single cell can indicate how long it has been in a quiescent state before returning to a proliferative state (MILLER et al., 2018).

In actively proliferative cells, the Ki-67 level is lower during the G1/S transition, and in less proliferative cells that have spent long periods in quiescence, Ki-67 is undetectable during the G1/S transition. Our results suggest that with the MCF7 cell line, treated cells showed mild and diffuse labeling in a few cells, and most of them did not show visible labeling, indicating that they may be in the G1/S transition after a long period in a quiescent state (Figure 3-A). As for MV3 melanoma cells, the treatments caused a more noticeable change compared to the control. In fact, control cells showed intense labeling, suggesting that most cells are in a state of high proliferative activity (S/M phases). However, after treatment with withanolides, we observed much weaker and diffuse labeling, indicating arrest in G1/G0 phase (Figure 3-B). After a quantitative analysis of cells positively marked for Ki-67, we observed no significant difference in the MCF-7 lineage. However, all three withanolides were able to decrease significantly the content of Ki-67-positive cells compared to the control (Figure 4).

This result contrasts with the mechanisms observed in withanolides withaferin-A or S5, which induce G2/M phase arrest in in vitro models of breast cancer and melanoma, respectively. However, it aligns with the effect observed in treating breast cancer cells with the withanolide tubocapsenolide A. This treatment resulted in G1 phase accumulation and apoptosis due to the inhibition of heat shock proteins. Notably, this mode of action is associated with withanolides that feature an instauration at carbons C2-C3 (WANG et al., 2012; ZHANG et al., 2023), highlighting the multi-target activity of withanolides.

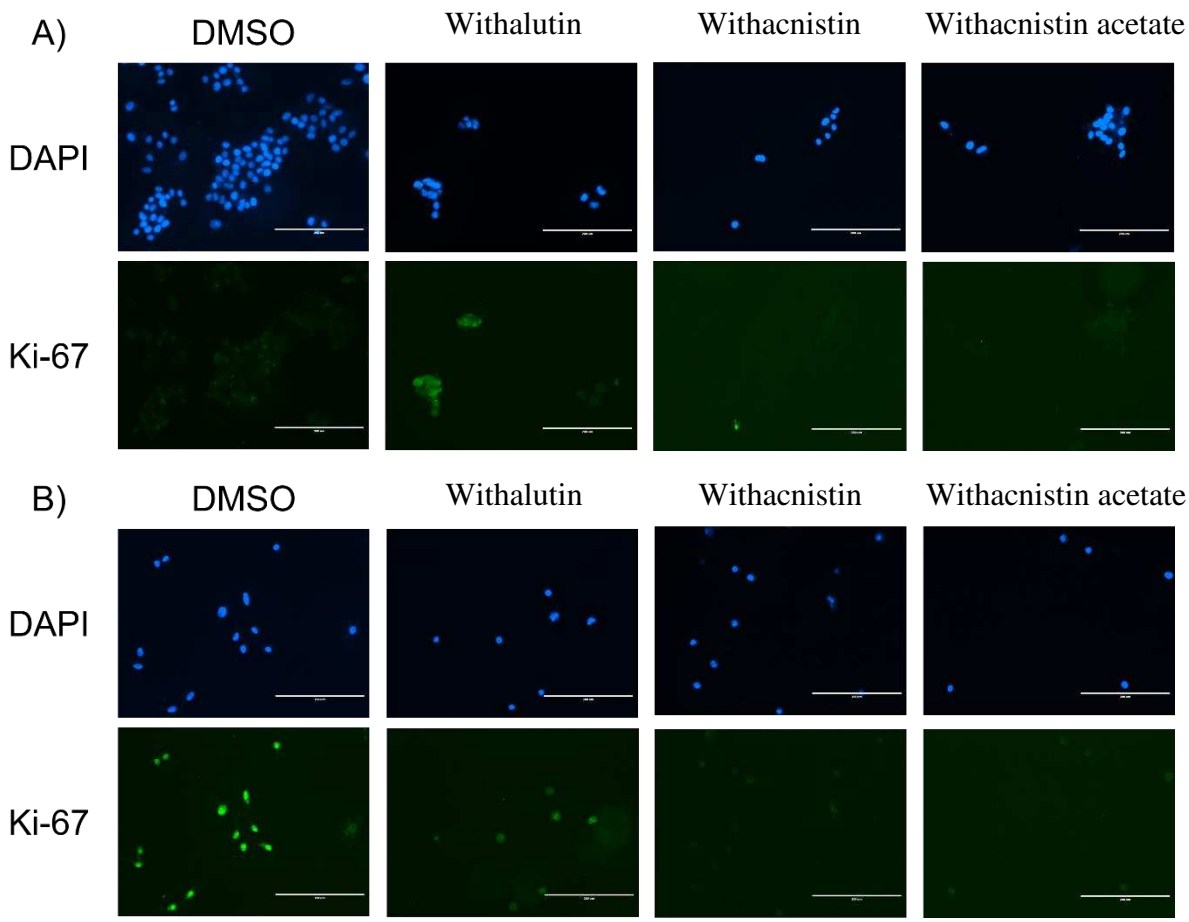

Fig. 3: Representative photomicrography of Ki-67 (green) and DAPI (blue) immunolabeling of (A) MCF-7 and (B) MV3 after 48h of treatments with DMSO (control) and the withanolides withalutin, withacnistin, and withacnistin acetate. Scale bar 200 µm.

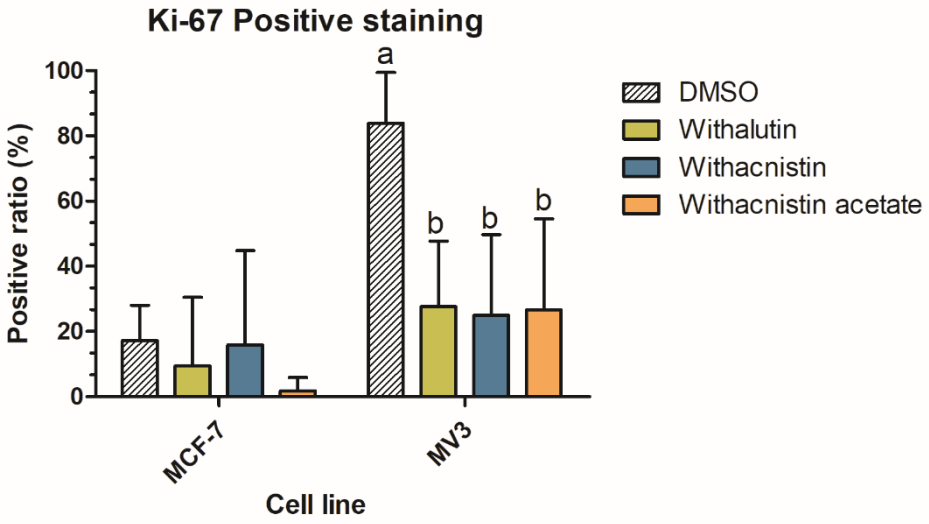

Fig. 4: Quantitative analysis of cell proliferation *in vitro.* Values in the bar graphs represent the mean and SD of Ki-67 positive cells, counted manually on randomely selected fields (n = 5 fields). The photomicrography of each

field are in Supplementary Material Figures S1-S8. The bars marked with different letters indicate significant differences as determined by ANOVA (p-value < 0.01).

Given that these molecules exhibit promising cytotoxicity and antiproliferative activitie in cellular models, we also proposed a potential molecular target based on the results observed and described in the literature by Zhang and colleagues (2014).

Signal transducers and activators of transcription (STAT) proteins are important targets for anticancer drugs. STAT3 is persistently activated in many metastatic tumors, and its phosphorylation is affected by treatment with different withanolides, such as withaferin A, physapubesin B, withaphysalin A, and also withacnistin, in multiple cancerous cell lines (ZHANG et al., 2014; ZHANG et al., 2023). This transcription factor is activated in response to many cytokines and growth factors (GFs) by binding to membrane receptors and then being phosphorylated by receptor tyrosine kinases (RTKs) like EGFR or non-RTKs (e.g., Src or JAK). After phosphorylation, STAT protein is dimerized through SH2-domain/phosphotyrosine interactions and then translocated to the nucleus to regulate several target genes (ZHANG et al., 2014).

Zhang and colleagues (2014) evaluated the activity of withacnistin in *in vitro* and *in vivo* breast cancer models. They observed that this molecule inhibits the recruitment of STAT3 and STAT5 to growth factor and cytokine receptors, tyrosine phosphorylation, nuclear translocation, and DNA binding. This resulted in the inactivation of these transcription factors and inhibition of the expression of target genes, anchorage-independent growth, invasion, induction of apoptosis, and regression of ErB2-driven mammary tumors in an in vivo model (ZHANG et al., 2014). STAT3 inhibition occurred completely within the first 30 minutes after treatment, while STAT5 took 60-120 minutes for complete inactivation. Additionally, the inactivation occurred after stimulation by different growth factors and cytokines and did not alter the autophosphorylation of EGFR and gp130 receptors. From this, we hypothesize that withacnistin may directly bind to a site on STAT3, blocking its interaction with EGFR. However, in STAT5, this interaction may be bypassed as it has multiple binding sites on the receptor.

We observed that the presence of the acetate group in withacnistin acetate does not seem to alter cytotoxicity when compared to withacnistin. However, the substitution of the epoxide ring at the C5-C6 position with an instauration reduced cytotoxicity in both cell lines but did not significantly affect antiproliferative activity. This suggests that this structural change may minimize the molecule's activity without altering the mechanism of action. That said, we

evaluated the mode of interaction of the three withanolides with the STAT3 transcription factor and highlighted the most favorable conformations and preferential interaction sites (Figure 5).

Molecular docking simulation

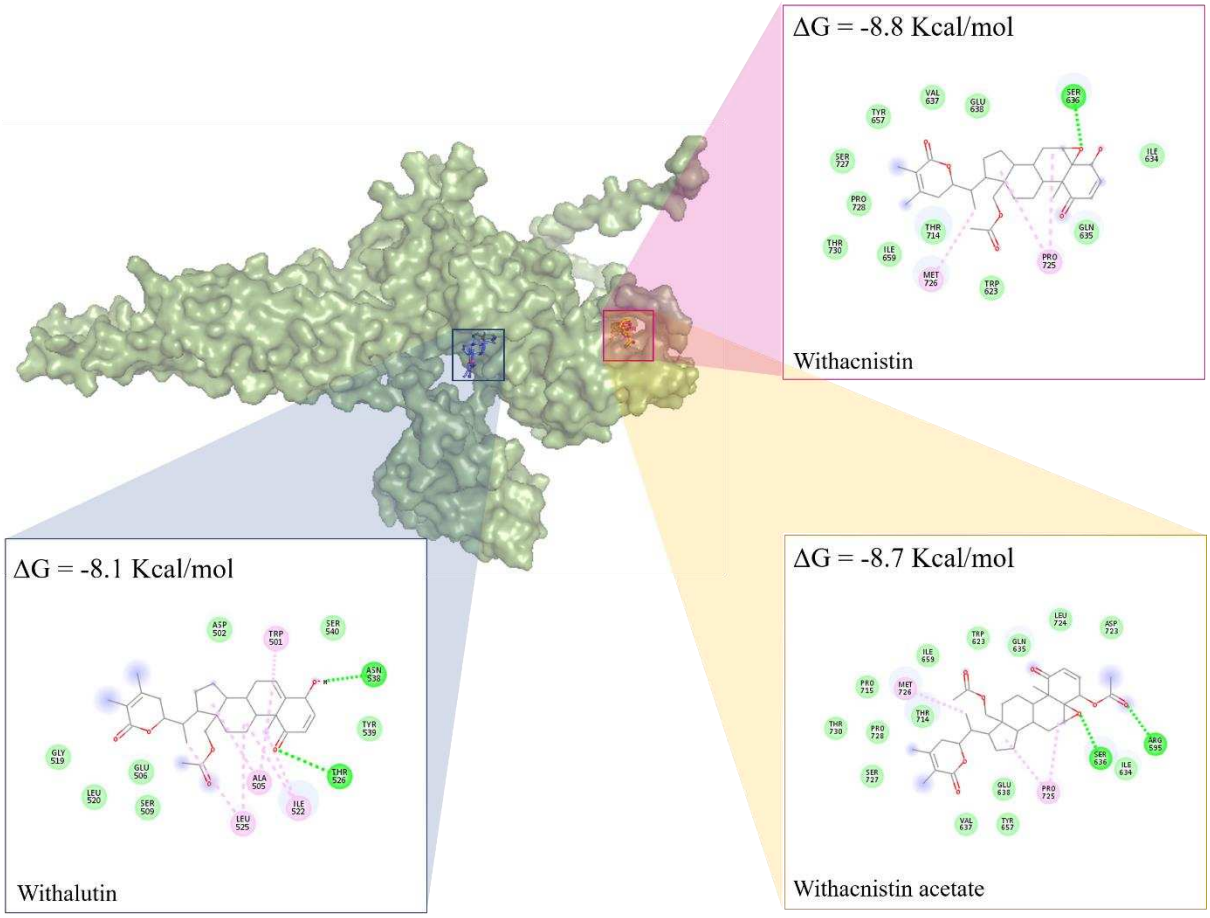

Fig. 5: The most favorable binding sites of each withanolide on the STAT3.

We observed that withanolides with an epoxide ring preferentially interact with the SH2 domain, responsible for the dimerization and activation of STAT3. However, withalutin presented a distinct preferred binding site compared to the others, in a DNA-binding region. Only the second conformational model interacted closer to the SH2 domain but with a less favorable binding affinity (-7.6 kcal/mol). This result suggests that these molecules may act to hinder phosphorylation and subsequent activation of STAT3. However, a more refined analysis is necessary to observe the impact of the epoxide ring on the stability of the ligand-protein complex within the SH2 domain.

2.5 Conclusions

The withanolides withalutin, withacnistin, and withacnistin acetate demonstrated excellent cytotoxic activity in *in vitro* models of breast cancer and melanoma. To date, this is the first report of the biological activity of withalutin in human cell lines. We observed significant antiproliferative activity in melanoma cells, and the structural variations among the molecules seem not to influence this activity. The presence of the acetate group did not yield significant differences in relation to the evaluated parameters when compared to non-acetylated withacnistin. However, the epoxide group at carbons C5-C6 proved to be relevant for the cytotoxicity, although withalutin also exhibited highly promising biological activity. These observations reinforce the multi-target nature of these natural products, indicating different modes of action due to their structural composition.

Regarding the mechanism by which these molecules act on tumor cells, we computationally investigated the interaction of these compounds with the transcription factor STAT3. Indeed, we observed differences in the binding sites of withalutin compared to withacnistin and its acetylated analogue, which may justify the observed discrepancy in cytotoxicity. Further studies are needed to validate the hypothesis that the inhibition of STAT3 is, at least in part, responsible for the anticancer activity of these withanolides.

2.6 Acknowledgements

This study was financed by the Fundação de Amparo à Pesquisa do Estado de Minas Gerais (FAPEMIG) and the Coordenação de Aperfeiçoamento de Pessoal de Nível Superior - Brasil (CAPES) - Finance Code 001.

2.7 Conflict of interest

Authors have no conflict of interest to declare.

2.8 References

ALMEIDA, A.A., COTA, B.B., RODRIGUES, L. M., DUTRA, L. L., KOHLHOFF, M., BRESSAN, G. C., BRANDÃO. G. C., LEITE, J. P. V. Withalutin, a new cytotoxic withanolide from *Athenaea velutina* (Sendtn.) D'Arcy. *Natural Product Research*, v. 13, p. 1-8, 2022. DOI: 10.1080/14786419.2022.2039135

ALMEIDA, A.A., LIMA, G.D.A., EITERER, M., RODRIGUES, L.A., DO VALE, J.A., ZANATTA, A.C., BRESSAN, G.C., DE OLIVEIRA, L.L., LEITE, J.P.V. A withanolide-rich fraction of *Athenaea velutina* induces apoptosis and cell cycle arrest in melanoma B16F10 cells. *Planta Medica*, 2021. DOI: 10.1055/a-1395-9046

ALMEIDA, A.A., LIMA, G.D.A., SIMÃO, M.V.R.C., MOREIRA, G.A., SIQUEIRA, R.P., ZANATTA, A.C., VILEGAS, W., MACHADO-NEVES, M., BRESSAN, G.C., LEITE, J.P.V. Screening of plants from the Brazilian Atlantic Forest led to the identification of *Athenaea*

velutina (Solanaceae) as a novel source of antimetastatic agentes. *International Journal of Experimental Pathology*, v.10, n.3-4, p. 106-121, 2020.

ALMEIDA-LAFETÁ, R. C., FERREIRA, M. J. P., EMERENCIANO, V. P., KAPLAN, M. A. C. Withanolides from *Aureliana fasciculata var. fasciculata. Helvetica Chimica Acta*, v. 93, 2010.

CHOUDHARY, M.I., YOUSUF, S., NAWAZ, S.A., AHMED, S., *et al.* Cholinesterase inhibiting withanolides from *Withania somnifera*. *Chemical and pharmaceutical bulletin*, v. 52, p. 1358–1361, 2004.

DUTRA, L.L., BORGES, R.J., MALTAROLLO, V.G., MENDES, T.A., BRESSAN, G.C. AND LEITE, J.P.V. *In silico* evaluation of pharmacokinetics properties of withanolides and simulation of their biological activities against Alzheimer's disease. *Journal of Biomolecular Structure and Dynamics*, p.1-16, 2023. DOI: 10.1080/07391102.2023.2206909

GUO, L., DONG, Z., ZHANG, X., YANG, Y., HU, X., JI, Y., CUI, H. Morusinol extracted from *Morus alba* induces cell cycle arrest and apoptosis via inhibition of DNA damage response in melanoma by CHK1 degradation through the ubiquitin-proteasome pathway. *Phytomedicine*, v. 114, p. 154765, 2023. DOI: 10.1016/j.phymed.2023.154765

JUMPER, J., EVANS, R., PRITZEL, A. *et al*. Highly accurate protein structure prediction with AlphaFold. *Nature,* v. 596, p. 583-589, 2021. DOI: 10.1038/s41586-021-03819-2 ABUHAMMAD, S. and ZIHlIF, M. Gene expression alteration in doxorubicin resistant MCF7 breast cancer cell line. *Genomics*, v. 101, p. 213-220, 2013. DOI: 10.1016/j.ygeno.2012.11.009

KUPCHAN, S.M., ANDERSON, W.K., BOLLINGER, P., DOSKOTCH, R.W., SMITH, R.M., SAENZ-RENAULD, J.A., SCHNOES, H.K., BURLINGAME, A.L. and SMITH, D.H. Tumor inhibitors. XXXIX. Active principles of *Acnistur arborescens*. Isolation and structural and spectral studies of withaferin A and withacnistin. *The Journal of organic chemistry, v.34,* p.3858-3866, 1969.

LIMA, S.C.D.M., PACHECO, J.D.S., MARQUES, A.M., VELTRI, E.R.P., ALMEIDA-LAFETÁ, R.D.C., FIGUEIREDO, M.R., KAPLAN, M.A.C., TORRES-SANTOS, E.C. Leishmanicidal activity of Withanolides from *Aureliana fasciculata var. fasciculata. Molecules*, v. 23, n.12, p.3160, 2018. DOI: 10.3390/molecules23123160

MILLER, I., MIN, M., YANG, C., TIAN, C., GOOKIN, S., CARTER, D., & SPENCER, S. L. Ki67 is a graded rather than a binary marker of proliferation versus quiescence. *Cell reports*, v. 24, p. 1105-1112, 2018. DOI: 10.1016/j.celrep.2018.06.110

OLMSTEAD, R. G., BOHS, L., MIGID, H. A., SANTIAGO-VALENTIN, E., GARCIA, V. F. E COLLIERET S. M. A molecular phylogeny of the Solanaceae. *Taxon*, v. 57, p. 1159-1181, 2008.

PERES, R.B., FIUZA, L.F.D.A., DA SILVA, P.B., BATISTA, M.M., CAMILLO, F.D.C., MARQUES, A.M., DE C. BRITO, L., FIGUEIREDO, M.R., SOEIRO, M.D.N. *In vitro* phenotypic activity and in silico analysis of natural products from Brazilian biodiversity on *Trypanosoma cruzi*. *Molecules*, v. 26, n. 18, p.5676, 2021. DOI: 10.3390/molecules26185676

PIRES, N., GOTA, V., GULIA, A., HINGORANI, L., AGARWAL, M., PURI, A. Safety and pharmacokinetics of Withaferin-A in advanced stage high grade osteosarcoma: A phase I trial.

Journal of Ayurveda and Integrative Medicine, v. 11, p. 68-72, 2020. DOI: 10.1016/j.jaim.2018.12.008

WANG,U. C., TSAI,Y. L., WU, Y. C., CHANG, F. R., LIU, M. H., CHEN, W. Y., WU, C. C. Withanolides-induced breast cancer cell death is correlated with their ability to inhibit heat protein 90. *Plos One*, v. 7, p. e37764, 2012. DOI: 10.1371/journal.pone.0037764

XIA, G.Y., CAO, S.J., CHEN, L.X., QIU, F. Natural withanolides, an update. *Natural Product Reports*, v. 39, n.4, p.784-813, 2022. DOI: 10.1039/D1NP00055A

ZHANG, X., BLASKOVICH, M.A., FORINASH, K.D., SEBTI, S.M. Withacnistin inhibits recruitment of STAT3 and STAT5 to growth factor and cytokine receptors and induces regression of breast tumours. *British journal of cancer*, v. 111, n.5, p. 894-902, 2014.

ZHANG, Z., YANG, Y., XU, Y., LIU, Y., LI, H., CHEN, L. Molecular targets and mechanisms of anti-cancer effects of withanolides. *Chemico-Biological Interactions*, v. 384, p. 110698, 2023. DOI: 10.1016/j.cbi.2023.110698

Chapter 3: The *Athenaea* genus as a promissing source of antitumoral agents

[1]Luana L. Dutra, [2]João Victor da Costa Santos, [1]Tiago A. O. Mendes, [1]Gustavo C. Bressan, [3]Markus Kohlhoff, and [1]João Paulo V. Leite

[1]Department of Biochemistry and Molecular Biology, Universidade Federal de Viçosa, Minas Gerais Brazil.

[2]Department of Vegetal Biology, Universidade Federal de Viçosa, Minas Gerais Brazil.

[3]Instituto Rene-Rachou, Fundação Oswaldo Cruz (Fiocruz), Belo Horizonte, Brazil.

Contributing authors: luanalucasdutra@gmail.com; tiagomendes@gmail.com; gustavo.bressan@ufv.br; markus.kohlhoff@fiocruz.br; pvleite@ufv.br.

Manuscript under preparation

3.1 Abstract

This study focused on identifying natural compounds with anticancer properties, singling out *Athenaea fasciculata* as a promising source. Small molecules such as withanolides from *Athenaea velutina, Withania somnifera*, and other Solanaceas demonstrated significant anticancer effects, inducing cell cycle arrest and apoptosis *in vitro* and *in vivo*. In this work we evaluated extracts from different *Athenaea* species against tumoral and non-tumoral cell lines, with *A. fasciculata* showing the most promise. Fractionation of its extract revealed increased cytotoxicity in specific fractions, supported by LC-MS/MS analysis that allowed annotation of glycosylated withanolides. These findings underscore *Athenaea* species as a valuable source of bioactive compounds with potential therapeutic applications, warranting continued investigation.

3.2 Introduction

Cancer is a leading global cause of death, accounting for nearly 10 million fatalities in 2020 (FERLAY et al., 2020). It constitutes a group of diseases originating from uncontrolled cell proliferation, influenced by various factors such as genetics, environment, and lifestyle. Despite the continuous advancements in cancer therapies, it remains a significant threat to human health.

The current drug development landscape faces challenges as numerous studies rely on methodologies centered around protein-ligand interaction and a linear comprehension of the

mechanism of action. This approach hinders the exploration of new molecules for inherently multifactorial diseases. In this context, natural products emerge as a promising solution due to their structural complexity and pharmacokinetics that extend beyond the specific single-target binding approach. They also induce physiological effects through physical mechanisms, such as altering membrane permeability, macromolecule mimicry, and synergistic effects within herbal complex mixtures (BIZZARRI et al., 2020).

Natural products offer structures that have evolved to interact with proteins and other biological targets and their pharmacokinetic properties go beyond the rule-of-5 due to their rich stereochemistry and three-dimensional structures, which correlated with increased binding specificity, reduced preclinical toxicity, and improved progression through clinical trials (STONE et al., 2022). From 1981 to 2019, 247 new drugs were approved for cancer treatment. This included 52 peptides/proteins, 18 natural products, 1 botanical drug (defined mixture), 43 derivatives of natural products, 29 synthetic compounds, 13 synthetic compounds with natural pharmacophores, and 36 natural product mimics (NEWMAN and CRAGG, 2019).

Throughout our studies aimed at identifying natural molecules with anti-tumor activity, we singled out *Athenaea velutina*, among various endemic species of the Atlantic Forest, as a promising source of compounds with antibacterial and anticancer effects against murine melanoma cells (B16F10) (ALMEIDA et al., 2019). The enriched fraction of withanolides obtained from the dichloromethane extract of *A. velutina* significantly reduced cellular proliferation, migration, and invasion processes. It induced cell cycle arrest in the G0/G1 phase and apoptosis in a murine in vitro model (ALMEIDA et al., 2021). Three withanolides isolated from this fraction, withalutin, withacnistin, and withacnistin acetate, exhibited excellent cytotoxicity in B16F10, MV3, and MCF-7 cell lines, along with significant antiproliferative activity in MV3 and promising properties related to ADMET (ALMEIDA et al., 2022; DUTRA et al., manuscript in preparation).

The genus *Athenaea* currently comprises twelve species found in neotropical climates, with a diversity center in the southeast region of Brazil. There are few studies on the phytochemistry of these plants and their potential therapeutic use (RODRIGUES et al., 2019; ALMEIDA-LAFETÁ et al., 2010; SILVA et al., 2018).

This study assessed the cytotoxic activity of different extracts obtained from three *Athenaea* species (*A. fasciculata, A. martiana, and A. tomentosa*) against human tumor and non-tumor cell lines. The most promising extract underwent fractionation, and its composition was evaluated using LC-MS/MS.

3.3 Methodology

Plant extracts and bioguided fractionation

The leaves of *A. tomentosa, A. fasciculata*, and *A. martiana* were collected from fragments of the Atlantic Forest in the municipality of Viçosa, state of Minas Gerais, Brazil. The plant material was dried, ground in a knife mill, and then subjected to exhaustive sequential percolation, with the extracting solventes of increasing polarity, hexane (degreasing step), dichloromethane, and ethanol. The respective dichloromethane and ethanolic extracts of each *Athenaea* species were concentrated using a rotary evaporator coupled with a vacuum pump (reduced pressure). After this concentration step, for complete solvent removal, all extracts were lyophilized. The fractionation of the most cytotoxic extract was carried out by liquid-liquid partitioning, starting with approximately 3.0 mg of extract and 150 ml of water. Three volumes of 150 ml of each extracting solvent (hexane, dichloromethane, and ethyl acetate) were used, and the organic fractions and the final aqueous fraction were concentrated using a rotary evaporator and lyophilized to remove residual water. The dichloromethane, ethyl acetate, and aqueous fractions were assessed for cytotoxicity in in vitro tumor models (MCF-7 and MV3) and non-tumoral (Hek-293) cells. Their composition was determined by LC-MS/MS.

Cell culture and cell viability assay

The study evaluated the anticancer activity of *Athenaea* spp. extracts using human melanoma (MV3), human breast cancer (MCF-7), and non-tumoral Human Embryonic Kidney (HEK-293). These cell lines were kindly provided by Dr. Anésia Aparecida dos Santos from the Department of General Biology at the Universidade Federal de Viçosa, Brazil. MV3 and HEK-293 cells were cultured in high-glucose DMEM medium, while MCF-7 cells were cultured in RPMI medium. The samples were solubilized in DMSO and stored at -20ºC. Cell viability assays were conducted by treating MV3 and MCF-7 cells with the extracts from different species of *Athenaea* at 100µg/mL. The IC_{50} was determined by treating cells with six different concentrations of the most active extract and it's fractions, or the vehicle solvent (DMSO) for 48 hours. MTT reagent was added, and the formazan salts were quantified at 540 nm. IC_{50} values were determined by nonlinear regression. The selectivity index (SI) for tumor cell lines was assessed by performing the same assay on the non-tumor cell line HEK-293.

LC-HRMS/MS analysis

The analyses were carried out using a Nexera UHPLC (Shimadzu, Japan) coupled to a maXis ESI-QTOF high resolution mass spectrometer (Bruker, Germany). The LC system

consisted of LC-30AD solvent pumps, a CBM-20A system controller, a CTO-20A column oven, a SIL-30AC automated sample injector, and an SPD-20A UV detector. The samples were diluted in DMSO:methanol (1:3) at 5 mg/mL concentration and centrifuged before injection. A sample volume of 2 µL was injected into a Shimadzu Shim-Pack XR-ODS-III column (C18, 2.2 µm, 2.0 x 150 mm). The temperature was maintained at 40 °C. The flow rate was maintained at 0.4 mL/min. For elution of the column, solvent A (0.1% formic acid in water) and solvent B (0.1% formic acid in acetonitrile) were used with the following program: 5% B (0 to 5 min), a linear gradient to 100% B in 40 min and a hold at 100% for 5 min. An analytical blank containing only the sample solvent was performed at the beginning of the sample batch. Mass spectra were acquired at *m/z* 100-1500 in positive mode at a rate of 5 Hz. Ion-source parameters were set to 500 V end plate offset, 4500 V capillary voltage, 3.0 bar nebulizer pressure and 8 L/min respective 200 °C dry gas flow and temperature. Data dependent fragment spectra were recorded at a collision energy range between 15 and 60 eV. Mass calibration was achieved by initial ion-source infusion of 20 µL 1 mM sodium formate in 50% 2-propanol and post-acquisition recalibration of the raw data. Compounds were detected by chromatographic peak dissection with subsequent formula determination according to exact mass and isotope pattern. The chromatograms were analysed with MZmine 3 (SCHMID et al, 2023), with default parameters.

3.4 Results and discussion

Selection of the extract for bioguided fractionation

The ethanolic extract of *A. fasciculata* (EeAf) exhibited the most potent cytotoxic activity against both tested cell lines in comparison to other five Athenaea genus extracts (Figure 1). Based on this result, we performed fractionation of this extract through liquid-liquid partitioning, resulting in four fractions (Table 1). The hexane-derived fraction (EeAf-HEX, 65.3 mg) was not evaluated due to being made of highly hydrophobic compounds. The dichloromethane (EeAf-DCM, 71.4 mg), ethyl acetate (EeAf-ACE, 25.5 mg), and aqueous (EeAf-WAT) fractions were assessed for cytotoxicity in *in vitro* tumor models (MCF-7 and MV3) and non-tumoral (Hek-293) cells. Their composition was determined by LC-MS/MS.

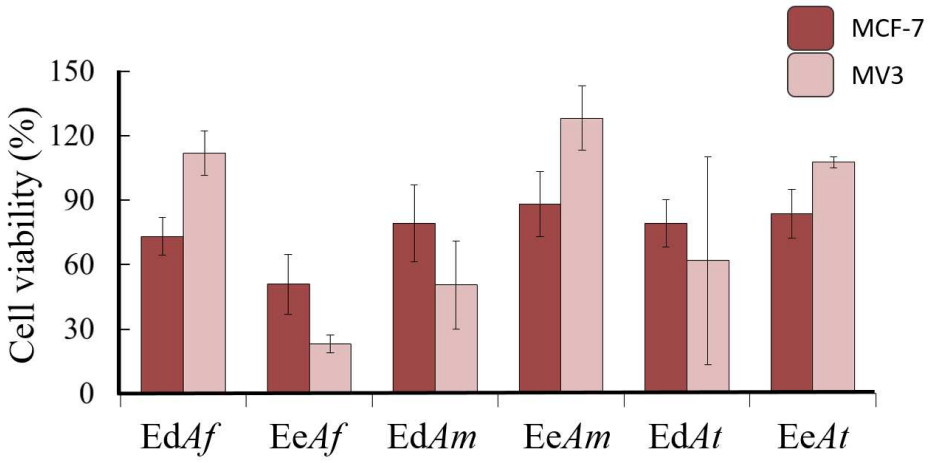

Fig. 1: MTT/formazan assay results depict the cytotoxic effects of dichloromethanic (Ed) and ethanolic (Ee) extracts produced by percolation of dry leaves from the *Athenaea* spp. *A. fasciculate* (*Af*), *A. martiana* (*Am*), and *A. tomentosa* (*At*). Cell viability was calculated relative to the control group (DMSO) using MCF-7 (red) and MV3 (pink) cell lines, and the graph represents the mean of two independent experiments, each conducted in triplicate.

We observed that the IC_{50} values of the all organic fractions decreased compared to the aqueous extract, indicating a separation of the active components according to polarity. The dichloromethane fraction exhibited a reduced IC_{50} value in both tumor cell lines and moderately decreased in the non-tumoral cell line. On the other hand, the fraction obtained with ethyl acetate (EeAf-ACE) presented the most surprising result. Its cytotoxicity increased considerably only in the two tumor cell lines, showing the statistically significant highest selectivity index among the fractions. The aqueous phase also demonstrated cytotoxic activity, though with IC_{50} values slightly higher than EeAf, indicating that there are still active compounds in this fraction.

Table 1: *In vitro* cytotoxic activity of the *A. fasciculate* extract and its fractions using the MTT/formazan assay.

	IC_{50} of each treatment, in µM (SD)			**IS**	
	MV3	MCF7	HEK-293	MV3	MCF-7
EeAf	16,98 (±5,22)	22,08 (±7,59)	10,60 (±1,45)[a]	0,6	0,5
EeAf-DCM	11,14 (±8,36)	14,95 (±9,26)	7,80 (±1,43)[a]	0,7	0,5
EeAf-ACE	7,01 (±0,50)	17,06 (±4,75)	85,86 (±61,43) [b]	12,2	5,0
EeAf-WAT	18,17 (±17,76)	27,54 (±18,92)	65,60 (±43,64) [b]	3,6	2,4

EeAf: extract ethanolic of *A. fasciculate*, EeAf-DCM: dichloromethane fraction of EeAf, EeAf-ACE: ethyl acetate fraction of EeAf, EeAf-WAT: aqueous fraction of EeAf. SI (selectivity index) = $IC_{50}^{HEK\text{-}293}/IC_{50}^{\text{cancer cell line}}$, Nonlinear regression analysis were performed to calculate de IC_{50} values, based on two independent experiment with three replicates each. Different superscript letters indicate statical significance differences between means after 1-way ANOVA and Bonferroni postests (p-value < 0.01).

LC-HRMS/MS analysis

Extracts obtained from percolation contain a mixture of structurally diverse molecules. Fractionation resulted in relatively less complex mixtures, yet the chromatograms of these fractions were quite similar (Figure 2). Withanolides are a class of natural products found in Solanaceae species, including *Athenaea velutina*, and are responsible for the antitumor activity of leaves extracts from this plant (ALMEIDA et al, 2021). They have a well-known fragmentation pattern, with the successive loss of water molecules and cleavage of the lactone group (ALMEIDA et al, 2021).

A total of 26 withanolides were annotated from the LC/MSMS data of EeAf and its fractions (Table 2). All the compounds were annotated based on the fragmentation pattern (loss of multiple water molecules) and the correspondence of mass (Erro ≤ 0.05 Da). The signals observed in the first 19 minutes of the chromatograms (Figure 2) correspond to more polar compounds, such as the ion *quasimolecular* $[M+H]^+$ at *m/z* 1075.5377, which exhibits fragmentations (*m/z* 913.4834) corresponding to the loss of a glucose unit (162 Da), followed by the loss of two deoxyhexose units of 146 Da (m/z 767.4235, 621.3650) and another glucose units (*m/z* 459.3115) attached to a putative withanolide core (*m/z* 459.3115, 441.3012, 423.2903).

This withanolide was annotated as being an aglycone derivative with a *quasimolecular* $[M+H]^+$ at *m/z* 459.3115. A withanolide compound, called pubesenolide, with identical molecular mass of this annotated aglycone was reported for the species *Physalis pubescens* (SAHAI et al., 1985), also belonging to the Solanaceae family and phylogenetically close to *A. fasciculata*. Thus, it suggests that the annotated withanolides (Rt 18.2-18.3 min.) are glycosylated derivatives of pubesenolide. The mass and fragmentation pattern supported the annotation, with successive losses of water molecules observed (*m/z* 441.3003, 423.2896, 405.2796), and a peak at *m/z* 157.1019 could corresponds to the ion referring to the aglycone group (ALMEIDA et al., 2021). This aglycone and its polyglycosylated derivatives were found mostly in the EeAf and EeAf-WAT (sample A and E). The isolated Pubesenolide-like withanolide and the derivative with only one glycoside were concentrated in the fraction EeAf-ACE (Sample D), along with the 20β-Hydroxy-1-oxo-(22R)-witha-2,5,24-trienolide-like compound.

Four compound were annotaded as derivatives of Withaferin A (Rt 28.7-29.1 min), due to the presence of fragments corresponding to loss of multiple waters (*m/z* 453.2658, 435.2551, 425.2707, 417.2446) and molecular mass correspondence (Erro 0.001-0.006 Da). They were found in the EeAf and the fraction EeAf-DCM, including two dimeric structures. This withanolide is known for its cytotoxicity and antitumoral activities (XIA et al., 2020). One

Withaferin A-like withanolide was annotated in the fraction EeAf-DCM (sample C) with similar mass and fragmentation patterns but different retention time (*m/z* 471.2439 and 958.5717, Rt: 24.3 to 24.7 min) compared to the same annotated structure in EeAf,suggesting that this fraction has multiple isomers of this molecule.

Withanolide B-like compounds were annotated in EeAf and the fractions EeAf-DCM and ACE (samples A, C, and D) (Rt 28.6-29.2 min). This molecule, first isolated from *Lycium chinense* (Solanaceae), has been described as a potential neurotherapeutic agent, but little is known about its antitumoral effects (RATH et al., 2019; GIRME et al., 2020; BALKRISHNA et al., 2023). The mass correspondence and fragments at m/z 455.2821, 437.2710, 419.2601 (loss of water) support that annotation.

25,25-dihydrowithanolide D-like withanolide, annotated based on the fragmentation pattern of multiple losses of water (m/z 455.2802, 437.2699, 419.2595) and mass correspondence, was concentrated in the fraction EeAf- DCM (sample C). That compound showed high cytotoxicity and selectivity towards lymphotropic virus type 1 (HTLV-1)-infected T-cell lines (MT-1 and MT-2) and fresh Adult T-cell leukemia/lymphoma (ATL) (NAKANO et al., 2013; KINJO et al., 2016).

There were three withanolides concentrated in the fractions EeAf-DCM and ACE (Samples C and D) were annotated as Sinubrasolide L (*m/z* 425.3063) and derivatives (*m/z* 407.2958 and 485.3280), based on the mass correspondence and the presence of fragments at m/z 407.2954 (loss of water) and m/z 425.3061 (loss of acetic acid). That molecule was isolated from a cultured soft coral *Sinularia brassica*, one of the few marine sources of withanolides, along with other eleven sinubrasolides (A-K). The cytotoxicity of Sinubrasilide L was evaluated against a panel of tumoral cell lines (leukemia and colon cancer) and showed no activity. Our results suggest that this molecule could be at least partially responsible for the cytotoxicity of EeAf-DCM and ACE against melanoma and breast cancer cells (HUANG et al., 2017).

The MS1 and MS2 spectra of the annotated withanolides are listed in the Supplementary material.

Table 2: Withanolides annotated from LC/MSMS analysis of EeAf and fractions.

RT (min)	m/z	Adduct	Fragments	Aglycone Formula	Annotation	Erro (Da)	Samples
18.2, 18.2	1075	[M+H]+	1075.5377, 913.4834, 767.4235, 621.3650, 459.3115, 441.3012, 423.2903, 269.1910	$C_{28}H_{42}O_5$ (MW 458)	Pubsenolide-like tetra-glycosylated (glu-rha-rha-glu)	-0.036	a, e
18.1-18.2, 18.1-18.2	929	[M+H]+	929.4809, 767.4248, 621.3649, 459.3117, 441.3012, 423.2910, 269.1912	$C_{28}H_{42}O_5$ (MW 458)	Pubsenolide-like tri-glycosylated (glu-rha-glu)	-0.016	a, e
18.1-18.2, 18.1-18.3	767	[M+H]+	767.4269, 621.3641, 459.3121, 441.3003, 423.9896, 269.1913	$C_{28}H_{42}O_5$ (MW 458)	Pubsenolide-like bi-glycosylated (rha-glu)	-0.015	a, e
18.2-18.3, 18.2	783	[M+H]+	783.4198, 621.3646, 459.3116, 441.3013, 423.2904, 405.2799, 269.1909	$C_{28}H_{42}O_5$ (MW 458)	Pubsenolide-like bi-glycosylated (glu-glu)	0.002	a, e
28.7-28.8, 29.0-29.1	958	[M+H+NH3]+	488.3035, 471.2763, 453.2665, 435.2552, 281.1552.	$C_{28}H_{38}O_6$ (MW 470)	Withaferin-A-like dimer	0.006	a, c
28.8, 29.0-29.1	941	[M+H]+	941.5473, 471.2765, 453.2660, 435.2551, 425.2709.	$C_{28}H_{38}O_6$ (MW 470)	Withaferin-A-like dimer	0.005	a, c
28.6-28-7, 29.0	488	[M+H+NH3]+	488.3031, 471.2762, 453.2656, 435.2555, 281.1556	$C_{28}H_{38}O_6$ (MW 470)	Withaferin-A-like	0.001	a, c
28.6-28.8, 28.9-29.0	471	[M+H]+	471.2766, 453.2658, 435.2551, 425.2707, 417.2446, 281.1554	$C_{28}H_{38}O_6$ (MW 470)	Withaferin-A-like	0.002	a, c
28.9-29.0, 29.1-29.4	926	[M+H+NH3]+	926.5813, 437.2709, 455.2818, 419.2600	$C_{28}H_{38}O_5$ (MW 454)	Withanolide B-like dimer	0.002	a, c
28.9-29.0, 29.2-29.4	909	[M+H]+	909.5565, 455.2818, 437.2706, 419.2603	$C_{28}H_{38}O_5$ (MW 454)	Withanolide B-like dimer	0.005	a, c
28.9-29.0, 29.2-29.4, 28.6	455	[M+H]+	455.2821, 437.2710, 419.2601, 401.2492, 281.1551	$C_{28}H_{38}O_5$ (MW 454)	Withanolide B-like	0.002	a, c, d
28.9, 29.2, 28.6	472	[M+H+NH3]+	455.2816, 437.2706, 419.2598	$C_{28}H_{38}O_5$ (MW 454)	Withanolide B-like	0.002	a, c, d
23.2	962	[M+H+NH3]+	945.5813, 473.3113, 455.2818, 437.2709, 419.2600	$C_{28}H_{40}O_6$ (MW 472)	24,25-dihydrowithanolide D-like dimer	0.004	c
23.1-23.2	473	[M+H]+	437.2699, 419.2595, 301.1810, 283.1703, 265.1597	$C_{28}H_{40}O_6$ (MW 472)	24,25-dihydrowithanolide D-like	0.001	c
23.1	490	[M+H+NH3]+	473.2907, 455.2818, 437.2709, 301.1809, 283.1709, 265.198	$C_{28}H_{40}O_6$ (MW 472)	24,25-dihydrowithanolide D-like	0.001	c
23.1-23.3	455	[M+H]+	455.2805, 437.2702, 419.2592, 301.1811, 283,1707, 265.1595, 171.0810	C28H38O5 (MW 454)	Withanolide B-like	0.001	c
23.9-24.0	459	[M+H]+	459.3117, 423.2905, 287.2017, 269.1911, 251.1809, 157.1020	$C_{28}H_{42}O_5$ (MW 458)	Pubsenolide-like	0.001	c
24.5	471	[M+H]+	453.2650, 435.2546, 417.2439, 299.1653, 281.1546	$C_{28}H_{38}O_6$ (MW 470)	Withaferin-A-like	0.001	c
24.6	958	[M+H+NH3]+	958.5736, 488.3016, 471.2757, 453.2648, 435.2545, 299.1648, 281.1549	$C_{28}H_{38}O_6$ (MW 470)	Withaferin-A-like dimer	0.005	c
24.6-24.7, 24.2-24.4	425	[M+H]+	425.3061, 407.2954, 253.1959, 157.1018	$C_{28}H_{40}O_3$ (MW 424)	Sinubrasolide L-like	0.000	c, d
24.7, 24.3	407	[M+H-H2O]	407.2958, 253.1962, 157.1016	$C_{28}H_{40}O_3$ (MW 424)	Sinubrasolide L-like - water	0.005	c, d
24.6-24.7, 24.3	485	[M+H+Ac]+	425.3061, 407.2954, 253.1964, 157.1018	$C_{28}H_{40}O_3$ (MW 424)	Sinubrasolide L-like acetate	-0.030	c, d
20.4-20.6	459	[M+H]+	456.3110, 423.2897, 287.2015, 269.1908, 251.1802, 157.1014	$C_{28}H_{42}O_5$ (MW 458)	Pubsenolide-like	0.001	d
20.5-20.9	621	[M+H]+	621.3633, 459.3113, 441.3006, 423.2901, 269.1909, 251.1804	$C_{28}H_{42}O_5$ (MW 458)	Pubsenolide-like glycosylated (glu)	-0.001	d
21.0-21.1	457	[M+H+H2O]+	457.2952, 439.2845, 287.2012, 269.1907, 251.1802	$C_{28}H_{38}O_4$ (MW 438)	20beta-Hydroxy-1-oxo-(22R)-witha-2,5,24-trienolide-like + water	-0.005	d
21.0	439	[M+H]+	439.2845, 269.1909, 251.1803	$C_{28}H_{38}O_4$ (MW 438)	20beta-Hydroxy-1-oxo-(22R)-witha-2,5,24-trienolide-like	0.000	d

Samples: EeAf (a), EeAf-DCM (c), EeAf-ACE (d), EeAf-WAT (e). RT: Retention time of the ion in each sample. Quasimolecular ions with similar *m/z* values and fragmentation patterns, but with different Rt were displayed on separate lines. The fragmentation pattern for withanolides described was observed in the sample firstly annotated. Aglycone formula corresponds to the formula of the annotated withanolide without glycosylation or adducts. Annotation was proposed based on the molecular ion mass and fragmentation patterns. The error of each annotation was calculated as (observed molecular mass) - (annotation mass). The mass values used for that calculation were: Pubsenolide (458.3032), Withaferin A (470.2668), Withanolide B (454.2719), 24,25-dihydrowithanolide D (472.2825), Sinubrasolide L (424.2984), 20β-Hydroxy-1-oxo-(22R)-witha-2,5,24-trienolide (438.2770).

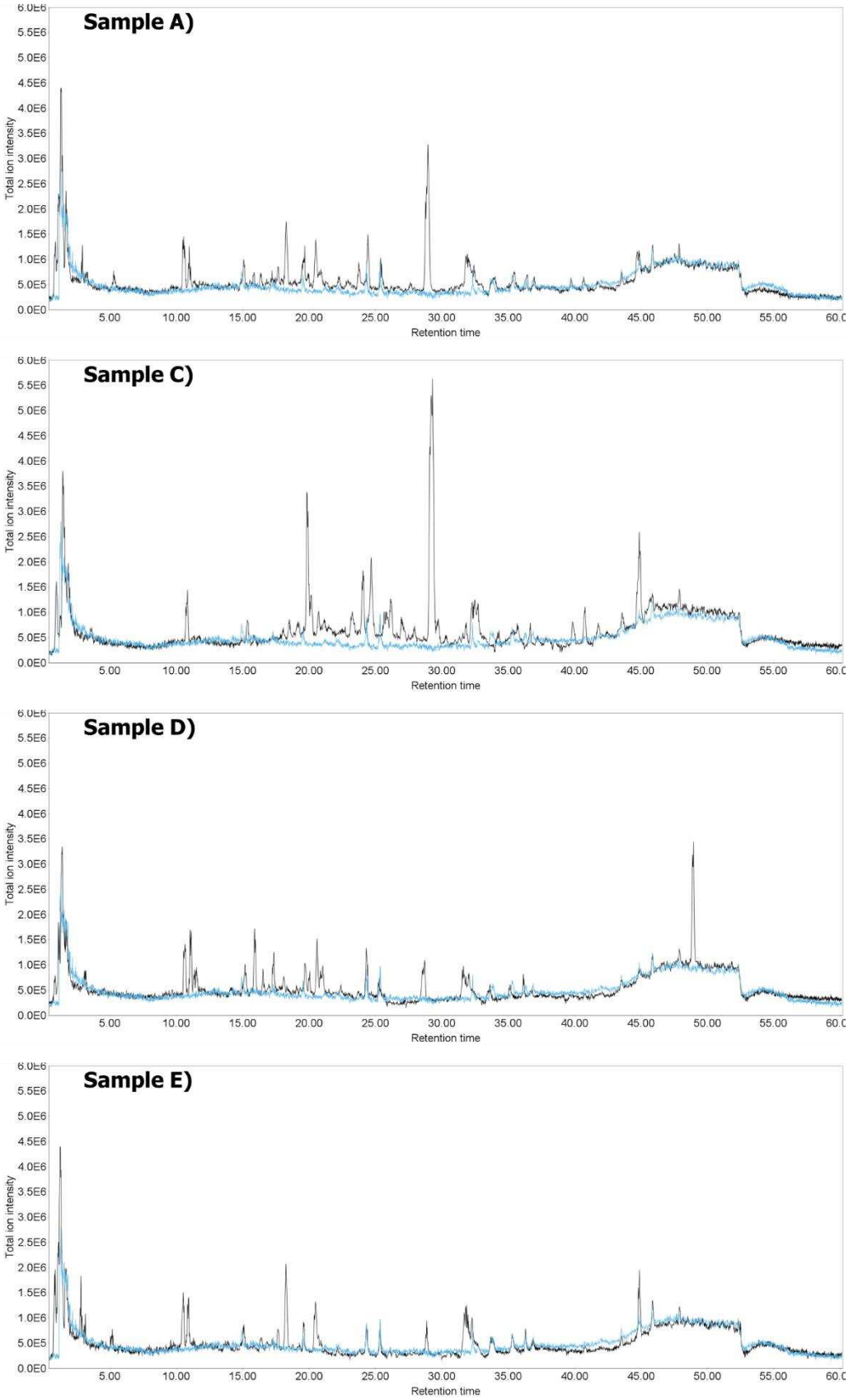

Figure 2: Total ion chromatogram of the ethanolic extract of A. fasciculate (EeAf-A), and its derivated dichloromethane (EeAf-DCM-C), ethyl acetate (EeAf-ACE-D), and aqueous (EeAf-WAT-E) fractions, analysed by LC-HRMS in positive mode. The blue chromatogram correspond to the solvente.

3.5 Conclusions

In our study, we reported the cytotoxic activity of extracts obtained from different species of the *Athenaea* genus. The ethanolic extract of *A. fasciculata* exhibited higher cytotoxicity in all the *in vitro* models evaluated. We initiated bioguided fractionation from this extract, resulting in three organic fractions (EeAf-HEX, EeAf-DCM, and EeAf-ACE) and one aqueous fraction (EeAf-WAT). All fractions maintained activity against the evaluated cell lines; however, the EeAf-ACE fraction demonstrated relatively superior cytotoxicity against the tumor cell lines and significantly lower cytotoxicity against the normal cell line. Fragmentation analysis suggests the presence of glycosylated withanolides in all three fractions, but the acetate fraction is less complex than the others and retains the bioactive compounds, making it the most promising for future fractionations aimed at isolating these bioactive molecules.

To our knowledge, this is the first report of cytotoxic activity in human cancer *in vitro* models for *A. fasciculata*, which may be attributed to the presence of glycosylated withanolides. Further studies will be conducted to isolate and characterize the active molecules in the ethyl acetate fraction.

3.6 Acknowledgements

This study was financed by the Fundação de Amparo à Pesquisa do Estado de Minas Gerais (FAPEMIG) and the Coordenação de Aperfeiçoamento de Pessoal de Nível Superior - Brasil (CAPES) - Finance Code 001.

3.7 Conflict of interest

Authors have no conflict of interest to declare.

3.8 References

ALMEIDA, A.A., COTA, B.B., RODRIGUES, L. M., DUTRA, L. L., KOHLHOFF, M., BRESSAN, G. C., BRANDÃO. G. C., LEITE, J. P. V. Withalutin, a new cytotoxic withanolide from *Athenaea velutina* (Sendtn.) D'Arcy. *Natural Product Research*, v. 13, p. 1-8, 2022. DOI: 10.1080/14786419.2022.2039135

ALMEIDA, A.A., LIMA, G.D.A., EITERER, M., RODRIGUES, L.A., DO VALE, J.A., ZANATTA, A.C., BRESSAN, G.C., DE OLIVEIRA, L.L., LEITE, J.P.V. A withanolide-rich fraction of *Athenaea velutina* induces apoptosis and cell cycle arrest in melanoma B16F10 cells. *Planta Medica*, 2021. DOI: 10.1055/a-1395-9046

ALMEIDA, A.A., LIMA, G.D.A., SIMÃO, M.V.R.C., MOREIRA, G.A., SIQUEIRA, R.P., ZANATTA, A.C., VILEGAS, W., MACHADO-NEVES, M., BRESSAN, G.C., LEITE, J.P.V. Screening of plants from the Brazilian Atlantic Forest led to the identification of *Athenaea*

velutina (Solanaceae) as a novel source of antimetastatic agentes. *International Journal of Experimental Pathology*, v.10, n.3-4, p. 106-121, 2020.

ALMEIDA-LAFETÁ, R. C., FERREIRA, M. J. P., EMERENCIANO, V. P., KAPLAN, M. A. C. Withanolides from *Aureliana fasciculata* var. *fasciculata*. *Helvetica Chimica Acta*, v. 93, 2010.

BALKRISHNA, A., BHATTACHARYA, K., SHUKLA, S. AND VARSHNEY, A. Neuroprotection by Polyherbal Medicine Divya-Medha-Vati Against Scopolamine-Induced Cognitive Impairment Through Modulation of Oxidative Stress, Acetylcholine Activity, and Cell Signaling. *Molecular Neurobiology*, p.1-20. 2023.

BIZZARRI, M., GIULIANI, A., MONTI, N., VERNA, R., PENSOTTI, A. AND CUCINA, A. Rediscovery of natural compounds acting via multitarget recognition and noncanonical pharmacodynamical actions. *Drug Discovery Today*, v. 25, p.920-927, 2020. DOI: 10.1016/j.drudis.2020.02.010

DUTRA, L.L., BORGES, R.J., MALTAROLLO, V.G., MENDES, T.A., BRESSAN, G.C. AND LEITE, J.P.V. *In silico* evaluation of pharmacokinetics properties of withanolides and simulation of their biological activities against Alzheimer's disease. *Journal of Biomolecular Structure and Dynamics*, p.1-16, 2023. DOI: 10.1080/07391102.2023.2206909

FERLAY, J., ERVIK, M., LAM, F., COLOMBET, M., MERY, L., PIÑEROS, M., et al. Global Cancer Observatory: Cancer Today. Lyon: International Agency for Research on Cancer; 2020 (https://gco.iarc.fr/today, accessed January 2024).

GIRME, A., SASTE, G., PAWAR, S., BALASUBRAMANIAM, A.K., MUSANDE, K., DARJI, B., SATTI, N.K., VERMA, M.K., ANAND, R., SINGH, R. AND VISHWAKARMA, R.A. Investigating 11 withanosides and withanolides by UHPLC–PDA and mass fragmentation studies from Ashwagandha (*Withania somnifera*). *ACS omega*, v.*5*, p.27933-27943. 2020.

HUANG, C.Y., AHMED, A.F., SU, J.H., SUNG, P.J., HWANG, T.L., CHIANG, P.L., DAI, C.F., LIAW, C.C. AND SHEU, J.H. Bioactive new withanolides from the cultured soft coral *Sinularia brassica*. *Bioorganic & Medicinal Chemistry Letters*, v.*27*, p.3267-3271. 2017.

KINJO, J., NAKANO, D., FUJIOKA, T. AND OKABE, H. Screening of promising chemotherapeutic candidates from plants extracts. *Journal of natural medicines*, v.*70*, p.335-360. 2016.

NAKANO, D., ISHITSUKA, K., KATSUYA, H., KUNAMI, N., NOGAMI, R., YOSHIMURA, Y., MATSUDA, M., KAMIKAWA, M., TSUCHIHASHI, R., OKAWA, M. AND IKEDA, T. Screening of promising chemotherapeutic candidates from plants against human adult T-cell leukemia/lymphoma (II): apoptosis of antiproliferactive principle (24, 25-dihydrowithanolide D) against ATL cell lines and structure–activity relationships with withanolides isolated from solanaceous plants. *Journal of natural medicines*, v.*67*, p.415-420. 2013.

NEWMAN, D.J., and CRAGG, G.M. Natural products as sources of new drugs over the nearly four decades from 01/1981 to 09/2019. *Journal of natural products*, v. 83(3), p.770-803, 2020.

RATH, S.N., JENA, L. and PATRI, M. Understanding ligands driven mechanism of wild and mutant aryl hydrocarbon receptor in presence of phytochemicals combating Parkinson's disease: an *in silico* and *in vivo* study. *Journal of Biomolecular Structure and Dynamics*, 2019.

RODRIGUES, I. M. C., KNAPP, S., STEHMANN, J. R. The nomenclatural re-establishment of *Athenaea* Sendtn. (Solenaceae) with a nomenclatural synopsis of the genus. *Taxon*, 2019. DOI:https://doi.org/10.1002/tax.12089

SAHAI, M. Pubesenolide, a new withanolide from *Physalis pubescens*. *Journal of Natural Products*, v.48, p.474-476.1985.

SCHMID, R., HEUCKEROTH, S., KORF, A., SMIRNOV, A., MYERS, O., DYRLUND, T.S., BUSHUIEV, R., MURRAY, K.J., HOFFMANN, N., LU, M., and SARVEPALLI, A. Integrative analysis of multimodal mass spectrometry data in MZmine 3. *Nature biotechnology*, v. 41(4), p.447-449, 2023.

SILVA, E. L., ALMEIDA-LAFETÁ, R. C., BORGES, R. M. e STAERK, D. Athenolide A, a new steroidal lactone from the leaves of *Athenaea martiana* (Solanaceae) determined by means of HPLC-HR-MS-SPE-NMR analysis. *Chem. Biodiversity*, v. 15, 2018. DOI: 1 0.1002/cbdv.201700455

STONE, S., NEWMAN, D.J., COLLETTI, S.L. AND TAN, D.S. Cheminformatic analysis of natural product-based drugs and chemical probes. *Natural Product Reports*, v.39, p.20-32, 2022. DOI: 10.1039/D1NP00039J

WANG, M., CARVER, J.J., PHELAN, V.V., SANCHEZ, L.M., GARG, N., PENG, Y., NGUYEN, D.D., WATROUS, J., KAPONO, C.A., LUZZATTO-KNAAN, T. AND PORTO, C. Sharing and community curation of mass spectrometry data with Global Natural Products Social Molecular Networking. *Nature biotechnology*, v. 34(8), p.828-837, 2016.

Overall conclusion

Withanolides are a promissing and diverse class of natural products, with many biological activities associated to them. In this study we aimed to elucidate how the structural diversity of withanolides influences their pharmacokinetic properties and interaction with potential molecular targets involved in the development of Alzheimer's Disease through a *in silico* approach. We highlighted the importance of unsaturations at carbons C5 and C16 or C17 as promoters of a better pharmacokinetic profile and better interaction with the catalytic site of cholinesterase enzymes, the most likely targets to thes small molecules. This study was published by Dutra and colleagues (2023), with the full text detailed in Chapter 1.

Building upon the work of Almeida and colleagues (2022), we also investigated how the structural differences of these molecules reflect on their cytotoxicity in human cancer cell models (melanoma and human breast cancer). While withalutin exhibited a higher IC_{50} value compared to the other two withanolides in both cell lines, all three significantly reduced cell proliferation in the melanoma model. A possible mechanism of action responsible for these activities could be the interaction with the transcription factor STAT3, preventing its activation and subsequent gene regulation. Our study revealed that withalutin does not share the same binding site as the other two withanolides in a blind molecular docking simulation. The absence of the epoxide ring at carbons C5 and C6 of withalutin results in a weaker interaction with the suggested target, which may justify its lower activity compared to the other two withanolides.

To continue to bioprospecting for new molecules with anticancer activity on the genus *Athenaea* we evaluated the cytotoxic activity of dichloromethane and ethanolic extracts generated by exhaustive percolation of dried leaves from *A. fasciculata, A. martiana, and A. tomentosa* species on *in vitro* human cell lines. Among these, the ethanolic extract of *A. fasciculata* (EEAf) showed lower IC_{50} values for both tumor cell lines (16.9 ± 5.2 µM in melanoma and 22.1 ± 7.6 µM in breast cancer). After fractionating this extract by liquid-liquid partition, increased cytotoxicity was observed in the dichloromethane and ethyl acetate fractions. The composition of the extract and its fractions was evaluated by LC-MS/MS and the chromatogram analysis sugest the presence of glycosilated withanolides, as awell other molecules that were find mainly on the EeAf-ACE fraction.

APÊNDICE A: tabelas suplementares ao capítulo 1

Supplementary information for *In silico* evaluation of pharmacokinetics properties of withanolides and simulation of their biological activities against Alzheimer's disease

Luana Lucas Dutra, Rafael J. Borges, Vinícius G. Maltarollo[1], Tiago Antônio de Oliveira Mendes, Gustavo Costa Bressan, João Paulo Viana Leite

Department of Biochemistry and Molecular Biology Universidade Federal de Viçosa
[1]Pharmaceutical Products Department- Faculty of Pharmacy Federal University of Minas Gerais
Minas Gerais, Brazil
Contributing authors: luanalucasdutra@gmail.com; rafael.j.borges@ufv.br; maltarollo@ufmg.br; tiagomendes@gmail.com; gustavo.bressan@ufv.br; jpvleite@ufv.br

Table 1: Identification of the withanolides evaluated. The SMILES structures were described by Xia et al (2020), except for the molecules 1, 3, and 17 (Almeida et al. 2022).

ID	NAME	SMILES
1	Withacnistine	[H][C@@]1(CC[C@@]2([H])[C@]3([H])C[C@H]4O[C@]44[C@@H](O)C=CC(=O)[C@]4(C)[C@@]3([H])CC[C@]12COC(C)=O)[C@H](C)[C@@]1([H])CC(C)=C(C)C(=O)O1
2	Withanolide D	O=C1[C@@]2(C)[C@@]([C@H]3C[C@]4([H])[C@]2([H])CC[C@@]5(C)[C@@]4([H])CC[C@]5([H])[C@@]([C@]6([H])OC(C(C)=C(C)C6)=O)(C)O)(O3)[C@@H](O)C=C1
3	Withacnistin-acetate	[H][C@@]1(CC[C@@]2([H])[C@]3([H])C[C@H]4O[C@]44[C@@H](OC(C)=O)C=CC(=O)[C@]4(C)[C@@]3([H])CC[C@]12COC(C)=O)[C@H](C)[C@@]1([H])CC(C)=C(C)C(=O)O1
4	Aurelianolide A	O=C1[C@@]2(C)[C@@]([C@H]3C[C@]4([H])[C@]2([H])CC[C@@]5(C)[C@]4(C[C@@H](OC(C)=O)[C@]5(O)[C@@H]([C@]6([H])OC(C(C)=C(C)C6)=O)C)[H])(O3)[C@@H](O)C=C1
5	28-Hydroxytubocapsanolide A	O=C1[C@@]2(C)[C@@]([C@H]3C[C@]4([H])[C@]2([H])CC[C@@]5(C)[C@@]4([H])C[C@@H](O6)[C@]56[C@@H]([C@]7([H])OC(C(C)=C(CO)C7)=O)C)(O3)[C@@H](O)C=C1
6	27-O-acetyl-withaferin A	O=C1[C@@]2(C)[C@@]([C@H]3C[C@]4([H])[C@]2([H])CC[C@@]5(C)[C@]4(CC[C@]5([H])[C@@H]([C@]6([H])OC(C(COC(C)=O)=C(C)C6)=O)C)[H])(O3)[C@@H](O)C=C1
7	5β,6β-Epoxy-4β-hydroxy-27-(1-formyloxy-1-methylethoxy)-1-oxo-witha-2,24-dienolide	O=C1[C@@]2(C)[C@@]([C@H]3C[C@]4([H])[C@]2([H])CC[C@@]5(C)[C@]4(CC[C@]5([H])[C@@H]([C@]6([H])OC(C(COC(C)(C)OC([H])=O)=C(C)C6)=O)C)[H])(O3)[C@@H](O)C=C1
8	27-O-acetyl-viscosalactone B	O=C1[C@@]2(C)[C@@]([C@H]3C[C@]4([H])[C@]2([H])CC[C@@]5(C)[C@]4(CC[C@]5([H])[C@@H]([C@]6([H])OC(C(COC(C)=O)=C(C)C6)=O)C)[H])(O3)[C@@H](O)[C@@H](O)C1
9	Tubocaapsanolide MAP	O=C1[C@@]2(C)[C@@]([C@H]3C[C@]4([H])[C@]2([H])CC[C@@]5(C)[C@]4(C[C@@H](O6)[C@]56[C@@H]([C@]7([H])OC(C(C)=C(C)C7)=O)C)[H])(O3)[C@@H](O)[C@H](OC)C1
10	2,3-Dihydrotubocapsanolide A	O=C1[C@@]2(C)[C@@]([C@H]3C[C@]4([H])[C@]2([H])CC[C@@]5(C)[C@@]4([H])C[C@@H](O6)[C@]56[C@@H]([C@]7([H])OC(C(C)=C(C)C7)=O)C)(O3)[C@@H](O)CC1
11	3β-Ethoxy-2,3-dihydrotubocapsanolide A	O=C1[C@@]2(C)[C@@]([C@H]3C[C@]4([H])[C@]2([H])CC[C@@]5(C)[C@@]4([H])C[C@@H](O6)[C@]56[C@@H]([C@]7([H])OC(C(C)=C(C)C7)=O)C)(O3)[C@@H](O)[C@@H](OCC)C1
12	3α-(Uracil-1-yl)-2,3-dihydrowithaferin A	O=C1[C@@]2(C)[C@@]([C@H]3C[C@]4([H])[C@]2([H])CC[C@@]5(C)[C@]4(CC[C@]5([H])[C@@H]([C@]6([H])OC(C(CO)=C(C)C6)=O)C)[H])(O3)[C@@H](O)[C@H](N7C(NC(C=C7)=O)=O)C1

13	3β-(Uracil-1-yl)-2,3-dihydrowithaferin A	O=C1[C@@]2(C)[C@@](C@H]3C[C@]4([H])[C@]2([H])CC[C@@]5(C)[C@]4(CC[C@]5([H])[C@@H]([C@]6([H])OC(C(CO)=C(C)C6)=O)C)[H])(O3)[C@@H](O)[C@@H](N7C(NC(C=C7)=O)=O)C1
14	3β-(Adenin-9-yl)-2,3-dihydrowithaferin A	O=C1[C@@]2(C)[C@@](C@H]3C[C@]4([H])[C@]2([H])CC[C@@]5(C)[C@]4(CC[C@]5([H])[C@@H]([C@]6([H])OC(C(CO)=C(C)C6)=O)C)[H])(O3)[C@@H](O)[C@@H](N7C=NC8=C(N)N=CN=C87)C1
15	14α,15α-Epoxywithaferin A	C[C@@]12[C@@](C@H]3C[C@]4([H])[C@]2([H])CC[C@@]5(C)[C@]4(O6)[C@H]6C[C@]5([H])[C@@H]([C@]7([H])OC(C(CO)=C(C)C7)=O)C)(O3)[C@@H](O)C=CC1=O
16	Withaoxylactone	C[C@@]12[C@@](C@H]3C[C@]4([H])[C@]2([H])CC[C@@]5(C)[C@]4(O6)[C@H]6C[C@]5([H])[C@@H]([C@]7([H])OC(C(CO)=C(C)C7)=O)C)(O3)[C@@H](O)[C@@H](O)CC1=O
17	Withalutin	[H][C@@]12CC[C@@H]([C@H](C)[C@H]3CC(C)=C(C)C(=O)O3)[C@@]1(COC(C)=O)CC[C@@]1([H])[C@@]2([H])CC=C2[C@@H](O)C=CC(=O)[C@]12C
18	5,6-deoxywithaferin A	O=C(C=C[C@@H]1O)[C@@]2(C)C1=CC[C@]3([H])[C@]2([H])CC[C@@]4(C)[C@]3(CC[C@]4([H])[C@@H]([C@]5([H])OC(C(CO)=C(C)C5)=O)C)[H]
19	Aurelianolide B	O=C(C=C[C@@H]1O)[C@@]2(C)C1=CC[C@]3([H])[C@]2([H])CC[C@@]4(C)[C@]3(C[C@@H](OC(C)=O)[C@]4(O)[C@@H]([C@]5([H])OC(C(C)=C(C)C5)=O)C)[H]
20	Obtusifonolide	CC(C1)=C(CO)C(O[C@@]1([H])[C@@H](C)[C@@]2([H])[C@H](OC(C)=O)C[C@@]3([H])[C@]4([H])CC=C([C@@]5(C)[C@@]4([H])CC[C@@]32C)CC=CC5=O)=O
21	Withacoagulin D	O=C(C=CC1)[C@@]2(C)C1=CC[C@]3([H])[C@]2([H])CC[C@@]4(C)[C@@]3(O)CC[C@@]4([C@@]([C@]5([H])OC(C(CO)=C(C)C5)=O)(C)O)O
22	Withacoagulin G	O=C(C=CC1)[C@@]2(C)C1=CC[C@]3([H])[C@]2([H])CC[C@@]4(C)[C@@]3([H])CC[C@@]4([C@@]([C@]5([H])OC(C(CO)=C(C)C5)=O)(C)O)O
23	Withacoagulin H	O=C(C=CC1)[C@@]2(C)C1=CC[C@]3([H])[C@]2([H])CC[C@@]4(C)C3=CC[C@@]4([C@@]([C@]5([H])OC(C(CO)=C(C)C5)=O)(C)O)O
24	(22R)-4α,17α,27-Trihydroxy-1-oxo-witha-2,5,24-trienolide	O=C(C=C[C@H]1O)[C@@]2(C)C1=CC[C@]3([H])[C@]2([H])CC[C@@]4(C)[C@@]3([H])CC[C@@]4([C@@H]([C@]5([H])OC(C(CO)=C(C)C5)=O)C)O
25	Withacoagulide C	O=C(C=CC1)[C@@]2(C)C1=CC[C@]3([H])[C@]2([H])CC[C@@]4(C)[C@@]3(CC[C@]4(O)[C@@]([C@]5([H])OC(C(C)=C(C)C5)=O)(C)O)O

26	Withasilolide A	O=C(C=CC1)[C@@]2(C)C1=C[C@@H](O)[C@]3([H])[C@]2([H])CC[C@@]4(C)[C@@]3([H])CC[C@]4([H])[C@@]([C@]5([H])OC(C(C)=C(C)C5)=O)(C)O
27	Withasilolide B	O=C(C=CC1)[C@@]2(C)C1=C[C@@H](O)[C@]3([H])[C@]2([H])CC[C@@]4(C)[C@@]3([H])CC[C@]4([H])[C@@]([C@]5([H])OC([C@H](C)[C@@H](C)C5)=O)(C)O
28	5,6-De-epoxy-5-en-7-one-17-hydroxy withaferin A	O=C(C=C[C@@H]1O)[C@@]2(C)C1=CC([C@]3([H])[C@]2([H])CC[C@@]4(C)[C@@]3([H])CC[C@@]4([C@@H](C5OC(C(CO)=C(C)C5)=O)C)O)=O
29	Withacoagulin I	O=C(CC=C1)[C@@]2(C)C1=CC[C@]3([H])[C@]2([H])CC[C@@]4(C)[C@]3(O)CC[C@@]4([C@@]([C@]5([H])OC(C(CO)=C(C)C5)=O)(C)O)O
30	Withacoagulide D	O=C(CC=C1)[C@@]2(C)C1=CC[C@]3([H])[C@]2([H])CC[C@@]4(C)[C@@]3(CC[C@]4(O)[C@@]([C@]5([H])OC(C(C)=C(C)C5)=O)(C)O)O
31	27-Hydroxywithanolide K	O=C(CC=C1)[C@@]2(C)C1=CC[C@]3([H])[C@]2([H])CC[C@@]4(C)[C@@]3(O)CC[C@]4(O)[C@@]([C@]5([H])OC(C(CO)=C(C)C5)=O)(C)O
32	27-Hydroxywithanolide I	O=C(CC=C1)[C@@]2(C)C1=CC[C@]3([H])[C@]2([H])CC[C@@]4(C)[C@@]3(O)CC[C@]4([H])[C@@H]([C@]5([H])OC(C(CO)=C(C)C5)=O)C
33	Withacoagulin F	O=C(CC=C1)[C@@]2(C)C1=CC[C@]3([H])[C@]2([H])CC[C@@]4(C)[C@]3(O)CC[C@]4([H])[C@@H]([C@]5([H])OC(C(C)=C(C)C5)=O)C
34	Withanolide H	O=C(CC=C1)[C@@]2(C)C1=CC[C@]3([H])[C@]2([H])CC[C@@]4(C)[C@@]3(O)CC[C@]4([H])[C@@]([C@]5([H])OC(C(CO)=C(C)C5)=O)(C)O
35	Withacoagulin E	O=C(CC=C1)[C@@]2(C)C1=CC[C@]3([H])[C@]2([H])CC[C@@]4(C)[C@]3(O)CC[C@]4([H])[C@@]([C@]5([H])OC(C(C)=C(C)C5)=O)(C)O
36	2,3-Dihydro-3β,27-dihydroxywithanolide I	O=C(C[C@H](O)C1)[C@@]2(C)C1=CC[C@]3([H])[C@]2([H])CC[C@@]4(C)[C@@]3(O)CC[C@]4([H])[C@@]([C@]5([H])OC(C(CO)=C(C)C5)=O)(C)O
37	2,3-Dihydro-3β-O-β-D-glucopyranosylwithanolide I	O=C(C[C@H](O[C@@H]([C@@H]1O)O[C@H](CO)[C@@H](O)[C@@H]1O)C2)[C@@]3(C)C2=CC[C@]4([H])[C@]3([H])CC[C@@]5(C)[C@@]4(O)CC[C@]5([H])[C@@]([C@]6([H])OC(C(C)=C(C)C6)=O)(C)O
38	14-Epicoagulin O	C[C@]12C(C[C@@H](O[C@@H]([C@@H]3O)O[C@H](CO)[C@@H](O)[C@@H]3O)CC2=O)=CC[C@]4([H])[C@]1([H])CC[C@@]5(C)[C@]4(O)CC[C@]5([H])[C@@]([C@]6([H])OC(C(C)=C(C)C6)=O)(C)O

39	14-Epicoagulansin B	C[C@]12C(C[C@@H](O)CC2=O)=CC[C@]3([H])[C@]1([H])CC[C@@]4(C)[C@]3(O)CC[C@]4([H])[C@@]([C@]5([H])OC([C@@H]([C@@H](C)C5)C)=O)(C)O
40	Withacoagulin A	C[C@]12C(C=CCC2=O)=CC[C@]3([H])[C@]1([H])CC[C@@]4(C)C3=CC[C@]4(O)[C@]([C@]5([H])OC(C(C)=C(C)C5)=O)(O)C
41	Withanolide P	C[C@]12C(CC=CC2=O)=CC[C@]3([H])[C@]1([H])CC[C@@]4(C)[C@]3(O)CC[C@]4(O)[C@@H]([C@]5([H])OC(C(C)=C(C)C5)=O)C
42	Wadpressine	O=C(C[C@H](O[C@@H]([C@@H]1O)O[C@H](CO)[C@@H](O[C@@H]([C@@H]2O)O[C@@H](C)[C@H](O)[C@H]2O)[C@@H]1O)C3)[C@@]4(C)C3=CC[C@@]5([H])[C@]4([H])CC[C@@]6(C)[C@]5(CC[C@@]6(O)[C@@]([C@]7([H])OC(C(C)=C(C)C7)=O)(C)O)O
43	(20R,22R)-14α,17,20β,27-Trihydroxy-1-oxowitha-5,24-dienolide-27-(O-β-D-glucopyranoside)	O=C(C[C@H](O[C@@H]([C@@H]1O)O[C@H](CO)[C@@H](O)[C@@H]1O)C2)[C@@]3(C)C2=CC[C@]4([H])[C@]3([H])CC[C@@]5(C)[C@@]4(O)CC[C@@]5(O)[C@@]([C@]6([H])OC(C(CO)=C(C)C6)=O)(C)O
44	Withanolide F	O=C(C=CC1)[C@@]2(C)C1=CC[C@]3([H])[C@]2([H])CC[C@@]4(C)[C@@]3(O)CC[C@@]4(O)[C@@]([C@]5([H])OC(C(C)=C(C)C5)=O)(C)O
45	27-Hydroxywithanolide F	O=C(C=CC1)[C@@]2(C)C1=CC[C@]3([H])[C@]2([H])CC[C@@]4(C)[C@@]3(O)CC[C@@]4(O)[C@@]([C@]5([H])OC(C(CO)=C(C)C5)=O)(C)O
46	2,3-Dihydro-3β-hydroxywithanolide F	O=C(C[C@H](O)C1)[C@@]2(C)C1=CC[C@]3([H])[C@]2([H])CC[C@@]4(C)[C@@]3(O)CC[C@@]4(O)[C@@]([C@]5([H])OC(C(C)=C(C)C5)=O)(C)O
47	15α-Hydroxycoagulin L	O=C(C[C@H](O[C@@H]([C@@H]1O)O[C@H](CO)[C@@H](O)[C@@H]1O)C2)[C@@]3(C)C2=CC[C@]4([H])[C@]3([H])CC[C@@]5(C)[C@@]4(O)[C@@H](O)C[C@@]5(O)[C@@]([C@]6([H])OC(C(C)=C(C)C6)=O)(C)O
48	14α,15α,17β,20-Tetrahydroxy-1-oxowitha-2,5,24-trienolide	C[C@]12C(CC=CC2=O)=CC[C@]3([H])[C@]1([H])CC[C@@]4(C)[C@@]3(O)[C@@H](O)C[C@@]4(O)[C@]([C@]5([H])OC(C(C)=C(C)C5)=O)(O)C
49	Withacoagulin C	C[C@]12C(C=CCC2=O)=CC[C@]3([H])[C@]1([H])CC[C@@]4(C)[C@@]3(O)[C@@H](O)C[C@@]4(O)[C@]([C@]5([H])OC(C(C)=C(C)C5)=O)(O)C
50	14α,15α-Epoxy-17β,20-dihydroxy-1-oxowitha-3,5,24-trienolide	C[C@]12C(C=CCC2=O)=CC[C@]3([H])[C@]1([H])CC[C@@]4(C)[C@@]3(O5)[C@@H]5C[C@@]4(O)[C@]([C@]6([H])OC(C(C)=C(C)C6)=O)(O)C
51	(4S,20S,22R)-4,27-Dihydroxy-1-oxo-witha-2,5,16,24-tetraenolide	O=C(C=C[C@@H]1O)[C@@]2(C)C1=CC[C@]3([H])[C@]2([H])CC[C@@]4(C)[C@@]3([H])CC=C4[C@@H]([C@]5([H])OC(C(CO)=C(C)C5)=O)C

52	(4S,20S,22R)-4-Hydroxy-1-oxo-witha-2,5,16,24-tetraenolide	O=C(C=C[C@@H]1O)[C@@]2(C)C1=CC[C@]3([H])[C@]2([H])CC[C@@]4(C)[C@@]3([H])CC=C4[C@@H]([C@]5([H])OC(C(C)=C(C)C5)=O)C
53	(20S,22R)-27-Hydroxy-1,4-dioxo-witha-2,5,16,24-tetraenolide	O=C(C=CC1=O)[C@@]2(C)C1=CC[C@]3([H])[C@]2([H])CC[C@@]4(C)[C@@]3([H])CC=C4[C@@H]([C@]5([H])OC(C(CO)=C(C)C5)=O)C
54	(4S,22R)-4,16β,27-Trihydroxy-1-oxo-witha-2,5,17(20),24-tetraenolide	O=C(C=C[C@@H]1O)[C@@]2(C)C1=CC[C@]3([H])[C@]2([H])CC[C@@]4(C)[C@@]3([H])C[C@H](O)/C4=C([C@]5([H])OC(C(CO)=C(C)C5)=O)/C
55	(22R)-16β,27-Dihydroxy-1-oxo-witha-2,5,17(20),24-tetraenolide	O=C(C=CC1)[C@@]2(C)C1=CC[C@]3([H])[C@]2([H])CC[C@@]4(C)[C@@]3([H])C[C@H](O)/C4=C([C@]5([H])OC(C(CO)=C(C)C5)=O)/C
56	(22R)-16β,27-Dihydroxy-1,4-dioxo-witha-2,5,17(20),24-tetraenolide	O=C(C=CC1=O)[C@@]2(C)C1=CC[C@]3([H])[C@]2([H])CC[C@@]4(C)[C@@]3([H])C[C@H](O)/C4=C([C@]5([H])OC(C(CO)=C(C)C5)=O)/C
57	Withasilolide D	O=C1[C@@]2(C)[C@]([C@@H](O3)[C@@H]3[C@]4([H])[C@]2([H])CC[C@@]5(C)[C@@]4([H])CC[C@]5([H])[C@@]([C@]6([H])OC(C(C)=C(C)[C@@H]6O)=O)(C)O)(O)CC=C1
58	Withasilolide C	O=C1[C@@]2(C)[C@]([C@@H](O3)[C@@H]3[C@]4([H])[C@]2([H])CC[C@@]5(C)[C@@]4([H])CC[C@]5(O)[C@@H]([C@]6([H])OC([C@H](C)[C@@H](C)C6)=O)C)(O)CC=C1
59	Withasilolide E	O=C1[C@@]2(C)[C@]([C@@H](O3)[C@@H]3[C@]4([H])[C@]2([H])CC[C@@]5(C)[C@@]4([H])C[C@@H](O)/C5=C(C)\[C@]6([H])OC(C(CO)=C(C)C6)=O)(O)CC=C1
60	Withasilolide F	O=C1[C@@]2(C)[C@]([C@@H](O3)[C@@H]3[C@]4([H])[C@]2([H])CC[C@@]5(C)[C@@]4([H])C[C@@H](OC(C)=O)/C5=C(C)\[C@]6([H])OC(C(CO)=C(C)C6)=O)(O)CC=C1
61	Withacoagulinyl tetraglucoside	O=C1[C@@]2(C)[C@]([C@@H](O[C@@H]([C@@H]3O)O[C@H](CO[C@@H]([C@@H]4O)O[C@H](CO[C@@H]([C@@H]5O)O[C@H](CO[C@@H]([C@@H]6O)O[C@H](CO)[C@@H](O)[C@@H]6O)[C@@H](O)[C@@H]5O)[C@@H](O)[C@@H]4O)[C@@H](O)[C@@H]3O)C[C@]7([H])[C@]2([H])CC[C@@]8(C)[C@@]7([H])CC[C@]8([H])[C@@]([C@]9([H])OC(C(C)=C(C)C9)=O)(C)OC(C)=O)(OC(C)=O)CC=C1
62	27-Acetoxy-4β,6α-dihydroxy-5β-chloro-1-oxowitha-2,24-dienolide	O=C1[C@@]2(C)[C@@]([C@@H](O)C[C@]3([H])[C@]2([H])CC[C@@]4(C)[C@@]3([H])CC[C@]4([H])[C@@H]([C@]5([H])OC(C(COC(C)=O)=C(C)C5)=O)C)(Cl)[C@@H](O)C=C1
63	6α-Chloro-5β,17α-dihydroxywithaferin A	O=C1[C@@]2(C)[C@@]([C@@H](Cl)C[C@]3([H])[C@]2([H])CC[C@@]4(C)[C@@]3([H])CC[C@]4(O)[C@@H]([C@]5([H])OC(C(CO)=C(C)C5)=O)C)(O)[C@@H](O)C=C1
64	3β,4β,5α,6β,27-Pentahydroxy-1-oxo-witha-24-enolide	O=C1[C@@]2(C)[C@]([C@H](O)C[C@]3([H])[C@]2([H])CC[C@@]4(C)[C@@]3([H])CC[C@]4([H])[C@@H]([C@]5([H])OC(C(CO)=C(C)C5)=O)C)(O)[C@@H](O)[C@@H](O)C1

65	Withasomniferolide A	[H][C@]12[C@@]([C@]([H])(CC[C@]3([H])[C@@H]([C@]4([H])OC(C(CO)=C(C)C4)=O)C)[C@]3(C)CC2)([H])C=CC([C@]51C)=CC=CC5=O
66	Withasomniferolide B	[H][C@]12[C@@]([C@]([H])(CC[C@]3([H])[C@]([C@]4([H])OC(C(C)=C(C)C4)=O)(O)C)[C@]3(C)CC2)([H])C=CC([C@]51C)=CC=CC5=O
67	Physaperuvin G, withanolide S	O=C1[C@@]2(C)[C@]([C@H](O)C[C@]3([H])[C@]2([H])CC[C@@]4(C)[C@@]3(O)CC[C@@]4(O)[C@@]([C@]5([H])OC(C(C)=C(C)C5)=O)(C)O)(O)CC=C1
68	Tubocapsanolide D	C[C@@]12[C@@]([C@@H](O)C[C@]3([H])[C@]2([H])CC[C@@]4(C)[C@@]3([H])CC[C@@]4(O)[C@@H]([C@]5([H])OC(C(C)=C(C)C5)=O)C)(O)[C@@H](O)C=CC1=O
69	Withaphysalin V	O=C(C=CC1)[C@@]2(C)C1=C[C@@H](O)[C@]3([H])[C@]2([H])CC[C@]45[C@]([C@](C)([C@]6([H])OC(C(C)=C(C)C6)=O)OC5O)([H])CC[C@@]34[H]
70	Withaphysalin W	O=C(CC=C1)[C@@]2(C)C1=C[C@@H](O)[C@]3([H])[C@]2([H])CC[C@]45[C@]([C@](C)([C@]6([H])OC(C(C)=C(C)C6)=O)OC5O)([H])CC[C@@]34[H]
71	Withaphysalin X	O=C(C=CC1)[C@@]2(C)C1=CC[C@]3([H])[C@]2([H])CC[C@@]4(O5)[C@]([C@](C)([C@]6([H])OC(C(CO)=C(C)C6)=O)OC4O)([H])CCC35O
72	4β-Hydroxyacnistin I	O=C1[C@@]2(C)[C@@]([C@H]3C[C@]4([H])[C@]2([H])CC[C@@]5(C)[C@@]4([H])C[C@@H](O)[C@]5([H])[C@]6([H])C[C@@]7(C)[C@@](C)(O)C(O[C@@H]6C7)=O)(O3)[C@@H](O)C=C1
73	25-Epi-anomanolide A	O=C1[C@@]2(C)[C@@]([C@H]3C[C@]4([H])[C@]2([H])CC[C@@]5(C)[C@@]4([H])CC[C@]5(O)[C@]6([H])C[C@@]7(C)[C@](C)(O)C(O[C@@H]6C7)=O)(O3)[C@@H](O)C=C1
74	4β-Hydroxyanomanolide E	O=C1[C@@]2(C)[C@@]([C@@H](O)C[C@]3([H])[C@]2([H])CC[C@@]4(C)[C@@]3([H])C[C@@H](O)[C@]4(O)[C@]5([H])C[C@@]6(C)[C@@](C)(O)C(O[C@@H]5C6)=O)(O)[C@@H](O)C=C1
75	2,3-Dihydroanomanolide A	O=C1[C@@]2(C)[C@@]([C@H]3C[C@]4([H])[C@]2([H])CC[C@@]5(C)[C@@]4([H])CC[C@]5(O)[C@]6([H])C[C@@]7(C)[C@@](C)(O)C(O[C@@H]6C7)=O)(O3)[C@@H](O)CC1
76	3β-Methoxy-2,3-dihydroanomanolide C	O=C1[C@@]2(C)[C@@]([C@H]3C[C@]4([H])[C@]2([H])CC[C@@]5(C)[C@@]4([H])C[C@@H](O)[C@]5(O)[C@]6([H])C[C@@]7(C)[C@@](C)(O)C(O[C@@H]6C7)=O)(O3)[C@@H](O)[C@@H](OC)C1
77	Withajardin J	O=C1[C@@]2(C)[C@@]([C@H]3C[C@]4([H])[C@]2([H])CC[C@@]5(C)[C@@]4([H])CC[C@]5(O)[C@@](C6)([H])[C@@H]7OC([C@]6([C@@](C)(O)C7)C)=O)(O3)[C@@H](O)C=C1

78	Withajardin K	O=C1[C@@]2(C)[C@@](C@H]3C[C@]4([H])[C@]2([H])CC[C@@]5(C)[C@@]4([H])CC=C5[C@@](C6)([H])[C@@H]7OC([C@]6([C@@](C)(O)C7)C)=O)(O3)[C@@H](O)C=C1
79	17-Epi-withajardin J	O=C1[C@@]2(C)[C@@](C@H]3C[C@]4([H])[C@]2([H])CC[C@@]5(C)[C@@]4([H])CC[C@@]5(O)[C@@](C6)([H])[C@@H]7OC([C@]6([C@@](C)(O)C7)C)=O)(O3)[C@@H](O)C=C1
80	Withacoagulin J	O=C1[C@@]2(C)C(C=C[C@]3([H])[C@]2([H])CC[C@@]4(C)[C@@]3(O5)CC[C@@]4(O)[C@]5([C@]6([H])OC(C(C)=C(C)C6)=O)C)=CCC1
81	Withacogulanoside-B	O=C(C[C@H](O)C1)[C@@]2(C)C1=CC[C@]3([H])[C@]2([H])CC[C@@]4(C)[C@@]3(O5)CC[C@@]4([H])[C@]5([C@]6([H])OC(C(CO[C@@](H])([C@](O)7[H])O[C@](H])(CO)[C@@](H])(O)[C@@]7(O)[H])=C(C)C6)=O)C
82	Physangulidine D	O=C(C=CC1)[C@@]2(C)C1=C[C@@H]3C4C2CC[C@](C)(O)[C@]4(CC5)O[C@]5([C@H]6C(O7)C[C@](O)(C)[C@@](C6)(C)C7=O)O3
83	Physangulidine E	O=C(CC=C1)[C@@]2(C)C1=C[C@@H]3C4C2CC[C@](C)(O)[C@]4(CC5)O[C@]5([C@H]6C(O7)C[C@](O)(C)[C@@](C6)(C)C7=O)O3
84	Physangulidine F	O=C1[C@@]2(C)C([C@H](O)[C@@H]3C4C2CC[C@](C)(O)[C@]4(CC5)O[C@]5([C@H]6C(O7)C[C@](O)(C)[C@@](C6)(C)C7=O)O3)=CC=C1
85	Physangulidine G	O=C1[C@@]2(C)[C@]3([C@H](O)[C@@H]4C5C2CC[C@](C)(O)[C@]5(CC6)O[C@]6([C@H]7C(O8)C[C@](O)(C)[C@@](C7)(C)C8=O)O4)C=C[C@H]1OO3
86	Physangulidine H	O=C1[C@@]2(C)[C@]3([C@H](O)[C@@H]4C5C2CC[C@](C)(O)[C@]5(CC6)O[C@]6([C@H]7C(O8)C[C@](O)(C)[C@@](C7)(C)C8=O)O4)[C@@H](O3)C=C1
87	5β,6β-epoxy-4β,16β,27-trihydroxy-1-oxo-witha-2,17(20),24-trienolide	O=C1[C@@]2(C)[C@@]([C@H]3C[C@]4([H])[C@]2([H])CC[C@@]5(C)[C@]4(C[C@H](O)/C5=C([C@]6([H])OC(C(CO)=C(C)C6)=O)/C)[H])(O3)[C@@H](O)C=C1
88	4β-Formyl-6β,27-dihydroxy-1-oxo-witha-2,24-dienolide	O=C1OC([C@@H](C)[C@@]2([H])CC[C@@]3([H])[C@]4([H])C[C@@H](O)[C@@]5(C([H])=O)[C@](C)(C(C=C5)=O)[C@@]4([H])CC[C@@]32C)CC(C)=C1CO
89	4β-Formyl-6β,27-dihydroxy-1-oxo-witha-24-enolide	O=C1OC([C@@H](C)[C@@]2([H])CC[C@@]3([H])[C@]4([H])C[C@@H](O)[C@@]5(C([H])=O)[C@](C)(C(CC5)=O)[C@@]4([H])CC[C@@]32C)CC(C)=C1CO
90	28-Hydroxytubocapsenolide A	O=C1[C@@]2(C)[C@@]([C@H]3C[C@]4([H])[C@]2([H])CCC5=C4C[C@@H](O)[C@@]5(C)[C@@H]([C@]6([H])OC(C(C)=C(CO)C6)=O)C)(O3)[C@@H](O)C=C1
91	3β-Ethoxy-2,3-dihydrotubocapsenolide A	O=C1[C@@]2(C)[C@@]([C@H]3C[C@]4([H])[C@]2([H])CCC5=C4C[C@@H](O)[C@@]5(C)[C@@H]([C@]6([H])OC(C(C)=C(C)C6)=O)C)(O3)[C@@H](O)[C@@H](OCC)C1

Table 2: Physicochemical properties of the withanolides. predicted by the server pkCSM.

ID	MOL_WEIGHT	LOGP	#ROTATABLE_BONDS	#ACCEPTORS	#DONORS	SURFACE_AREA
1	512.643	39.237	4	7	1	218.528
2	470.606	34.954	2	6	2	201.317
3	554.68	44.945	5	8	0	235.739
4	528.642	3.037	3	8	2	223.322
5	484.589	24.842	3	7	2	205.425
6	512.643	39.237	4	7	1	218.528
7	556.696	42.863	7	8	1	236.371
8	530.658	31.185	4	8	2	224.012
9	500.632	33.607	3	7	1	212.799
10	470.606	37.358	2	6	1	201.320
11	514.659	37.508	4	7	1	219.164
12	582.694	22.781	4	9	3	244.036
13	582.694	22.781	4	9	3	244.036
14	605.736	3.15	4	11	3	256.163
15	484.589	24.842	3	7	2	205.425
16	502.604	1.679	3	8	3	210.909
17	484.589	23.879	2	7	3	205.422
18	454.607	41.417	3	5	2	196.520
19	512.643	38.258	3	7	2	218.525
20	496.644	47.125	4	6	1	213.730
21	486.605	25.156	3	7	4	206.108
22	470.606	34.007	3	6	3	201.314
23	468.59	33.208	3	6	3	200.624
24	470.606	32.566	3	6	3	201.314
25	470.606	35.432	2	6	3	201.314
26	454.607	42.842	2	5	2	196.520

27	456.623	4.22	2	5	2	197.209
28	484.589	24.356	3	7	3	205.476
29	486.605	25.156	3	7	4	206.108
30	470.606	35.432	2	6	3	201.314
31	486.605	25.156	3	7	4	206.108
32	454.607	42.858	3	5	2	196.520
33	438.608	53.134	2	4	1	191.726
34	470.606	34.007	3	6	3	201.314
35	454.607	44.283	2	5	2	196.520
36	488.621	25.955	3	7	4	206.798
37	634.763	14.473	5	11	6	263.797
38	634.763	14.473	5	11	6	263.797
39	474.638	35.589	2	6	3	202.693
40	452.591	43.484	2	5	2	195.830
41	454.607	44.283	2	5	2	196.520
42	796.904	-0.586	7	16	9	325.591
43	666.761	-0.4654	6	13	8	273.386
44	470.606	35.432	2	6	3	201.314
45	486.605	25.156	3	7	4	206.108
46	488.621	2.738	2	7	4	206.798
47	666.761	-0.467	5	13	8	273.386
48	486.605	2.514	2	7	4	206.108
49	486.605	2.514	2	7	4	206.108
50	468.59	35.596	2	6	2	200.627
51	452.591	40.618	3	5	2	195.830
52	436.592	50.894	2	4	1	191.036
53	450.575	4.27	3	5	1	195.197
54	468.59	31.767	2	6	3	200.624
55	452.591	42.059	2	5	2	195.830

56	466.574	33.849	2	6	2	199.992
57	486.605	24.662	2	7	3	206.111
58	472.622	34.312	2	6	2	202.007
59	484.589	23.879	2	7	3	205.422
60	526.626	29.587	3	8	2	222.632
61	-	-	-	-	-	-
62	549.104	41.246	4	7	2	229.518
63	523.066	26.687	3	7	4	217.101
64	506.636	15.021	3	8	5	212.282
65	436.592	49.469	3	4	1	191.036
66	436.592	50.894	2	4	1	191.036
67	504.62	17.088	2	8	5	211.592
68	488.621	24.498	2	7	4	206.798
69	468.59	36.206	1	6	2	200.627
70	468.59	36.206	1	6	2	200.627
71	500.588	24.636	2	8	3	210.535
72	486.605	2.156	1	7	3	205.795
73	486.605	23.001	1	7	3	205.795
74	520.619	0.2253	1	9	6	216.070
75	488.621	25.241	1	7	3	206.485
76	534.646	11.198	2	9	4	222.757
77	486.605	23.001	1	7	3	205.795
78	468.59	31.053	1	6	2	200.311
79	486.605	23.001	1	7	3	205.795
80	452.591	45.888	1	5	1	195.833
81	632.747	14.653	5	11	5	263.111
82	484.589	29.759	1	7	2	205.425
83	484.589	29.759	1	7	2	205.425
84	500.588	19.467	1	8	3	210.219

85	532.586	10.895	1	10	3	220.059
86	516.587	11.579	1	9	3	215.016
87	484.589	23.879	2	7	3	205.422
88	470.606	34.006	4	6	2	201.371
89	472.622	36.246	4	6	2	202.061
90	484.589	23.879	3	7	3	205.422
91	514.659	36.545	4	7	2	219.161

Table 3: Absorption properties of the withanolides. predicted by the server pkCSM.

ID	Water solubility	Caco2 permeability	Intestinal absorption	Skin Permeability	P-glycoprotein substrate	P-glycoprotein I inhibitor	P-glycoprotein II inhibitor
1	-4.874	0.9	100	-3.115	Yes	Yes	Yes
2	-5.131	0.798	85.205	-3.258	Yes	Yes	Yes
3	-5.27	0.884	100	-2.917	No	Yes	Yes
4	-5.54	0.759	73.561	-3.061	Yes	Yes	Yes
5	-4.866	0.813	87.132	-3.193	Yes	Yes	No
6	-5.304	0.787	94.715	-3.119	No	Yes	Yes
7	-5.463	0.763	89.32	-2.96	No	Yes	Yes
8	-5.096	0.62	83.84	-3.047	Yes	Yes	Yes
9	-5.125	0.86	90.497	-3.145	Yes	Yes	Yes
10	-5.076	1.309	98.169	-3.276	No	Yes	No
11	-5.216	0.847	91.255	-3.122	Yes	Yes	Yes
12	-4.464	0.311	73.943	-2.851	Yes	Yes	No
13	-4.464	0.311	73.943	-2.851	Yes	Yes	No
14	-2.961	-0.288	84.193	-2.735	Yes	No	No
15	-4.893	0.883	88.261	-3.215	Yes	Yes	No
16	-4.874	0.999	78.189	-3.078	Yes	No	No
17	-5.286	0.981	98.545	-3.615	Yes	Yes	Yes
18	-5.216	0.919	97.084	-3.433	Yes	Yes	Yes
19	-4.98	0.854	78.815	-3.666	Yes	Yes	Yes
20	-5.518	1.023	99.32	-3.58	Yes	Yes	Yes
21	-4.895	0.719	65.025	-3.282	Yes	Yes	No
22	-5.152	0.761	77.184	-3.825	Yes	Yes	No
23	-5.126	0.764	76.974	-3.831	Yes	Yes	No
24	-4.866	0.838	80.513	-3.938	Yes	Yes	Yes
25	-4.333	0.736	67.908	-3.239	Yes	No	No
26	-4.837	0.93	98.416	-3.219	Yes	Yes	Yes

27	-4.829	0.936	98.597	-3.224	Yes	Yes	Yes
28	-4.789	0.819	69.734	-3.944	Yes	Yes	Yes
29	-4.895	0.719	65.025	-3.282	Yes	Yes	No
30	-4.333	0.736	67.908	-3.239	Yes	No	No
31	-4.662	0.707	65.092	-3.392	Yes	Yes	No
32	-5.281	0.961	96.414	-3.939	Yes	Yes	No
33	-5.788	0.91	97.335	-3.742	Yes	Yes	Yes
34	-5.308	0.817	79.694	-4.168	Yes	No	No
35	-5.635	1.078	96.793	-4.282	Yes	No	No
36	-4.777	0.767	74.293	-3.631	Yes	Yes	No
37	-3.792	-0.28	42.115	-2.742	Yes	No	No
38	-3.656	-0.341	46.474	-2.739	Yes	No	No
39	-5.269	0.855	82.753	-4.295	Yes	No	No
40	-5.296	1.002	95.186	-4.367	Yes	Yes	Yes
41	-5.304	1.121	96.047	-4.192	Yes	No	No
42	-2.15	-0.487	10.722	-2.735	Yes	No	No
43	-2.697	-0.498	16.587	-2.735	Yes	No	No
44	-4.858	0.781	73.113	-3.621	Yes	No	No
45	-4.662	0.707	65.092	-3.392	Yes	Yes	No
46	-4.514	0.731	67.712	-3.447	Yes	No	No
47	-2.226	-0.499	9.416	-2.735	Yes	No	No
48	-4.346	0.72	71.337	-3.266	Yes	Yes	No
49	-4.346	0.72	71.337	-3.266	Yes	Yes	No
50	-5.16	0.922	91.014	-3.259	Yes	No	No
51	-5.138	0.939	97.787	-3.831	Yes	Yes	Yes
52	-5.631	0.889	98.709	-3.509	Yes	Yes	Yes
53	-5.439	0.933	100	-4.14	Yes	Yes	Yes
54	-4.568	0.877	77.607	-3.399	Yes	Yes	Yes
55	-5.566	0.952	96.928	-4.085	Yes	Yes	Yes

56	-5.173	0.856	82.891	-4.112	Yes	Yes	Yes
57	-4.601	0.666	67.578	-2.932	Yes	Yes	No
58	-5.026	0.852	88.671	-3.47	Yes	Yes	No
59	-4.983	0.813	78.028	-3.191	Yes	No	No
60	-5.076	0.823	83.253	-3.143	Yes	Yes	Yes
61	-	-	-	-	-	-	-
62	-5.413	0.819	84.146	-2.899	Yes	Yes	Yes
63	-5.232	0.686	67.172	-3.132	Yes	Yes	Yes
64	-4.385	0.309	55.835	-2.917	Yes	Yes	No
65	-5.817	0.915	97.653	-3.762	Yes	Yes	Yes
66	-5.717	0.911	97.461	-3.888	No	Yes	Yes
67	-3.548	-0.095	45.044	-2.829	Yes	No	No
68	-4.5	0.734	66.387	-3.439	Yes	Yes	No
69	-4.569	0.975	93.396	-2.897	Yes	Yes	Yes
70	-4.569	0.975	93.396	-2.897	Yes	Yes	Yes
71	-5.275	0.745	72.516	-3.298	Yes	Yes	No
72	-5.14	0.764	86.484	-3.227	Yes	Yes	No
73	-5.204	0.777	82	-3.191	Yes	Yes	No
74	-4.037	0.407	62.211	-2.835	Yes	No	No
75	-5.254	0.768	82.852	-3.188	Yes	Yes	No
76	-4.941	0.429	72.494	-2.98	Yes	No	No
77	-4.914	0.799	87.206	-3.183	Yes	Yes	No
78	-4.753	0.822	94.013	-3.196	Yes	Yes	No
79	-4.914	0.799	87.206	-3.183	Yes	Yes	No
80	-5.482	0.977	96.753	-3.763	Yes	Yes	No
81	-3.942	-0.2	51.831	-2.761	Yes	No	No
82	-4.997	0.857	100	-3.562	Yes	No	No
83	-4.997	0.857	100	-3.562	Yes	No	No
84	-4.608	0.837	95.398	-3.529	Yes	No	No

85	-4.176	0.799	94.024	-3.042	Yes	No	No
86	-4.341	1.301	97.149	-2.931	No	No	No
87	-5.174	0.78	74.521	-3.278	Yes	No	Yes
88	-4.769	0.842	85.491	-3.378	Yes	Yes	Yes
89	-4.831	0.833	86.344	-3.358	Yes	Yes	Yes
90	-5.133	0.78	77.574	-3.304	Yes	Yes	No
91	-5.497	0.814	81.696	-3.203	Yes	Yes	No

Table 4: Distribution properties of the withanolides. predicted by the server pkCSM.

ID	VDss (human)	Fraction unbound (human)	BBB permeability	CNS permeability
1	-0.248	0	-0.554	-2.642
2	-0.02	0.104	-0.31	-2.886
3	-0.221	0	-0.926	-2.585
4	0.165	0.157	-0.718	-2.959
5	0.087	0.191	-0.579	-3.118
6	-0.309	0.012	-0.675	-2.937
7	-0.374	0.009	-0.952	-3.085
8	-0.694	0.09	-0.905	-3.244
9	0.07	0.106	-0.644	-2.957
10	0.168	0.099	-0.425	-2.788
11	0.087	0.085	-0.668	-2.945
12	-0.88	0.153	-1.378	-3.648
13	-0.88	0.153	-1.378	-3.648
14	-0.004	0.39	-1.37	-3.724
15	0.289	0.217	-0.64	-3.064
16	0.117	0.278	-1.056	-3.522
17	-0.273	0	-0.489	-2.486
18	-0.322	0	0.257	-1.957
19	-0.001	0.051	-0.098	-2.601
20	-0.087	0	-0.475	-2.382
21	0.162	0.343	-0.731	-3.428
22	0.012	0.217	-0.588	-3.344
23	0.01	0.221	-0.576	-3.346
24	-0.073	0.129	-0.623	-2.788
25	0.017	0.309	-0.868	-4.015
26	-0.137	0	0.267	-1.86

27	-0.137	0.001	0.268	-1.874
28	-0.143	0.176	-0.722	-2.961
29	0.162	0.343	-0.731	-3.428
30	0.017	0.309	-0.868	-4.015
31	0.042	0.335	-0.95	-3.773
32	0.284	0.079	-0.177	-2.888
33	0.398	0	-0.18	-2.767
34	0.26	0.206	-0.68	-2.984
35	0.323	0.125	-0.071	-2.861
36	0.143	0.269	-0.786	-3.055
37	-0.221	0.39	-1.516	-4.664
38	-0.046	0.399	-1.5	-4.689
39	0.176	0.179	-0.711	-2.925
40	0.194	0.079	-0.072	-1.844
41	0.234	0.117	-0.129	-3.168
42	0.048	0.462	-1.984	-6.054
43	-0.068	0.495	-1.867	-5.58
44	0.009	0.258	-0.884	-3.65
45	0.042	0.335	-0.95	-3.773
46	-0.113	0.316	-0.99	-3.729
47	-0.115	0.506	-2.016	-6.243
48	-0.16	0.309	-1.008	-4.082
49	-0.16	0.309	-1.008	-4.082
50	0.435	0.21	-0.242	-2.921
51	-0.032	0.023	0.18	-1.984
52	0.117	0	-0.038	-1.577
53	0.011	0.008	-0.223	-1.938
54	-0.113	0.13	-0.689	-2.662
55	0.061	0.073	-0.129	-1.902

56	-0.139	0.109	-0.354	-2.634
57	-0.424	0.157	-0.79	-3.054
58	-0.033	0.154	-0.016	-2.789
59	-0.072	0.194	-0.773	-2.932
60	-0.193	0.13	-0.751	-2.892
61	-	-	-	-
62	-0.909	0	-0.376	-2.848
63	-0.319	0.227	-0.868	-3.179
64	-1.018	0.217	-1.008	-3.406
65	0.035	0	-0.037	-1.684
66	0.163	0	0.042	-1.561
67	0.048	0.433	-1.179	-4.526
68	-0.241	0.247	-0.877	-3.078
69	-0.073	0.011	0.14	-2.449
70	-0.073	0.011	0.14	-2.449
71	0.326	0.297	-0.904	-3.055
72	0.013	0.196	-0.757	-3.165
73	0.134	0.209	-0.788	-3.117
74	-0.085	0.303	-1.072	-3.987
75	0.141	0.199	-0.821	-3.112
76	-0.052	0.248	-1.107	-3.613
77	0.123	0.239	-0.722	-3.139
78	0.097	0.159	-0.349	-2.982
79	0.123	0.239	-0.722	-3.139
80	0.5	0.149	-0.102	-2.812
81	0.149	0.317	-1.666	-4.688
82	0.482	0.27	-0.522	-3.061
83	0.482	0.27	-0.522	-3.061
84	0.523	0.295	-0.93	-3.14

85	0.594	0.331	-1.234	-3.299
86	0.578	0.342	-1.048	-3.239
87	-0.032	0.208	-0.776	-3.051
88	-0.275	0.023	-0.368	-2.606
89	-0.27	0.014	-0.375	-2.577
90	0.187	0.237	-0.804	-3.075
91	0.176	0.124	-0.622	-3.002

Table 5: Metabolism properties of the withanolides. predicted by the server pkCSM.

ID	CYP2D6 substrate	CYP3A4 substrate	CYP1A2 inhibitior	CYP2C19 inhibitior	CYP2C9 inhibitior	CYP2D6 inhibitior	CYP3A4 inhibitior
1	No	Yes	No	No	No	No	No
2	No	Yes	No	No	No	No	No
3	No	Yes	No	No	No	No	No
4	No	Yes	No	No	No	No	No
5	No	Yes	No	No	No	No	No
6	No	Yes	No	No	No	No	No
7	No	Yes	No	No	No	No	No
8	No	Yes	No	No	No	No	No
9	No	Yes	No	No	No	No	No
10	No	Yes	No	No	No	No	No
11	No	Yes	No	No	No	No	No
12	No	Yes	No	No	No	No	No
13	No	Yes	No	No	No	No	No
14	No	No	No	No	No	No	Yes
15	No	Yes	No	No	No	No	No
16	No	Yes	No	No	No	No	No
17	No	Yes	No	No	No	No	No
18	No	Yes	No	No	No	No	No
19	No	Yes	No	No	No	No	No
20	No	Yes	No	No	No	No	No
21	No	No	No	No	No	No	No
22	No	No	No	No	No	No	No
23	No	No	No	No	No	No	No
24	No	Yes	No	No	No	No	No
25	No	No	No	No	No	No	No
26	No	Yes	No	No	No	No	No

27	No	Yes	No	No	No	No	No
28	No	Yes	No	No	No	No	No
29	No	No	No	No	No	No	No
30	No	No	No	No	No	No	No
31	No	No	No	No	No	No	No
32	No	Yes	No	No	No	No	Yes
33	No	Yes	No	No	No	No	Yes
34	No	Yes	No	No	No	No	No
35	No	Yes	No	No	No	No	No
36	No	No	No	No	No	No	No
37	No	No	No	No	No	No	No
38	No	No	No	No	No	No	No
39	No	Yes	No	No	No	No	No
40	No	Yes	No	No	No	No	Yes
41	No	Yes	No	No	No	No	No
42	No	No	No	No	No	No	No
43	No	No	No	No	No	No	No
44	No	Yes	No	No	No	No	No
45	No	No	No	No	No	No	No
46	No	No	No	No	No	No	No
47	No	No	No	No	No	No	No
48	No	No	No	No	No	No	No
49	No	No	No	No	No	No	No
50	No	Yes	No	No	No	No	No
51	No	Yes	No	No	No	No	No
52	No	Yes	No	No	No	No	No
53	No	Yes	No	No	No	No	No
54	No	No	No	No	No	No	No
55	No	No	No	No	No	No	No

56	No	Yes	No	No	No	No	No
57	No	Yes	No	No	No	No	No
58	No	Yes	No	No	No	No	No
59	No	No	No	No	No	No	No
60	No	Yes	No	No	No	No	No
61	-	-	-	-	-	-	-
62	No	Yes	No	No	No	No	No
63	No	Yes	No	No	No	No	No
64	No	Yes	No	No	No	No	No
65	No	Yes	No	No	No	No	Yes
66	No	Yes	No	No	No	No	No
67	No	No	No	No	No	No	No
68	No	Yes	No	No	No	No	No
69	No	Yes	No	No	No	No	No
70	No	Yes	No	No	No	No	No
71	No	No	No	No	No	No	No
72	No	Yes	No	No	No	No	No
73	No	Yes	No	No	No	No	No
74	No	No	No	No	No	No	No
75	No	Yes	No	No	No	No	No
76	No	Yes	No	No	No	No	No
77	No	Yes	No	No	No	No	No
78	No	Yes	No	No	No	No	No
79	No	Yes	No	No	No	No	No
80	No	Yes	No	No	No	No	No
81	No	No	No	No	No	No	No
82	No	Yes	No	No	No	No	No
83	No	Yes	No	No	No	No	No
84	No	Yes	No	No	No	No	No

85	No	Yes	No	No	No	No	No
86	No	Yes	No	No	No	No	No
87	No	Yes	No	No	No	No	No
88	No	Yes	No	No	No	No	No
89	No	Yes	No	No	No	No	No
90	No	Yes	No	No	No	No	No
91	No	Yes	No	No	No	No	Yes

Table 6: Excretion properties of the withanolides. predicted by the server pkCSM.

ID	Total Clearance	Renal OCT2 substrate
1	0.348	No
2	0.355	Yes
3	0.237	Yes
4	0.351	No
5	0.373	Yes
6	0.319	No
7	0.285	No
8	0.353	No
9	0.361	Yes
10	0.316	Yes
11	0.392	Yes
12	0.12	No
13	0.12	No
14	0.266	No
15	0.358	No
16	0.395	No
17	0.428	Yes
18	0.504	No
19	0.424	No
20	0.42	Yes
21	0.551	No
22	0.529	No
23	0.521	No
24	0.544	No
25	0.498	No
26	0.428	No

27	0.383	No
28	0.494	No
29	0.566	No
30	0.513	No
31	0.57	No
32	0.525	No
33	0.458	No
34	0.521	No
35	0.453	No
36	0.52	No
37	0.503	No
38	0.507	No
39	0.403	No
40	0.461	Yes
41	0.485	No
42	0.528	No
43	0.618	No
44	0.486	No
45	0.554	No
46	0.501	No
47	0.582	No
48	0.513	No
49	0.528	No
50	0.388	No
51	0.508	No
52	0.441	Yes
53	0.427	Yes
54	0.504	No
55	0.485	Yes

56	0.422	Yes
57	0.375	No
58	0.348	Yes
59	0.415	No
60	0.323	No
61	-	-
62	-0.062	No
63	0.067	No
64	0.599	No
65	0.481	No
66	0.402	Yes
67	0.54	No
68	0.545	No
69	0.352	No
70	0.367	No
71	0.431	No
72	0.158	No
73	0.169	No
74	0.33	No
75	0.184	No
76	0.261	No
77	0.135	No
78	0.108	Yes
79	0.135	No
80	0.365	No
81	0.413	No
82	0.128	No
83	0.144	No
84	0.155	No

85	0.159	No
86	0.083	No
87	0.429	No
88	0.476	No
89	0.488	No
90	0.492	No
91	0.513	No

Table 7: Toxicity properties of the withanolides. predicted by the server pkCSM.

ID	AMES toxicity	Max. tolerated Dose (MRTD)	hERG I inhibitor	hERG II inhibitor	Oral Rat Acute Toxicity (LD50)	Oral Rat Chronic Toxicity (LOAEL)	Hepatotoxicity	Skin Sensitisation	*T.Pyriformis* toxicity	Minnow toxicity
1	No	-0.443	No	No	2.907	1.368	No	No	0.292	1.484
2	No	-0.522	No	No	2.799	1.543	Yes	No	0.301	0.39
3	No	-0.256	No	No	2.953	0.1	No	No	0.288	0.819
4	No	-0.95	No	No	3.733	1.946	No	No	0.287	1.297
5	Yes	-0.582	No	No	3.18	1.69	No	No	0.289	1.634
6	No	-0.466	No	No	2.782	1.312	No	No	0.299	0.725
7	No	-0.459	No	No	2.975	0.393	No	No	0.29	0.921
8	No	-0.52	No	No	3.153	1.913	No	No	0.29	1.284
9	No	-0.638	No	No	2.939	1.771	No	No	0.29	1.124
10	No	-0.562	No	No	2.702	1.697	No	No	0.296	0.867
11	No	-0.685	No	No	2.904	1.803	No	No	0.289	0.958
12	No	-0.855	No	No	3.6	1.887	Yes	No	0.286	1.327
13	No	-0.855	No	No	3.6	1.887	Yes	No	0.286	1.327
14	No	0.495	No	No	2.481	1.34	Yes	No	0.285	0.501
15	No	-0.961	No	No	3.439	1.688	No	No	0.287	2.499
16	No	-1.001	No	No	3.996	1.979	No	No	0.286	2.971
17	No	-0.294	No	No	2.156	0.521	No	No	0.337	-0.27
18	No	-1.537	No	No	3.419	1.803	No	No	0.364	0.71
19	No	-1.419	No	No	3.166	1.838	No	No	0.296	1.225
20	No	-0.585	No	No	2.937	0.224	No	No	0.328	1.1
21	No	-0.711	No	No	2.736	2.12	No	No	0.285	2.13
22	No	-0.827	No	No	2.393	1.793	No	No	0.288	0.707
23	No	-0.823	No	No	2.383	1.798	No	No	0.288	0.75
24	No	-1.376	No	No	3.071	1.501	Yes	No	0.313	1.439
25	No	-0.147	No	No	2.499	2.105	No	No	0.285	0.243

26	No	-1.283	No	No	3.003	1.556	Yes	No	0.33	0.355
27	No	-1.285	No	No	2.997	1.56	No	No	0.33	0.348
28	No	-1.268	No	No	3.061	1.595	Yes	No	0.298	2.19
29	No	-0.711	No	No	2.736	2.12	No	No	0.285	2.13
30	No	-0.147	No	No	2.499	2.105	No	No	0.285	0.243
31	No	-0.514	No	No	2.912	2.123	No	No	0.285	1.967
32	No	-0.857	No	No	2.607	-0.706	No	No	0.37	0.739
33	No	-0.537	No	No	2.228	1.468	No	No	0.449	0.033
34	No	-0.863	No	No	2.675	1.68	No	No	0.301	1.494
35	No	-0.593	No	No	2.319	1.671	No	No	0.342	0.675
36	No	-1.152	No	No	3.278	1.52	No	No	0.288	2.577
37	No	-1.604	No	Yes	4.135	3.435	No	No	0.285	4.709
38	No	-1.481	No	Yes	4.007	3.65	No	No	0.285	4.989
39	No	-0.834	No	No	2.767	1.353	No	No	0.302	2.234
40	No	-0.703	No	No	2.244	1.696	Yes	No	0.347	1.168
41	No	-0.747	No	No	2.699	1.631	No	No	0.323	0.758
42	No	-1.675	No	Yes	3.242	4.959	No	No	0.285	6.043
43	No	-1.565	No	Yes	3.954	3.284	No	No	0.285	6.343
44	No	-0.284	No	No	2.578	2.106	No	No	0.287	0.93
45	No	-0.514	No	No	2.912	2.123	No	No	0.285	1.967
46	No	-0.621	No	No	3.111	2.069	No	No	0.286	1.992
47	No	-1.377	No	Yes	3.501	4.05	No	No	0.285	6.468
48	No	-0.278	No	No	3.181	2.529	No	No	0.285	2.696
49	No	-0.278	No	No	3.181	2.529	No	No	0.285	2.696
50	No	-0.747	No	No	3.197	1.7	No	No	0.293	1.633
51	No	-1.317	No	No	3.041	1.985	No	No	0.379	0.755
52	No	-0.858	No	No	2.675	1.465	No	No	0.448	0.13
53	No	-0.767	No	No	2.044	0.595	No	No	0.404	-0.081
54	No	-1.563	No	No	3.717	1.486	Yes	No	0.314	1.92

55	No	-1.24	No	No	2.878	1.598	Yes	No	0.388	0.537
56	No	-1.225	No	No	2.908	1.656	No	No	0.333	1.085
57	No	-0.817	No	No	3.407	2.439	No	No	0.285	1.029
58	No	-0.988	No	No	3.179	1.747	No	No	0.292	0.65
59	Yes	-1.51	No	No	3.676	1.746	Yes	No	0.288	2.59
60	Yes	-1.056	No	No	3.628	1.804	No	No	0.287	2.415
61	-	-	-	-	-	-	-	-	-	-
62	No	-1.238	No	No	2.42	1.487	No	No	0.291	0.619
63	No	-1.169	No	No	2.178	1.685	No	No	0.287	1.425
64	No	-1.751	No	No	3.479	2.229	No	No	0.285	2.622
65	No	-0.506	No	No	2.532	1.458	No	No	0.457	0.288
66	No	-0.361	No	No	2.297	1.457	Yes	No	0.454	0.303
67	No	-0.253	No	No	3.319	2.921	No	No	0.285	2.586
68	No	-1.057	No	No	3.381	2.188	No	No	0.286	2.339
69	No	-1.217	No	No	3.338	1.769	No	No	0.289	1.393
70	No	-1.217	No	No	3.338	1.769	No	No	0.289	1.393
71	No	-1.249	No	No	2.8	2.077	No	No	0.286	2.848
72	No	-1.158	No	No	3.43	1.632	No	No	0.289	2.17
73	No	-0.915	No	No	3.378	1.721	No	No	0.288	2.19
74	No	-1.551	No	Yes	3.505	2.966	No	No	0.285	4.298
75	No	-0.925	No	No	3.377	1.707	No	No	0.288	2.111
76	No	-1.23	No	No	4.159	2.354	No	No	0.285	3.203
77	Yes	-1.034	No	No	3.362	1.428	No	No	0.286	2.565
78	No	-0.633	No	No	2.701	1.295	No	No	0.288	1.715
79	Yes	-1.034	No	No	3.362	1.428	No	No	0.286	2.565
80	No	-0.537	No	No	2.244	0.378	No	No	0.31	0.27
81	No	-2.231	No	No	4.251	3.072	No	No	0.285	3.921
82	No	-1.098	No	No	2.879	1.417	No	No	0.286	1.941
83	No	-1.098	No	No	2.879	1.417	No	No	0.286	1.941

84	No	-1.386	No	No	3.475	1.575	No	No	0.285	3.238
85	No	-1.568	No	No	3.632	1.728	No	No	0.285	4.848
86	No	-1.428	No	No	4.352	1.595	No	No	0.285	4.02
87	No	-1.315	No	No	3.538	1.609	Yes	No	0.295	2.063
88	No	-0.711	No	No	2.803	0.042	No	No	0.298	-0.107
89	No	-0.706	No	No	2.826	0.008	No	No	0.298	-0.186
90	No	-0.728	No	No	3.436	1.607	No	No	0.292	1.994
91	No	-0.948	No	No	3.169	1.646	No	No	0.294	1.319

Table 8: Physicochemical properties of the withanolides. predicted by the server SwissADME.

ID	Formula	MW	#Heavy atoms	#Aromatic heavy atoms	Fraction Csp3	#Rotatable bonds	#H-bond acceptors	#H-bond donors	MR	TPSA
1	C30H40O7	512.63	37	0	0.77	5	7	1	137.23	102.43
2	C28H38O6	470.60	34	0	0.79	2	6	2	127.53	96.36
3	C32H42O8	554.67	40	0	0.75	7	8	0	146.96	108.50
4	C30H40O8	528.63	38	0	0.77	4	8	2	138.43	122.66
5	C28H36O7	484.58	35	0	0.79	3	7	2	126.50	108.89
6	C30H40O7	512.63	37	0	0.77	5	7	1	137.23	102.43
7	C32H44O8	556.69	40	0	0.78	7	8	1	148.35	111.66
8	C30H42O8	530.65	38	0	0.83	5	8	2	138.86	122.66
9	C29H40O7	500.62	36	0	0.86	3	7	1	131.70	97.89
10	C28H38O6	470.60	34	0	0.86	2	6	1	125.81	88.66
11	C30H42O7	514.65	37	0	0.87	4	7	1	136.51	97.89
12	C32H42N2O8	582.68	42	6	0.75	4	8	3	153.63	151.22
13	C32H42N2O8	582.68	42	6	0.75	4	8	3	153.63	151.22
14	C33H43N5O6	605.72	44	9	0.73	4	9	3	162.03	165.98
15	C28H36O7	484.58	35	0	0.79	3	7	2	126.50	108.89
16	C28H38O8	502.60	36	0	0.86	3	8	3	128.13	129.12
17	C30H40O6	496.64	36	0	0.70	5	6	1	137.74	89.90
18	C28H38O5	454.60	33	0	0.71	3	5	2	128.01	83.83
19	C30H40O7	512.63	37	0	0.70	4	7	2	138.94	110.13
20	C30H40O6	496.64	36	0	0.70	5	6	1	137.74	89.90
21	C28H38O7	486.60	35	0	0.71	3	7	4	130.44	124.29
22	C28H38O6	470.60	34	0	0.71	3	6	3	129.24	104.06
23	C28H36O6	468.58	34	0	0.64	3	6	3	128.77	104.06
24	C28H38O6	470.60	34	0	0.71	3	6	3	129.21	104.06
25	C28H38O6	470.60	34	0	0.71	2	6	3	129.28	104.06
26	C28H38O5	454.60	33	0	0.71	2	5	2	128.04	83.83

27	C28H40O5	456.61	33	0	0.79	2	5	2	128.52	83.83
28	C28H36O7	484.58	35	0	0.68	3	7	3	129.41	121.13
29	C28H38O7	486.60	35	0	0.71	3	7	4	130.44	124.29
30	C28H38O6	470.60	34	0	0.71	2	6	3	129.28	104.06
31	C28H38O7	486.60	35	0	0.71	3	7	4	130.44	124.29
32	C28H38O5	454.60	33	0	0.71	3	5	2	128.04	83.83
33	C28H38O4	438.60	32	0	0.71	2	4	1	126.88	63.60
34	C28H38O6	470.60	34	0	0.71	3	6	3	129.24	104.06
35	C28H38O5	454.60	33	0	0.71	2	5	2	128.08	83.83
36	C28H40O7	488.61	35	0	0.79	3	7	4	130.88	124.29
37	C34H50O11	634.75	45	0	0.82	5	11	6	162.10	183.21
38	C34H50O11	634.75	45	0	0.82	5	11	6	162.10	183.21
39	C28H42O6	474.63	34	0	0.86	2	6	3	130.19	104.06
40	C28H36O5	452.58	33	0	0.64	2	5	2	127.61	83.83
41	C28H38O5	454.60	33	0	0.71	2	5	2	128.08	83.83
42	-	-	-	-	-	-	-	-	-	-
43	C34H50O13	666.75	47	0	0.82	6	13	8	164.46	223.67
44	C28H38O6	470.60	34	0	0.71	2	6	3	129.28	104.06
45	C28H38O7	486.60	35	0	0.71	3	7	4	130.44	124.29
46	C28H40O7	488.61	35	0	0.79	2	7	4	130.92	124.29
47	C34H50O13	666.75	47	0	0.82	5	13	8	164.46	223.67
48	C28H38O7	486.60	35	0	0.71	2	7	4	130.44	124.29
49	C28H38O7	486.60	35	0	0.71	2	7	4	130.44	124.29
50	C28H36O6	468.58	34	0	0.71	2	6	2	127.09	96.36
51	C28H36O5	452.58	33	0	0.64	3	5	2	127.53	83.83
52	C28H36O4	436.58	32	0	0.64	2	4	1	126.37	63.60
53	C28H34O5	450.57	33	0	0.61	3	5	1	126.57	80.67
54	C28H36O6	468.58	34	0	0.64	2	6	3	128.69	104.06
55	C28H36O5	452.58	33	0	0.64	2	5	2	127.53	83.83

56	C28H34O6	466.57	34	0	0.61	2	6	2	127.73	100.90
57	C28H38O7	486.60	35	0	0.79	2	7	3	128.69	116.59
58	C28H40O6	472.61	34	0	0.86	2	6	2	128.00	96.36
59	C28H36O7	484.58	35	0	0.71	2	7	3	128.18	116.59
60	C30H38O8	526.62	38	0	0.70	4	8	2	137.91	122.66
61	-	-	-	-	-	-	-	-	-	-
62	C30H41ClO7	549.10	38	0	0.77	5	7	2	144.21	110.13
63	C28H39ClO7	523.06	36	0	0.79	3	7	4	135.68	124.29
64	C28H42O8	506.63	36	0	0.86	3	8	5	132.48	144.52
65	C28H36O4	436.58	32	0	0.64	3	4	1	126.37	63.60
66	C28H36O4	436.58	32	0	0.64	2	4	1	126.41	63.60
67	C28H40O8	504.61	36	0	0.79	2	8	5	132.12	144.52
68	C28H40O7	488.61	35	0	0.79	2	7	4	130.88	124.29
69	C28H36O6	468.58	34	0	0.71	1	6	2	127.02	93.06
70	C28H36O6	468.58	34	0	0.71	1	6	2	127.02	93.06
71	C28H36O8	500.58	36	0	0.71	2	8	3	129.60	122.52
72	C28H38O7	486.60	35	0	0.86	1	7	3	126.79	116.59
73	C28H38O7	486.60	35	0	0.86	1	7	3	126.83	116.59
74	C28H40O9	520.61	37	0	0.86	1	9	6	131.34	164.75
75	C28H40O7	488.61	35	0	0.93	1	7	3	127.30	116.59
76	C29H42O9	534.64	38	0	0.93	2	9	4	134.36	146.05
77	C28H38O7	486.60	35	0	0.86	1	7	3	126.83	116.59
78	C28H36O6	468.58	34	0	0.79	1	6	2	125.15	96.36
79	C28H38O7	486.60	35	0	0.86	1	7	3	126.83	116.59
80	C28H36O5	452.58	33	0	0.71	1	5	1	125.93	72.83
81	C34H48O11	632.74	45	0	0.82	5	11	5	159.91	172.21
82	C28H36O7	484.58	35	0	0.79	1	7	2	126.57	102.29
83	C28H36O7	484.58	35	0	0.79	1	7	2	126.57	102.29
84	C28H36O8	500.58	36	0	0.79	1	8	3	127.74	122.52

85	C28H36O10	532.58	38	0	0.86	1	10	3	128.30	140.98
86	C28H36O9	516.58	37	0	0.86	1	9	3	127.22	135.05
87	C28H36O7	484.58	35	0	0.71	2	7	3	128.18	116.59
88	C28H38O6	470.60	34	0	0.75	4	6	2	128.42	100.90
89	C28H40O6	472.61	34	0	0.82	4	6	2	128.89	100.90
90	C28H36O7	484.58	35	0	0.71	3	7	3	128.18	116.59
91	C30H42O7	514.65	37	0	0.80	4	7	2	138.19	105.59

Table 9: Lipophilicity properties of the withanolides. predicted by the server SwissADME.

ID	iLOGP	XLOGP3	WLOGP	MLOGP	Silicos-IT Log P	Consensus Log P
1	3.85	3.70	3.92	3.07	4.44	3.80
2	3.80	3.12	3.50	2.75	3.78	3.39
3	4.11	4.27	4.49	3.39	4.96	4.25
4	3.33	2.52	3.04	2.28	3.66	2.97
5	3.29	1.69	2.48	1.95	3.76	2.64
6	4.20	3.85	3.92	3.07	4.44	3.90
7	4.39	4.43	4.29	3.06	4.64	4.16
8	4.01	2.87	3.12	2.37	3.96	3.27
9	3.84	2.49	3.36	2.24	4.44	3.27
10	3.73	2.93	3.74	2.84	4.78	3.60
11	4.04	2.86	3.75	2.43	4.84	3.59
12	2.99	2.51	2.28	1.68	3.60	2.61
13	3.11	2.51	2.28	1.68	3.60	2.64
14	3.45	2.91	3.16	1.50	2.53	2.71
15	3.24	2.24	2.48	1.95	3.76	2.74
16	3.20	1.26	1.68	1.26	3.28	2.14
17	4.09	4.36	4.71	3.79	4.60	4.31
18	3.47	4.50	4.14	3.48	4.09	3.94
19	4.11	3.18	3.83	2.99	3.82	3.58
20	3.82	4.84	4.71	3.79	4.60	4.35
21	2.74	1.71	2.52	1.87	3.23	2.41
22	3.40	2.77	3.40	2.67	3.72	3.19
23	3.07	2.21	3.32	2.58	3.71	2.98
24	3.41	2.88	3.26	2.67	3.59	3.16
25	3.10	2.41	3.54	2.67	3.83	3.11
26	3.72	3.78	4.28	3.48	3.94	3.84

27	3.56	4.36	4.22	3.57	3.55	3.85
28	2.92	1.82	2.44	1.79	3.29	2.45
29	3.01	1.64	2.52	1.87	3.23	2.45
30	3.05	2.34	3.54	2.67	3.83	3.09
31	2.40	1.64	2.52	1.87	3.23	2.33
32	3.53	3.93	4.29	3.48	4.49	3.94
33	3.94	4.63	5.31	4.31	5.09	4.66
34	3.44	2.70	3.40	2.67	3.72	3.19
35	3.65	3.40	4.43	3.48	4.33	3.86
36	2.81	1.59	2.60	1.95	3.24	2.44
37	3.70	0.69	1.45	0.40	1.76	1.60
38	3.44	0.69	1.45	0.40	1.76	1.55
39	3.42	2.86	3.56	2.84	3.46	3.23
40	3.20	2.84	4.35	3.40	4.32	3.62
41	3.76	3.64	4.43	3.48	4.59	3.98
42	-	-	-	-	-	-
43	2.17	-1.06	-0.47	-1.11	0.67	0.04
44	3.33	2.41	3.54	2.67	3.83	3.16
45	4.04	1.71	2.52	1.87	3.23	2.67
46	3.33	1.23	2.74	1.95	3.35	2.52
47	3.23	-1.34	-0.47	-1.11	0.39	0.14
48	3.15	1.44	2.51	1.87	2.94	2.38
49	2.93	1.37	2.51	1.87	2.94	2.32
50	3.78	2.36	3.56	2.67	4.16	3.31
51	3.38	3.57	4.06	3.40	4.08	3.70
52	3.73	4.27	5.09	4.23	4.69	4.40
53	3.35	4.07	4.27	3.32	4.67	3.93
54	3.20	2.54	3.18	2.58	3.32	2.96
55	3.54	3.65	4.21	3.40	4.21	3.80

56	3.10	3.04	3.38	2.51	3.90	3.19
57	3.41	2.69	2.47	1.95	2.89	2.68
58	2.85	3.63	3.43	2.84	3.66	3.28
59	2.99	2.01	2.39	1.87	3.16	2.48
60	2.80	2.58	2.96	2.20	3.67	2.84
61	-	-	-	-	-	-
62	3.71	4.13	4.12	3.26	4.35	3.91
63	1.35	2.50	2.67	2.15	3.34	2.40
64	2.73	1.85	1.50	1.26	2.23	1.92
65	3.63	5.64	4.95	4.23	4.58	4.60
66	3.79	4.92	5.09	4.23	4.42	4.49
67	3.52	0.75	1.71	1.17	2.46	1.92
68	2.86	1.92	2.45	1.95	2.83	2.40
69	3.19	2.85	3.62	3.07	3.23	3.19
70	3.43	2.78	3.62	3.07	3.23	3.23
71	2.61	1.56	2.46	1.89	2.60	2.23
72	3.14	2.28	2.16	2.04	2.60	2.44
73	3.09	2.01	2.30	2.04	2.99	2.49
74	1.90	0.04	0.23	0.48	0.89	0.71
75	3.09	2.00	2.52	2.14	3.40	2.63
76	2.44	0.59	1.12	0.77	2.17	1.42
77	2.62	1.68	2.30	2.04	2.99	2.33
78	3.40	2.36	3.11	2.75	3.48	3.02
79	3.12	1.68	2.30	2.04	2.99	2.43
80	3.83	3.17	4.59	3.48	4.79	3.97
81	3.91	0.44	1.47	0.40	2.08	1.66
82	3.53	1.65	2.98	2.36	3.21	2.75
83	3.25	1.58	2.98	2.36	3.21	2.68
84	2.82	0.74	1.95	1.57	2.32	1.88

85	2.75	0.35	1.09	0.93	1.49	1.32
86	2.92	0.01	1.16	0.88	2.16	1.43
87	3.22	1.87	2.39	1.87	3.16	2.50
88	2.91	4.29	3.40	2.67	4.08	3.47
89	3.09	4.09	3.62	2.75	4.48	3.61
90	3.32	0.74	2.39	1.87	3.42	2.35
91	4.08	1.92	3.65	2.34	4.51	3.30

Table 10: Water solubility of the withanolides. predicted by the server SwissADME.

ID	ESOL Log S	ESOL Solubility (mg/ml)	ESOL Solubility (mol/l)	ESOL Class	Ali Log S	Ali Solubility (mg/ml)	Ali Solubility (mol/l)	Ali Class	Silicos-IT LogSw	Silicos-IT Solubility (mg/ml)	Silicos-IT Solubility (mol/l)	Silicos-IT class
1	-5.02	4.90e-03	9.56e-06	MS	-5.54	1.47e-03	2.87e-06	MS	-4.40	2.04e-02	3.98e-05	MS
2	-4.59	1.21e-02	2.56e-05	MS	-4.81	7.25e-03	1.54e-05	MS	-3.78	7.85e-02	1.67e-04	S
3	-5.51	1.73e-03	3.11e-06	MS	-6.26	3.04e-04	5.49e-07	PS	-5.00	5.53e-03	9.98e-06	MS
4	-4.44	1.91e-02	3.62e-05	MS	-4.74	9.57e-03	1.81e-05	MS	-3.78	8.83e-02	1.67e-04	S
5	-3.71	9.42e-02	1.94e-04	S	-3.59	1.24e-01	2.56e-04	S	-3.50	1.53e-01	3.15e-04	S
6	-5.11	3.94e-03	7.69e-06	MS	-5.70	1.03e-03	2.01e-06	MS	-4.40	2.04e-02	3.98e-05	MS
7	-5.62	1.33e-03	2.40e-06	MS	-6.49	1.79e-04	3.21e-07	PS	-4.52	1.67e-02	3.00e-05	MS
8	-4.61	1.31e-02	2.47e-05	MS	-5.11	4.16e-03	7.85e-06	MS	-4.04	4.83e-02	9.10e-05	MS
9	-4.31	2.43e-02	4.85e-05	MS	-4.19	3.23e-02	6.45e-05	MS	-4.41	1.96e-02	3.92e-05	MS
10	-4.47	1.59e-02	3.38e-05	MS	-4.45	1.66e-02	3.52e-05	MS	-4.54	1.35e-02	2.86e-05	MS
11	-4.57	1.39e-02	2.70e-05	MS	-4.57	1.37e-02	2.66e-05	MS	-4.80	8.23e-03	1.60e-05	MS
12	-4.88	7.76e-03	1.33e-05	MS	-5.33	2.72e-03	4.66e-06	MS	-4.66	1.27e-02	2.18e-05	MS
13	-4.88	7.76e-03	1.33e-05	MS	-5.33	2.72e-03	4.66e-06	MS	-4.66	1.27e-02	2.18e-05	MS
14	-5.32	2.92e-03	4.83e-06	MS	-6.06	5.32e-04	8.78e-07	PS	-4.97	6.48e-03	1.07e-05	MS
15	-4.06	4.24e-02	8.76e-05	MS	-4.16	3.33e-02	6.88e-05	MS	-3.50	1.53e-01	3.15e-04	S
16	-3.55	1.41e-01	2.81e-04	S	-3.57	1.35e-01	2.69e-04	S	-3.15	3.60e-01	7.16e-04	S
17	-5.34	2.29e-03	4.61e-06	MS	-5.96	5.40e-04	1.09e-06	MS	-4.68	1.04e-02	2.10e-05	MS
18	-5.30	2.30e-03	5.06e-06	MS	-5.98	4.75e-04	1.04e-06	MS	-4.07	3.86e-02	8.49e-05	MS
19	-4.76	8.96e-03	1.75e-05	MS	-5.16	3.52e-03	6.86e-06	MS	-4.06	4.51e-02	8.79e-05	MS
20	-5.64	1.14e-03	2.30e-06	MS	-6.46	1.72e-04	3.45e-07	PS	-4.68	1.04e-02	2.10e-05	MS
21	-3.74	8.93e-02	1.84e-04	S	-3.94	5.64e-02	1.16e-04	S	-3.56	1.35e-01	2.77e-04	S
22	-4.30	2.33e-02	4.96e-05	MS	-4.61	1.15e-02	2.45e-05	MS	-3.93	5.53e-02	1.17e-04	S
23	-3.94	5.39e-02	1.15e-04	S	-4.03	4.38e-02	9.34e-05	MS	-3.91	5.73e-02	1.22e-04	S
24	-4.37	1.99e-02	4.23e-05	MS	-4.73	8.86e-03	1.88e-05	MS	-3.70	9.41e-02	2.00e-04	S
25	-4.14	3.38e-02	7.18e-05	MS	-4.24	2.72e-02	5.79e-05	MS	-4.13	3.48e-02	7.40e-05	MS
26	-4.91	5.62e-03	1.24e-05	MS	-5.23	2.65e-03	5.83e-06	MS	-4.05	4.01e-02	8.83e-05	MS

27	-5.29	2.36e-03	5.18e-06	MS	-5.84	6.66e-04	1.46e-06	MS	-3.62	1.09e-01	2.39e-04	S
28	-3.79	7.80e-02	1.61e-04	S	-3.98	5.03e-02	1.04e-04	S	-3.57	1.30e-01	2.67e-04	S
29	-3.69	9.89e-02	2.03e-04	S	-3.86	6.67e-02	1.37e-04	S	-3.56	1.35e-01	2.77e-04	S
30	-4.10	3.74e-02	7.95e-05	MS	-4.16	3.22e-02	6.84e-05	MS	-4.13	3.48e-02	7.40e-05	MS
31	-3.69	9.89e-02	2.03e-04	S	-3.86	6.67e-02	1.37e-04	S	-3.56	1.35e-01	2.77e-04	S
32	-4.94	5.26e-03	1.16e-05	MS	-5.39	1.85e-03	4.08e-06	MS	-4.52	1.37e-02	3.01e-05	MS
33	-5.34	1.99e-03	4.53e-06	MS	-5.69	8.93e-04	2.04e-06	MS	-5.09	3.53e-03	8.05e-06	MS
34	-4.26	2.58e-02	5.49e-05	MS	-4.54	1.36e-02	2.90e-05	MS	-3.93	5.53e-02	1.17e-04	S
35	-4.67	9.75e-03	2.15e-05	MS	-4.84	6.57e-03	1.45e-05	MS	-4.50	1.42e-02	3.13e-05	MS
36	-3.67	1.04e-01	2.12e-04	S	-3.81	7.55e-02	1.54e-04	S	-3.57	1.31e-01	2.67e-04	S
37	-3.88	8.36e-02	1.32e-04	S	-4.11	4.88e-02	7.68e-05	MS	-2.34	2.88e+00	4.54e-03	S
38	-3.88	8.36e-02	1.32e-04	S	-4.11	4.88e-02	7.68e-05	MS	-2.34	2.88e+00	4.54e-03	S
39	-4.45	1.67e-02	3.53e-05	MS	-4.70	9.38e-03	1.98e-05	MS	-3.71	9.17e-02	1.93e-04	S
40	-4.30	2.25e-02	4.97e-05	MS	-4.26	2.49e-02	5.51e-05	MS	-4.49	1.47e-02	3.26e-05	MS
41	-4.82	6.89e-03	1.51e-05	MS	-5.09	3.70e-03	8.15e-06	MS	-4.72	8.60e-03	1.89e-05	MS
42	-	-	-	-	-	-	-	-	-	-	-	-
43	-2.91	8.20e-01	1.23e-03	S	-3.15	4.74e-01	7.11e-04	S	-1.39	2.75e+01	4.12e-02	S
44	-4.14	3.38e-02	7.18e-05	MS	-4.24	2.72e-02	5.79e-05	MS	-4.13	3.48e-02	7.40e-05	MS
45	-3.74	8.93e-02	1.84e-04	S	-3.94	5.64e-02	1.16e-04	S	-3.56	1.35e-01	2.77e-04	S
46	-3.51	1.50e-01	3.07e-04	S	-3.44	1.78e-01	3.65e-04	S	-3.77	8.20e-02	1.68e-04	S
47	-2.80	1.06e+00	1.59e-03	S	-2.86	9.25e-01	1.39e-03	S	-1.14	4.86e+01	7.29e-02	S
48	-3.63	1.14e-01	2.33e-04	S	-3.66	1.08e-01	2.21e-04	S	-3.31	2.39e-01	4.91e-04	S
49	-3.59	1.26e-01	2.58e-04	S	-3.58	1.27e-01	2.61e-04	S	-3.31	2.39e-01	4.91e-04	S
50	-4.10	3.72e-02	7.94e-05	MS	-4.02	4.44e-02	9.47e-05	MS	-4.21	2.88e-02	6.15e-05	MS
51	-4.70	9.09e-03	2.01e-05	MS	-5.02	4.36e-03	9.63e-06	MS	-4.05	3.99e-02	8.81e-05	MS
52	-5.10	3.43e-03	7.85e-06	MS	-5.32	2.10e-03	4.81e-06	MS	-4.63	1.03e-02	2.36e-05	MS
53	-5.00	4.51e-03	1.00e-05	MS	-5.47	1.53e-03	3.40e-06	MS	-4.75	7.99e-03	1.77e-05	MS
54	-4.21	2.87e-02	6.12e-05	MS	-4.37	1.99e-02	4.24e-05	MS	-3.46	1.61e-01	3.44e-04	S
55	-4.81	6.95e-03	1.54e-05	MS	-5.10	3.60e-03	7.96e-06	MS	-4.29	2.34e-02	5.18e-05	MS

56	-4.52	1.42e-02	3.05e-05	MS	-4.82	6.99e-03	1.50e-05	MS	-4.16	3.23e-02	6.92e-05	MS
57	-4.42	1.85e-02	3.81e-05	MS	-4.79	7.87e-03	1.62e-05	MS	-2.96	5.40e-01	1.11e-03	S
58	-4.93	5.62e-03	1.19e-05	MS	-5.34	2.15e-03	4.55e-06	MS	-3.56	1.29e-01	2.73e-04	S
59	-3.98	5.09e-02	1.05e-04	S	-4.09	3.98e-02	8.22e-05	MS	-3.19	3.15e-01	6.50e-04	S
60	-4.47	1.80e-02	3.42e-05	MS	-4.80	8.26e-03	1.57e-05	MS	-3.79	8.54e-02	1.62e-04	S
61	-	-	-	-	-	-	-	-	-	-	-	-
62	-5.52	1.67e-03	3.05e-06	MS	-6.15	3.89e-04	7.09e-07	PS	-4.66	1.19e-02	2.17e-05	MS
63	-4.46	1.81e-02	3.47e-05	MS	-4.76	9.18e-03	1.76e-05	MS	-3.69	1.07e-01	2.05e-04	S
64	-3.95	5.70e-02	1.13e-04	S	-4.51	1.58e-02	3.12e-05	MS	-2.54	1.48e+00	2.92e-03	S
65	-5.90	5.47e-04	1.25e-06	MS	-6.74	7.95e-05	1.82e-07	PS	-4.43	1.63e-02	3.74e-05	MS
66	-5.51	1.34e-03	3.06e-06	MS	-5.99	4.44e-04	1.02e-06	MS	-4.41	1.70e-02	3.90e-05	MS
67	-3.31	2.48e-01	4.91e-04	S	-3.36	2.18e-01	4.32e-04	S	-2.95	5.65e-01	1.12e-03	S
68	-3.95	5.52e-02	1.13e-04	S	-4.15	3.43e-02	7.02e-05	MS	-3.09	3.94e-01	8.05e-04	S
69	-4.47	1.57e-02	3.35e-05	MS	-4.46	1.61e-02	3.44e-05	MS	-3.65	1.04e-01	2.22e-04	S
70	-4.43	1.74e-02	3.71e-05	MS	-4.39	1.91e-02	4.07e-05	MS	-3.65	1.04e-01	2.22e-04	S
71	-3.79	8.04e-02	1.61e-04	S	-3.74	9.05e-02	1.81e-04	S	-3.25	2.81e-01	5.61e-04	S
72	-4.23	2.88e-02	5.93e-05	MS	-4.37	2.10e-02	4.31e-05	MS	-2.85	6.92e-01	1.42e-03	S
73	-4.06	4.27e-02	8.77e-05	MS	-4.09	4.00e-02	8.22e-05	MS	-3.30	2.46e-01	5.05e-04	S
74	-3.03	4.89e-01	9.40e-04	S	-3.05	4.61e-01	8.86e-04	S	-1.57	1.40e+01	2.70e-02	S
75	-4.06	4.22e-02	8.64e-05	MS	-4.07	4.11e-02	8.41e-05	MS	-3.76	8.45e-02	1.73e-04	S
76	-3.39	2.16e-01	4.03e-04	S	-3.23	3.14e-01	5.88e-04	S	-2.80	8.45e-01	1.58e-03	S
77	-3.85	6.88e-02	1.41e-04	S	-3.74	8.80e-02	1.81e-04	S	-3.30	2.46e-01	5.05e-04	S
78	-4.17	3.20e-02	6.82e-05	MS	-4.02	4.44e-02	9.47e-05	MS	-3.65	1.04e-01	2.22e-04	S
79	-3.85	6.88e-02	1.41e-04	S	-3.74	8.80e-02	1.81e-04	S	-3.30	2.46e-01	5.05e-04	S
80	-4.58	1.20e-02	2.65e-05	MS	-4.37	1.93e-02	4.26e-05	MS	-5.25	2.53e-03	5.60e-06	MS
81	-3.71	1.23e-01	1.95e-04	S	-3.62	1.50e-01	2.38e-04	S	-2.89	8.13e-01	1.29e-03	S
82	-3.82	7.37e-02	1.52e-04	S	-3.41	1.88e-01	3.88e-04	S	-3.83	7.23e-02	1.49e-04	S
83	-3.77	8.16e-02	1.68e-04	S	-3.34	2.22e-01	4.58e-04	S	-3.83	7.23e-02	1.49e-04	S
84	-3.34	2.27e-01	4.53e-04	S	-2.89	6.42e-01	1.28e-03	S	-3.00	4.97e-01	9.93e-04	S

85	-3.30	2.69e-01	5.05e-04	S	-2.87	7.10e-01	1.33e-03	S	-2.45	1.90e+00	3.57e-03	S
86	-2.98	5.37e-01	1.04e-03	S	-2.40	2.07e+00	4.00e-03	S	-2.73	9.73e-01	1.88e-03	S
87	-3.89	6.24e-02	1.29e-04	S	-3.94	5.56e-02	1.15e-04	S	-3.19	3.15e-01	6.50e-04	S
88	-5.20	2.99e-03	6.36e-06	MS	-6.12	3.55e-04	7.55e-07	PS	-3.96	5.14e-02	1.09e-04	S
89	-5.08	3.90e-03	8.26e-06	MS	-5.91	5.76e-04	1.22e-06	MS	-4.43	1.76e-02	3.73e-05	MS
90	-3.11	3.74e-01	7.72e-04	S	-2.77	8.28e-01	1.71e-03	S	-3.41	1.90e-01	3.93e-04	S
91	-3.98	5.43e-02	1.06e-04	S	-3.76	8.92e-02	1.73e-04	S	-4.70	1.03e-02	2.00e-05	MS

S = soluble
PS = poorly soluble
MS = moderately soluble

Table 11: Pharmacokinetics properties of the withanolides. predicted by the server SwissADME.

ID	GI absorption	BBB permeant	Pgp substrate	CYP1A2 inhibitor	CYP2C19 inhibitor	CYP2C9 inhibitor	CYP2D6 inhibitor	CYP3A4 inhibitor	log Kp (cm/s)
1	High	No	Yes	No	No	No	No	No	-6.80
2	High	No	Yes	No	No	No	No	No	-6.96
3	High	No	Yes	No	No	No	No	No	-6.65
4	High	No	Yes	No	No	No	No	No	-7.74
5	High	No	Yes	No	No	No	No	No	-8.06
6	High	No	Yes	No	No	No	No	No	-6.69
7	High	No	Yes	No	No	No	No	No	-6.55
8	High	No	Yes	No	No	No	No	No	-7.50
9	High	No	Yes	No	No	No	No	No	-7.59
10	High	No	Yes	No	No	No	No	No	-7.09
11	High	No	Yes	No	No	No	No	No	-7.41
12	Low	No	Yes	No	No	No	No	No	-8.07
13	Low	No	Yes	No	No	No	No	No	-8.07
14	Low	No	Yes	No	No	No	Yes	No	-7.93
15	High	No	Yes	No	No	No	No	No	-7.67
16	High	No	Yes	No	No	No	No	No	-8.47
17	High	No	Yes	No	No	Yes	No	No	-6.23
18	High	No	Yes	No	No	Yes	No	No	-5.88
19	High	No	Yes	No	No	No	No	No	-7.17
20	High	No	Yes	No	No	Yes	No	No	-5.89
21	High	No	Yes	No	No	No	No	No	-8.05
22	High	No	Yes	No	No	No	No	Yes	-7.20
23	High	No	Yes	No	No	No	No	No	-7.59
24	High	No	Yes	No	No	No	No	No	-7.13
25	High	No	Yes	No	No	No	No	No	-7.46
26	High	No	Yes	No	No	No	No	No	-6.39

27	High	No	Yes	No	No	No	No	No	-5.99
28	High	No	Yes	No	No	No	No	No	-7.96
29	High	No	Yes	No	No	No	No	No	-8.10
30	High	No	Yes	No	No	No	No	No	-7.51
31	High	No	Yes	No	No	No	No	No	-8.10
32	High	No	Yes	No	No	Yes	No	Yes	-6.28
33	High	No	Yes	No	No	Yes	No	No	-5.69
34	High	No	Yes	No	No	No	No	Yes	-7.25
35	High	No	Yes	No	No	No	No	No	-6.66
36	High	No	Yes	No	No	No	No	No	-8.15
37	Low	No	Yes	No	No	No	No	No	-9.68
38	Low	No	Yes	No	No	No	No	No	-9.68
39	High	No	Yes	No	No	No	No	No	-7.16
40	High	No	Yes	No	No	No	No	No	-7.04
41	High	No	Yes	No	No	Yes	No	No	-6.49
42	-	-	-	-	-	-	-	-	-
43	Low	No	No	No	No	No	No	No	-11.12
44	High	No	Yes	No	No	No	No	No	-7.46
45	High	No	Yes	No	No	No	No	No	-8.05
46	High	No	Yes	No	No	No	No	No	-8.41
47	Low	No	No	No	No	No	No	No	-11.32
48	High	No	Yes	No	No	No	No	No	-8.25
49	High	No	Yes	No	No	No	No	No	-8.30
50	High	No	Yes	No	No	No	No	No	-7.48
51	High	No	Yes	No	No	Yes	No	Yes	-6.53
52	High	Yes	Yes	No	No	Yes	No	No	-5.93
53	High	No	Yes	No	No	Yes	No	No	-6.16
54	High	No	Yes	No	No	No	No	No	-7.35
55	High	No	Yes	No	No	Yes	No	Yes	-6.47

56	High	No	Yes	No	No	Yes	No	No	-6.99
57	High	No	Yes	No	No	No	No	No	-7.36
58	High	No	Yes	No	No	No	No	No	-6.61
59	High	No	Yes	No	No	No	No	No	-7.83
60	High	No	Yes	No	No	No	No	No	-7.68
61	-	-	-	-	-	-	-	-	-
62	High	No	Yes	No	No	No	No	No	-6.72
63	High	No	Yes	No	No	No	No	Yes	-7.72
64	Low	No	Yes	No	No	No	No	No	-8.08
65	High	Yes	Yes	No	No	Yes	No	No	-4.96
66	High	Yes	Yes	No	No	Yes	No	No	-5.47
67	Low	No	Yes	No	No	No	No	No	-8.85
68	High	No	Yes	No	No	No	No	No	-7.92
69	High	No	Yes	No	No	No	No	No	-7.13
70	High	No	Yes	No	No	No	No	No	-7.18
71	High	No	Yes	No	No	No	No	No	-8.25
72	High	No	Yes	No	No	No	No	No	-7.65
73	High	No	Yes	No	No	No	No	No	-7.84
74	Low	No	Yes	No	No	No	No	No	-9.45
75	High	No	Yes	No	No	No	No	No	-7.86
76	Low	No	Yes	No	No	No	No	No	-9.14
77	High	No	Yes	No	No	No	No	No	-8.08
78	High	No	Yes	No	No	No	No	No	-7.48
79	High	No	Yes	No	No	No	No	No	-8.08
80	High	No	Yes	No	No	No	No	No	-6.81
81	Low	No	Yes	No	No	No	No	No	-9.85
82	High	No	Yes	No	No	No	No	No	-8.08
83	High	No	Yes	No	No	No	No	No	-8.13
84	High	No	Yes	No	No	No	No	No	-8.83

85	High	No	Yes	No	No	No	No	No	-9.30
86	High	No	Yes	No	No	No	No	No	-9.44
87	High	No	Yes	No	No	No	No	No	-7.93
88	High	No	Yes	No	No	Yes	No	No	-6.12
89	High	No	Yes	No	No	No	No	No	-6.28
90	High	No	Yes	No	No	No	No	No	-8.73
91	High	No	Yes	No	No	No	No	No	-8.08

Table 12: Druglikeness properties of the withanolides. predicted by the server SwissADME.

ID	Lipinski #violations	Ghose #violations	Veber #violations	Egan #violations	Muegge #violations	Bioavailability Score
1	1	3	0	0	0	0.55
2	0	1	0	0	0	0.55
3	1	3	0	0	0	0.55
4	1	3	0	0	0	0.55
5	0	2	0	0	0	0.55
6	1	3	0	0	0	0.55
7	1	3	0	0	0	0.55
8	1	3	0	0	0	0.55
9	1	3	0	0	0	0.55
10	0	1	0	0	0	0.55
11	1	3	0	0	0	0.55
12	1	3	1	1	1	0.55
13	1	3	1	1	1	0.55
14	2	3	1	1	3	0.17
15	0	2	0	0	0	0.55
16	1	2	0	0	0	0.55
17	0	3	0	0	0	0.55
18	0	1	0	0	0	0.55
19	1	3	0	0	0	0.55
20	0	3	0	0	0	0.55
21	0	3	0	0	0	0.55
22	0	1	0	0	0	0.55
23	0	0	0	0	0	0.55
24	0	1	0	0	0	0.55
25	0	1	0	0	0	0.55
26	0	1	0	0	0	0.55

27	0	1	0	0	0	0.55
28	0	2	0	0	0	0.55
29	0	3	0	0	0	0.55
30	0	1	0	0	0	0.55
31	0	3	0	0	0	0.55
32	0	1	0	0	0	0.55
33	1	0	0	0	0	0.55
34	0	1	0	0	0	0.55
35	0	1	0	0	0	0.55
36	0	3	0	0	0	0.55
37	3	3	1	1	4	0.17
38	3	3	1	1	4	0.17
39	0	2	0	0	0	0.55
40	0	0	0	0	0	0.55
41	0	1	0	0	0	0.55
42	-	-	-	-	-	-
43	3	4	1	1	4	0.17
44	0	1	0	0	0	0.55
45	0	3	0	0	0	0.55
46	0	3	0	0	0	0.55
47	3	4	1	1	4	0.17
48	0	3	0	0	0	0.55
49	0	3	0	0	0	0.55
50	0	0	0	0	0	0.55
51	0	0	0	0	0	0.55
52	1	0	0	0	0	0.55
53	0	0	0	0	0	0.55
54	0	0	0	0	0	0.55
55	0	0	0	0	0	0.55

56	0	0	0	0	0	0.55
57	0	2	0	0	0	0.55
58	0	1	0	0	0	0.55
59	0	2	0	0	0	0.55
60	1	3	0	0	0	0.55
61	-	-	-	-	-	-
62	1	3	0	0	0	0.55
63	1	3	0	0	0	0.55
64	1	3	1	1	0	0.55
65	1	0	0	0	1	0.55
66	1	0	0	0	0	0.55
67	1	3	1	1	0	0.55
68	0	3	0	0	0	0.55
69	0	0	0	0	0	0.55
70	0	0	0	0	0	0.55
71	1	2	0	0	0	0.55
72	0	2	0	0	0	0.55
73	0	2	0	0	0	0.55
74	2	3	1	1	2	0.17
75	0	2	0	0	0	0.55
76	1	3	1	1	0	0.55
77	0	2	0	0	0	0.55
78	0	0	0	0	0	0.55
79	0	2	0	0	0	0.55
80	0	0	0	0	0	0.55
81	2	3	1	1	3	0.17
82	0	2	0	0	0	0.55
83	0	2	0	0	0	0.55
84	1	2	0	0	0	0.55

85	1	2	1	1	1	0.55
86	1	2	0	1	1	0.55
87	0	2	0	0	0	0.55
88	0	1	0	0	0	0.55
89	0	1	0	0	0	0.55
90	0	2	0	0	0	0.55
91	1	3	0	0	0	0.55

Table 13: Medicinal chemistry properties of the withanolides. predicted by the server SwissADME.

ID	PAINS #alerts	Brenk #alerts	Leadlikeness #violations	Synthetic Accessibility
1	0	2	2	7.06
2	0	1	1	6.85
3	0	2	2	7.31
4	0	2	1	7.22
5	0	1	1	6.93
6	0	2	2	7.03
7	0	4	2	7.43
8	0	2	1	7.11
9	0	1	1	7.02
10	0	1	1	6.78
11	0	1	1	7.14
12	0	1	1	7.00
13	0	1	1	7.00
14	0	1	1	7.13
15	0	1	1	7.18
16	0	1	1	7.20
17	0	2	2	6.49
18	0	1	2	6.29
19	0	2	1	6.68
20	0	2	2	6.52
21	0	1	1	6.37
22	0	1	1	6.28
23	0	1	1	6.22
24	0	1	1	6.32
25	0	1	1	6.33
26	0	1	2	6.33

27	0	1	2	6.26
28	0	0	1	6.29
29	0	0	1	6.48
30	0	0	1	6.45
31	0	0	1	6.48
32	0	0	2	6.38
33	0	0	2	6.32
34	0	0	1	6.45
35	0	0	1	6.40
36	0	1	1	6.49
37	0	1	1	7.78
38	0	1	1	7.78
39	0	1	1	6.39
40	0	1	1	6.31
41	0	1	2	6.28
42	-	-	-	-
43	0	1	1	7.85
44	0	1	1	6.33
45	0	1	1	6.37
46	0	1	1	6.50
47	0	1	1	7.90
48	0	1	1	6.44
49	0	0	1	6.56
50	0	1	1	6.89
51	0	1	2	6.27
52	0	1	2	6.21
53	0	1	2	6.08
54	0	1	1	6.25
55	0	1	2	6.14

56	0	1	1	6.08
57	0	1	1	6.55
58	0	1	2	6.35
59	0	2	1	6.39
60	0	3	1	6.59
61	-	-	-	-
62	0	2	2	6.74
63	0	1	1	6.53
64	0	0	1	6.55
65	0	0	2	6.43
66	0	0	2	6.43
67	0	0	1	6.53
68	0	0	1	6.47
69	0	1	1	6.89
70	0	0	1	7.01
71	0	1	1	6.93
72	0	1	1	7.65
73	0	1	1	7.61
74	0	0	1	7.32
75	0	1	1	7.29
76	0	1	1	7.54
77	0	1	1	7.55
78	0	2	1	7.52
79	0	1	1	7.55
80	0	0	1	6.81
81	0	1	1	8.09
82	0	1	1	7.83
83	0	0	1	8.00
84	0	0	1	8.12

85	0	2	1	8.83
86	0	1	1	8.48
87	0	2	1	6.84
88	0	1	2	6.44
89	0	1	2	6.21
90	0	2	1	6.95
91	0	2	1	7.25

Table 14: Medicinal chemistry properties of the withanolides. predicted by the server ADMET Lab2.

ID	NonBiodegradable	QED	Synth	Fsp3	MCE-18	Natural Product-likeness	Alarm_NMR	BMS	Chelating	PAINS	Lipinski	Pfizer	GSK	GoldenTriangle
1	3	0.316	6.041	0.8	145.185	2.585	1	0	0	0	Accepted	Accepted	Rejected	Rejected
2	3	0.486	5.738	0.821	150.333	3.109	2	0	0	0	Accepted	Accepted	Rejected	Accepted
3	3	0.208	6.174	0.75	146.429	2.527	1	0	0	0	Accepted	Accepted	Rejected	Rejected
4	3	0.337	6.17	0.8	156.074	2.412	1	0	0	0	Accepted	Accepted	Rejected	Rejected
5	3	0.345	6.334	0.857	167.885	2.68	2	1	0	0	Accepted	Accepted	Rejected	Accepted
6	3	0.408	5.698	0.8	145.185	2.943	2	0	0	0	Accepted	Accepted	Rejected	Rejected
7	3	0.192	6.051	0.812	150.621	2.694	2	1	0	0	Accepted	Accepted	Rejected	Rejected
8	3	0.42	5.841	0.833	149.836	3.3	2	0	0	0	Accepted	Accepted	Rejected	Rejected
9	3	0.361	6.404	0.862	168.667	2.933	1	0	0	0	Accepted	Accepted	Rejected	Rejected
10	3	0.489	6.123	0.857	166.154	3.388	2	0	0	0	Accepted	Accepted	Rejected	Accepted
11	3	0.348	6.408	0.867	167.571	2.67	1	0	0	0	Accepted	Accepted	Rejected	Rejected
12	3	0.361	5.934	0.75	213.571	2.732	2	0	0	0	Accepted	Accepted	Rejected	Rejected
13	3	0.361	5.934	0.75	213.571	2.732	2	0	0	0	Accepted	Accepted	Rejected	Rejected
14	3	0.305	6.222	0.727	231.579	2.597	2	0	0	0	Rejected	Accepted	Rejected	Rejected
15	3	0.485	6.348	0.821	165	3.24	2	0	0	0	Accepted	Accepted	Rejected	Accepted

16	3	0.393	6.475	0.857	169.846	3.316	2	0	0	0	Accepted	Accepted	Rejected	Rejected
17	1	0.408	5.476	0.733	87.615	2.328	1	0	0	0	Accepted	Accepted	Rejected	Accepted
18	1	0.504	5.124	0.75	86.204	3.017	2	0	0	0	Accepted	Accepted	Rejected	Accepted
19	1	0.45	5.614	0.733	95.346	2.283	1	0	0	0	Accepted	Accepted	Rejected	Rejected
20	1	0.453	5.512	0.7	86.667	2.721	1	0	0	0	Accepted	Accepted	Rejected	Accepted
21	1	0.452	5.427	0.714	98.167	3.434	2	0	0	0	Accepted	Accepted	Rejected	Accepted
22	1	0.546	5.261	0.714	93	3.31	2	0	0	0	Accepted	Accepted	Rejected	Accepted
23	1	0.434	5.407	0.643	90.783	3.516	2	0	0	0	Accepted	Accepted	Rejected	Accepted
24	1	0.483	5.347	0.75	91.429	2.846	2	0	0	0	Accepted	Accepted	Rejected	Accepted
25	1	0.534	5.349	0.714	98.167	3.318	2	0	0	0	Accepted	Accepted	Rejected	Accepted
26	1	0.609	5.246	0.714	90.417	3.384	2	0	0	0	Accepted	Accepted	Rejected	Accepted
27	1	0.608	5.441	0.786	92.4	3.346	1	0	0	0	Accepted	Accepted	Rejected	Accepted
28	1	0.467	5.452	0.714	93	2.743	2	0	0	0	Accepted	Accepted	Rejected	Accepted
29	1	0.452	5.427	0.714	98.167	3.434	2	0	0	0	Accepted	Accepted	Rejected	Accepted
30	1	0.534	5.349	0.714	98.167	3.318	2	0	0	0	Accepted	Accepted	Rejected	Accepted
31	1	0.452	5.427	0.714	98.167	3.434	2	0	0	0	Accepted	Accepted	Rejected	Accepted

32	1	0.622	5.201	0.714	87.833	3.585	2	0	0	0	Accepted	Accepted	Rejected	Accepted
33	1	0.593	5.116	0.714	87.833	3.466	2	0	0	0	Accepted	Rejected	Rejected	Accepted
34	1	0.546	5.282	0.714	93	3.622	2	0	0	0	Accepted	Accepted	Rejected	Accepted
35	1	0.603	5.2	0.714	93	3.508	2	0	0	0	Accepted	Accepted	Rejected	Accepted
36	1	0.356	5.275	0.786	97.68	3.432	2	0	0	0	Accepted	Accepted	Rejected	Accepted
37	2	0.19	5.637	0.824	120.484	3.113	2	0	0	0	Rejected	Accepted	Rejected	Rejected
38	2	0.19	5.637	0.824	120.484	3.113	2	0	0	0	Rejected	Accepted	Rejected	Rejected
39	1	0.418	5.384	0.857	99.615	3.303	1	0	0	0	Accepted	Accepted	Rejected	Accepted
40	1	0.481	5.331	0.643	90.783	3.399	2	0	0	0	Accepted	Accepted	Rejected	Accepted
41	1	0.603	5.378	0.714	93	3.29	2	0	0	0	Accepted	Accepted	Rejected	Accepted
42	2	0.115	6.207	0.85	148.649	2.777	2	1	0	0	Rejected	Accepted	Rejected	Rejected
43	2	0.133	5.837	0.824	125.839	3.053	2	1	0	0	Rejected	Accepted	Rejected	Rejected
44	1	0.534	5.349	0.714	98.167	3.318	2	0	0	0	Accepted	Accepted	Rejected	Accepted
45	1	0.452	5.427	0.714	98.167	3.434	2	0	0	0	Accepted	Accepted	Rejected	Accepted
46	1	0.348	5.34	0.786	102.96	3.136	2	0	0	0	Accepted	Accepted	Rejected	Accepted
47	2	0.138	5.935	0.824	128.516	2.967	2	1	0	0	Rejected	Accepted	Rejected	Rejected

48	1	0.442	5.573	0.714	100.75	3.345	2	0	0	0	Accepted	Accepted	Rejected	Accepted
49	1	0.442	5.573	0.714	100.75	3.345	2	0	0	0	Accepted	Accepted	Rejected	Accepted
50	3	0.475	5.981	0.714	150.5	3.289	2	0	0	0	Accepted	Accepted	Rejected	Accepted
51	1	0.509	5.296	0.679	84.255	2.918	2	0	0	0	Accepted	Accepted	Rejected	Accepted
52	1	0.431	5.214	0.679	84.255	2.749	2	0	0	0	Accepted	Rejected	Rejected	Accepted
53	1	0.517	5.354	0.607	82.133	2.987	4	1	0	0	Accepted	Accepted	Rejected	Accepted
54	1	0.475	5.464	0.679	88.255	2.708	2	0	0	0	Accepted	Accepted	Rejected	Accepted
55	1	0.484	5.356	0.643	84.652	3.169	2	0	0	0	Accepted	Accepted	Rejected	Accepted
56	1	0.479	5.521	0.607	86.133	2.775	4	1	0	0	Accepted	Accepted	Rejected	Accepted
57	3	0.35	5.782	0.821	112	2.707	1	0	0	0	Accepted	Accepted	Rejected	Accepted
58	3	0.363	5.76	0.857	110.385	2.946	1	0	0	0	Accepted	Accepted	Rejected	Accepted
59	3	0.313	5.852	0.714	105	3.023	2	0	0	0	Accepted	Accepted	Rejected	Accepted
60	3	0.327	6.017	0.7	106.118	2.521	1	0	0	0	Accepted	Accepted	Rejected	Rejected
61	2	0.03	7.452	0.857	191.154	1.523	1	1	0	0	Rejected	Accepted	Rejected	Rejected
62	2	0.405	5.269	0.8	97.296	2.639	2	1	0	0	Accepted	Accepted	Rejected	Rejected
63	2	0.384	5.516	0.821	101.333	2.805	2	1	0	0	Accepted	Accepted	Rejected	Rejected

64	1	0.362	5.408	0.857	99.615	3.242	2	0	0	0	Accepted	Accepted	Rejected	Rejected
65	1	0.636	5.13	0.643	80.696	3.234	3	0	0	0	Accepted	Rejected	Rejected	Accepted
66	1	0.613	5.173	0.643	85.739	3.141	3	0	0	0	Accepted	Rejected	Rejected	Accepted
67	1	0.282	5.633	0.786	108.24	3.108	2	0	0	0	Accepted	Accepted	Rejected	Rejected
68	1	0.511	5.364	0.821	101.333	2.817	2	0	0	0	Accepted	Accepted	Rejected	Accepted
69	2	0.571	5.987	0.714	143	3.47	2	0	0	0	Accepted	Accepted	Rejected	Accepted
70	2	0.571	5.987	0.714	143	3.47	2	0	0	0	Accepted	Accepted	Rejected	Accepted
71	2	0.495	6.807	0.714	146.667	3.388	2	0	0	0	Accepted	Accepted	Rejected	Rejected
72	3	0.433	6.737	0.893	178.245	2.868	1	0	0	0	Accepted	Accepted	Rejected	Accepted
73	3	0.433	6.687	0.893	182.038	2.764	1	0	0	0	Accepted	Accepted	Rejected	Accepted
74	1	0.313	6.401	0.893	128.453	2.764	1	0	0	0	Accepted	Accepted	Rejected	Rejected
75	3	0.384	6.701	0.929	183.111	3.196	1	0	0	0	Accepted	Accepted	Rejected	Accepted
76	3	0.302	6.986	0.931	189.286	3.316	1	0	0	0	Accepted	Accepted	Rejected	Rejected
77	3	0.433	6.697	0.893	182.038	2.696	0	0	0	0	Accepted	Accepted	Rejected	Accepted
78	3	0.359	6.693	0.821	172.275	2.925	0	0	0	0	Accepted	Accepted	Rejected	Accepted
79	3	0.433	6.697	0.893	182.038	2.696	0	0	0	0	Accepted	Accepted	Rejected	Accepted

80	2	0.589	6.219	0.714	107.625	3.164	2	0	0	0	Accepted	Rejected	Rejected	Accepted
81	2	0.22	6.484	0.824	130.065	2.936	2	0	0	0	Rejected	Accepted	Rejected	Rejected
82	2	0.552	7.277	0.786	174.84	2.655	1	0	0	0	Accepted	Accepted	Rejected	Accepted
83	2	0.552	7.277	0.786	174.84	2.655	1	0	0	0	Accepted	Accepted	Rejected	Accepted
84	2	0.526	7.388	0.821	179.765	2.434	1	0	0	0	Accepted	Accepted	Rejected	Rejected
85	2	0.336	6.38	0.857	203.538	2.451	1	1	0	0	Accepted	Accepted	Rejected	Rejected
86	3	0.347	7.871	0.857	203.538	2.611	1	0	0	0	Accepted	Accepted	Rejected	Rejected
87	3	0.352	6.039	0.75	146.122	2.863	2	0	0	0	Accepted	Accepted	Rejected	Accepted
88	1	0.482	5.386	0.75	91.429	3.325	4	1	0	0	Accepted	Accepted	Rejected	Accepted
89	1	0.479	5.291	0.821	93.333	3.264	3	1	0	0	Accepted	Accepted	Rejected	Accepted
90	3	0.284	6.295	0.786	147.2	2.859	2	1	0	0	Accepted	Accepted	Rejected	Accepted
91	3	0.336	6.372	0.8	147.296	2.736	1	0	0	0	Accepted	Accepted	Rejected	Rejected

Table 15: Physicochemical properties of the withanolides. predicted by the server ADMET Lab2.

ID	LogS	LogD	LogP	MW	Vol	Dense	nHA	nHD	TPSA	nRot	nRing	MaxRing	nHet	fChar	nRig	Flex	nStereo
1	-4.734	3.984	4.246	512.28	524.447	0.977	7	0	99.27	5	6	18	7	0	32	0.156	11
2	-4.637	3.687	3.897	470.27	483.701	0.972	6	1	93.2	2	6	18	6	0	31	0.065	10
3	-4.949	3.822	4.615	554.29	565.192	0.981	8	0	108.5	7	6	18	8	0	32	0.219	11
4	-4.68	2.661	3.441	528.27	533.237	0.991	8	1	119.5	4	6	18	8	0	32	0.125	12
5	-4.633	2.671	2.939	484.25	483.935	1.001	7	0	102.57	3	7	19	7	0	34	0.088	13
6	-4.783	3.92	4.109	512.28	524.447	0.977	7	0	99.27	5	6	18	7	0	32	0.156	10
7	-4.808	3.753	4.518	556.3	567.829	0.98	8	0	108.5	7	6	18	8	0	32	0.219	10
8	-4.385	3.505	3.359	530.29	535.873	0.99	8	2	122.66	5	6	18	8	0	31	0.161	12
9	-4.979	3.072	3.864	500.28	503.867	0.993	7	1	97.89	3	7	19	7	0	32	0.094	14
10	-4.888	3.698	4.004	470.27	477.781	0.984	6	1	88.66	2	7	19	6	0	32	0.062	12
11	-5.084	3.499	4.139	514.29	521.163	0.987	7	1	97.89	4	7	19	7	0	32	0.125	14
12	-3.929	2.743	2.437	582.29	578.629	1.006	10	3	151.22	4	7	18	10	0	38	0.105	12
13	-4.055	2.404	2.172	582.29	578.629	1.006	10	3	151.22	4	7	18	10	0	38	0.105	12
14	-3.253	2.572	1.937	605.32	600.142	1.009	11	4	166.71	4	8	18	11	0	41	0.098	12
15	-4.595	2.884	3.003	484.25	483.935	1.001	7	1	105.73	3	7	19	7	0	33	0.091	11
16	-4.111	2.265	2.222	502.26	495.361	1.014	8	3	129.12	3	7	19	8	0	32	0.094	13
17	-4.187	3.413	4.194	496.28	521.576	0.952	6	0	86.74	5	5	17	6	0	30	0.167	10
18	-4.174	3.305	3.619	454.27	480.831	0.945	5	1	80.67	3	5	17	5	0	29	0.103	9
19	-4.302	1.927	3.426	512.28	530.367	0.966	7	1	106.97	4	5	17	7	0	30	0.133	11
20	-4.502	3.672	4.327	496.28	521.576	0.952	6	1	89.9	5	5	17	6	0	29	0.172	10
21	-4.181	1.096	1.605	486.26	498.411	0.976	7	4	124.29	3	5	17	7	0	28	0.107	8
22	-4.224	2.553	2.793	470.27	489.621	0.96	6	3	104.06	3	5	17	6	0	28	0.107	8
23	-4.211	2.156	2.959	468.25	486.984	0.962	6	3	104.06	3	5	17	6	0	28	0.107	7
24	-4.059	1.955	2.574	470.27	489.621	0.96	6	2	100.9	3	5	17	6	0	29	0.103	9
25	-4.372	1.849	2.662	470.27	489.621	0.96	6	3	104.06	2	5	17	6	0	28	0.071	8

26	-4.363	3.317	3.583	454.27	480.831	0.945	5	2	83.83	2	5	17	5	0	28	0.071	9
27	-4.43	3.384	3.743	456.29	483.467	0.944	5	2	83.83	2	5	17	5	0	28	0.071	11
28	-3.806	0.658	1.917	484.25	495.775	0.977	7	2	117.97	3	5	17	7	0	30	0.1	8
29	-4.046	1.061	1.68	486.26	498.411	0.976	7	4	124.29	3	5	17	7	0	28	0.107	8
30	-4.372	1.849	2.662	470.27	489.621	0.96	6	3	104.06	2	5	17	6	0	28	0.071	8
31	-4.181	1.096	1.605	486.26	498.411	0.976	7	4	124.29	3	5	17	7	0	28	0.107	8
32	-4.636	3.082	3.313	454.27	480.831	0.945	5	2	83.83	3	5	17	5	0	28	0.107	8
33	-4.968	3.957	4.437	438.28	472.04	0.928	4	1	63.6	2	5	17	4	0	28	0.071	8
34	-4.527	1.593	2.324	470.27	489.621	0.96	6	3	104.06	3	5	17	6	0	28	0.107	8
35	-4.744	2.54	3.485	454.27	480.831	0.945	5	2	83.83	2	5	17	5	0	28	0.071	8
36	-4.525	0.828	2.025	488.28	501.048	0.975	7	4	124.29	3	5	17	7	0	28	0.107	9
37	-3.849	0.795	1.897	634.34	631.428	1.005	11	6	183.21	5	6	17	11	0	34	0.147	14
38	-3.801	0.741	1.891	634.34	631.428	1.005	11	6	183.21	5	6	17	11	0	34	0.147	14
39	-4.822	2.028	3.189	474.3	494.894	0.958	6	3	104.06	2	5	17	6	0	28	0.071	11
40	-4.567	3.234	4.002	452.26	478.194	0.946	5	2	83.83	2	5	17	5	0	28	0.071	7
41	-4.712	2.352	3.361	454.27	480.831	0.945	5	2	83.83	2	5	17	5	0	28	0.071	8
42	-3.324	-0.065	1.136	796.39	770.598	1.033	16	9	262.36	7	7	17	16	0	40	0.175	19
43	-3.271	-0.221	0.662	666.33	649.008	1.027	13	8	223.67	6	6	17	13	0	34	0.176	14
44	-4.458	1.922	2.594	470.27	489.621	0.96	6	3	104.06	2	5	17	6	0	28	0.071	8
45	-4.107	1.136	1.653	486.26	498.411	0.976	7	4	124.29	3	5	17	7	0	28	0.107	8
46	-4.455	1.108	2.214	488.28	501.048	0.975	7	4	124.29	2	5	17	7	0	28	0.071	9
47	-3.362	0.057	1.099	666.33	649.008	1.027	13	8	223.67	5	6	17	13	0	34	0.147	15
48	-4.214	1.56	2.262	486.26	498.411	0.976	7	4	124.29	2	5	17	7	0	28	0.071	9
49	-4.214	1.56	2.262	486.26	498.411	0.976	7	4	124.29	2	5	17	7	0	28	0.071	9
50	-4.632	2.025	2.764	468.25	481.064	0.973	6	2	96.36	2	6	18	6	0	30	0.067	9
51	-3.966	2.876	3.557	452.26	478.194	0.946	5	1	80.67	3	5	17	5	0	29	0.103	8
52	-4.348	3.755	4.82	436.26	469.404	0.929	4	0	60.44	2	5	17	4	0	29	0.069	8

53	-4.186	3.015	3.702	450.24	475.558	0.947	5	1	80.67	3	5	17	5	0	29	0.103	8
54	-3.331	2.067	2.164	468.25	486.984	0.962	6	2	100.9	2	5	17	6	0	30	0.067	8
55	-3.849	2.865	3.043	452.26	478.194	0.946	5	2	83.83	2	5	17	5	0	29	0.069	7
56	-3.699	2.299	2.482	466.24	484.348	0.963	6	2	100.9	2	5	17	6	0	30	0.067	8
57	-4.039	1.406	3.165	486.26	492.491	0.987	7	2	113.43	2	6	18	7	0	31	0.065	13
58	-4.537	3.157	3.657	472.28	486.337	0.971	6	2	96.36	2	6	18	6	0	30	0.067	13
59	-4.069	2.111	2.096	484.25	489.855	0.989	7	3	116.59	2	6	18	7	0	31	0.065	10
60	-4.161	2.2	2.52	526.26	530.6	0.992	8	2	122.66	4	6	18	8	0	32	0.125	11
61	-2.745	-0.509	-0.363	1204.51	1130.431	1.066	28	13	432.8	18	9	17	28	0	54	0.333	31
62	-4.187	3.69	3.859	548.25	548.214	1	7	1	106.97	5	5	17	8	0	30	0.167	10
63	-4.481	2.776	2.934	522.24	516.259	1.012	7	3	121.13	3	5	17	8	0	29	0.103	10
64	-3.718	2.461	2.176	506.29	512.474	0.988	8	5	144.52	3	5	17	8	0	28	0.107	12
65	-4.807	3.892	4.508	436.26	469.404	0.929	4	1	63.6	3	5	17	4	0	28	0.107	8
66	-4.923	3.819	4.919	436.26	469.404	0.929	4	1	63.6	2	5	17	4	0	28	0.071	8
67	-3.888	0.362	1.714	504.27	509.838	0.989	8	5	144.52	2	5	17	8	0	28	0.071	10
68	-4.084	2.964	2.877	488.28	501.048	0.975	7	3	121.13	2	5	17	7	0	29	0.069	10
69	-4.198	2.511	2.426	468.25	481.064	0.973	6	2	93.06	1	6	20	6	0	32	0.031	10
70	-4.198	2.511	2.426	468.25	481.064	0.973	6	2	93.06	1	6	20	6	0	32	0.031	10
71	-4.109	0.686	1.517	500.24	498.645	1.003	8	3	122.52	2	6	20	8	0	33	0.061	9
72	-4.503	3.236	2.356	486.26	486.571	0.999	7	2	113.43	1	7	18	7	0	34	0.029	13
73	-4.418	2.424	2.417	486.26	486.571	0.999	7	2	113.43	1	7	18	7	0	34	0.029	12
74	-3.53	1.298	1.481	520.27	512.708	1.015	9	5	161.59	1	6	17	9	0	32	0.031	13
75	-4.277	2.397	2.167	488.28	489.208	0.998	7	3	116.59	1	7	18	7	0	33	0.03	13
76	-4.051	2.01	1.804	534.28	524.084	1.019	9	4	146.05	2	7	18	9	0	33	0.061	15
77	-4.461	2.119	2.485	486.26	486.571	0.999	7	2	113.43	1	8	18	7	0	34	0.029	12
78	-4.567	3.05	3.458	468.25	475.144	0.985	6	1	93.2	1	8	18	6	0	34	0.029	11
79	-4.625	2.245	2.326	486.26	486.571	0.999	7	2	113.43	1	8	18	7	0	34	0.029	12

80	-4.818	2.392	3.09	452.26	472.274	0.958	5	1	72.83	1	6	6	5	0	31	0.032	8
81	-4.322	1.022	1.828	632.32	622.871	1.015	11	5	172.21	5	7	6	11	0	37	0.135	14
82	-4.172	1.436	1.504	484.25	483.935	1.001	7	2	102.29	1	8	17	7	0	34	0.029	11
83	-4.172	1.436	1.504	484.25	483.935	1.001	7	2	102.29	1	8	17	7	0	34	0.029	11
84	-3.507	0.661	1.045	500.24	492.725	1.015	8	2	119.36	1	8	17	8	0	35	0.029	12
85	-4.088	0.755	1.098	532.23	504.385	1.055	10	3	140.98	1	10	0	10	0	37	0.027	13
86	-4.146	0.362	0.942	516.24	495.595	1.042	9	3	135.05	1	9	18	9	0	36	0.028	14
87	-4.059	2.471	2.129	484.25	489.855	0.989	7	2	113.43	2	6	18	7	0	32	0.062	9
88	-4.252	2.795	2.58	470.27	489.621	0.96	6	2	100.9	4	5	16	6	0	28	0.143	10
89	-4.34	2.83	2.562	472.28	492.257	0.959	6	2	100.9	4	5	16	6	0	28	0.143	10
90	-4.152	1.051	1.828	484.25	489.855	0.989	7	1	110.27	3	6	18	7	0	32	0.094	11
91	-4.472	2.428	3.198	514.29	527.083	0.976	7	2	105.59	4	6	18	7	0	30	0.133	12

Table 16: Absorption. distribution. and excretion properties of the withanolides. predicted by the server ADMET Lab2.

ID	Pgp-inh	Pgp-sub	HIA	F(20%)	F(30%)	Caco-2	MDCK	BBB	PPB	VDss	Fu	CL	T12
1	0.999	0.648	0.006	0.786	0.996	-5.13	3.52E-05	0.962	65.71%	1.066	17.33%	9.539	0.454
2	0.998	0.355	0.005	0.848	0.98	-4.896	2.24E-05	0.981	80.63%	1.233	11.28%	12.501	0.752
3	1	0.948	0.01	0.975	0.995	-5.112	4.34E-05	0.965	64.03%	1.106	23.42%	5.483	0.353
4	0.999	0.992	0.006	0.83	0.974	-5.313	7.00E-05	0.977	55.67%	1.015	29.64%	7.189	0.64
5	0.995	0.01	0.003	0.606	0.979	-5.235	5.03E-05	0.984	54.44%	1.269	53.33%	17.36	0.569
6	0.998	0.366	0.004	0.979	0.994	-5.097	3.27E-05	0.829	81.34%	0.805	7.06%	14.624	0.772
7	0.995	0.068	0.002	0.954	0.978	-5.014	3.53E-05	0.974	79.77%	1.401	6.35%	13.061	0.791
8	0.996	0.995	0.025	0.798	0.989	-5.222	3.65E-05	0.503	66.26%	0.601	17.36%	10.931	0.811
9	0.999	0.95	0.004	0.082	0.938	-5.22	3.88E-05	0.664	62.83%	1.403	29.68%	12.803	0.481
10	0.995	0.989	0.003	0.773	0.983	-5.146	2.95E-05	0.901	68.97%	1.808	14.72%	16.019	0.743
11	0.999	0.896	0.003	0.078	0.793	-5.229	3.73E-05	0.765	64.80%	1.344	22.87%	13.417	0.335
12	0.896	0.992	0.205	0.768	0.991	-5.567	1.11E-05	0.135	37.66%	0.477	21.05%	9.748	0.833
13	0.858	0.983	0.093	0.258	0.977	-5.592	9.62E-06	0.151	44.05%	0.434	20.03%	8.87	0.862
14	0.297	0.999	0.816	0.062	0.994	-5.964	4.65E-06	0.247	47.47%	1.001	32.17%	10.678	0.906
15	0.853	0.993	0.006	0.778	0.994	-5.255	1.58E-05	0.857	76.11%	1.034	10.45%	12.167	0.827
16	0.203	0.998	0.043	0.171	0.99	-5.342	1.93E-05	0.253	55.41%	0.615	18.91%	8.935	0.85
17	1	0.142	0.023	0.029	0.851	-4.807	2.21E-05	0.974	54.56%	0.929	23.73%	11.324	0.207
18	0.998	0.489	0.011	0.008	0.017	-4.78	2.14E-05	0.647	89.43%	0.525	4.03%	17.098	0.728
19	1	0.962	0.008	0.033	0.363	-5.002	5.68E-05	0.967	51.99%	0.926	27.47%	6.738	0.441
20	1	0.253	0.492	0.813	0.634	-4.727	2.52E-05	0.957	66.98%	0.932	18.81%	8.259	0.603
21	0.917	0.83	0.485	0.105	0.585	-4.877	2.15E-05	0.945	72.85%	0.545	17.63%	2.928	0.85
22	0.995	0.642	0.056	0.031	0.026	-4.842	2.53E-05	0.871	80.05%	0.751	9.22%	5.779	0.869
23	0.989	0.743	0.114	0.038	0.051	-4.845	2.26E-05	0.958	81.70%	0.876	13.21%	4.933	0.851
24	0.993	0.888	0.013	0.007	0.011	-4.811	1.65E-05	0.732	61.10%	0.417	15.09%	14.435	0.709
25	0.994	0.97	0.096	0.579	0.936	-4.894	2.21E-05	0.985	82.29%	1.068	13.05%	4.434	0.762

26	1	0.847	0.12	0.436	0.053	-4.732	2.96E-05	0.951	87.03%	1.64	10.99%	11.885	0.85
27	1	0.277	0.03	0.427	0.044	-4.712	2.46E-05	0.952	75.81%	1.278	16.50%	11.45	0.624
28	0.169	0.885	0.019	0.349	0.014	-4.881	1.08E-05	0.533	59.24%	0.389	26.16%	9.644	0.759
29	0.963	0.976	0.378	0.07	0.463	-4.962	1.95E-05	0.904	70.21%	0.516	18.09%	3.138	0.843
30	0.994	0.97	0.096	0.579	0.936	-4.894	2.21E-05	0.985	82.29%	1.068	13.05%	4.434	0.762
31	0.917	0.83	0.485	0.105	0.585	-4.877	2.15E-05	0.945	72.85%	0.545	17.63%	2.928	0.85
32	0.997	0.348	0.386	0.879	0.921	-4.88	2.56E-05	0.235	89.92%	0.842	3.26%	5.455	0.784
33	0.999	0.778	0.038	0.975	0.983	-4.909	2.58E-05	0.564	92.41%	1.266	3.71%	9.055	0.61
34	0.994	0.377	0.627	0.502	0.631	-4.791	2.61E-05	0.945	82.94%	0.771	8.42%	3.335	0.867
35	0.999	0.832	0.205	0.898	0.958	-4.802	2.52E-05	0.979	87.35%	1.31	9.62%	5.471	0.812
36	0.307	0.949	0.269	0.548	0.039	-4.842	6.74E-06	0.808	61.02%	0.492	20.17%	2.96	0.772
37	0.956	0.862	0.867	0.888	0.775	-5.45	3.28E-05	0.052	74.53%	0.56	10.85%	1.507	0.824
38	0.964	0.996	0.897	0.497	0.61	-5.643	4.54E-05	0.117	60.40%	0.466	15.89%	1.631	0.85
39	0.953	0.983	0.01	0.081	0.272	-4.757	2.24E-05	0.891	59.93%	0.842	27.35%	5.72	0.363
40	0.998	0.706	0.046	0.313	0.724	-4.815	2.54E-05	0.991	90.02%	1.68	8.39%	6.853	0.715
41	0.997	0.966	0.042	0.916	0.971	-4.921	2.43E-05	0.949	83.81%	0.995	10.96%	8.241	0.523
42	0.421	1	0.94	0.928	0.997	-6.388	0.000115	0.125	49.26%	0.384	20.68%	0.964	0.752
43	0.321	0.988	0.89	0.926	0.846	-6.313	3.87E-05	0.147	38.00%	0.396	22.67%	1.247	0.81
44	0.993	0.939	0.06	0.398	0.857	-4.821	2.29E-05	0.988	84.81%	1.062	10.57%	4.23	0.725
45	0.965	0.954	0.227	0.036	0.15	-4.856	2.01E-05	0.923	74.20%	0.481	16.65%	3.02	0.815
46	0.518	0.995	0.012	0.071	0.131	-4.931	9.44E-06	0.961	66.89%	0.514	18.66%	3.795	0.505
47	0.708	0.999	0.834	0.636	0.913	-6.334	6.16E-05	0.139	46.62%	0.401	21.24%	1.189	0.799
48	0.995	0.994	0.261	0.302	0.551	-4.871	2.06E-05	0.967	82.78%	0.906	14.20%	3.09	0.822
49	0.995	0.994	0.261	0.302	0.551	-4.871	2.06E-05	0.967	82.78%	0.906	14.20%	3.09	0.822
50	0.995	0.987	0.033	0.829	0.978	-4.935	1.91E-05	0.989	83.80%	1.528	11.18%	6.714	0.801
51	0.992	0.659	0.007	0.006	0.003	-4.737	2.62E-05	0.864	77.02%	0.711	11.69%	16.893	0.451
52	0.998	0.222	0.007	0.016	0.05	-4.707	2.85E-05	0.919	92.22%	1.399	6.77%	18.011	0.205

53	0.997	0.132	0.01	0.007	0.013	-4.729	3.77E-05	0.198	88.48%	1.396	8.66%	12.513	0.065
54	0.993	0.996	0.008	0.005	0.003	-4.803	1.68E-05	0.791	53.98%	0.438	30.54%	11.834	0.844
55	0.998	0.992	0.047	0.068	0.006	-4.847	2.41E-05	0.9	84.07%	0.905	12.63%	10.756	0.834
56	0.998	0.98	0.011	0.007	0.015	-4.913	2.07E-05	0.84	81.29%	0.761	15.60%	9.226	0.2
57	0.997	0.005	0.018	0.007	0.011	-4.735	4.13E-05	0.945	50.50%	1.182	52.51%	8.072	0.658
58	0.997	0.012	0.006	0.01	0.372	-4.88	4.11E-05	0.942	54.80%	0.783	28.04%	11.125	0.389
59	0.937	0.99	0.029	0.007	0.013	-4.961	1.19E-05	0.785	33.57%	0.575	40.82%	4.212	0.831
60	0.997	0.989	0.023	0.184	0.103	-5.23	9.79E-05	0.442	34.99%	0.64	59.44%	3.703	0.663
61	0.992	0.999	1	0.908	1	-6.492	0.000708	0.119	33.20%	0.056	30.43%	0.123	0.914
62	0.998	0.993	0.01	0.463	0.82	-5.216	2.78E-05	0.971	88.76%	0.566	6.89%	13.637	0.732
63	0.871	0.938	0.007	0.008	0.162	-5.095	1.29E-05	0.914	68.59%	0.479	16.48%	5.277	0.86
64	0.936	0.996	0.877	0.045	0.662	-5.382	1.78E-05	0.308	59.13%	0.399	18.00%	3.906	0.891
65	0.999	0.106	0.019	0.763	0.008	-4.953	2.43E-05	0.054	92.07%	1.462	2.99%	8.766	0.239
66	1	0.036	0.014	0.861	0.059	-4.816	2.68E-05	0.242	93.02%	2.262	4.47%	5.93	0.131
67	0.057	0.987	0.037	0.054	0.811	-5.312	7.76E-06	0.899	32.16%	0.45	28.35%	2.193	0.71
68	0.986	0.993	0.068	0.091	0.965	-4.983	1.32E-05	0.943	80.64%	0.642	10.56%	6.24	0.797
69	0.999	0.977	0.387	0.725	0.433	-4.851	2.47E-05	0.928	78.80%	1.803	19.13%	10.886	0.918
70	0.999	0.977	0.387	0.725	0.433	-4.851	2.47E-05	0.928	78.80%	1.803	19.13%	10.886	0.918
71	0.994	0.952	0.795	0.915	0.969	-5.053	1.88E-05	0.824	73.63%	1.169	14.33%	4.736	0.882
72	0.934	0.716	0.006	0.584	0.982	-5.293	1.72E-05	0.945	60.51%	0.674	21.23%	7.003	0.763
73	0.845	0.19	0.005	0.412	0.978	-5.312	1.92E-05	0.947	66.31%	0.578	14.66%	8.928	0.582
74	0.115	0.996	0.076	0.641	0.977	-5.366	3.88E-05	0.854	60.74%	0.332	23.53%	2.742	0.773
75	0.52	0.108	0.005	0.74	0.949	-5.287	1.94E-05	0.916	65.84%	0.739	17.10%	6.318	0.678
76	0.187	0.959	0.035	0.588	0.973	-5.392	3.08E-05	0.596	54.75%	0.444	30.49%	3.613	0.679
77	0.422	0.138	0.005	0.816	0.972	-5.327	2.06E-05	0.895	63.85%	0.404	16.88%	8.769	0.652
78	0.871	0.044	0.004	0.064	0.83	-5.275	1.53E-05	0.96	59.78%	0.682	20.70%	12.996	0.438
79	0.498	0.006	0.007	0.91	0.976	-5.285	1.53E-05	0.948	66.69%	0.502	18.42%	6.626	0.668

80	0.998	0.824	0.028	0.974	0.992	-4.917	1.95E-05	0.988	87.11%	1.84	7.26%	9.328	0.798
81	0.459	0.964	0.696	0.924	0.985	-5.471	1.78E-05	0.048	66.13%	0.654	13.76%	1.927	0.81
82	0.998	0.001	0.022	0.978	0.562	-5.229	1.87E-05	0.809	77.11%	1.51	10.71%	7.888	0.374
83	0.998	0.001	0.022	0.978	0.562	-5.229	1.87E-05	0.809	77.11%	1.51	10.71%	7.888	0.374
84	0.993	0.001	0.257	0.956	0.709	-5.233	1.84E-05	0.925	64.06%	0.936	26.39%	8.543	0.26
85	0.974	0.565	0.634	0.989	0.948	-5.384	2.08E-05	0.564	48.44%	0.608	30.43%	5.763	0.276
86	0.937	0.05	0.833	0.994	0.947	-5.402	2.15E-05	0.641	42.74%	0.712	31.33%	6.89	0.292
87	0.979	0.999	0.006	0.01	0.256	-5.202	1.87E-05	0.783	58.07%	0.501	31.05%	11.318	0.868
88	0.976	0.948	0.401	0.585	0.43	-5.181	1.27E-05	0.865	59.66%	0.905	21.03%	9.15	0.204
89	0.96	0.991	0.034	0.066	0.969	-5.156	9.39E-06	0.555	58.51%	0.711	22.60%	9.537	0.682
90	0.985	0.979	0.011	0.093	0.986	-5.117	3.82E-05	0.876	61.52%	1.245	47.29%	10.755	0.538
91	0.999	0.994	0.007	0.248	0.94	-5.089	2.57E-05	0.273	72.77%	1.446	13.61%	11.902	0.165

Table 17: Metabolism properties of the withanolides. predicted by the server ADMET Lab2.

ID	CYP1A2-inh	CYP1A2-sub	CYP2C19-inh	CYP2C19-sub	CYP2C9-inh	CYP2C9-sub	CYP2D6-inh	CYP2D6-sub	CYP3A4-inh	CYP3A4-sub
1	0.039	0.533	0.212	0.809	0.112	0.015	0.008	0.061	0.871	0.736
2	0.036	0.522	0.342	0.851	0.257	0.033	0.013	0.125	0.788	0.757
3	0.038	0.148	0.197	0.661	0.123	0.011	0.006	0.048	0.853	0.758
4	0.02	0.673	0.033	0.742	0.028	0.01	0.004	0.053	0.641	0.676
5	0.007	0.79	0.02	0.836	0.012	0.012	0.004	0.1	0.857	0.906
6	0.043	0.244	0.493	0.871	0.562	0.025	0.014	0.077	0.881	0.899
7	0.017	0.611	0.363	0.895	0.435	0.014	0.007	0.083	0.864	0.88
8	0.021	0.132	0.052	0.749	0.113	0.035	0.006	0.102	0.772	0.683
9	0.014	0.905	0.014	0.797	0.013	0.007	0.004	0.111	0.79	0.687
10	0.023	0.485	0.098	0.903	0.202	0.031	0.007	0.379	0.879	0.792
11	0.014	0.935	0.019	0.802	0.014	0.008	0.006	0.11	0.814	0.675
12	0.008	0.461	0.025	0.177	0.039	0.058	0.004	0.08	0.815	0.747
13	0.007	0.47	0.026	0.197	0.029	0.063	0.005	0.097	0.81	0.772
14	0.018	0.358	0.105	0.133	0.049	0.054	0.253	0.067	0.771	0.758
15	0.014	0.263	0.072	0.877	0.201	0.029	0.004	0.13	0.838	0.911
16	0.008	0.12	0.016	0.764	0.038	0.038	0.002	0.183	0.587	0.724
17	0.07	0.253	0.214	0.531	0.114	0.041	0.01	0.101	0.906	0.375
18	0.062	0.489	0.294	0.623	0.355	0.091	0.013	0.283	0.866	0.568
19	0.036	0.302	0.047	0.52	0.043	0.031	0.007	0.099	0.742	0.366
20	0.039	0.157	0.042	0.726	0.066	0.055	0.005	0.061	0.868	0.489
21	0.02	0.297	0.053	0.616	0.061	0.077	0.009	0.054	0.731	0.924
22	0.05	0.362	0.132	0.742	0.133	0.06	0.023	0.043	0.883	0.922
23	0.033	0.282	0.076	0.704	0.128	0.068	0.018	0.049	0.887	0.919
24	0.029	0.44	0.07	0.724	0.05	0.065	0.006	0.141	0.866	0.679
25	0.029	0.574	0.256	0.735	0.266	0.055	0.033	0.037	0.842	0.931

26	0.088	0.257	0.452	0.725	0.533	0.098	0.167	0.121	0.851	0.59
27	0.05	0.296	0.056	0.746	0.054	0.069	0.005	0.112	0.816	0.603
28	0.007	0.21	0.027	0.837	0.017	0.082	0.004	0.126	0.775	0.859
29	0.016	0.452	0.038	0.651	0.051	0.056	0.005	0.039	0.682	0.931
30	0.029	0.574	0.256	0.735	0.266	0.055	0.033	0.037	0.842	0.931
31	0.02	0.297	0.053	0.616	0.061	0.077	0.009	0.054	0.731	0.924
32	0.043	0.285	0.37	0.795	0.497	0.264	0.158	0.142	0.916	0.88
33	0.064	0.32	0.824	0.866	0.865	0.181	0.35	0.103	0.93	0.894
34	0.026	0.19	0.116	0.63	0.112	0.181	0.042	0.15	0.817	0.736
35	0.041	0.196	0.395	0.733	0.421	0.133	0.155	0.107	0.876	0.739
36	0.015	0.146	0.058	0.636	0.055	0.167	0.007	0.093	0.787	0.47
37	0.006	0.113	0.017	0.505	0.025	0.074	0.003	0.054	0.513	0.26
38	0.005	0.115	0.013	0.499	0.015	0.045	0.002	0.045	0.479	0.285
39	0.016	0.209	0.035	0.738	0.029	0.081	0.002	0.062	0.836	0.516
40	0.069	0.327	0.52	0.786	0.656	0.075	0.221	0.045	0.919	0.918
41	0.028	0.381	0.376	0.812	0.32	0.076	0.062	0.054	0.866	0.925
42	0.003	0.808	0.01	0.465	0.004	0.016	0.001	0.012	0.229	0.162
43	0.005	0.535	0.009	0.463	0.002	0.033	0.001	0.014	0.235	0.719
44	0.03	0.625	0.303	0.742	0.229	0.066	0.041	0.031	0.847	0.932
45	0.016	0.536	0.041	0.66	0.043	0.063	0.006	0.034	0.707	0.932
46	0.018	0.585	0.121	0.757	0.131	0.067	0.007	0.023	0.837	0.917
47	0.005	0.245	0.01	0.478	0.005	0.031	0.001	0.019	0.359	0.261
48	0.017	0.358	0.049	0.674	0.121	0.058	0.008	0.042	0.796	0.841
49	0.017	0.358	0.049	0.674	0.121	0.058	0.008	0.042	0.796	0.841
50	0.033	0.41	0.335	0.785	0.409	0.034	0.021	0.069	0.896	0.912
51	0.054	0.517	0.225	0.596	0.17	0.074	0.026	0.108	0.931	0.552
52	0.111	0.599	0.808	0.815	0.735	0.09	0.142	0.108	0.948	0.587

53	0.072	0.595	0.229	0.712	0.139	0.043	0.033	0.066	0.905	0.577
54	0.027	0.462	0.072	0.728	0.066	0.071	0.005	0.138	0.85	0.535
55	0.045	0.292	0.161	0.795	0.165	0.078	0.023	0.067	0.914	0.792
56	0.036	0.564	0.087	0.739	0.057	0.051	0.005	0.078	0.808	0.536
57	0.023	0.918	0.021	0.663	0.01	0.03	0.003	0.121	0.628	0.32
58	0.031	0.819	0.033	0.787	0.016	0.035	0.003	0.107	0.79	0.73
59	0.024	0.367	0.053	0.696	0.036	0.074	0.006	0.141	0.63	0.566
60	0.026	0.694	0.036	0.542	0.02	0.042	0.003	0.093	0.685	0.396
61	0	0.054	0.002	0.054	0	0	0.008	0.023	0.046	0.007
62	0.08	0.342	0.349	0.746	0.331	0.051	0.017	0.042	0.889	0.886
63	0.022	0.488	0.05	0.841	0.022	0.063	0.004	0.109	0.791	0.906
64	0.019	0.126	0.012	0.722	0.013	0.072	0.003	0.098	0.393	0.392
65	0.147	0.251	0.536	0.818	0.761	0.06	0.283	0.075	0.914	0.884
66	0.229	0.232	0.777	0.758	0.759	0.058	0.424	0.089	0.877	0.734
67	0.01	0.831	0.036	0.595	0.052	0.075	0.005	0.044	0.618	0.819
68	0.024	0.558	0.152	0.846	0.089	0.066	0.008	0.067	0.845	0.881
69	0.027	0.414	0.092	0.767	0.386	0.05	0.024	0.145	0.821	0.572
70	0.027	0.414	0.092	0.767	0.386	0.05	0.024	0.145	0.821	0.572
71	0.006	0.474	0.019	0.713	0.022	0.052	0.003	0.185	0.649	0.71
72	0.009	0.782	0.039	0.857	0.047	0.024	0.002	0.067	0.835	0.851
73	0.008	0.917	0.037	0.815	0.057	0.016	0.002	0.053	0.777	0.929
74	0.003	0.762	0.014	0.785	0.009	0.036	0.001	0.065	0.488	0.746
75	0.008	0.804	0.026	0.834	0.036	0.033	0.002	0.108	0.757	0.872
76	0.002	0.723	0.009	0.801	0.007	0.019	0.001	0.101	0.533	0.567
77	0.005	0.938	0.028	0.824	0.047	0.02	0.002	0.053	0.777	0.934
78	0.011	0.89	0.057	0.834	0.072	0.02	0.004	0.043	0.913	0.924
79	0.005	0.925	0.034	0.839	0.056	0.03	0.003	0.056	0.766	0.931

80	0.042	0.562	0.861	0.909	0.732	0.058	0.197	0.092	0.931	0.931
81	0.003	0.556	0.014	0.696	0.015	0.037	0.002	0.101	0.47	0.448
82	0.004	0.909	0.083	0.869	0.061	0.048	0.004	0.08	0.6	0.933
83	0.004	0.909	0.083	0.869	0.061	0.048	0.004	0.08	0.6	0.933
84	0.003	0.972	0.023	0.846	0.018	0.037	0.003	0.081	0.502	0.914
85	0.004	0.969	0.027	0.826	0.024	0.041	0.003	0.109	0.465	0.918
86	0.002	0.967	0.016	0.807	0.012	0.025	0.001	0.086	0.287	0.918
87	0.016	0.33	0.042	0.832	0.035	0.035	0.002	0.074	0.682	0.855
88	0.015	0.239	0.03	0.575	0.015	0.051	0.067	0.022	0.931	0.846
89	0.015	0.354	0.025	0.746	0.013	0.075	0.053	0.057	0.925	0.809
90	0.005	0.194	0.021	0.84	0.012	0.053	0.003	0.08	0.883	0.867
91	0.01	0.339	0.02	0.798	0.02	0.031	0.004	0.098	0.831	0.589

Table 18: Toxicity properties of the withanolides. predicted by the server ADMET Lab2.

ID	hERG	H-HT	DILI	Ames	ROA	FDAMDD	SkinSen	Carcinogenicity	EC	EI	Respiratory	BCF	IGC50	LC50	LC50DM
1	0.056	0.689	0.802	0.166	0.217	0.199	0.415	0.444	0.035	0.255	0.94	0.509	4.401	5.357	5.103
2	0.513	0.228	0.595	0.127	0.739	0.518	0.857	0.868	0.038	0.082	0.963	0.436	3.451	4.014	3.922
3	0.028	0.583	0.764	0.08	0.236	0.058	0.872	0.322	0.897	0.358	0.964	0.399	4.244	5.213	4.799
4	0.112	0.827	0.727	0.109	0.317	0.332	0.411	0.207	0.006	0.037	0.937	0.542	4.632	5.681	5.81
5	0.894	0.591	0.848	0.049	0.235	0.735	0.85	0.812	0.092	0.174	0.966	0.415	4.748	4.375	4.147
6	0.403	0.147	0.665	0.203	0.312	0.889	0.73	0.766	0.038	0.041	0.943	0.46	4.477	4.699	3.773
7	0.128	0.338	0.573	0.669	0.458	0.695	0.825	0.907	0.004	0.014	0.95	0.162	3.53	4.032	3.522
8	0.709	0.808	0.443	0.022	0.5	0.935	0.603	0.755	0.018	0.015	0.978	0.456	3.493	4.622	4.02
9	0.881	0.978	0.886	0.038	0.87	0.894	0.463	0.085	0.012	0.022	0.98	0.959	4.619	6.638	7.386
10	0.957	0.937	0.789	0.013	0.951	0.967	0.862	0.797	0.144	0.091	0.975	0.531	3.698	5.164	5.527
11	0.872	0.973	0.856	0.028	0.739	0.788	0.519	0.14	0.015	0.022	0.984	0.975	4.557	6.585	7.145
12	0.66	0.955	0.959	0.021	0.815	0.95	0.542	0.795	0.003	0.009	0.945	0.32	2.586	4.027	4.421
13	0.355	0.943	0.963	0.016	0.524	0.908	0.584	0.742	0.003	0.01	0.957	0.354	2.393	3.88	4.083
14	0.8	0.972	0.944	0.045	0.952	0.933	0.926	0.181	0.003	0.012	0.978	0.23	2.814	4.619	4.254
15	0.161	0.842	0.904	0.022	0.157	0.459	0.607	0.689	0.057	0.705	0.938	0.448	4.042	4.776	4.152
16	0.384	0.971	0.861	0.011	0.281	0.858	0.664	0.405	0.023	0.098	0.976	0.508	3.282	4.771	4.394
17	0.043	0.674	0.712	0.066	0.298	0.195	0.21	0.212	0.014	0.044	0.954	0.609	4.31	5.606	6.015
18	0.044	0.279	0.38	0.041	0.46	0.369	0.382	0.366	0.01	0.027	0.932	0.442	2.958	4.783	4.224
19	0.055	0.935	0.637	0.024	0.294	0.246	0.14	0.077	0.004	0.015	0.895	0.693	4.561	6.12	6.649
20	0.709	0.522	0.335	0.016	0.724	0.757	0.866	0.528	0.004	0.011	0.963	0.462	3.181	4.777	4.655
21	0.1	0.625	0.037	0.01	0.468	0.937	0.946	0.856	0.003	0.016	0.927	0.12	2.041	3.073	3.87
22	0.256	0.514	0.05	0.013	0.299	0.927	0.954	0.851	0.004	0.015	0.973	0.113	1.914	3.125	3.683
23	0.155	0.594	0.032	0.008	0.655	0.929	0.89	0.899	0.004	0.012	0.962	0.117	2.098	3.325	3.851
24	0.042	0.312	0.308	0.019	0.43	0.693	0.243	0.704	0.004	0.017	0.901	0.386	2.144	3.843	3.999
25	0.262	0.666	0.036	0.009	0.379	0.953	0.921	0.971	0.004	0.013	0.964	0.02	2.028	2.67	3.475

26	0.896	0.481	0.079	0.01	0.91	0.903	0.956	0.829	0.008	0.018	0.975	0.369	2.471	3.713	3.748
27	0.895	0.615	0.116	0.008	0.834	0.843	0.954	0.781	0.007	0.015	0.976	0.408	2.614	3.655	3.799
28	0.002	0.176	0.075	0.006	0.935	0.872	0.02	0.615	0.003	0.015	0.629	0.143	2.693	3.775	4.271
29	0.101	0.655	0.035	0.011	0.336	0.948	0.933	0.953	0.004	0.015	0.965	-0.06	1.676	2.81	3.698
30	0.262	0.666	0.036	0.009	0.379	0.953	0.921	0.971	0.004	0.013	0.964	0.02	2.028	2.67	3.475
31	0.1	0.625	0.037	0.01	0.468	0.937	0.946	0.856	0.003	0.016	0.927	0.12	2.041	3.073	3.87
32	0.507	0.517	0.132	0.009	0.101	0.895	0.962	0.633	0.014	0.102	0.961	0.414	3.338	4.422	4.273
33	0.914	0.485	0.204	0.008	0.191	0.917	0.947	0.706	0.015	0.033	0.976	0.557	2.91	4.011	3.679
34	0.33	0.417	0.056	0.013	0.573	0.932	0.96	0.49	0.004	0.063	0.917	0.385	3.382	5.027	4.6
35	0.715	0.464	0.052	0.008	0.892	0.945	0.949	0.693	0.004	0.024	0.952	0.408	2.893	4.37	4.055
36	0.009	0.194	0.079	0.065	0.223	0.905	0.767	0.704	0.003	0.057	0.435	0.365	3.456	4.921	4.832
37	0.043	0.208	0.08	0.302	0.082	0.207	0.105	0.277	0.003	0.012	0.027	0.484	3.675	5.183	4.647
38	0.061	0.205	0.051	0.228	0.122	0.563	0.082	0.421	0.003	0.011	0.044	0.459	2.877	4.054	4.287
39	0.045	0.361	0.083	0.012	0.373	0.909	0.304	0.764	0.003	0.021	0.659	0.379	3.084	3.954	4.286
40	0.53	0.621	0.037	0.007	0.676	0.933	0.735	0.925	0.004	0.011	0.963	0.2	2.161	3.205	3.606
41	0.549	0.642	0.046	0.01	0.51	0.958	0.906	0.956	0.005	0.013	0.979	0.086	2.029	2.826	3.405
42	0.084	0.233	0.051	0.111	0.604	0.54	0.061	0.931	0.003	0.007	0.788	0.458	2.324	2.472	3.591
43	0.041	0.198	0.056	0.164	0.051	0.776	0.063	0.971	0.003	0.01	0.699	0.109	1.484	2.363	3.543
44	0.237	0.662	0.036	0.009	0.28	0.954	0.912	0.977	0.004	0.014	0.967	0.098	2.066	2.746	3.503
45	0.094	0.642	0.034	0.012	0.253	0.949	0.924	0.965	0.004	0.017	0.968	0.011	1.724	2.88	3.738
46	0.034	0.417	0.036	0.046	0.108	0.949	0.125	0.992	0.003	0.013	0.892	0.113	2.041	2.507	3.663
47	0.086	0.183	0.034	0.098	0.741	0.966	0.095	0.978	0.003	0.009	0.966	0.228	1.651	2.206	3.62
48	0.343	0.591	0.027	0.008	0.925	0.974	0.911	0.971	0.004	0.015	0.981	0.107	1.971	2.614	3.784
49	0.343	0.591	0.027	0.008	0.925	0.974	0.911	0.971	0.004	0.015	0.981	0.107	1.971	2.614	3.784
50	0.867	0.883	0.039	0.01	0.809	0.961	0.917	0.919	0.008	0.018	0.978	0.31	2.502	3.161	3.675
51	0.014	0.132	0.114	0.042	0.659	0.83	0.242	0.858	0.015	0.039	0.974	0.386	3.984	4.798	4.312
52	0.019	0.126	0.184	0.033	0.606	0.776	0.15	0.854	0.028	0.033	0.974	0.439	3.581	5.029	4.191

53	0.021	0.078	0.093	0.101	0.758	0.897	0.733	0.84	0.006	0.026	0.979	0.6	5.31	6.43	5.338
54	0.093	0.467	0.209	0.092	0.882	0.951	0.313	0.854	0.008	0.018	0.94	0.431	3.887	5.168	4.646
55	0.842	0.314	0.072	0.028	0.952	0.974	0.953	0.883	0.018	0.023	0.98	0.282	2.999	4.75	3.865
56	0.195	0.143	0.153	0.138	0.883	0.967	0.611	0.847	0.004	0.013	0.967	0.617	5.282	6.565	6.163
57	0.079	0.355	0.486	0.01	0.607	0.12	0.314	0.732	0.136	0.03	0.958	0.386	3.74	4.03	4.437
58	0.358	0.333	0.358	0.019	0.772	0.22	0.268	0.844	0.011	0.031	0.975	0.408	2.202	2.915	3.675
59	0.071	0.338	0.127	0.111	0.903	0.957	0.386	0.881	0.011	0.069	0.946	0.416	2.965	4.894	4.304
60	0.048	0.828	0.469	0.358	0.768	0.282	0.17	0.206	0.004	0.016	0.915	0.586	3.93	6.787	6.915
61	0.722	0.549	0.102	0.096	0.043	0.001	0.092	0.082	0.003	0.005	0.924	0.922	3.313	5.786	6.837
62	0.116	0.157	0.409	0.174	0.548	0.914	0.851	0.807	0.087	0.023	0.987	0.377	4.085	4.24	3.815
63	0.057	0.246	0.42	0.156	0.23	0.871	0.681	0.579	0.004	0.034	0.954	0.315	2.309	2.85	3.67
64	0.136	0.219	0.099	0.034	0.842	0.885	0.656	0.408	0.005	0.028	0.968	0.353	2.008	3.343	4.095
65	0.854	0.487	0.406	0.309	0.729	0.864	0.979	0.683	0.003	0.013	0.98	0.627	4.389	5.674	4.776
66	0.925	0.525	0.407	0.235	0.909	0.888	0.976	0.795	0.003	0.013	0.957	0.768	4.469	6.032	5.305
67	0.054	0.29	0.043	0.057	0.919	0.947	0.235	0.98	0.004	0.026	0.953	0.218	2.134	3.275	3.868
68	0.053	0.208	0.151	0.026	0.69	0.873	0.309	0.535	0.005	0.024	0.965	0.284	1.942	2.395	3.507
69	0.878	0.527	0.044	0.027	0.953	0.956	0.947	0.866	0.004	0.014	0.974	0.497	2.664	4.923	4.739
70	0.878	0.527	0.044	0.027	0.953	0.956	0.947	0.866	0.004	0.014	0.974	0.497	2.664	4.923	4.739
71	0.508	0.917	0.045	0.11	0.75	0.944	0.922	0.782	0.003	0.014	0.957	0.38	2.94	5.111	4.873
72	0.787	0.177	0.306	0.07	0.409	0.574	0.453	0.614	0.02	0.03	0.942	0.376	2.832	2.871	3.157
73	0.314	0.219	0.278	0.118	0.774	0.886	0.846	0.847	0.035	0.038	0.956	0.267	2.93	1.982	3.2
74	0.089	0.292	0.061	0.038	0.063	0.881	0.322	0.567	0.005	0.019	0.971	0.281	1.472	1.547	2.299
75	0.888	0.859	0.185	0.019	0.951	0.961	0.835	0.886	0.018	0.021	0.972	0.338	2.241	2.627	3.6
76	0.678	0.811	0.334	0.036	0.542	0.592	0.474	0.826	0.013	0.019	0.979	0.426	2.196	2.375	3.185
77	0.28	0.214	0.258	0.061	0.568	0.909	0.374	0.853	0.032	0.048	0.953	0.286	3.277	2.182	3.342
78	0.228	0.107	0.147	0.06	0.704	0.919	0.168	0.892	0.226	0.108	0.976	0.266	4.324	3.009	3.485
79	0.491	0.2	0.237	0.064	0.738	0.872	0.447	0.807	0.028	0.073	0.938	0.305	3.018	2.524	3.391

80	0.905	0.912	0.07	0.025	0.867	0.94	0.911	0.912	0.003	0.016	0.959	0.398	2.93	3.947	3.947
81	0.091	0.631	0.083	0.149	0.247	0.936	0.158	0.407	0.003	0.011	0.875	0.486	4.096	5.041	4.716
82	0.864	0.551	0.053	0.058	0.259	0.948	0.608	0.899	0.003	0.008	0.898	0.679	3.879	3.691	4.176
83	0.864	0.551	0.053	0.058	0.259	0.948	0.608	0.899	0.003	0.008	0.898	0.679	3.879	3.691	4.176
84	0.121	0.23	0.265	0.009	0.882	0.945	0.297	0.928	0.003	0.009	0.898	0.502	4.049	3.857	4.819
85	0.41	0.887	0.062	0.01	0.675	0.948	0.431	0.92	0.003	0.008	0.951	0.298	2.342	2.71	3.89
86	0.459	0.783	0.105	0.011	0.688	0.944	0.342	0.906	0.003	0.008	0.96	0.588	3.319	3	4.302
87	0.189	0.285	0.288	0.248	0.885	0.953	0.66	0.91	0.033	0.08	0.966	0.36	4.174	4.723	3.888
88	0.531	0.432	0.073	0.048	0.895	0.919	0.981	0.516	0.013	0.027	0.979	0.385	3.514	4.624	4.929
89	0.348	0.33	0.076	0.066	0.679	0.679	0.958	0.455	0.044	0.089	0.972	0.326	2.669	4.055	4.411
90	0.072	0.483	0.352	0.027	0.279	0.854	0.786	0.874	0.005	0.035	0.723	0.399	4.754	4.603	3.692
91	0.506	0.965	0.472	0.022	0.778	0.879	0.405	0.404	0.004	0.014	0.981	0.704	4.519	6.536	6.971

Table 19: Continuation of toxicity properties of the withanolides. predicted by the server ADMET Lab2

ID	NR-AR	NR-AR-LBD	NR-AhR	NR-Aromatase	NR-ER	NR-ER-LBD	NR-PPAR-gamma	SR-ARE	SR-ATAD5	SR-HSE	SR-MMP	SR-p53
1	0.983	0.97	0.014	0.689	0.917	0.757	0.364	0.551	0.266	0.153	0.844	0.955
2	0.987	0.973	0.026	0.7	0.827	0.272	0.008	0.067	0.024	0.032	0.457	0.71
3	0.978	0.945	0.01	0.705	0.837	0.741	0.541	0.728	0.376	0.372	0.858	0.974
4	0.977	0.944	0.019	0.847	0.805	0.268	0.033	0.505	0.12	0.041	0.826	0.918
5	0.972	0.971	0.019	0.884	0.708	0.379	0.823	0.624	0.296	0.047	0.808	0.956
6	0.976	0.963	0.029	0.613	0.887	0.72	0.026	0.375	0.021	0.185	0.647	0.93
7	0.961	0.919	0.02	0.454	0.889	0.703	0.011	0.393	0.018	0.094	0.745	0.909
8	0.962	0.961	0.015	0.484	0.81	0.316	0.052	0.623	0.023	0.081	0.751	0.92
9	0.861	0.925	0.012	0.894	0.595	0.155	0.895	0.764	0.65	0.093	0.856	0.972
10	0.965	0.968	0.026	0.879	0.756	0.146	0.806	0.672	0.175	0.065	0.78	0.964
11	0.897	0.941	0.008	0.859	0.613	0.148	0.894	0.751	0.429	0.059	0.836	0.97
12	0.95	0.906	0.01	0.49	0.547	0.055	0.005	0.311	0.017	0.035	0.489	0.901
13	0.971	0.936	0.009	0.297	0.627	0.096	0.003	0.338	0.015	0.03	0.453	0.841
14	0.931	0.91	0.041	0.93	0.206	0.033	0.143	0.823	0.032	0.033	0.777	0.938
15	0.927	0.946	0.1	0.848	0.805	0.151	0.764	0.748	0.136	0.191	0.793	0.977
16	0.878	0.941	0.065	0.841	0.608	0.03	0.746	0.827	0.117	0.068	0.807	0.971
17	0.99	0.966	0.014	0.013	0.939	0.81	0.005	0.045	0.013	0.078	0.814	0.553
18	0.944	0.886	0.025	0.04	0.742	0.374	0.003	0.058	0.006	0.11	0.658	0.209
19	0.944	0.766	0.014	0.166	0.688	0.038	0.017	0.076	0.032	0.054	0.784	0.495
20	0.973	0.95	0.009	0.596	0.637	0.155	0.012	0.52	0.01	0.129	0.708	0.501
21	0.996	0.994	0.076	0.95	0.549	0.007	0.004	0.579	0.141	0.042	0.506	0.712
22	0.997	0.993	0.029	0.882	0.775	0.024	0.003	0.66	0.023	0.03	0.386	0.514
23	0.99	0.978	0.089	0.949	0.685	0.013	0.007	0.847	0.082	0.055	0.625	0.824
24	0.963	0.953	0.015	0.48	0.744	0.013	0.004	0.05	0.013	0.024	0.53	0.5
25	0.998	0.995	0.049	0.96	0.88	0.027	0.009	0.913	0.377	0.04	0.809	0.906

26	0.992	0.968	0.029	0.555	0.742	0.065	0.002	0.463	0.009	0.024	0.529	0.108
27	0.994	0.964	0.009	0.208	0.714	0.065	0.002	0.379	0.008	0.019	0.555	0.043
28	0.841	0.94	0.05	0.824	0.188	0.549	0.473	0.489	0.828	0.069	0.9	0.931
29	0.997	0.996	0.044	0.96	0.841	0.01	0.006	0.851	0.188	0.028	0.67	0.875
30	0.998	0.995	0.049	0.96	0.88	0.027	0.009	0.913	0.377	0.04	0.809	0.906
31	0.996	0.994	0.076	0.95	0.549	0.007	0.004	0.579	0.141	0.042	0.506	0.712
32	0.95	0.927	0.106	0.795	0.435	0.012	0.015	0.65	0.026	0.381	0.602	0.824
33	0.975	0.971	0.097	0.867	0.893	0.465	0.273	0.911	0.194	0.593	0.837	0.931
34	0.973	0.966	0.086	0.858	0.331	0.008	0.02	0.466	0.149	0.221	0.515	0.761
35	0.989	0.984	0.071	0.898	0.807	0.033	0.093	0.851	0.492	0.283	0.806	0.897
36	0.882	0.869	0.06	0.803	0.222	0.009	0.015	0.286	0.051	0.167	0.526	0.647
37	0.674	0.764	0.039	0.817	0.461	0.032	0.014	0.459	0.284	0.035	0.481	0.709
38	0.805	0.895	0.028	0.87	0.612	0.018	0.021	0.599	0.374	0.04	0.582	0.846
39	0.955	0.914	0.019	0.868	0.554	0.02	0.066	0.54	0.159	0.27	0.884	0.785
40	0.992	0.974	0.103	0.949	0.771	0.036	0.01	0.908	0.206	0.096	0.772	0.871
41	0.99	0.983	0.032	0.953	0.909	0.039	0.033	0.892	0.435	0.054	0.834	0.931
42	0.942	0.874	0.008	0.953	0.588	0.071	0.005	0.269	0.593	0.015	0.541	0.847
43	0.973	0.95	0.011	0.948	0.688	0.009	0.003	0.347	0.134	0.008	0.359	0.583
44	0.998	0.99	0.031	0.957	0.9	0.03	0.006	0.897	0.419	0.027	0.872	0.862
45	0.998	0.992	0.025	0.957	0.868	0.01	0.004	0.784	0.212	0.019	0.769	0.798
46	0.992	0.956	0.02	0.95	0.842	0.012	0.005	0.563	0.201	0.028	0.882	0.814
47	0.981	0.925	0.013	0.949	0.737	0.008	0.004	0.412	0.199	0.007	0.673	0.614
48	0.999	0.987	0.047	0.961	0.898	0.027	0.005	0.839	0.326	0.017	0.91	0.81
49	0.999	0.987	0.047	0.961	0.898	0.027	0.005	0.839	0.326	0.017	0.91	0.81
50	0.996	0.995	0.07	0.958	0.926	0.338	0.339	0.933	0.875	0.071	0.921	0.978
51	0.955	0.911	0.027	0.062	0.726	0.419	0.004	0.074	0.006	0.047	0.469	0.157
52	0.966	0.901	0.035	0.074	0.803	0.777	0.005	0.084	0.007	0.089	0.562	0.187

53	0.955	0.909	0.01	0.426	0.667	0.537	0.013	0.767	0.011	0.165	0.555	0.763
54	0.913	0.883	0.036	0.056	0.727	0.013	0.007	0.054	0.006	0.025	0.528	0.061
55	0.975	0.958	0.031	0.799	0.775	0.061	0.009	0.586	0.006	0.041	0.386	0.151
56	0.921	0.894	0.014	0.395	0.647	0.029	0.026	0.672	0.011	0.078	0.613	0.638
57	0.988	0.966	0.006	0.271	0.57	0.137	0.007	0.041	0.038	0.013	0.771	0.405
58	0.992	0.968	0.006	0.833	0.783	0.029	0.006	0.412	0.044	0.015	0.859	0.846
59	0.952	0.887	0.03	0.827	0.707	0.011	0.004	0.238	0.011	0.025	0.611	0.418
60	0.932	0.878	0.015	0.813	0.755	0.018	0.014	0.81	0.013	0.033	0.823	0.539
61	0.837	0.95	0.002	0.305	0.838	0.439	0.005	0.075	0.776	0.001	0.25	0.483
62	0.993	0.986	0.025	0.526	0.945	0.816	0.004	0.515	0.009	0.022	0.665	0.674
63	0.991	0.982	0.026	0.868	0.77	0.012	0.001	0.053	0.016	0.013	0.326	0.391
64	0.97	0.945	0.012	0.432	0.751	0.026	0.001	0.081	0.01	0.02	0.354	0.104
65	0.981	0.942	0.013	0.818	0.541	0.123	0.003	0.933	0.013	0.131	0.729	0.782
66	0.992	0.967	0.014	0.809	0.535	0.041	0.003	0.906	0.027	0.053	0.548	0.642
67	0.998	0.983	0.037	0.97	0.829	0.007	0.004	0.494	0.699	0.017	0.925	0.875
68	0.992	0.982	0.039	0.853	0.757	0.008	0.001	0.036	0.018	0.012	0.573	0.27
69	0.993	0.963	0.057	0.692	0.78	0.06	0.008	0.77	0.016	0.035	0.747	0.724
70	0.993	0.963	0.057	0.692	0.78	0.06	0.008	0.77	0.016	0.035	0.747	0.724
71	0.691	0.938	0.206	0.883	0.306	0.012	0.561	0.864	0.292	0.441	0.719	0.981
72	0.981	0.973	0.036	0.888	0.775	0.022	0.008	0.062	0.111	0.037	0.826	0.885
73	0.994	0.998	0.024	0.949	0.966	0.448	0.142	0.832	0.683	0.018	0.937	0.965
74	0.997	0.995	0.067	0.929	0.841	0.007	0.002	0.046	0.121	0.004	0.802	0.345
75	0.994	0.997	0.02	0.94	0.866	0.011	0.196	0.656	0.617	0.021	0.925	0.952
76	0.989	0.991	0.025	0.936	0.727	0.011	0.047	0.265	0.463	0.016	0.856	0.947
77	0.996	0.999	0.04	0.948	0.971	0.517	0.121	0.907	0.687	0.018	0.957	0.974
78	0.995	0.996	0.044	0.907	0.959	0.782	0.326	0.921	0.304	0.035	0.951	0.958
79	0.995	0.998	0.064	0.937	0.89	0.019	0.05	0.737	0.581	0.031	0.945	0.948

80	0.976	0.997	0.145	0.962	0.718	0.05	0.794	0.958	0.948	0.531	0.905	0.979
81	0.541	0.678	0.07	0.709	0.239	0.02	0.253	0.492	0.1	0.107	0.542	0.947
82	0.022	0.995	0.025	0.963	0.162	0.135	0.954	0.977	0.969	0.88	0.97	0.998
83	0.022	0.995	0.025	0.963	0.162	0.135	0.954	0.977	0.969	0.88	0.97	0.998
84	0.291	0.996	0.023	0.941	0.31	0.488	0.983	0.93	0.973	0.701	0.975	0.997
85	0.02	0.997	0.028	0.959	0.481	0.601	0.988	0.967	0.991	0.785	0.98	1
86	0.027	0.997	0.017	0.947	0.344	0.499	0.988	0.968	0.984	0.722	0.977	0.999
87	0.967	0.959	0.032	0.805	0.811	0.064	0.02	0.159	0.014	0.023	0.476	0.649
88	0.991	0.99	0.011	0.894	0.882	0.623	0.626	0.916	0.077	0.174	0.929	0.954
89	0.984	0.988	0.017	0.834	0.92	0.491	0.095	0.607	0.017	0.108	0.926	0.906
90	0.971	0.904	0.023	0.891	0.863	0.492	0.092	0.596	0.013	0.11	0.612	0.825
91	0.957	0.897	0.008	0.834	0.798	0.326	0.315	0.615	0.023	0.057	0.742	0.924

Table 20: Docking results between the withanolides and the AD-related targets. Docking score values were predicted by Gold 2021.3 default scoring function.

ID	1EVE	6ESJ	2QP8	4AU8	6HK7	2V5Z
1	86.88	71.92	50.13	38.83	49.17	-3.77
2	78.48	66.03	54.97	39.3	53.02	39.45
3	92.84	77.33	59.15	38.86	59.65	-10.51
4	75.39	59.53	47.9	25.74	49.59	18.23
5	84.92	66.23	57.2	36.05	59.98	56.49
6	83.35	73.8	63.8	40.53	56.65	28.57
7	85.05	67.41	57.59	39.88	51.63	25.39
8	76.37	78.76	52.08	46.2	61.35	25.6
9	85.36	67.35	46.34	47.93	52.88	32.55
10	85.45	69.47	56.9	41.13	56.21	40.25
11	74.6	66.67	54.44	39.38	53.64	35.48
12	90.5	72.96	51.08	38.97	64.4	-12.66
13	81.79	84.97	32.65	49.65	64.67	-36.92
14	81.48	76.31	42.54	49.95	56.55	-68.71
15	67.35	64.61	55.58	40.53	51.23	20.57
16	79.59	63.2	56.09	23.44	56.13	21.68
17	76.17	79.5	55.07	50.48	50.44	14.35
18	79.48	68.51	59.21	47.4	57.93	54.5
19	70.99	71.71	43.69	27.26	56.14	16.47
20	83.15	71.38	46.15	36.26	56.83	21.46
21	75.37	68.79	58.07	26.35	57.22	38.07
22	76.5	69.93	50.34	28.18	57.55	38.97
23	79.64	74.82	68.25	39.48	59.35	44.19
24	79.27	70.16	52.74	36.5	58.15	45.18
25	66.43	68.57	42.28	38.49	50.26	18.00
26	73.28	72.53	66.37	34.84	56.39	50.57

27	74.89	70.81	56.59	32.02	47.73	44.19
28	79.07	70.54	52.81	45.69	55.79	45.57
29	71.43	75.91	46.18	33.42	56.28	29.92
30	67.87	75.77	48.66	33.59	54.95	29.35
31	77.81	70.12	52.00	30.75	58.67	35.36
32	86.1	62.00	54.06	50.38	55.12	57.7
33	71.75	69.8	48.63	24.64	56.46	32.8
34	83.95	69.44	54.42	38.59	58.24	62.33
35	71.18	75.82	57.3	41.13	56.34	34.88
36	77.57	75.15	54.6	33.34	58.71	49.4
37	104.3	72.94	53.57	64.11	60.84	-37.09
38	105.00	77.99	46.61	55.61	53.33	-40.64
39	68.33	62.48	56.82	31.67	51.68	10.35
40	79.09	71.22	52.51	41.69	58.29	43.9
41	68.69	65.32	44.57	40.18	50.97	29.3
42	69.05	65.22	64.71	65.21	58.00	-132.03
43	78.24	68.92	61.36	57.18	64.05	-26.4
44	58.43	65.28	42.85	45.09	54.83	19.54
45	63.83	65.61	34.11	40.36	57.84	19.29
46	62.04	67.99	43.5	6.78	56.6	8.39
47	76.98	74.07	34.57	58.64	59.24	-43.48
48	62.37	69.46	32.69	39.65	55.57	13.39
49	68.83	68.76	43.54	36.00	52.26	11.13
50	74.97	68.48	47.19	42.62	54.6	11.1
51	84.71	75.01	56.22	51.83	64.51	58.64
52	81.86	69.64	62.82	47.31	53.52	61.36
53	87.73	74.76	59.36	46.08	65.68	60.48
54	75.54	66.42	60.65	57.59	54.97	54.45
55	75.32	68.35	51.32	57.82	59.85	61.85

56	75.15	69.03	59.53	58.07	53.12	54.55
57	67.94	57.23	54.44	20.58	51.62	41.09
58	71.62	63.68	43.94	37.2	52.21	48.32
59	75.12	62.83	60.21	30.75	54.12	49.5
60	72.44	66.14	54.82	44.78	54.6	33.81
61	27.2	97.94	88.9	65.65	74.85	-310.05
62	71.75	78.46	42.71	52.53	50.42	35.37
63	68.55	61.56	50.53	49.34	51.2	52.57
64	77.47	64.4	49.72	28.26	56.6	31.82
65	84.77	72.05	54.81	52.14	71.47	62.31
66	74.62	64.69	50.00	41.7	58.7	64.33
67	58.4	60.36	46.67	10.94	45.45	20.02
68	64.33	50.73	46.25	59.45	55.25	13.97
69	78.95	61.24	60.32	33.7	52.42	43.85
70	80.62	65.11	57.9	40.97	54.41	43.38
71	94.44	67.11	62.49	35.06	65.86	-2.33
72	77.52	62.81	40.89	25.18	47.23	20.36
73	70.13	58.84	36.56	23.48	49.68	17.16
74	68.41	53.47	47.92	38.66	48.23	9.22
75	67.52	60.92	51.21	26.26	54.74	20.9
76	67.2	61.00	29.66	34.45	43.00	-36.03
77	79.08	55.44	37.69	21.2	57.83	20.73
78	77.91	55.5	46.7	35.05	51.96	49.31
79	63.59	56.87	45.57	20.06	57.46	5.06
80	59.57	62.8	49.84	39.52	53.63	-14.31
81	109.86	83.9	51.01	60.02	63.21	-46.29
82	72.26	60.00	50.22	37.79	40.31	-44.15
83	70.18	57.44	42.49	40.85	42.5	-39.63
84	71.43	60.76	42.00	44.72	46.52	-57.28

85	69.67	58.33	40.69	32.35	36.17	-88.71
86	52.7	51.49	40.08	30.91	33.21	-70.16
87	71.02	66.00	55.21	50.68	54.21	51.01
88	80.44	69.42	56.94	41.7	61.32	50.3
89	78.8	75.96	58.22	46.26	54.26	49.15
90	63.05	55.13	39.98	14.26	45.41	3.68
91	56.21	70.28	55.03	52.41	52.28	10.9

APÊNDICE B: figuras suplementares ao capítulo 1

Supplementary information for

In silico evaluation of pharmacokinetics properties of withanolides and simulation of their biological activities against Alzheimer's disease

Figure S1: 2D structures of the evaluated withanolides.

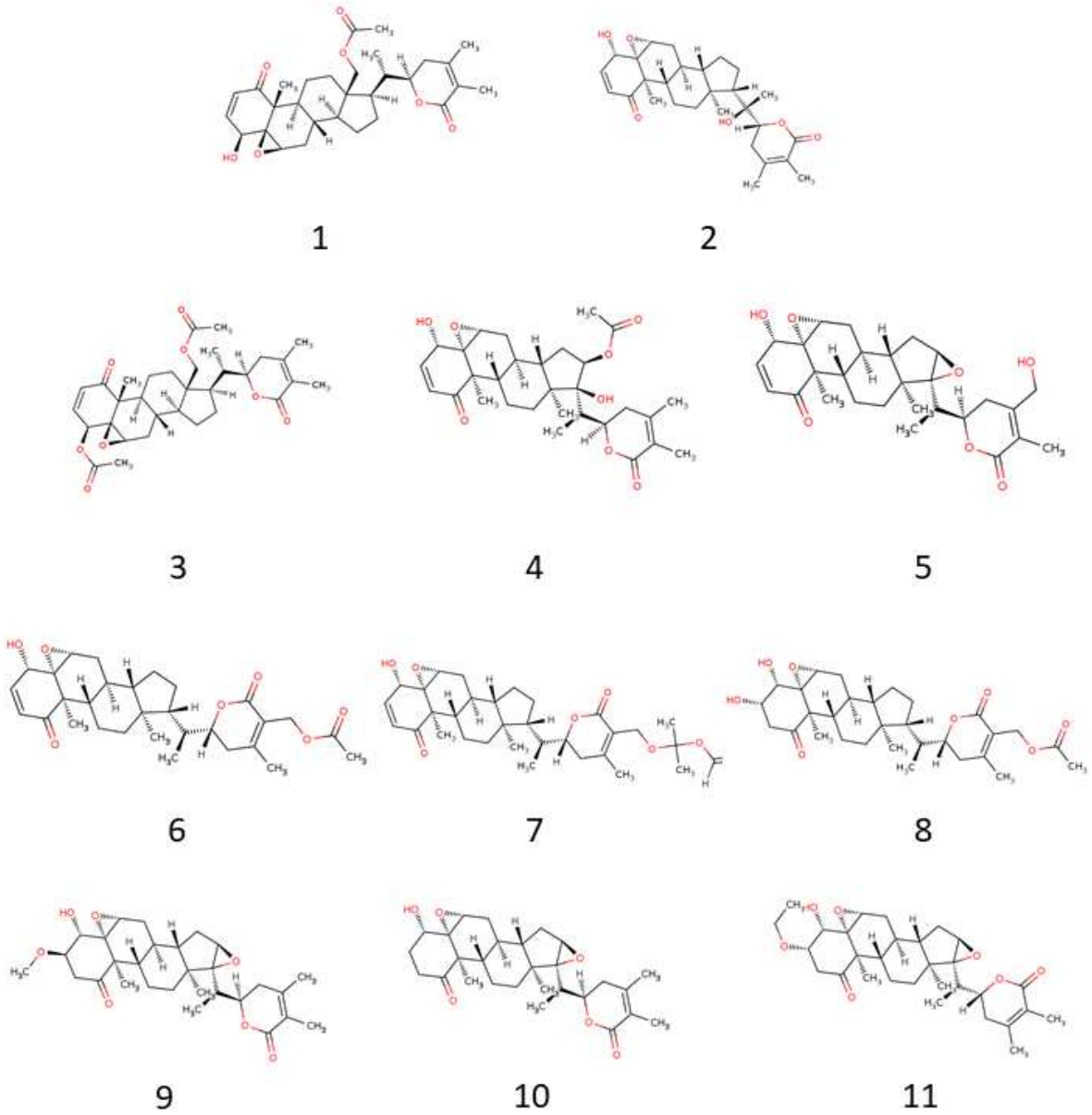

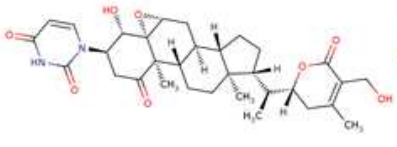

12

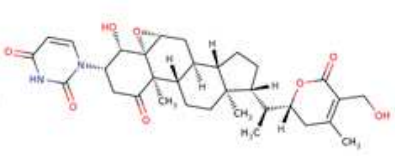

13

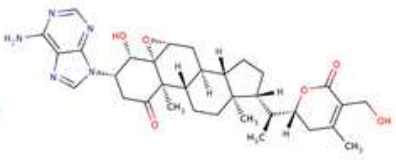

14

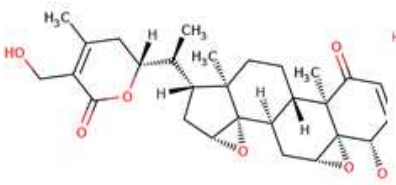

15

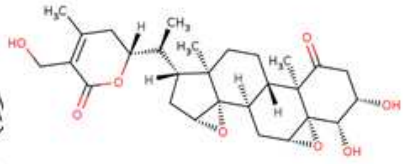

16

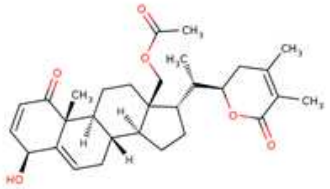

17

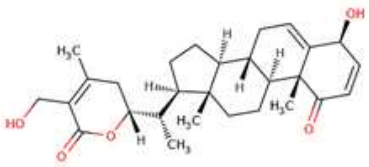

18

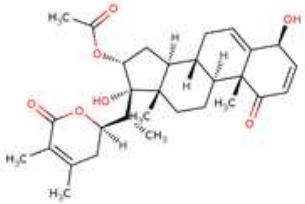

19

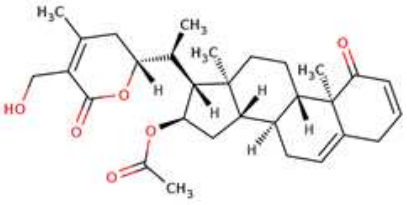

20

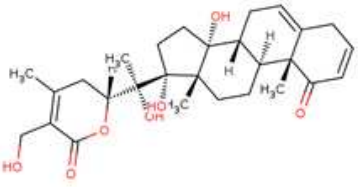

21

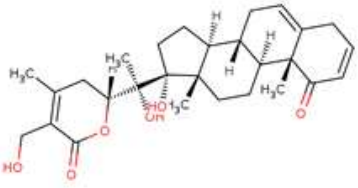

22

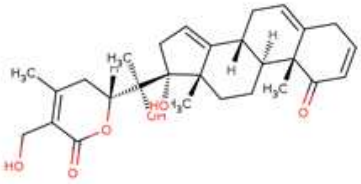

23

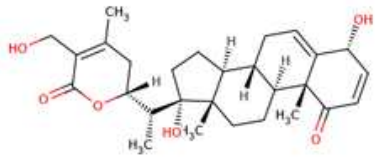

24

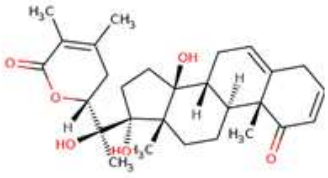

25

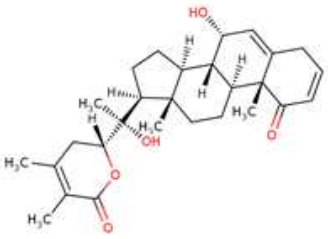

26

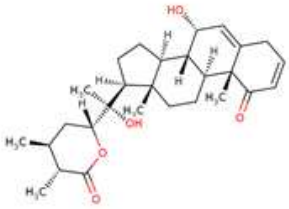

27

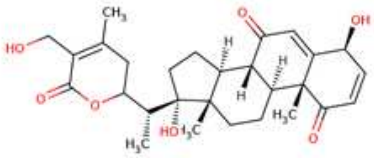

28

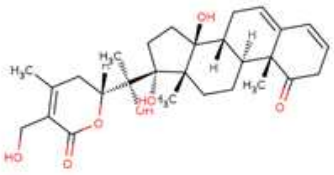

29

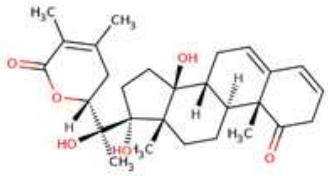

30

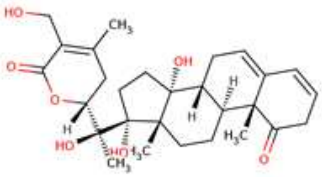

31

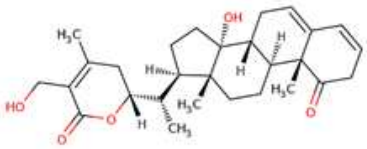

32

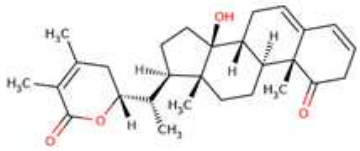

33

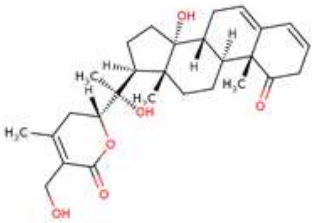

34

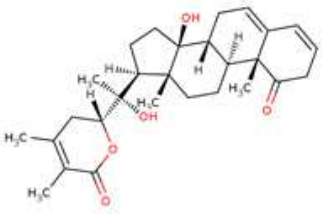

35

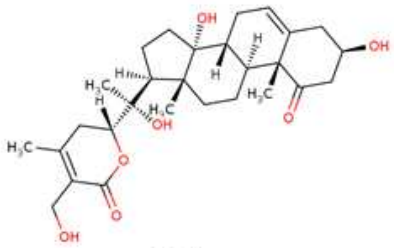

36

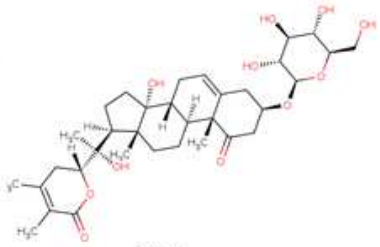

37

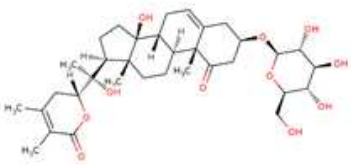

38

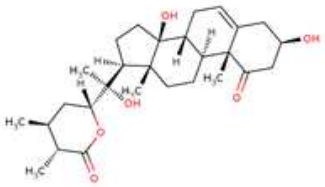

39

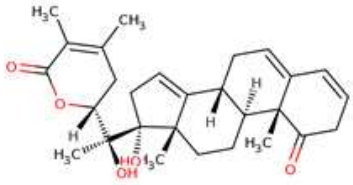

40

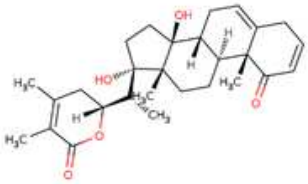

41

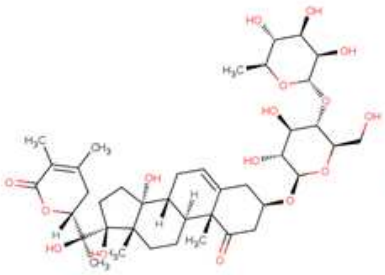

42

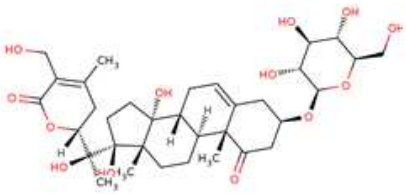

43

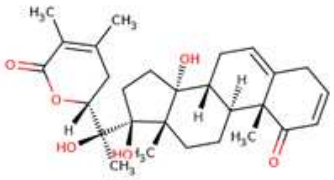

44

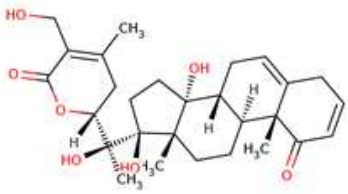

45

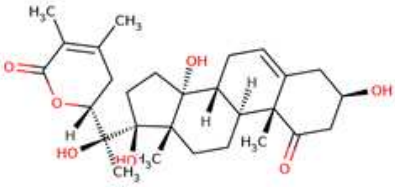

46

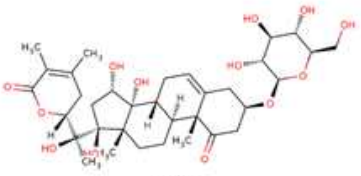

47

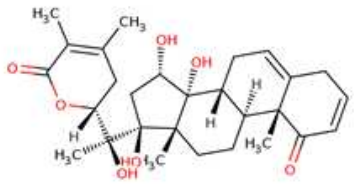

48

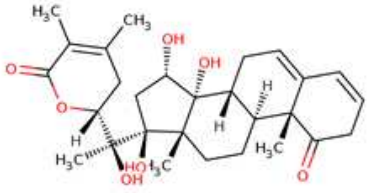

49

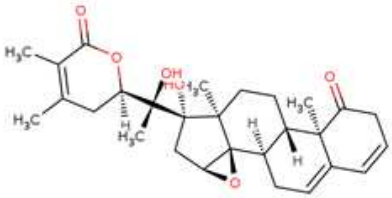

50

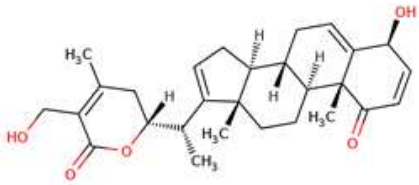

51

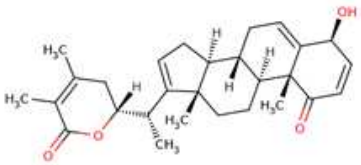

52

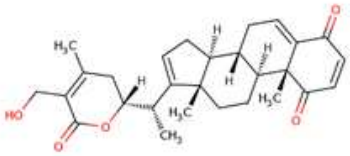

53

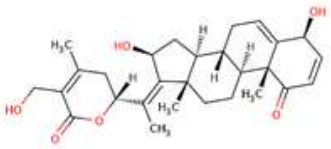

54

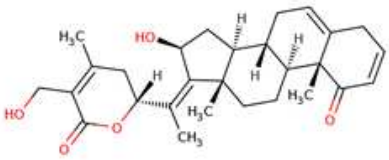

55

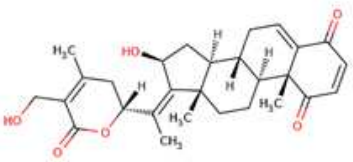

56

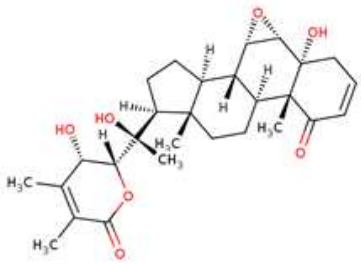

57

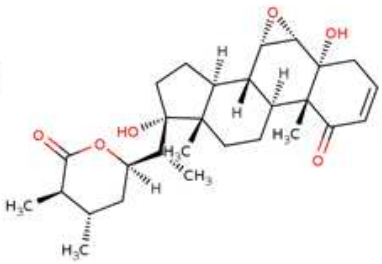

58

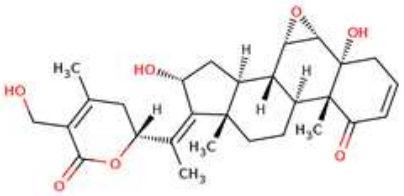

59

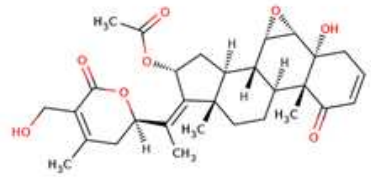

60

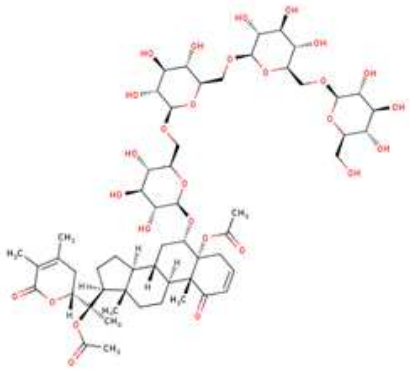

61

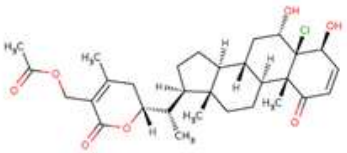

62

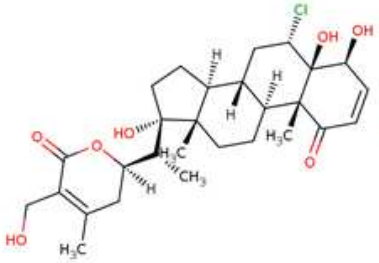

63

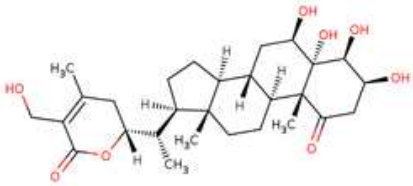

64

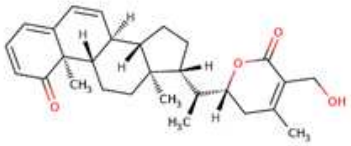

65

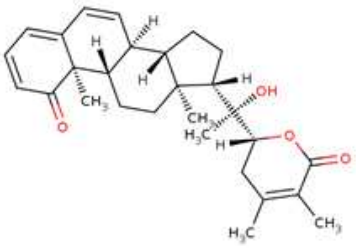

66

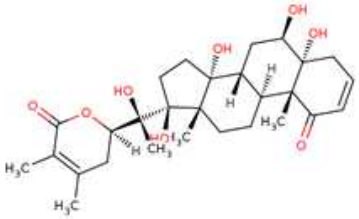

67

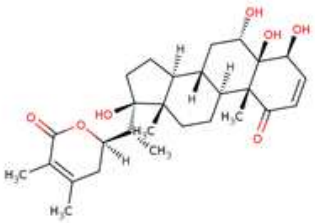

68

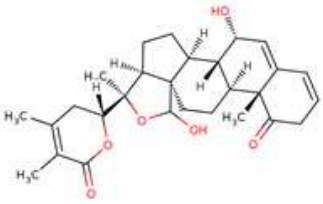

69

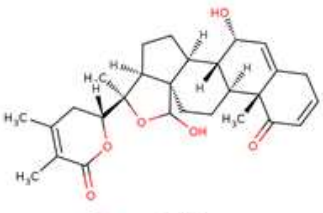

70

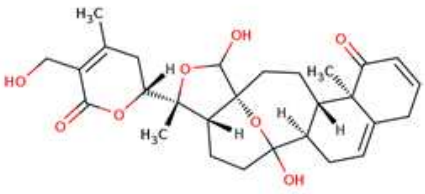

71

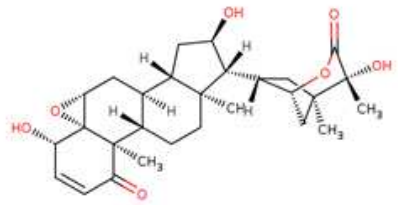

72

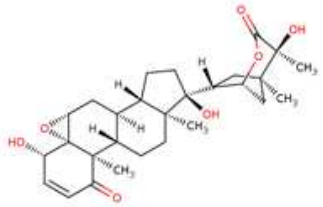

73

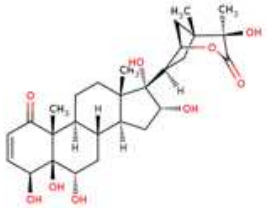

74

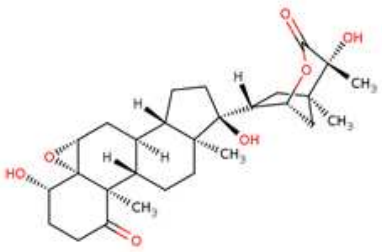

75

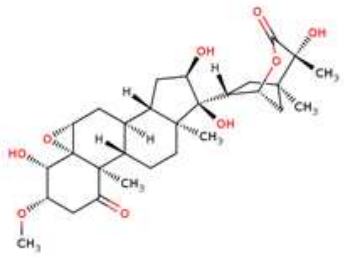

76

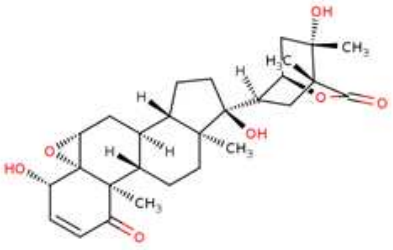

77

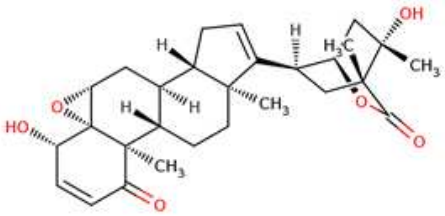

78

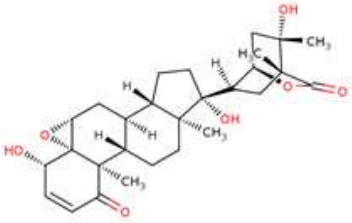

79

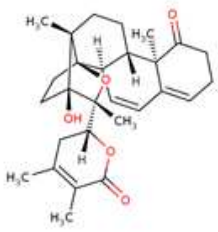

80

81

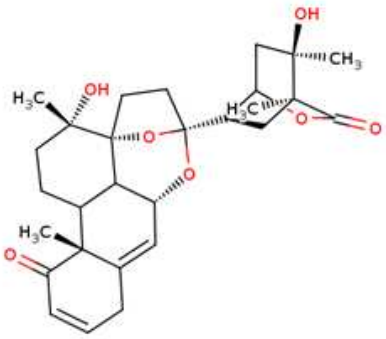

82

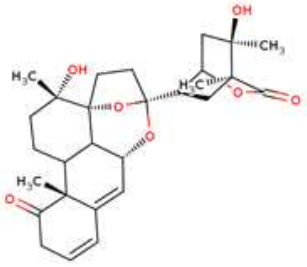

83

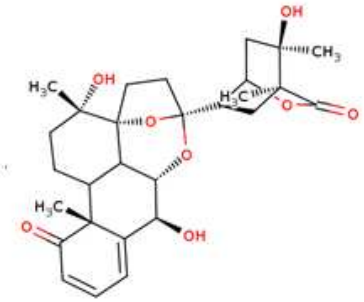

84

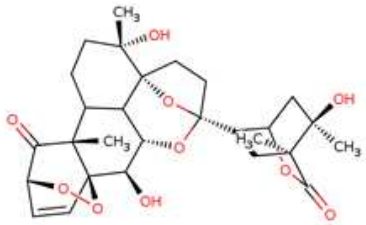

85

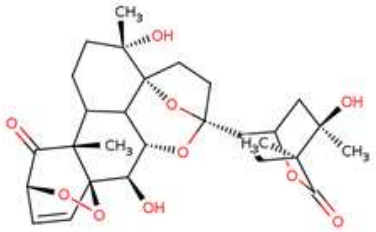

86

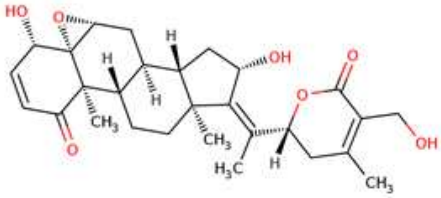

87

88

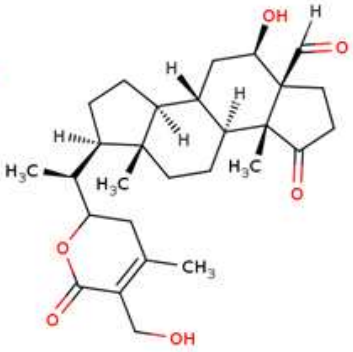

89

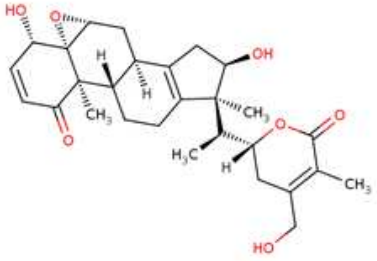

90

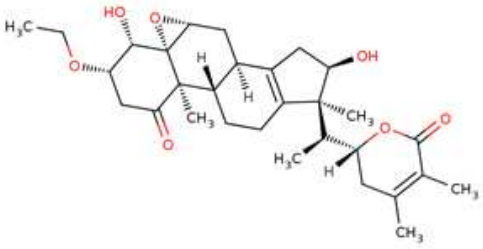

91

Figure S2: Redocking of the crystallized ligands. The original structure (blue) and the docking result (pink) are shown with their respective targets (cartoon) and RMSD values.

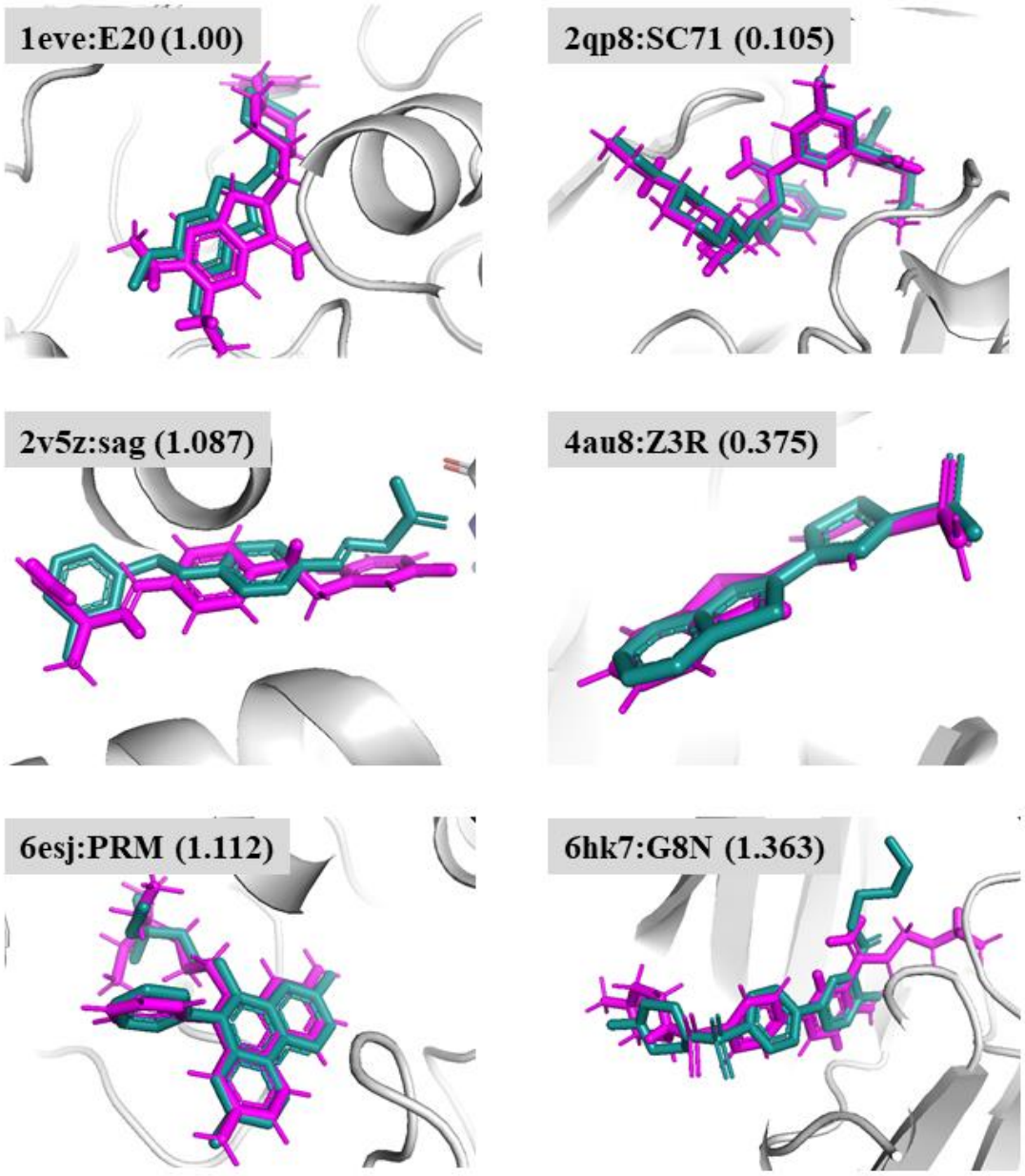

Figure S3:Solvent Accessible Surface Area (SASA) of the complex A) AChE-withanolide 53 and B) BChE-withanolide 53.

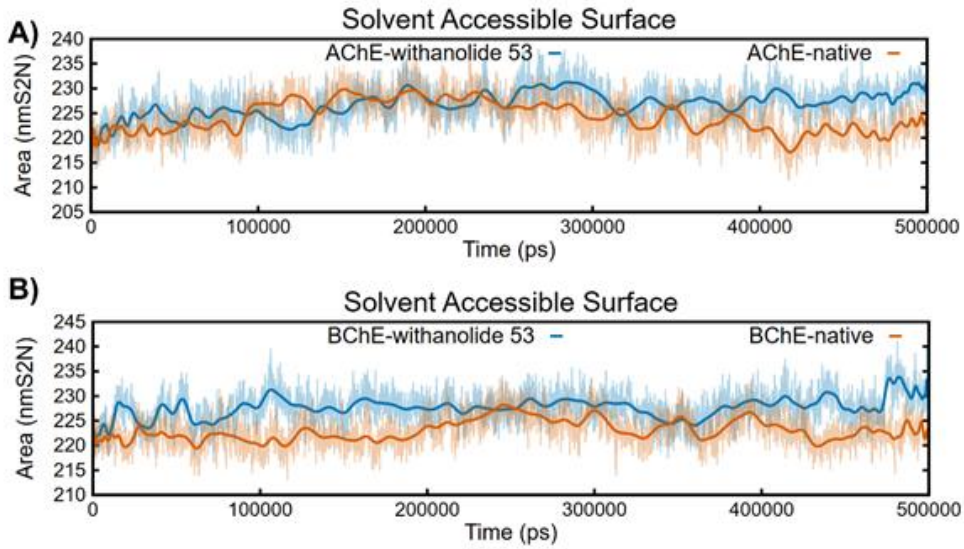

Figure S4:Radius of gyration (Rg) of the complex A) AChE-withanolide 53 and B) BChE-withanolide 53.

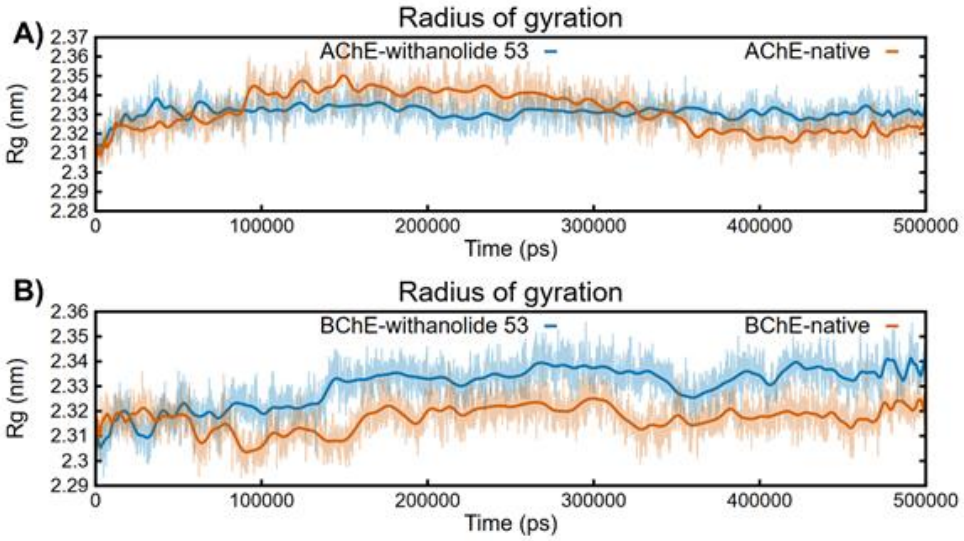

APÊNDICE C: figuras suplementares ao capítulo 2

Figure S1: Mcf7 cells treated with DMSO. On the right is shown the DAPI staining (brightness 20%), and on the left the Ki67-Alexa Fluor 488 staining (brightness 40%) of five different frames.

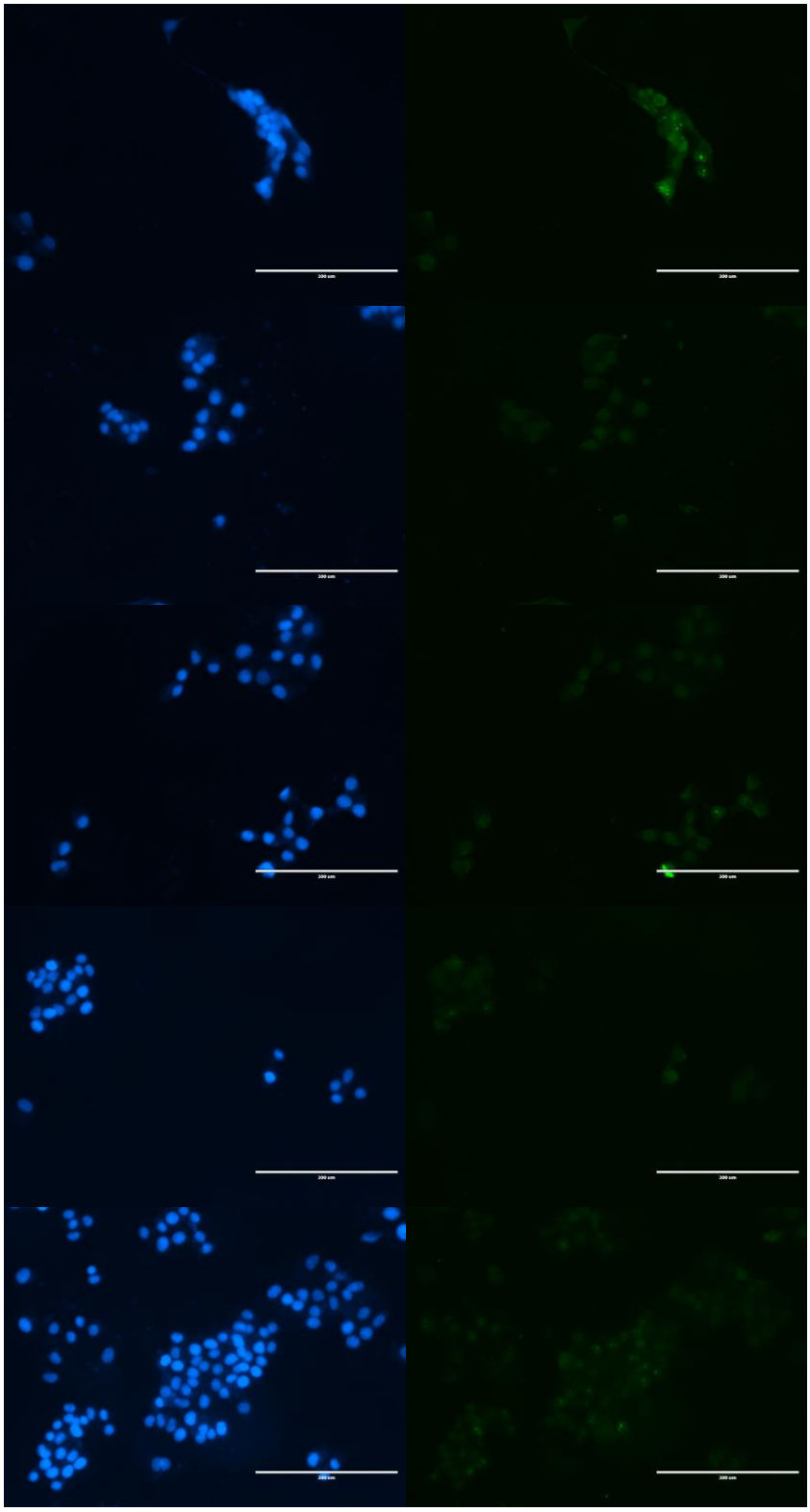

Figure S2: Mcf7 cells treated with withalutin (compound 1). On the right is shown the DAPI staining (brightness 20%), and on the left the Ki67-Alexa Fluor 488 staining (brightness 40%) of five different frames.

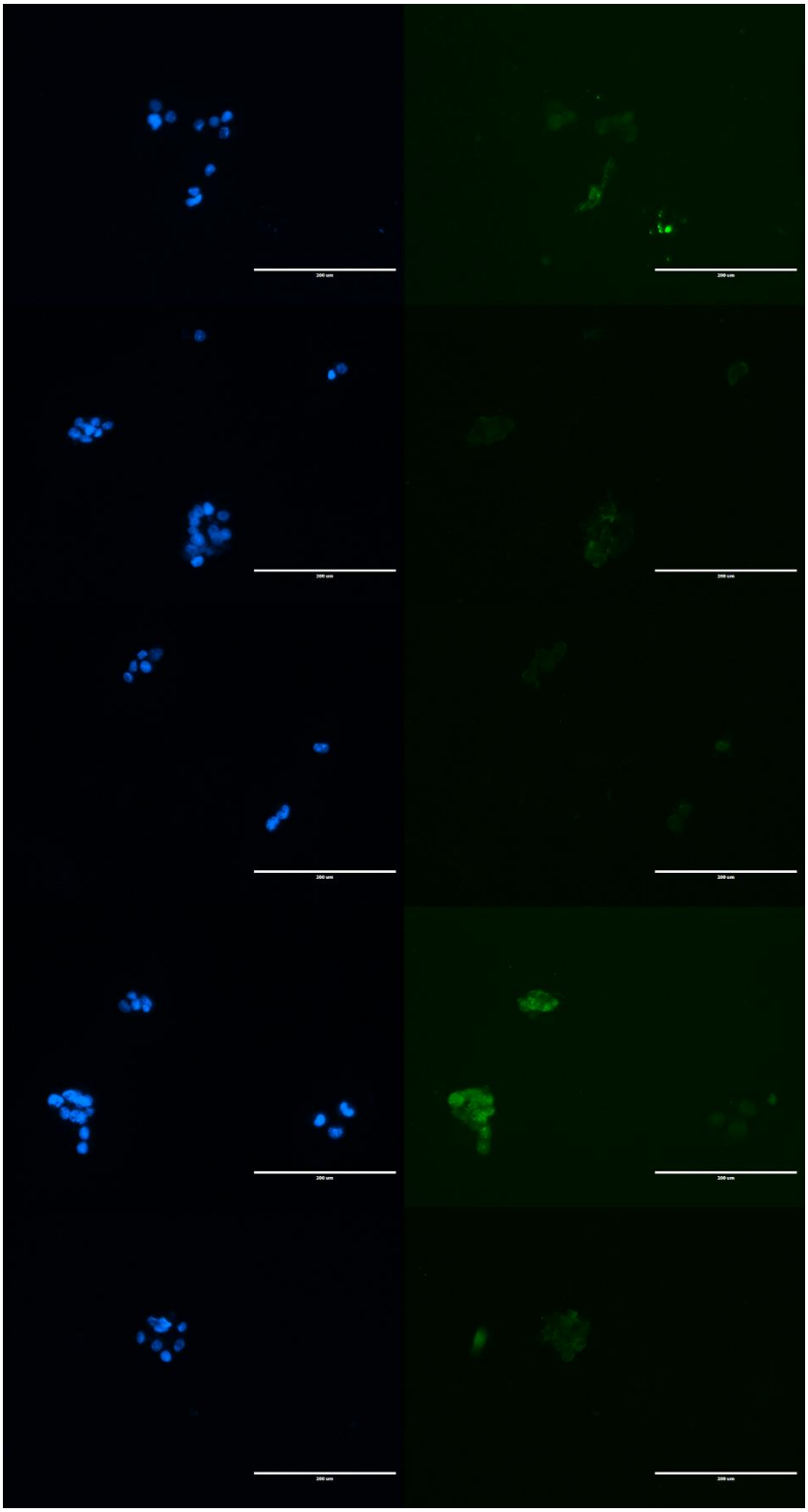

Figure S3: Mcf7 cells treated with withacnistin (compound 2). On the right is shown the DAPI staining (brightness 20%), and on the left the Ki67-Alexa Fluor 488 staining (brightness 40%) of five different frames.

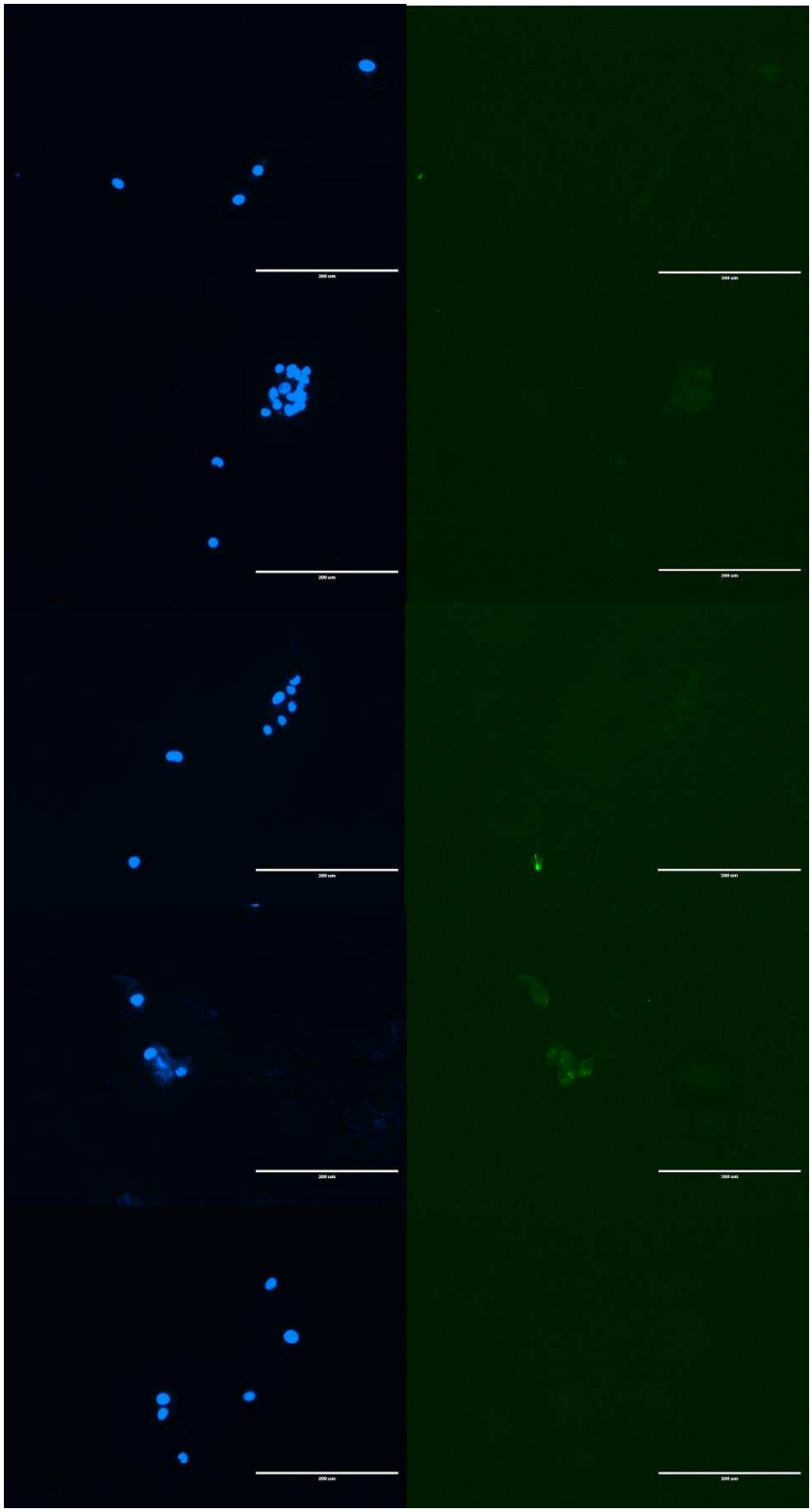

Figure S4: Mcf7 cells treated with withacnistin acetate (compound 3). On the right is shown the DAPI staining (brightness 20%), and on the left the Ki67-Alexa Fluor 488 staining (brightness 40%) of five different frames.

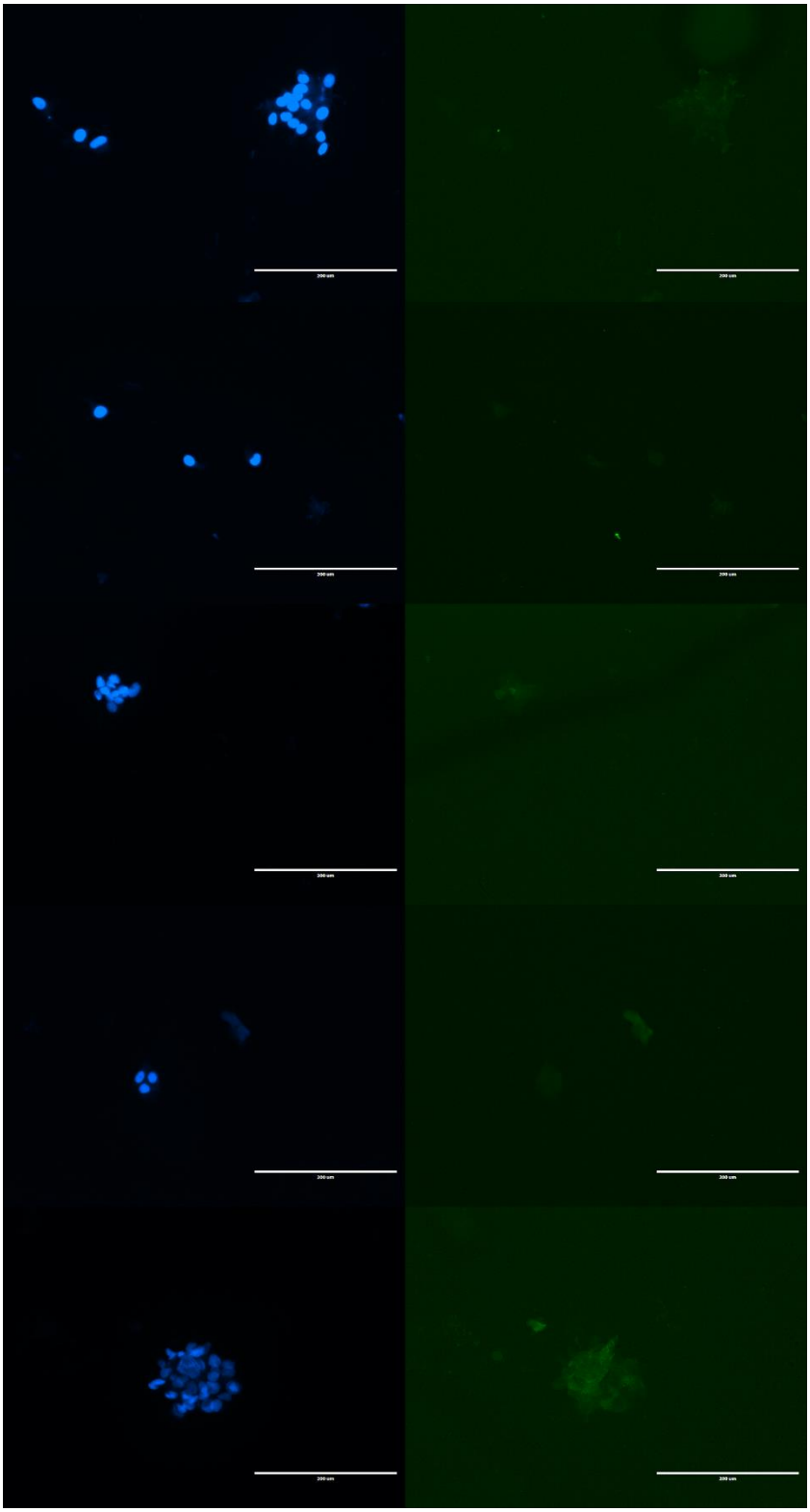

Figure S5: MV3 cells treated with DMSO. On the right is shown the DAPI staining (brightness 20%), and on the left the Ki67-Alexa Fluor 488 staining (brightness 40%) of five different frames.

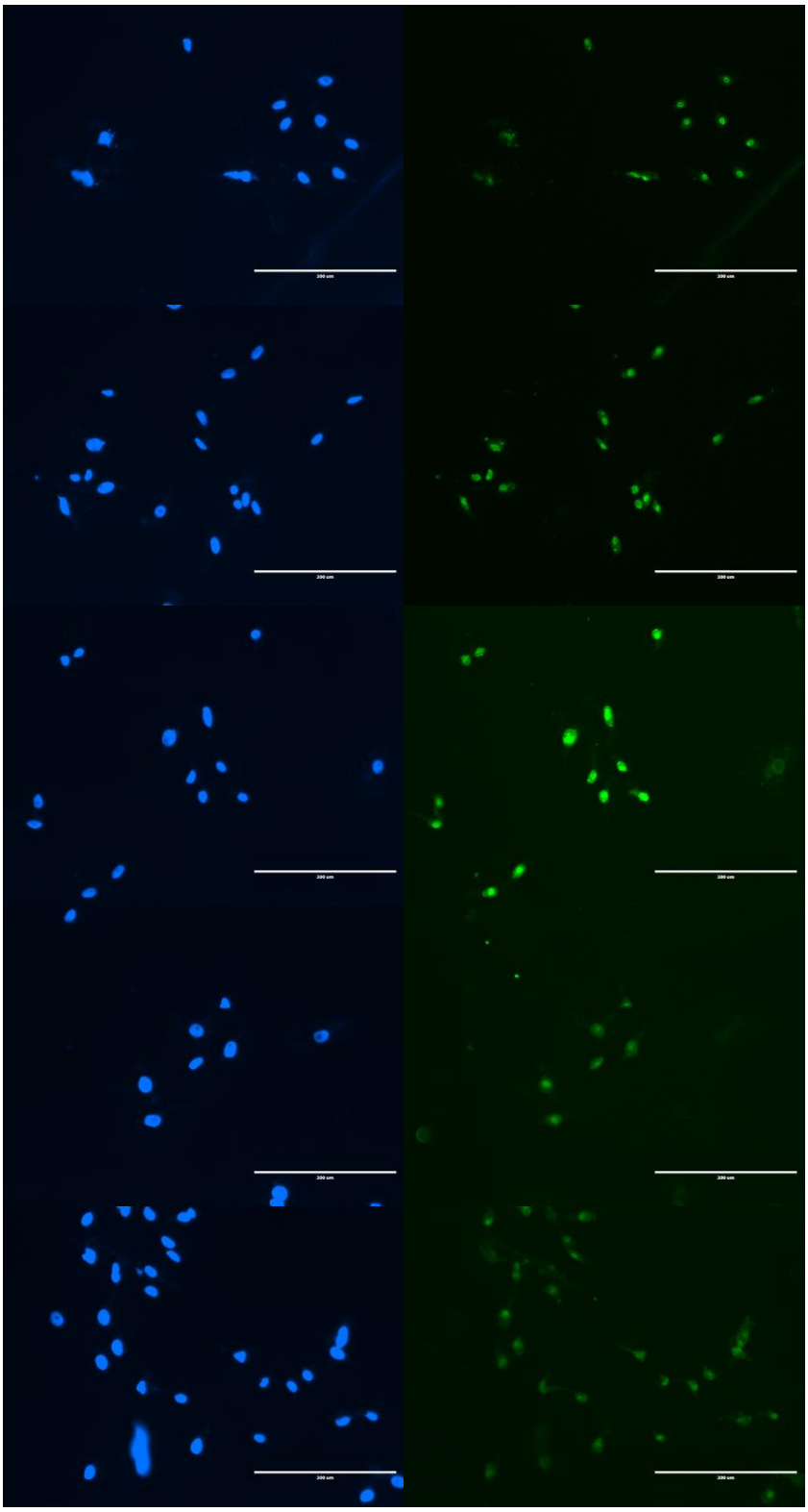

Figure S6: MV3 cells treated with withalutin (compound 1). On the right is shown the DAPI staining (brightness 20%), and on the left the Ki67-Alexa Fluor 488 staining (brightness 40%) of five different frames.

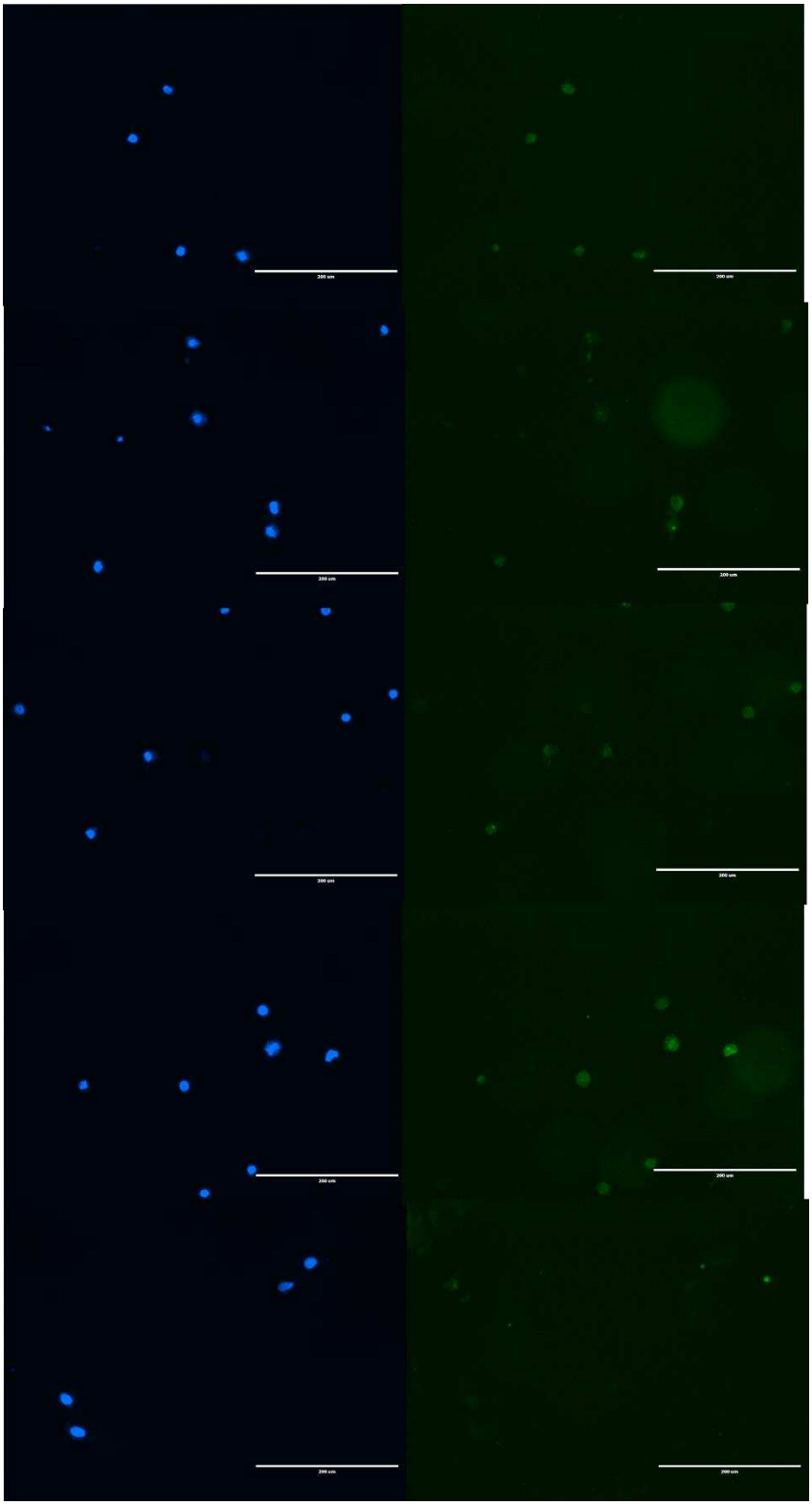

Figure S7: MV3 cells treated with withacnistin (compound 2). On the right is shown the DAPI staining (brightness 20%), and on the left the Ki67-Alexa Fluor 488 staining (brightness 40%) of five different frames.

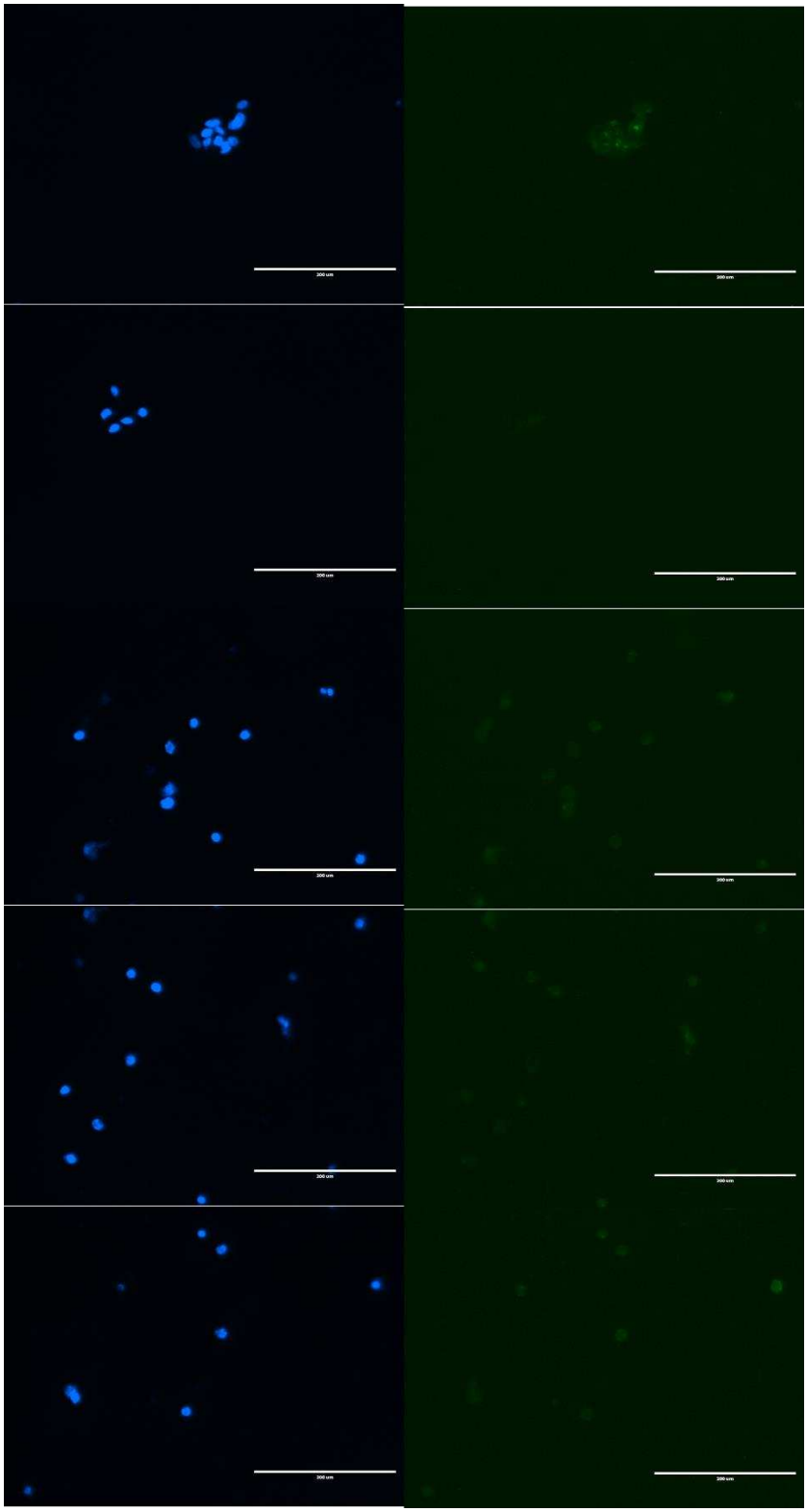

Figure S8: MV3 cells treated with withacnistin acetate (compound 3). On the right is shown the DAPI staining (brightness 20%), and on the left the Ki67-Alexa Fluor 488 staining (brightness 40%) of five different frames.

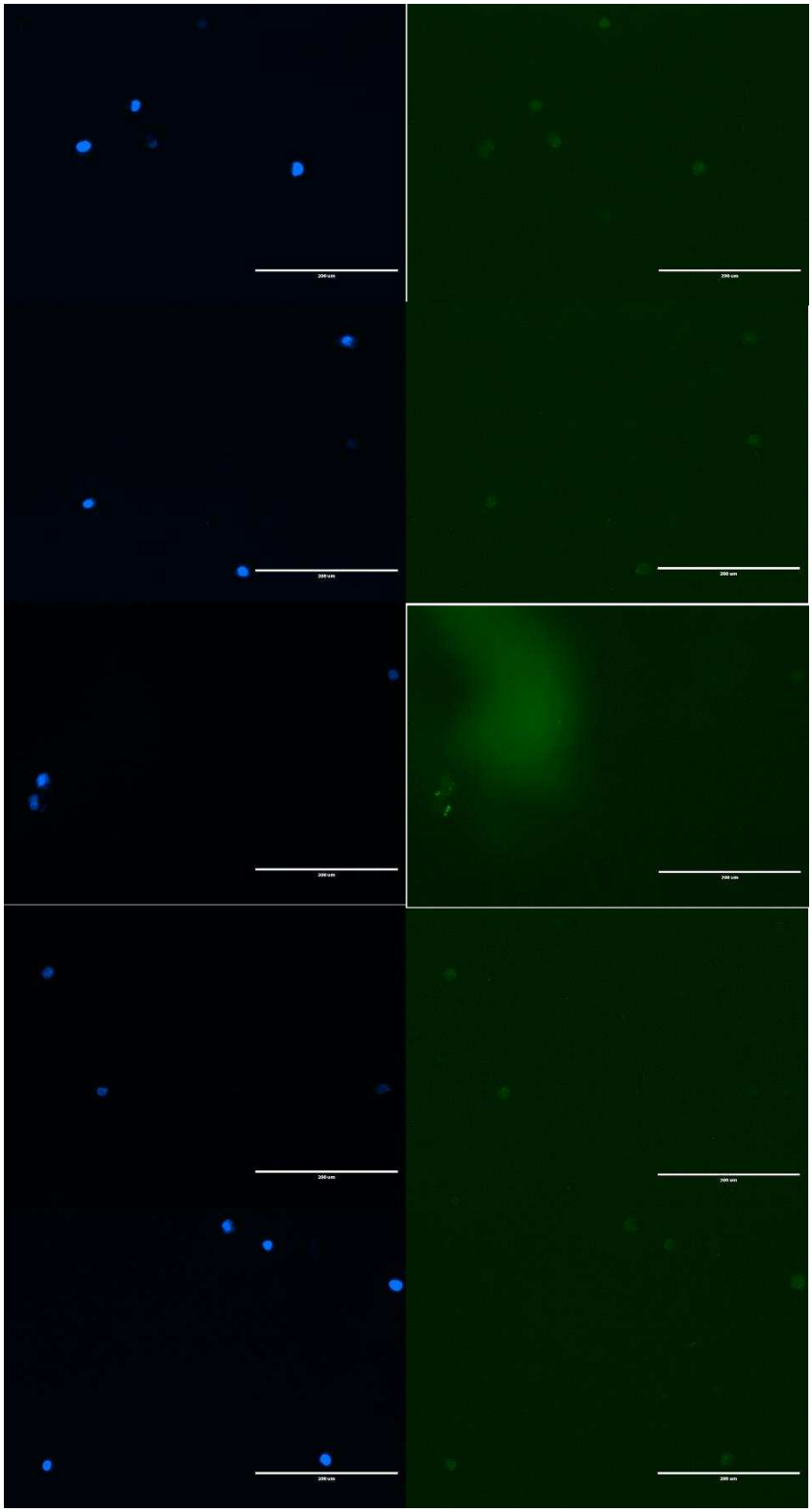

APÊNDICE D: figuras suplementares ao capítulo 3

Figure 1

Sample A: Mass spectrum referring to the m/z peak 1075.5377, 929.4792, 767.4248 (Rt 18.0-18.4 min.).

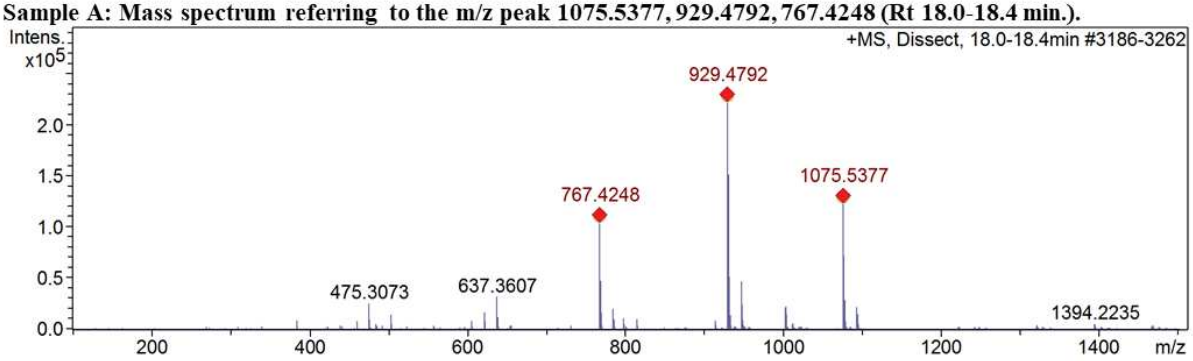

Figure 2

Sample A: MS2 of ion *m/z* 1075.5377 $[M+H]^+$. Anotation C28H42O5: (Pubesenolide-like) tetraglicosilado (glu-rha-rha-glu)

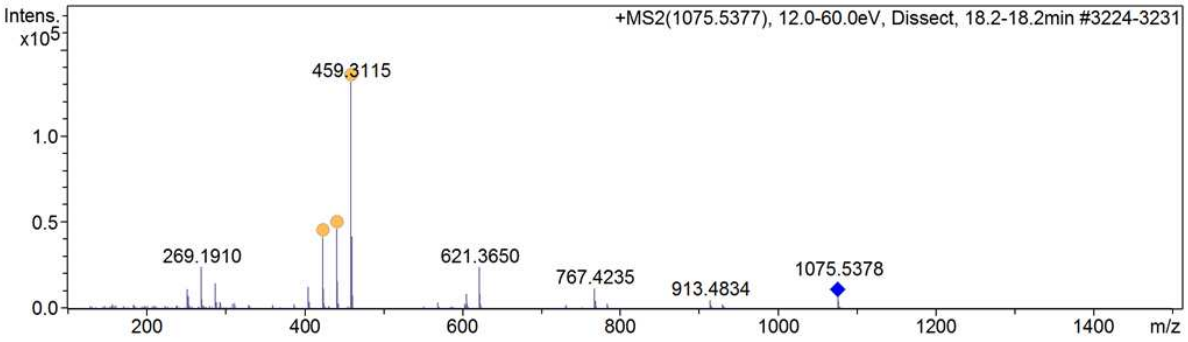

Figure 3

Sample A: MS2 of ion *m/z* 929.4792 $[M+H]^+$. Anotation C28H42O5: (Pubesenolide-like) triglicosilado (glu-rha-glu)

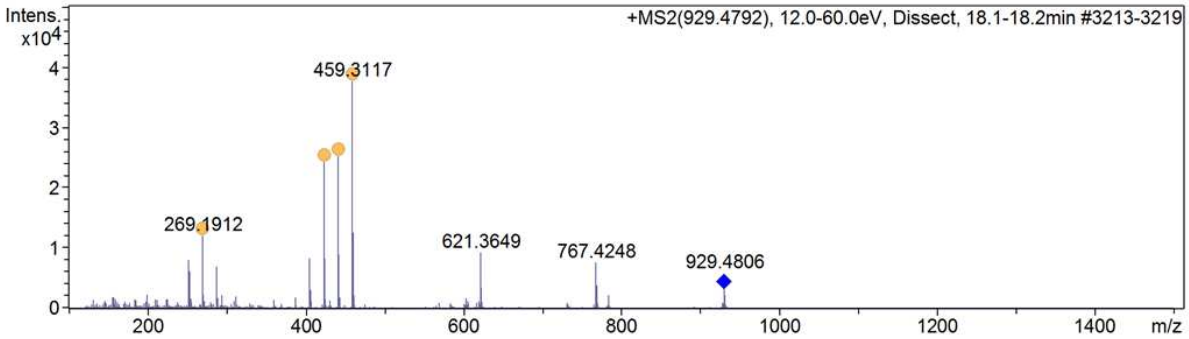

Figure 4

Sample A: MS2 of ion *m/z* 767.4248 [M+H]⁺. Anotation C28H42O5: (Pubesenolide-like) biglicosilado (rha-glu)

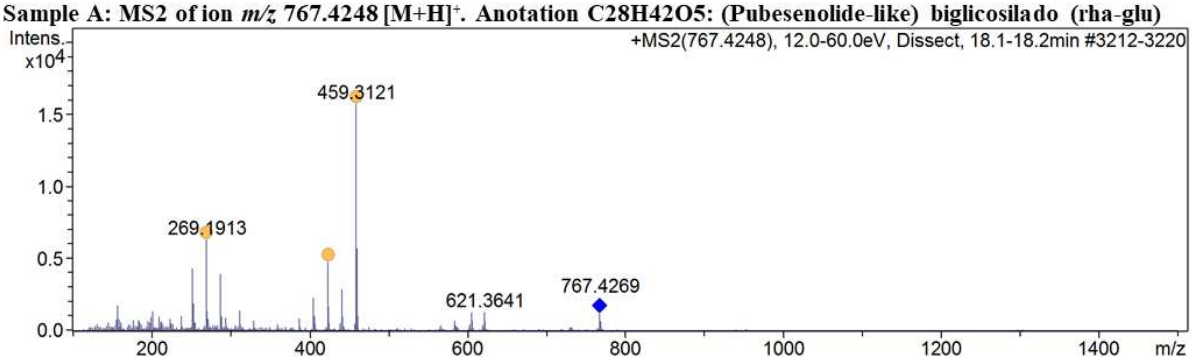

Figure 5

Sample A: Mass spectrum referring to the m/z peak 783.4207 (Rt 18.1-18.6 min.).

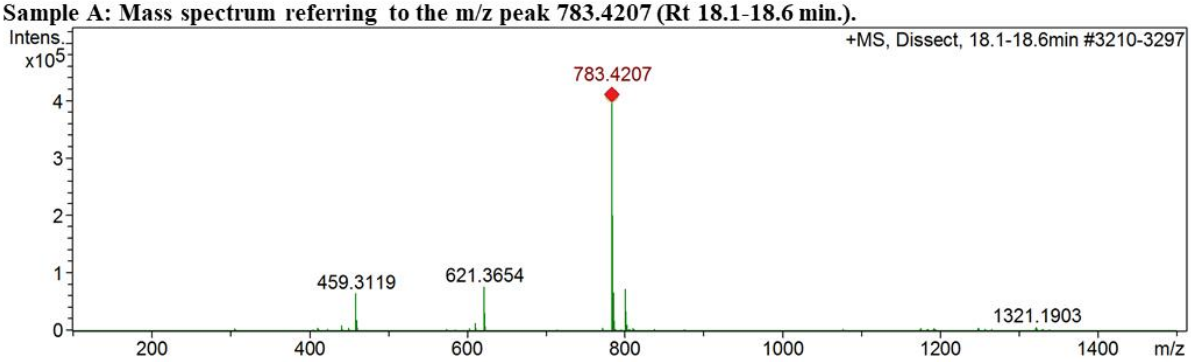

Figure 6

Sample A: MS2 of ion *m/z* 783.4207 [M+H]⁺. Anotation C28H42O5: (Pubesenolide-like) diglicosilado (glu-glu)

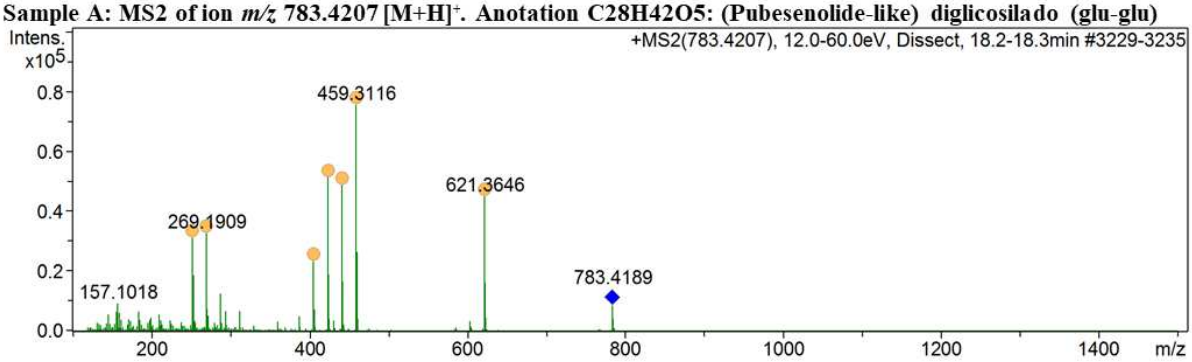

Figure 7

Sample A: Mass spectrum referring to the m/z peak 958.5751, 941.5484, 488.3040, 471.2773 (Rt 28.6-28.9 min.).

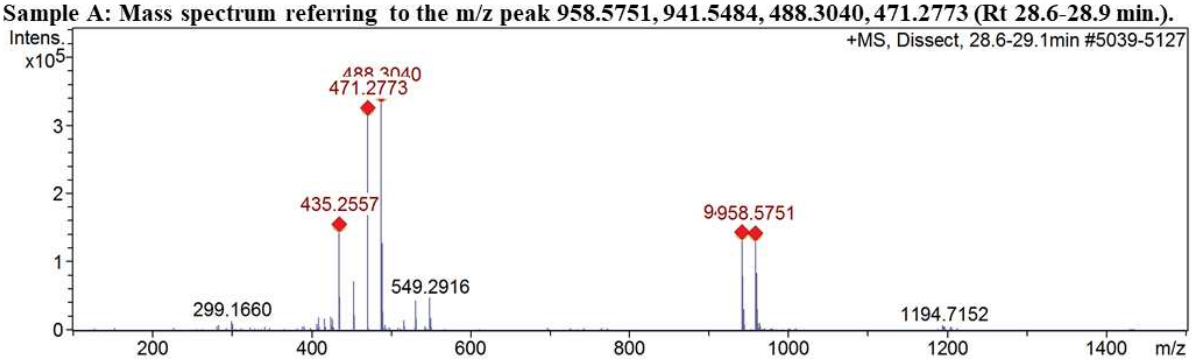

Figure 8

Sample A: MS2 of ion *m/z* 958.5751 [M+H+NH3]$^+$. Anotation C28H38O6: (Withaferin A-like dimer)

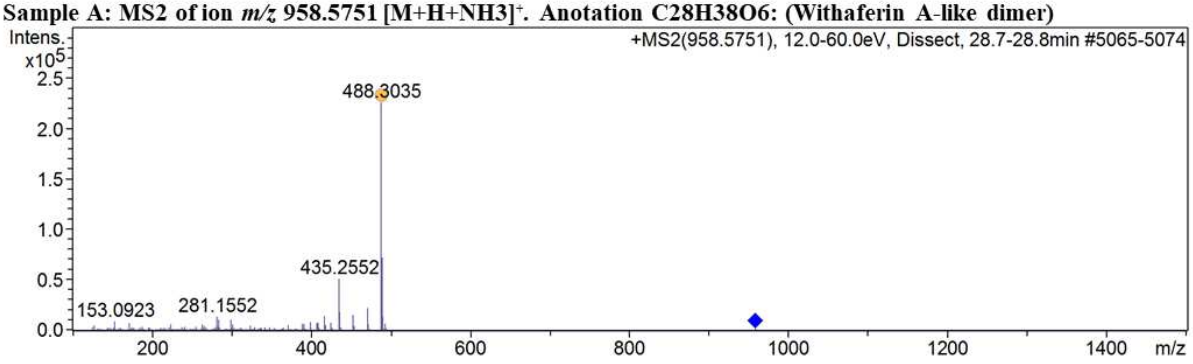

Figure 9

Sample A: MS2 of ion *m/z* 941.5484 [M+H]. Anotation C28H38O6: (Withaferin A-like dimer)

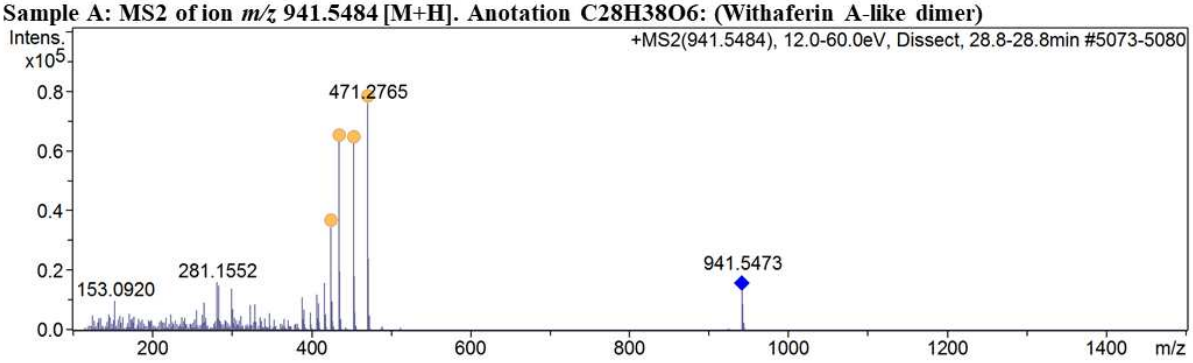

Figure 10

Sample A: MS2 of ion *m/z* 488.3040 [M+H+NH3]$^+$. Anotation C28H38O6: (Withaferin A-like)

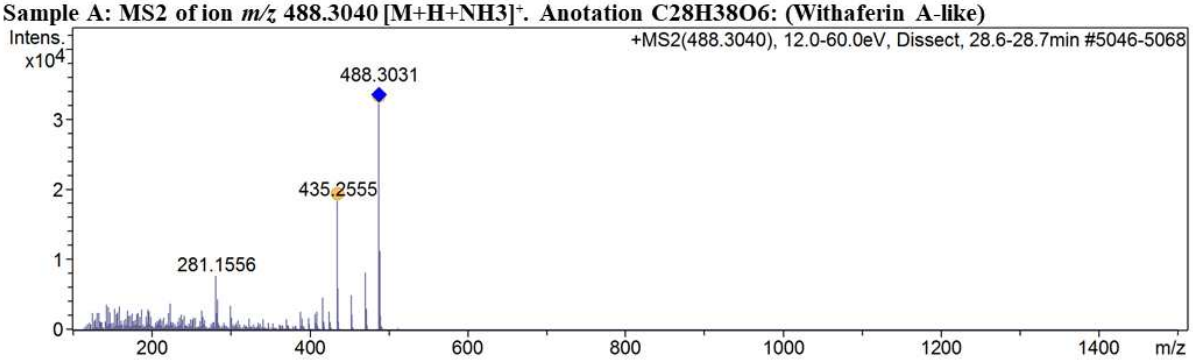

Figure 11

Sample A: MS2 of ion *m/z* 471.2773 [M+H]$^+$. Anotation C28H38O6: (Withaferin A-like)

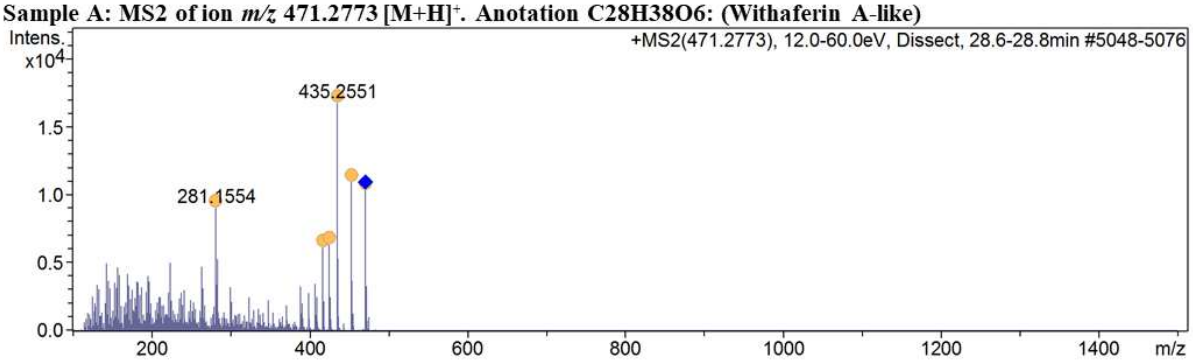

Figure 12

Sample A: Mass spectrum referring to the m/z peak 926.5846, 909.5585, 455.2831, 472.3087 (Rt 28.7-29.3 min.).

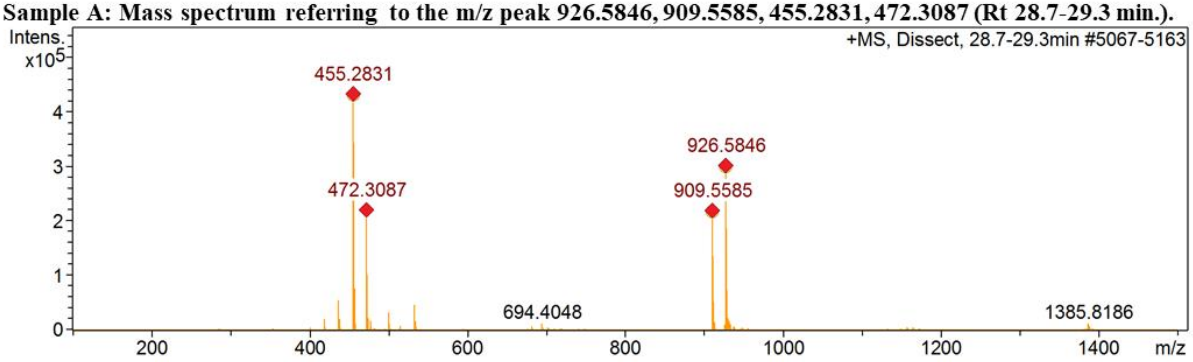

Figure 13

Sample A: MS2 of ion *m/z* 926.5846 $[M+H+NH3]^+$. Anotation C56H76O10: (withanolide B-like dimer)

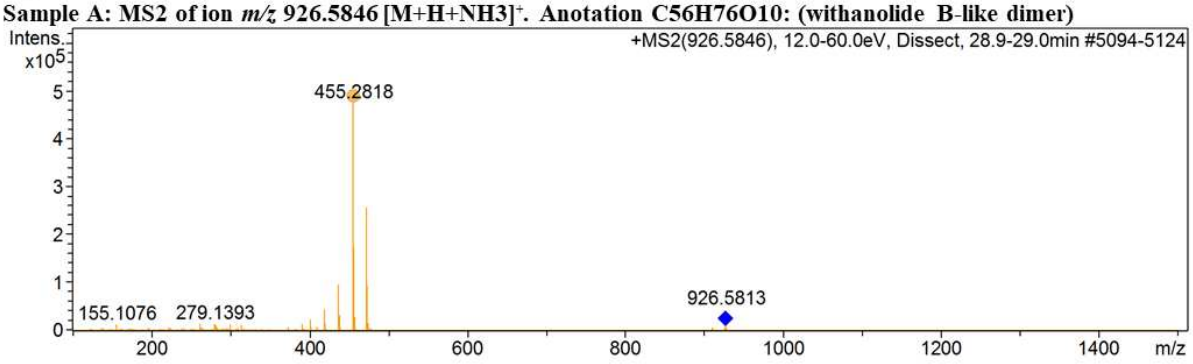

Figure 14

Sample A: MS2 of ion *m/z* 909.5585 $[M+H]^+$. Anotation C56H76O10: (withanolide B-like dimer)

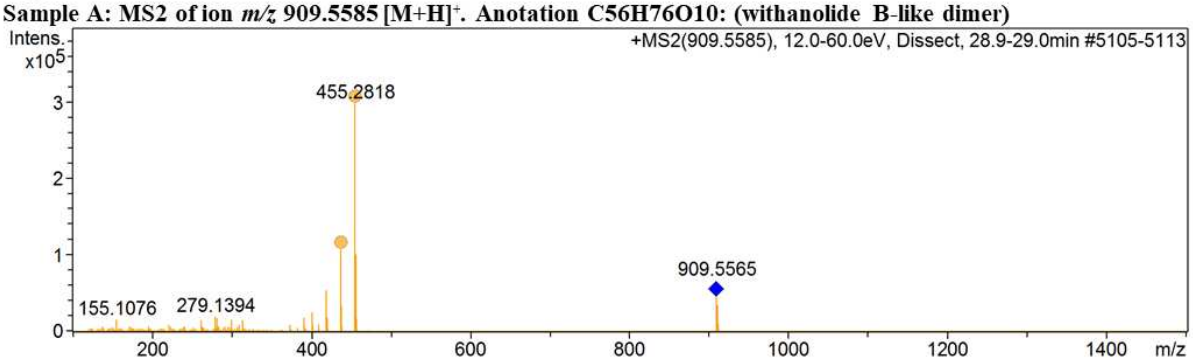

Figure 15

Sample A: MS2 of ion *m/z* 455.2831 $[M+H]^+$. Anotation C28H38O5: (withanolide B-like)

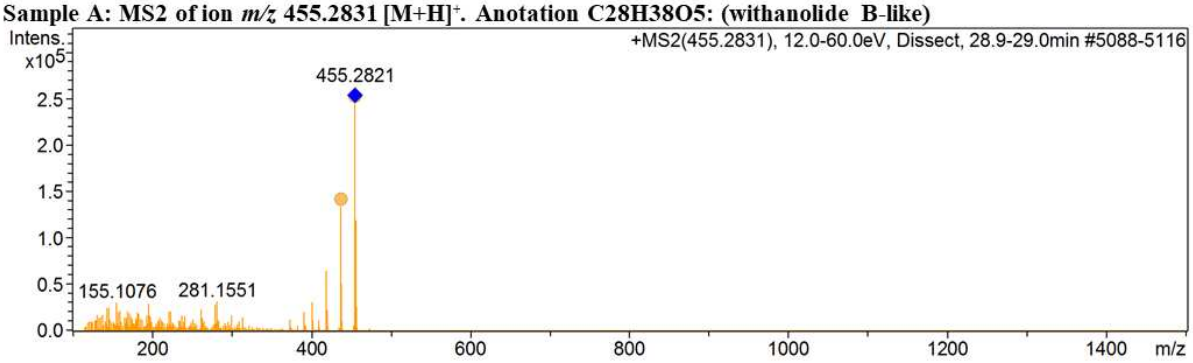

Figure 16

Sample A: MS2 of ion *m/z* 472.3087 $[M+H+NH3]^+$. Anotation C28H38O5: (withanolide B-like)

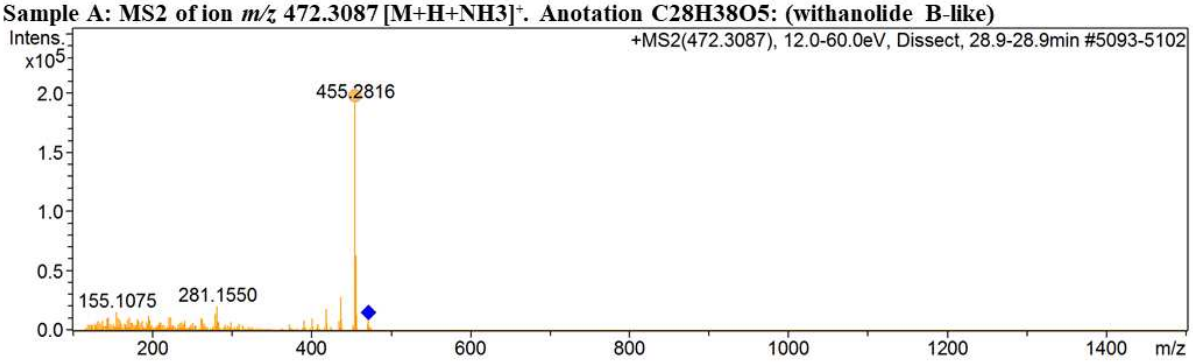

Figure 17

Sample C: Mass spectrum referring to the m/z peak 926.6032, 473.2914, 490.3181, 455.2809 (Rt 23.0-23.5 min)

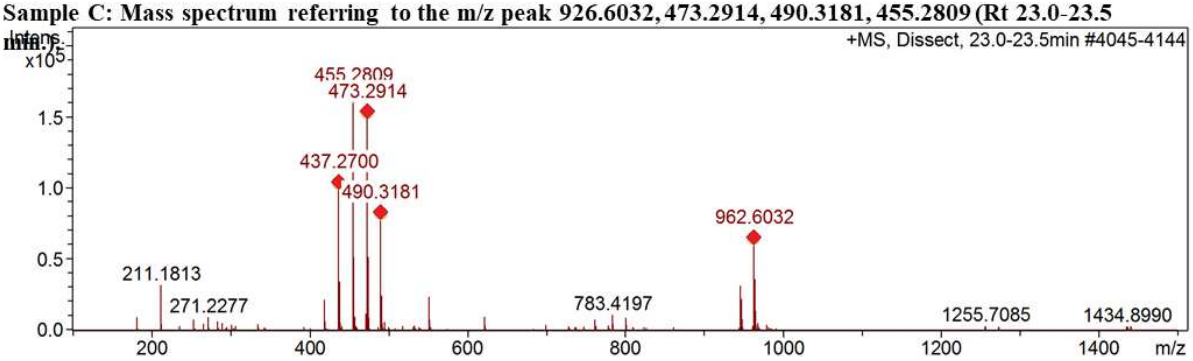

Figure 18

Sample C: MS2 of ion *m/z* 962.6032 $[M+H+NH3]^+$. Anotation C28H40O6: (24,25-dihydrowithanolide D-like

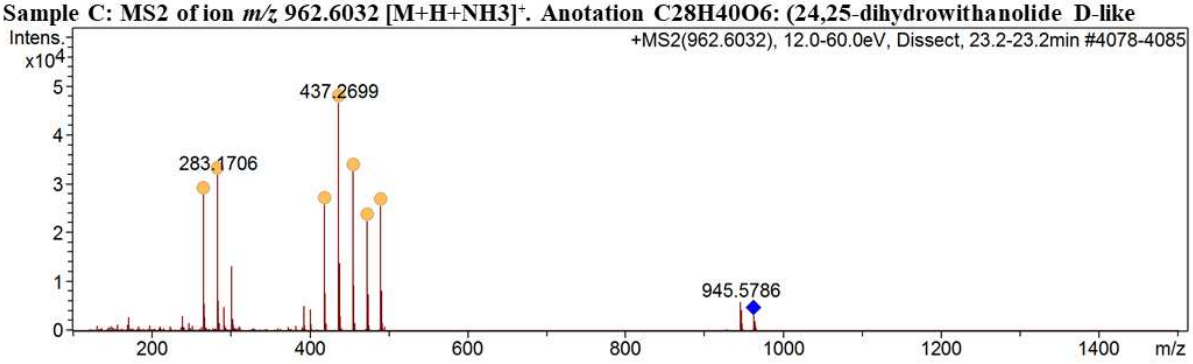

Figure 19

Sample C: MS2 of ion *m/z* 473.2914 $[M+H]^+$. Anotation C28H40O6: (24,25-dihydrowithanolide D-like)

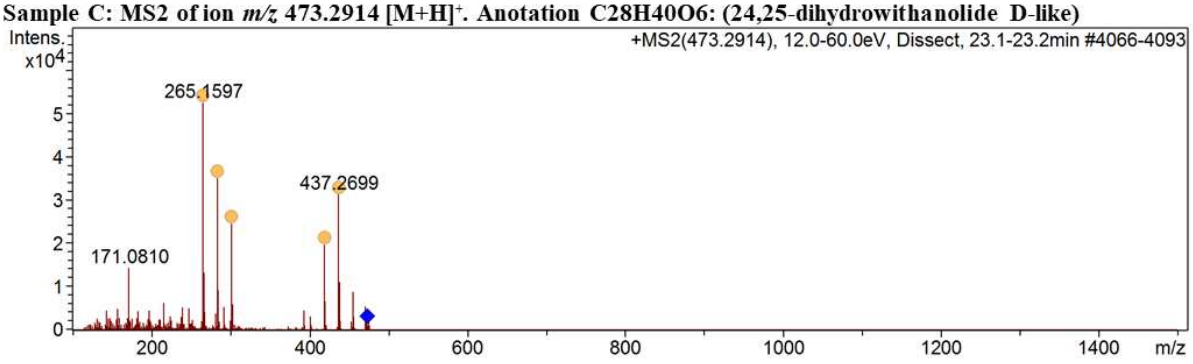

Figure 20

Sample C: MS2 of ion *m/z* 490.3181 [M+H+NH3]$^+$. Anotation C28H40O6: (24,25-dihydrowithanolide D-like)

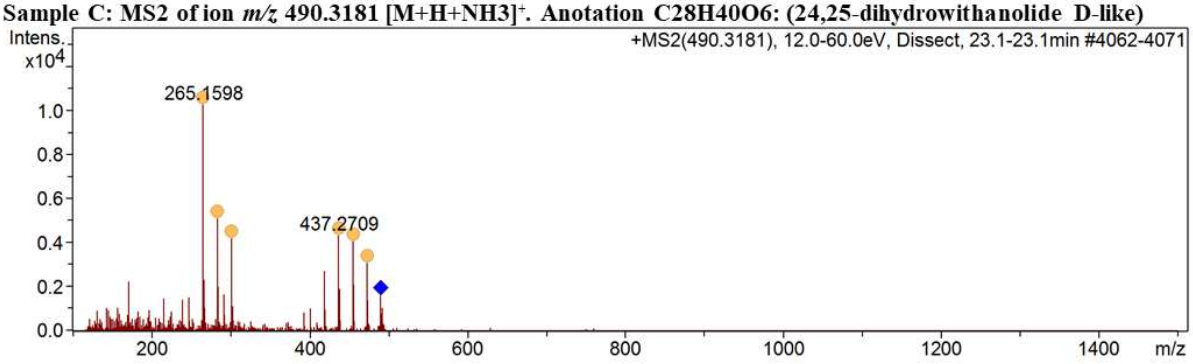

Figure 21

Sample C: MS2 of ion *m/z* 455.2809 [M+H]$^+$. Anotation C28H38O5: (Withanolide B-like)

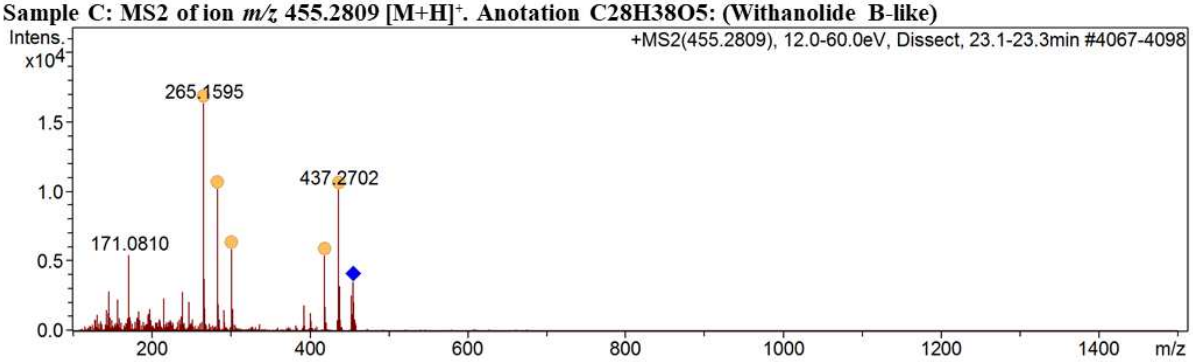

Figure 22

Sample C: Mass spectrum referring to the m/z peak 459.3132 (Rt 23.8-24.4 min.).

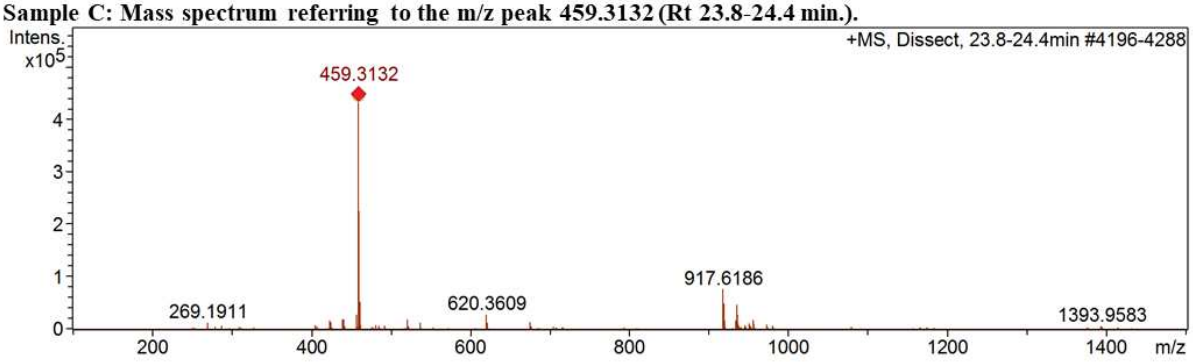

Figure 23

Sample C: MS2 of ion *m/z* 459.3132 [M+H]$^+$. Anotation C28H42O5: (Pubsenolide-like)

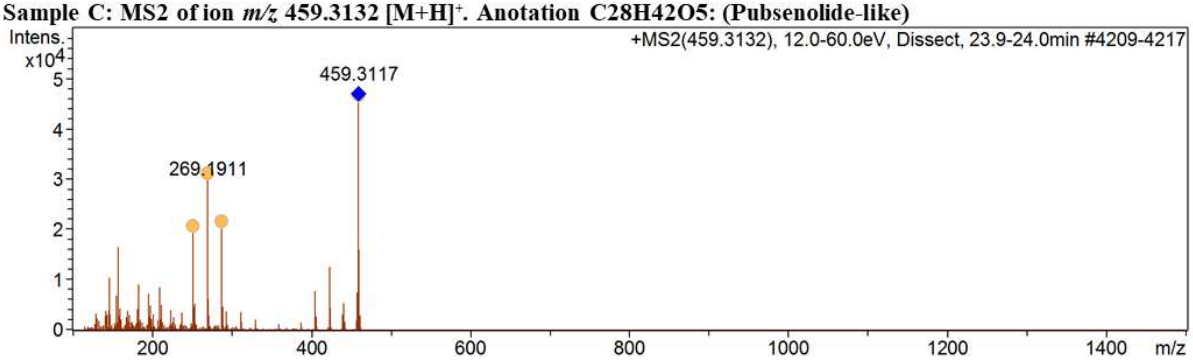

Figure 24

Sample C: Mass spectrum referring to the m/z peak 958.5717, 471.2760 (Rt 24.3-24.9 min.).

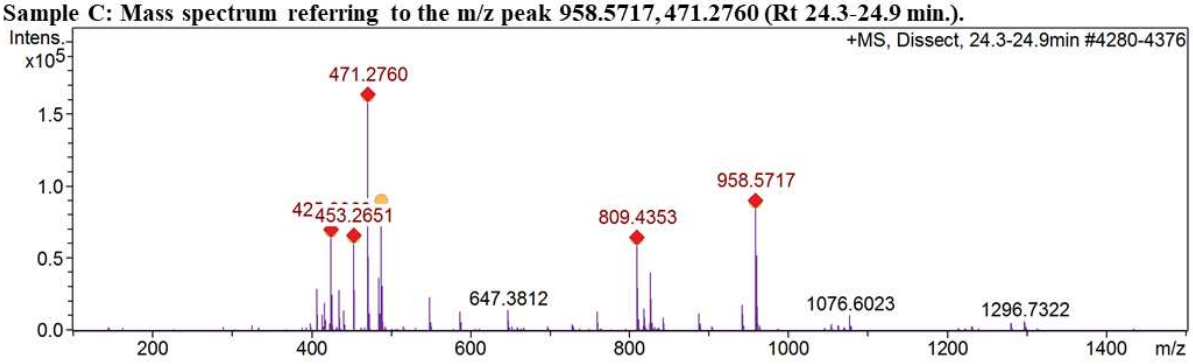

Figure 25

Sample C: MS2 of ion *m/z* 958.5717 $[M+H+NH3]^+$. Anotation C28H42O5: (Withaferin A-like dimer)

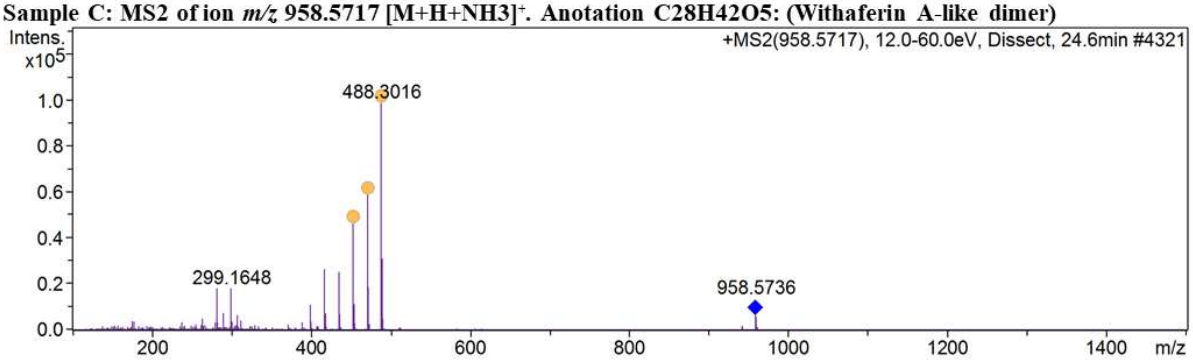

Figure 26

Sample C: MS2 of ion *m/z* 471.2760 $[M+H]^+$. Anotation C28H38O6: (Withaferin A-like)

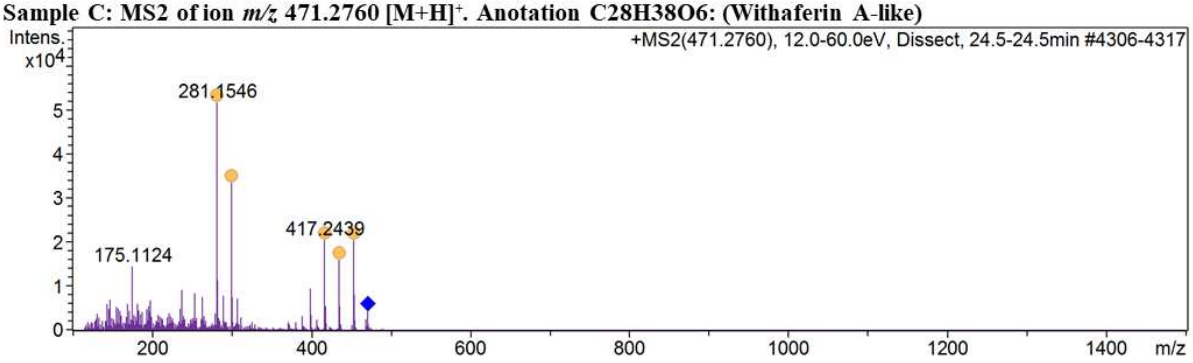

Figure 27

Sample C: Mass spectrum referring to the m/z peak 425.3063, 485.3280, 407.2958 (Rt 24.5-25.0 min.).

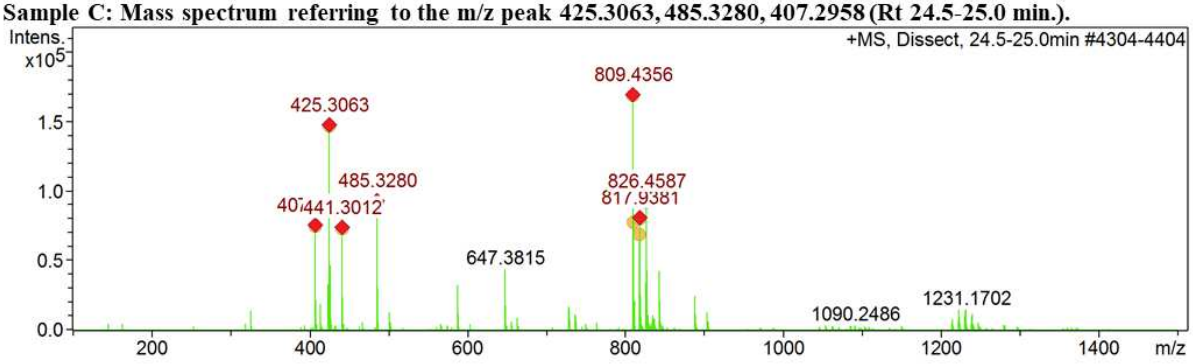

Figure 28

Sample C: MS2 of ion *m/z* 425.3063 [M+H]$^+$. Anotation C28H40O3: (Sinubrasolide L-like)

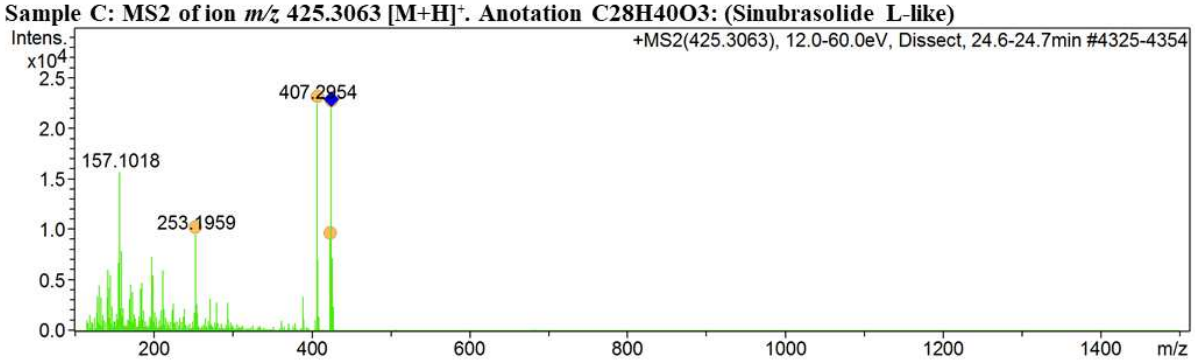

Figure 29

Sample C: MS2 of ion *m/z* 485.3280 [M+H+Ac]$^+$. Anotation C28H40O3: (Sinubrasolide L-like acetate)

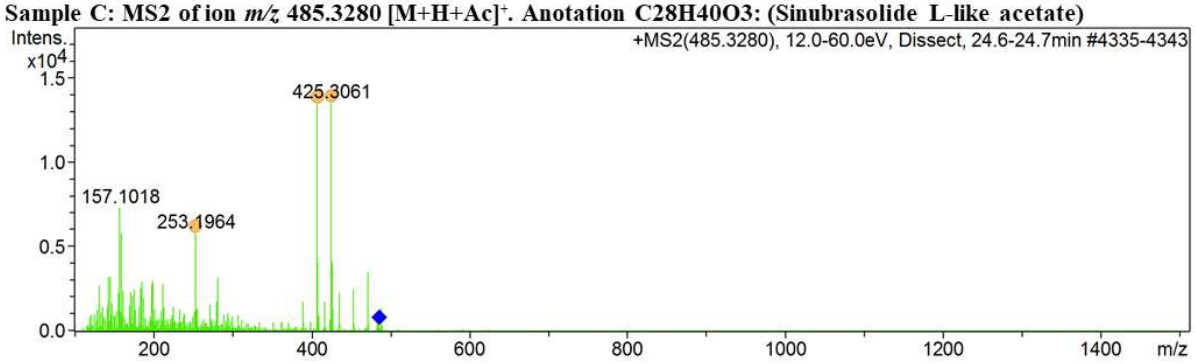

Figure 30

Sample C: MS2 of ion *m/z* 407.2958 [M+H-H2O]$^+$. Anotation C28H40O3: (Sinubrasolide L-like - water)

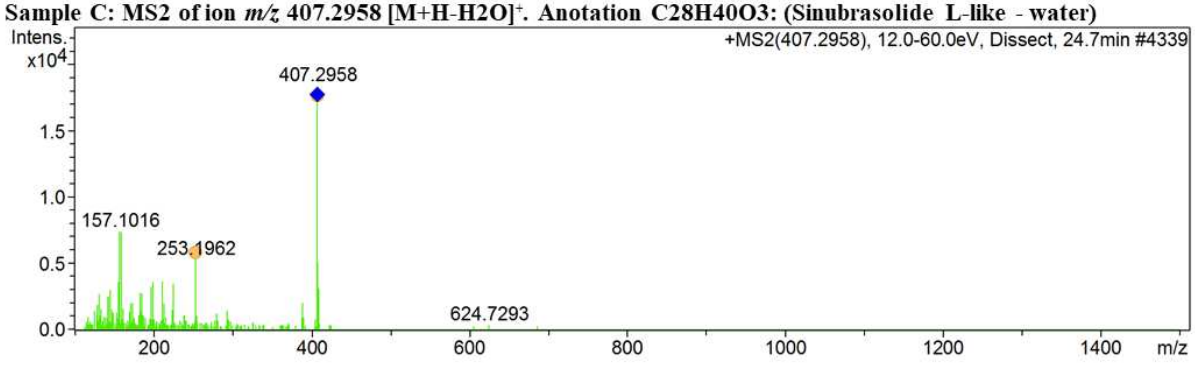

Figure 31

Sample C: Mass spectrum referring to the m/z peak 958.5725, 941.5469, 488.3028, 471.2763 (Rt 28.9-29.4

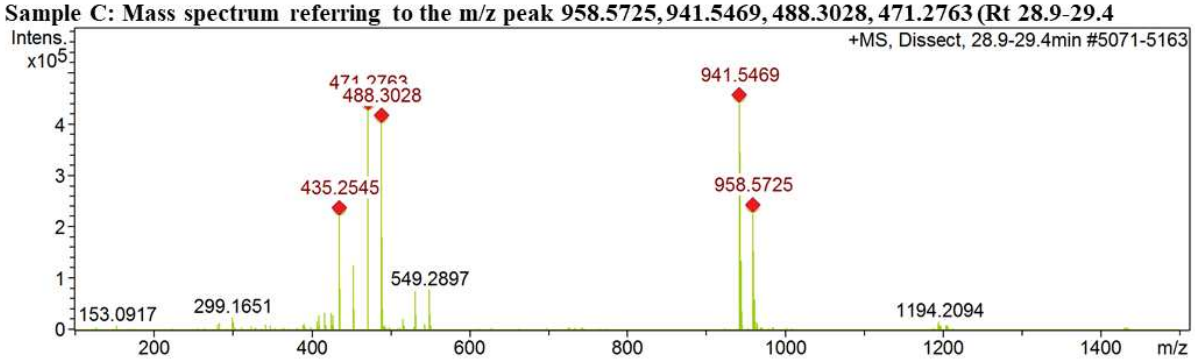

Figure 32

Sample C: Mass spectrum referring to the m/z peak 909.5569, 455.2820, 472.3071 (Rt 28.9-29.6 min.).

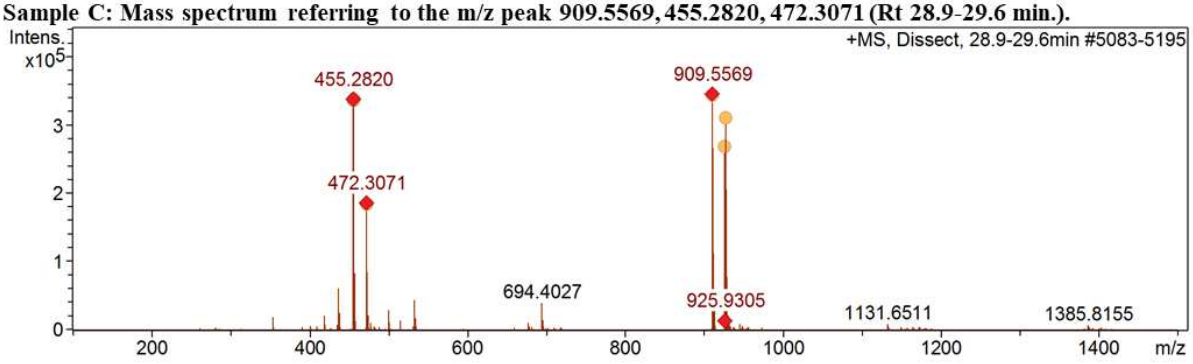

Figure 33

Sample C: Mass spectrum referring to the m/z peak 926.5823, 909.5573, 455.2827, 472.3076 (Rt 29.0-29.6

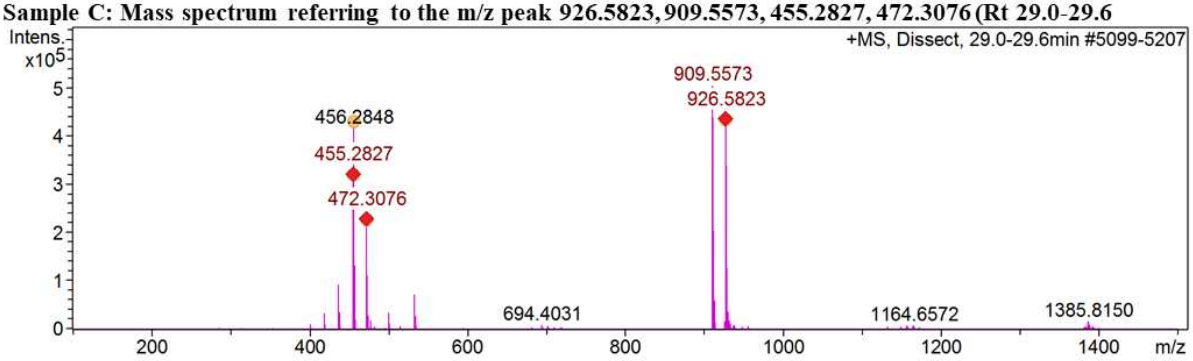

Figure 34

Sample D: Mass spectrum referring to the m/z peak 621.3648, 459.3116 (Rt 20.4-20.9 min.).

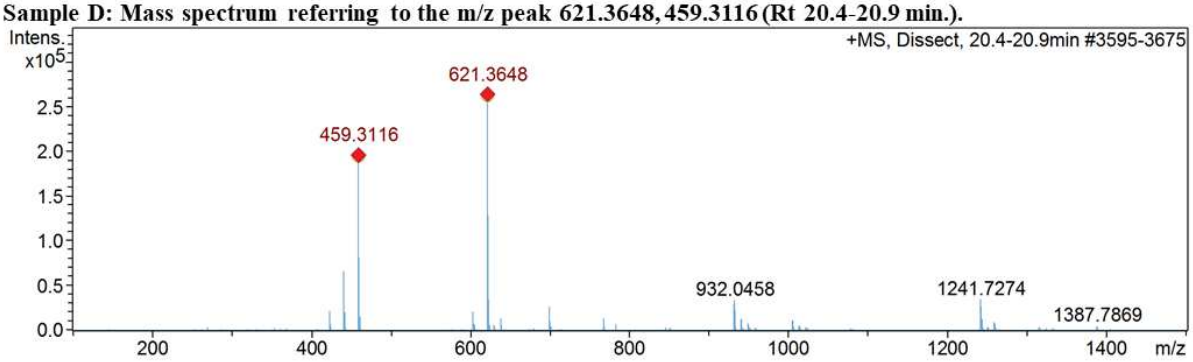

Figure 35

Sample D: MS2 of ion *m/z* 459.3116 $[M+H]^+$. Anotation C28H38O6: (Pubsenolide-like)

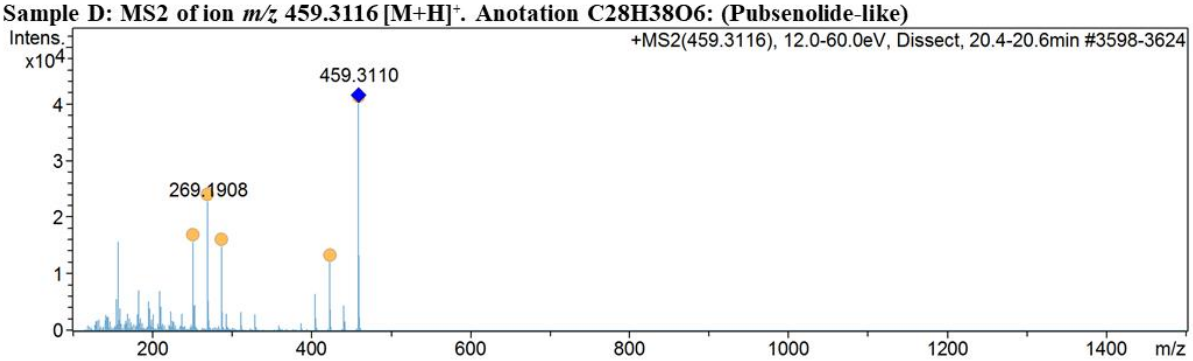

Figure 36

Sample D: MS2 of ion *m/z* 621.3648 $[M+H]^+$. Anotation C28H38O6: (Pubsenolide-like) glycosylated (glu)

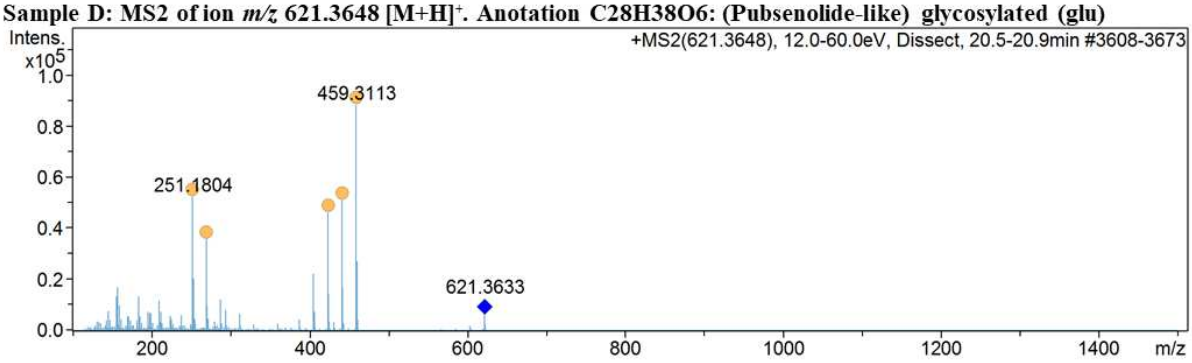

Figure 37

Sample D: Mass spectrum referring to the m/z peak 439.2851, 457.2956 (Rt 20.8-21.3 min.).

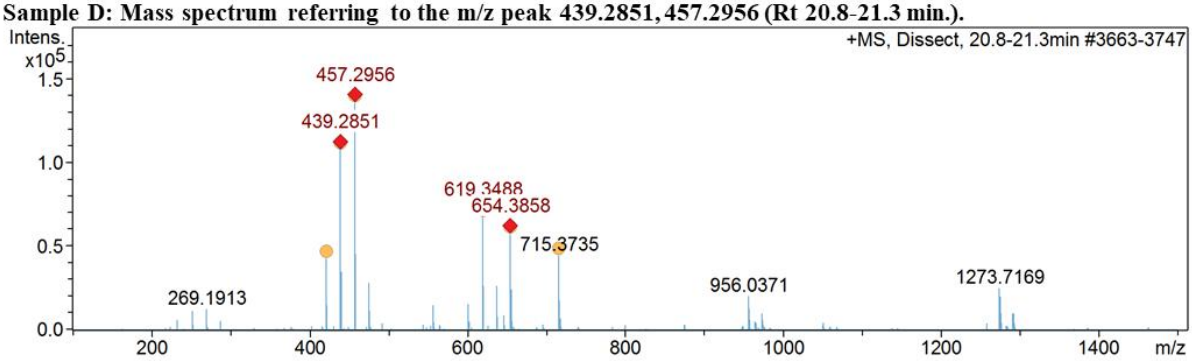

Figure 38

Sample D: MS2 of ion *m/z* 439.2851 $[M+H]^+$. Anotation C28H38O4: (20beta-hydroxy-1-oxo-(22R)-witha-2,5,24-trienolide-like)

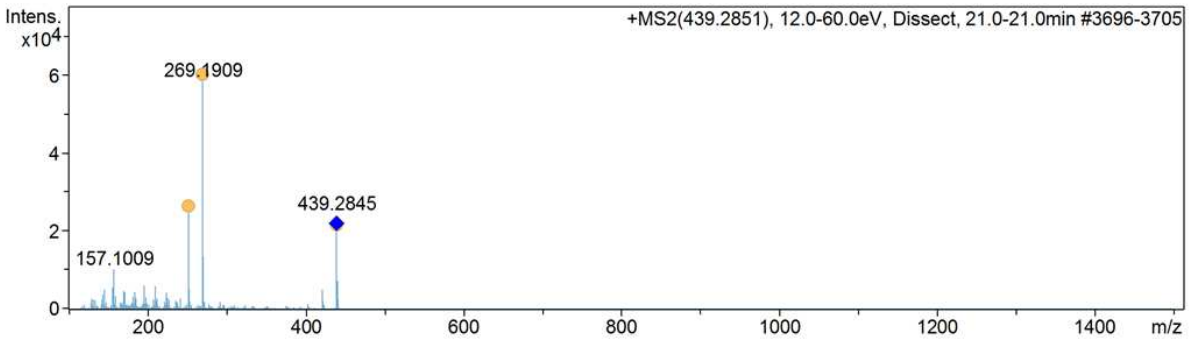

Figure 39

Sample D: MS2 of ion *m/z* 457.2956$[M+H+H2O]^+$. Anotation C28H38O4: (20beta-hydroxy-1-oxo-(22R)-witha-2,5,24-trienolide-like)

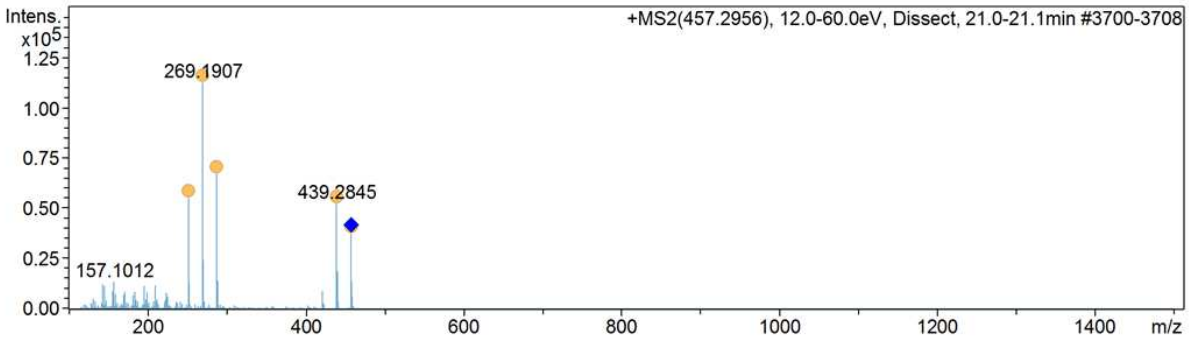

Figure 40

Sample D: Mass spectrum referring to the m/z peak 425.3063, 485.3272, 407.2956 (Rt 24.1-24.6 min.).

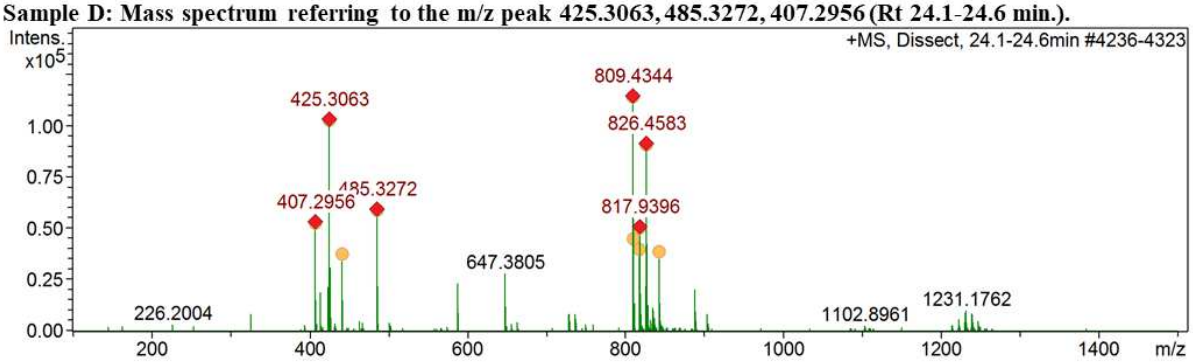

Figure 41

Sample D: Mass spectrum referring to the m/z peak 455.2811, 472.3072 (Rt 28.4-29.0 min.).

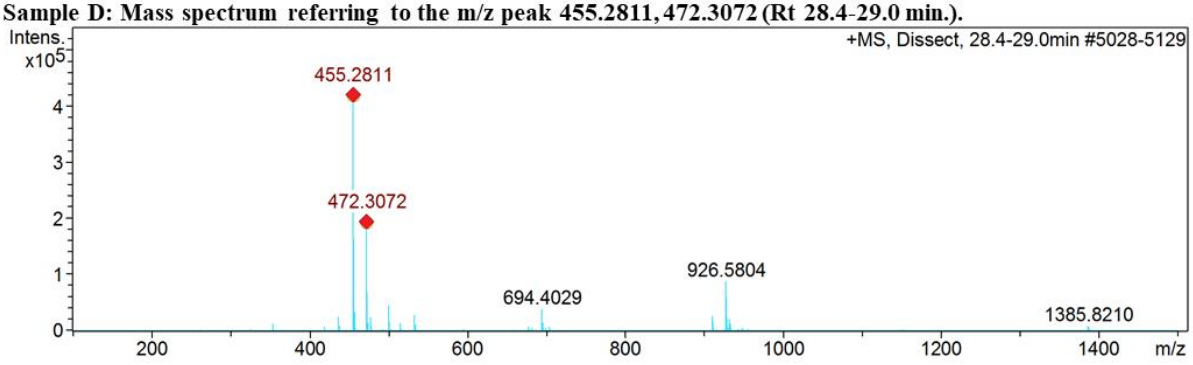

Figure 42

Sample E: Mass spectrum referring to the m/z peak 1075.5353, 929.4771. 767.4233 (Rt 18.0-18.4 min.).

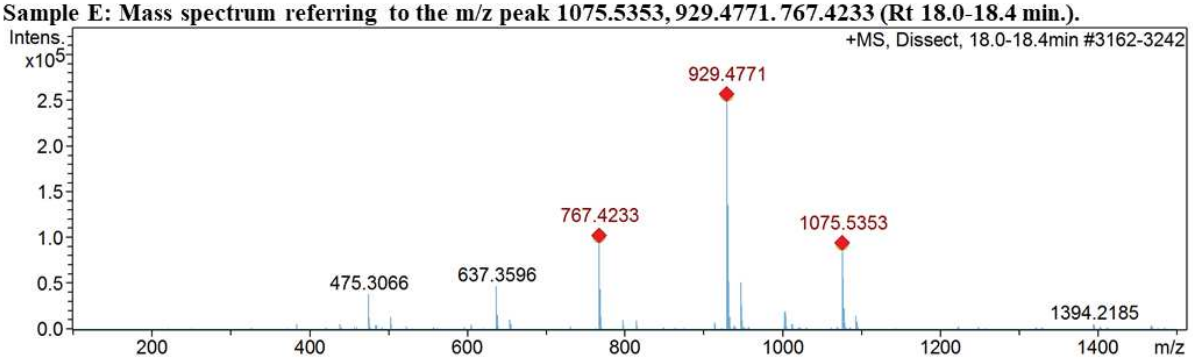

Figure 43

Sample E: Mass spectrum referring to the m/z peak 783.4191 (Rt 18.0-18.6 min.).